

N73-29811

Bell Aerospace DIVISION OF **textron**

POST OFFICE BOX ONE BUFFALO, NEW YORK 14240

CASE FILE COPY

EARTH STORABLE BIMODAL ENGINE FINAL REPORT PHASE I

Report No. 8706-933005

Contract No. 953530

March 1973

Jet Propulsion Laboratory
California Institute of Technology

This work was performed for the Jet Propulsion Laboratory,
California Institute of Technology, sponsored by the
National Aeronautics and Space Administration under
Contract NAS7-100.

Bell Aerospace DIVISION OF **textron**

POST OFFICE BOX ONE BUFFALO, NEW YORK 14240

**EARTH STORABLE BIMODAL ENGINE
FINAL REPORT PHASE I**

Report No. 8706-933005

Contract No. 953530

March 1973

Jet Propulsion Laboratory
California Institute of Technology

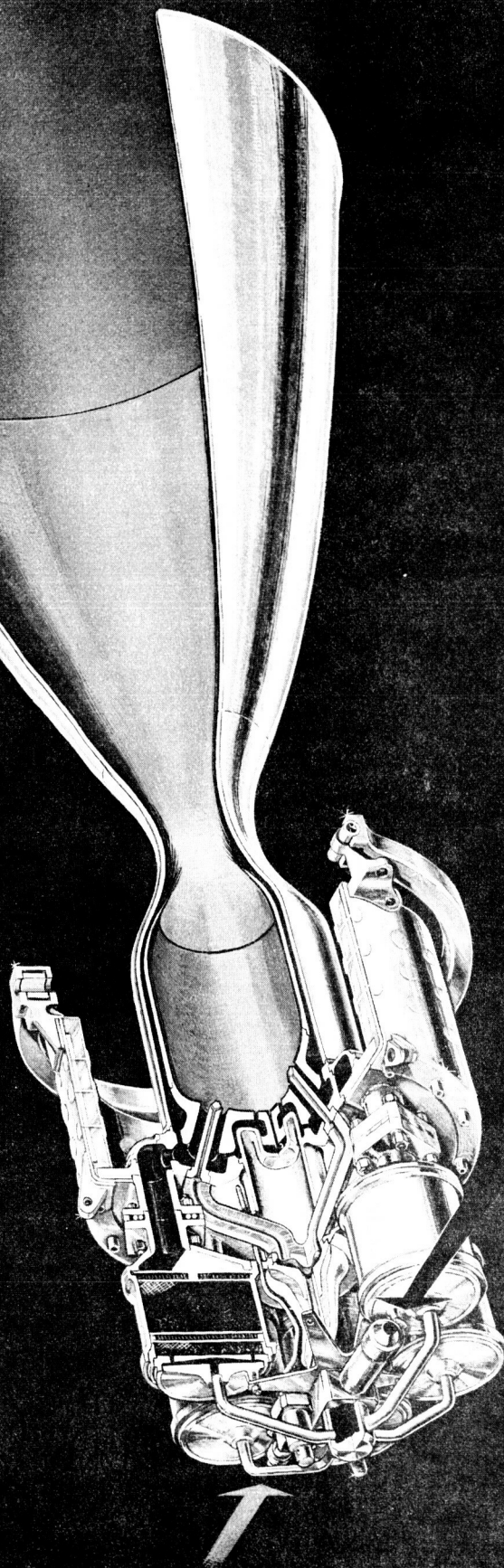
~~This work was performed for the Jet Propulsion Laboratory,
California Institute of Technology, sponsored by the
National Aeronautics and Space Administration under
Contract NAS7-100.~~

Approved by: N. R. Roth
 BAC Program Manager/Technical Director
 ESB Engine Program

JPL Program Manager: R. W. Riebling
JPL Technical Manager: C. H. Dodge

Bell Aerospace DIVISION OF **textron**

**FILM COOLED BIMODAL
THRUST CHAMBER ASSEMBLY**



FOREWORD

This study effort was sponsored by the Jet Propulsion Laboratory, California, Institute of Technology under Contract 953530. The JPL Program Manager was Mr. Robert W. Riebling and the JPL Technical Manager was Mr. Charles H. Dodge. The BAC Program Manager/Technical Director was Mr. Nelson R. Roth. The BAC Project Director was Mr. Neil I. Safeer, assisted by Messrs., Arthur H. Blessing, George E. Sabak, Kenneth McIlroy, and Nels W. Larson.

ABSTRACT

During Phase I, the main objective was to conduct an in-depth study of an Earth Storable Bimodal (ESB) Engine using earth storable propellants N_2O_4/N_2H_4 and operating in either a monopropellant or bipropellant mode. Detailed studies were completed for both a hot-gas, regeneratively cooled thrust chamber and a ducted hot-gas, film-cooled thrust chamber. Hydrazine decomposition products were used for cooling in either configuration. The various arrangements and configurations of hydrazine reactors, secondary injectors, chambers and gimbal methods were considered. The two basic materials selected for the major components were columbium alloys and L-605. The secondary injector types considered were previously demonstrated by JPL and consisted of a liquid-on-gas triplet, a liquid-on-gas doublet, and a liquid-on-gas coaxial injector. Various design tradeoffs were made with different reactor types located at: the secondary injector station, the thrust chamber throat, and the nozzle/extension interface. Associated thermal, structural, and mass analyses were completed.

The "preferred" regenerative chamber configurations consisted of six cylindrical individual L-605 reactors located at the columbium secondary injector station. The selected coolant passages for the columbium throat section was either a mini-channel or annular configuration and an annular configuration for the columbium chamber (barrel) section. The "preferred" ducted film-cooled chamber configuration consisted of six cylindrical individual L-605 reactors located at the columbium secondary injector station. A columbium chamber and liner are welded to the columbium injector. The selected injector was the liquid-on-gas coaxial injector.

A planned Phase II program, which was intended to allow detailed design, fabrication, and testing of the selected design, will not be funded due to budget limitations.

CONTENTS

Section		Page
1.	INTRODUCTION	1
2.	PROGRAM OBJECTIVES	1
3.	PROGRAM APPROACH	1
	Task 1 - Regenerative Thrust Chamber Design Study	1
	Task 2 - Bimodal Engine Configuration Study	1
4.	PROGRAM PLAN	2
5.	SUMMARY OF TECHNICAL DISCUSSION	3
5.1	Task 1 - Regenerative Thrust Chamber Design Study	3
5.1.1	Program Schedule	3
5.1.2	Task 1 Evaluation Plan	3
5.1.3	Preliminary System Requirements	4
5.1.4	Regeneratively Cooled Thrust Chamber Layouts	4
5.1.5	Thermal, Structural, Mass and Performance Analyses	6
5.1.6	Regenerative Chamber Configuration Rating and Selection	6
5.1.7	Preliminary Regenerative Chamber Design Review	7
5.1.8	Regenerative Chamber Layout Design	7
5.2	Task 2 - Bimodal Engine Configuration Study	8
5.2.1	Design Layouts of Coaxial Injectors	8
5.2.2	Mechanical Interface Details	10
5.2.3	Ducted Film-Cooled Engine Designs	10
5.2.4	Thermal, Structural and Mass Analyses	10
5.2.5	System Mass/Performance Tradeoffs	10
5.2.6	Rating and Selection of Final Configurations	10
6.	TECHNICAL DISCUSSION - TASK 1 (REGENERATIVE THRUST CHAMBER DESIGN STUDY)	11
6.1	General	11
6.2	Regeneratively Cooled Engine Evaluation Plan	12
6.3	Regenerative Chamber Conceptual Layouts	14
6.3.1	Reactor at Secondary Injectors	14
6.3.2	Reactors at Chamber Throat	15
6.3.3	Reactors at the Nozzle Extension Interface	16
6.4	Thermal Analyses	18
6.4.1	Throat Station	19
6.4.2	Radiation Cooled Nozzle Temperatures	20
6.4.3	Chamber Passage Design	21
6.4.4	Typical Channel Design at Throat Station	21
6.5	Structural Analysis	22
6.6	Mass Analyses	28
6.7	Regenerative Chamber Configuration Rating and Selection	31
6.7.1	Rationale and Results	31
6.8	Regenerative Chamber Layout	33

CONTENTS (CONT)

Section	Page
7. TECHNICAL DISCUSSION - TASK 2 (BIMODAL ENGINE CONFIGURATION STUDY).....	34
7.1 Design Layout of Coaxial Injectors	34
7.1.1 Selection Criteria and Combinations	34
7.1.2 Coaxial Injector Design Criteria	35
7.2 Mechanical Joints.....	37
7.3 Reactor/Injector/Chamber Interface	40
7.4 Ducted Film-Cooled Thrust Chamber Designs	40
7.5 Thermal Analyses.....	40
7.5.1 Partial Fuel Cooled Injector.....	41
7.5.2 Oxidizer Cooled Injector	41
7.5.3 Heat Gain by the Oxidizer Flow Through the Oxidizer Circuit.....	41
7.5.4 Chamber Wall Temperature	41
7.5.5 Discussion of Bimodal Engine, DJ-339 Test Results (JPL - Edwards Test Station)	41
7.5.6 Parametric Thermal Study to Determine Influence of Engine Variables on Wall Temperatures.....	42
7.6 Structural Analyses.....	44
7.7 Mass Analyses.....	49
7.8 System Mass/Performance Tradeoff.....	49
7.9 Rating and Selection of Final Bimodal Thruster Configurations.....	49
7.9.1 Ratings of Secondary Injectors.....	50
7.9.2 Ratings of Reactor/Injector Combinations with the Reactor at the Secondary Injection Station.....	51
7.9.3 Ratings of Preferred Reactor/Liner/Secondary Injector with Reactor at the Nozzle Extension Interface.....	54
7.10 Final Designs	56
7.11 Recommendations and Conclusions.....	56
7.12 New Technology.....	57

TABLES

Number		Page
1	Bimodal Regenerative Thrust Chamber Requirements	59
2	Flight-Type Bimodal Engine Requirements	60
3	Summary of Regenerative Throat Wall Temperatures for Various Configurations	61
4	Bimodal Engine Configurations Mass Analysis	62
5	Regeneratively Cooled Bimodal Engine Mass Analysis Inputs.	63
6	Bimodal Engine Single Bed Reactor Throat Mounted Gimbal Ring	64
7	Bimodal Engine 6 Cylindrical Reactors Head Mounted Gimbal Ring	65
8	Bimodal Engine 6 Cylindrical Reactors Throat Mounted Gimbal Ring.	66
9	Bimodal Engine Configuration Mass Analysis.	67
10	Summary of Table 9.	68
11	Bimodal Chamber Assembly Configurations - Channel, Drilled Annular.	69
12	Bimodal Configuration Changes, Head-Mounted Reactor (6).	70
13	Bimodal Configuration Changes, Throat-Mounted Reactor (6).	70
14	Regenerative Chamber Mass Comparison	71
15	Evaluation Ratings for Regenerative Chambers, Reactors and Nozzle Extensions	72
16	Summary - Regenerative Chamber Design Parameter Effect on Throat Temperature.	75
17	Oxidizer Temperature Rise and Injector Face Temperature	76
18	Final Mass Analyses	77
19	Secondary Injectors	78
20	Reactor/Injector Combinations - Reactor at Secondary Injector Station	79
21	Reactor/Liner/Secondary Injectors - Reactor at Nozzle Extension Interface	80

ILLUSTRATIONS

Figure		Page
1	Major Component Combinations	105
2	Regenerative Chamber Passage Combinations	107
3	Flow Chart.	108
4	Secondary Injector Station, Single Cylinder Reactor – Annular Passage Welded Interface.	109
5	Secondary Injector Station, Multiple Cylindrical Reactors – Annular Passage Welded Interface Cluster of 6 (Typical)	110
6	Secondary Injector Station, Annular Reactor, Flanged Interface	111
7	Secondary Injector Station – Annular Passage, Welded Interface.	112
8	Secondary Injector Station Radial in Feed – Annular Reactor – Annular Passage. .	113
9	Throat Station, Multiple Cylindrical, Welded Reactors, Cluster of 6 (Typical).	114
10	Throat Station, Radial in Feed Toroidal Reactor	115
11	Throat Station, Radial In-Feed, Annular Reactor, Split Section, All-Welded Columbium Alloy Design	116

ILLUSTRATIONS (CONT)

Figure		Page
12	Throat Station, Axial Feed Annular Reactor – Split Sections All Welded	117
13	Divergent Nozzle Station – Axial Flow Reactor Bed Loading Comparison	118
14	Divergent Nozzle Stations, $\epsilon = 10$ and $\epsilon = 13$ Axial Flow Reactor, Welded Joints.	119
15	Nozzle/Extension, Annular Reactor Axial Feed Reactor Bolted to Thrust Chamber.	120
16	Nozzle/Extension Station, Axial Flow Reactor L-605 Annular Reactor.	121
17	Nozzle/Extension Station, Annular Reactor Axial Feed Top Bed Bolted Configuration	122
18	Nozzle/Extension Station Axial Flow Injector, Annular Chamber Only Inner Liner and Injector Face Fabricated From Columbium Alloy	123
19	Nozzle Extension Station Annular Configuration Radial in Feed Reactor Bolted Joint	124
20	Thermal Conductivity.	125
21	Influence of Inlet Manifold Pressure on Cooling Passage Design Variables	126
22	Influence of Coolant Passage Design Parameters on Maximum Throat Temperature.	127
23	Influence of Coolant Passage Design Parameters on Maximum Throat Temperature	128
24	Influence of Coolant Passage Design Parameters on Maximum Throat Temperature.	129
25	Influence of Percent Land Width on Maximum Throat Temperature	130
26	Influence of Wall Thermal Conductivity and Land Width on Maximum Throat Temperature	131
27	Hot Gas Film Coefficient versus Contraction Ratio	132
28	Influence of Coolant Passage Design Parameters on Maximum Throat Temperature.	133
29	Influence of Coolant Passage Design Parameters on Maximum Throat Temperature.	134
30	Influence of Coolant Passage Design Parameters on Maximum Throat Temperature.	135
31	Influence of Percent Land Width on Maximum Throat Temperature	136
32	Annular Passage Wall Temperature at the Throat	137
33	Nozzle Extension Temperature versus Area Ratio	138
34	Annular Passage Wall Temperature - Chamber.	139
35	Drilled Passages - Wall Temperature - Chamber.	140
36	Wall Temperature at Throat Station versus Hot Gas Film Coefficient	141
37	Tensile Strength versus Temperature SCb-291 Columbium.	142
38	Effect of Temperature on Modulus of Elasticity for SCb-291 Columbium.	143
39	Stress Necessary to Produce a Creep Strain of 0.05% in SCb-291	144
40	Material SCb-291 Stress Necessary to Produce Indicated Creep Strain at Temperature.	145
41	Material SCb-291 Stress versus Temperature for Indicated Creep Strain at $t = 1000$ sec	146

ILLUSTRATIONS (CONT)

Figure		Page
42	Material SCb-291 Creep Characteristic Stress-Strain Diagrams at t = 1000 sec	147
43	Material SCb-291 Creep Characteristic Stress-Strain Diagram at t = 1000 sec	148
44	Bimode Engine Axial Temperature versus Distance	149
45	Bimodal Engine, Film-Cooled Triplet Injector Reactor Mounted at Secondary Injector Station.	150
46	Bimodal Engine, Film Cooled Triplet Injector Reactor Mounted at Secondary Injector Station.	151
47	Coaxial Injector	152
48	Columbium/L-605 Injector with Center Fuel Cooling	153
49	Bimodal Engine, Regeneratively Cooled L-605 Reactor and Secondary Injector Back Plate, Columbium Alloy Thrust Chamber. Six Cylindrical Integral Reactors	154
50	Fuel Orifice Variations (to Allow Axial Removal of Oxidizer Orifices)	155
51	Nut and Bolt Installation	156
52	Stud and Nut Installation.	157
53	Stud and Nut (Welded Stud).	158
54	Chamber and Liner Temperatures Test DJ-339.	159
55	Test DJ-339 - Throat Location.	160
56	Influence of Ammonia Dissociation on Liner and Wall Temperatures	161
57	Influence of Film Coolant Flow Rate on Liner and Wall Temperatures	162
58	Influence of Annular Gap on Liner and Wall Temperatures	163
59	Influence of Heat Transfer Coefficient on Throat Station Wall Temperature	164
60	Influence of Chamber Heat Transfer Coefficient on Chamber Liner and Wall Temperatures.	165
61	Axial Temperature Distribution of Film Coolant, Liner and Chamber Wall	166
62	Larsen-Miller Master Plot for Recrystallized C103	167
63	Material C-103 Creep Characteristic Stress-Strain Diagrams at t = 1000 sec	168
64	Material - SCb-291 Creep Characteristics Stress-Strain Diagram at t = 1000 sec	169
65	System Weight Comparison versus Total Impulses, Bimode Engine Weight and I_{sp}	170
66	Bimode Engine System Weight versus I_{sp} and Engine Weight.	171
67	Bimode Engine System Weight versus I_{sp} and Engine Weight.	172
68	Specific Impulse Values	173
69	Specific Impulse Values	174
70	Specific Impulse Values	175
71	Reactor Located at Secondary Injector Station	176
72	Regeneratively Cooled Thruster, Reactor Located at Nozzle Extension Interface . .	177
73	Prototype Regenerative Cooled Bimodal Thrust Chamber with Integral Six Cylindrical Reactor at Injector.	178
74	Prototype Regenerative Cooled Bimodal Thrust Chamber with Annular Reactor at Nozzle/Extension Interface.	179

ILLUSTRATIONS (CONT)

Figure		Page
75	Prototype Film-Cooled Bimodal Thrust Chamber with Six Individual Cylindrical Reactors at Injector.	180
76	Preprototype Film-Cooled Thrust Chamber with 100% Fuel Cooled Injector Face	181
77	Preprototype Film-Cooled Thrust Chamber with 6% Fuel Cooled Injector Face	182

I. INTRODUCTION

This report is submitted in compliance with the documentation requirements of the Jet Propulsion Laboratory, California Institute of Technology for Contract 953530. It summarizes the efforts performed on the Earth Storable Bimodal Engine.

2. PROGRAM OBJECTIVES

This program is Phase I of a planned two (2) phase effort leading to the development of an Earth Storable (ESB) Engine using earth storable propellants N_2O_4 and N_2H_4 and operating on command in either a monopropellant or bipropellant mode.

The objective of Phase I is to conduct an in-depth study of a gas regeneratively cooled thrust chamber, and an optimum packaging of various types of injectors and thrust chambers, into a flight-type engine configuration.

3. PROGRAM APPROACH

To accomplish the objectives the Phase I program is arranged in three (3) tasks:

- Task 1 Regenerative Thrust Chamber Design Study
- Task 2 Bimodal Engine Configuration Study
- Task 3 Documentation

The definition of the two (2) major tasks; Task 1 and Task 2 is as follows:

Task 1 - Regenerative Thrust Chamber Design Study

Conduct a detailed study to determine the optimum configuration for a metallic thrust chamber for the ESB engine. The chamber shall be regeneratively cooled by hydrazine decomposition products and can utilize each or any of the following alternate types of secondary injectors:

- 1) Canted liquid-on-gas triplet
- 2) Canted liquid-on-gas doublet
- 3) Canted liquid-on-gas coaxial

The regenerative thrust chamber shall be double walled, all metal with the coolant gases flowing counter to the direction of the exhaust gases. An uncooled nozzle extension shall be used at some appropriate area ratio in the divergent nozzle.

The requirements for the regenerative chamber are listed in Table 1.

Task 2 - Bimodal Engine Configuration Study

Establish a near-optimum configuration for a flight-type engine embodying the ultimately selected injector type and thrust chamber cooling concept. A detailed morphological study of possible ESB Engine configurations shall be made using the requirements listed in Table 2.

The secondary injector types to be considered are listed in the Task 1 definition section. The thrust chamber cooling concepts to be considered are:

- 1) Gaseous-regenerative/radiation cooling
- 2) Gaseous-film/radiation cooling of the configuration evaluated by JPL in its parallel in-house program.
- 3) Alternatives, technically justified approach(es).

In preparing the documentation, all technical reporting shall employ the use of SI units except on design layouts and drawings.

4. PROGRAM PLAN

The program duration of Phase I is 6 months with the Interim Report scheduled in the beginning of the 7th month.

Various regeneratively cooled thrust chamber designs will be studied in Task 1 with consideration for columbium alloys and L-605 as the two (2) primary classes of materials. Reactor locations will be studied at both the secondary injector station and at the nozzle/throat region. Both free standing and integral regenerative configurations will be considered. Tradeoff studies will consist of layouts, analyses, scoring, rating and final recommended regenerative cooled thrust chamber design. Following approval by JPL, a detail design will be completed including detail drawings of the optimum regenerative cooled thrust chamber and analyses in the areas of thermal, structural, performance, life, fabricability, weight, system interfaces, and cost.

The engine assembly configuration trade study will be accomplished in Task 2. Particular attention shall be given to such details as: reactor packaging, reactor types, thrust take-out provisions, insulation requirements, if any, material selection, instrumentation provisions, etc. A minimum of two reactor packaging arrangements of three types of reactors, three types of injectors and three chamber cooling configurations will be considered.

The Phase I final report (interim report) will reflect the configuration selected as well as the Task 1 study results. This Phase I effort will provide the necessary understanding to allow a transition to a Phase II program consisting of the design, fabrication and testing of a prototype flight configuration ESB Engine.

5. SUMMARY OF TECHNICAL DISCUSSION

5.1 TASK 1 - REGENERATIVE THRUST CHAMBER DESIGN STUDY

The activities accomplished in this task were:

- BAC submittal and JPL approval of the Program Schedule,
- BAC submittal and JPL approval of the Task 1 Evaluation Plan (rating and selection plan),
- JPL submittal of Preliminary System Requirements,
- Regeneratively cooled thrust chamber layouts,
- Thermal, structural, mass and performance analyses,
- Rating and selection of the regenerative chamber configurations,
- Preliminary Regenerative Chamber Design Review, and
- Regenerative chamber layout design.

5.1.1 Program Schedule

The preliminary Program Schedule (Report No. 8706-910002) was approved by JPL as submitted. Three copies of this plan were submitted to JPL. This submittal consisted of a schedule chart, a milestone chart, a man-hour/cost projection summary and associated program rationale.

5.1.2 Task 1 Evaluation Plan

The Task 1 Evaluation Plan (Report No. 8706-910001) was approved by JPL. This plan established a practical method for rating and evaluating regeneratively cooled thrust chamber concepts. The plan provides for a combination of a numerical rating system and an "engineering logic and judgment" system. To allow consideration of the various "arrangements" of components for regeneratively cooled Bimodal engines, the basic engine was divided into five major components:

- The reactor
- The secondary injector
- The regenerative chamber
- The nozzle extension, and
- The valves

Three major classes of engines were established:

- Reactor at the secondary injector station
- Reactor at the throat station, and
- Reactor at the nozzle/extension interface.

Note: *All appropriate Tables and Figures are provided in both S.I. and English units following the text and are separated for ease of reference. Each Table is provided in both the S.I. and English section, whereas all Figures are provided in the S.I. sections with Figures 20 through 44 and 54 through 64 repeated in the English section.*

Each of the five major components could be rated separately for fabrication from selected materials with six major elements being:

- Performance,
- Durability/Life,
- Fabrication,
- Risk,
- Cost, and
- Weight.

Following the individual ratings, a preliminary selection of the "preferred" component design was made. "All-welded" versus "flanged" interface comparisons were made followed by consideration of gimbaling for the more favored designs.

5.1.3 Preliminary System Requirements

To provide initial insight into the basic regeneratively cooled thrust chamber design preliminary system requirements were submitted by JPL. These were established using the Viking vehicle requirements as a guideline until more defined requirements are known. The major items consist of:

- | | |
|--------------------------------|--|
| 1. Gimbal Angle | $\pm 9^\circ$ |
| 2. Gimbal Actuation | Electrical – for near – Sun vehicles
Hydraulic – for Jupiter-type vehicles |
| 3. Chamber Pressure Transducer | Flight type as on Viking – need thermal standoff from hot injector. |
| 4. Envelope | A 20-inch diameter cylinder 20 inches long from valve inlet to throat station |
| 5. Structure Insulation | To be located on structure, not exterior of engine unless necessary for N_2H_4 line insulation |
| 6. Valve Actuation | Probably electrical |
| 7. Throttle Valve | No immediate need, could use Surveyor type, if needed |
| 8. Valve Installation | Initially a separate fuel and oxidizer valve were to be installed on the engine. During the Design Review it was agreed to locate the valves on the vehicle structure. |
| 9. Fuel Venturi | To be installed as close to reactor injector(s) as practical. |

5.1.4 Regeneratively Cooled Thrust Chamber Layouts

As described in the summary of the Evaluation Plan the regeneratively cooled engine has been separated into five basic elements. Of these five elements the reactor type and location and the regenerative chamber configuration were considered most significant in the initial tradeoff and study of the

regenerative thrust chamber. So, the major effort was concentrated in the combinations and configurations of these two elements.

5.1.4.1 Reactor

The reactor can be located at three different stations:

- At the Secondary Injector
- At the Throat
- At the Nozzle/Extension Interface

Three major forms of reactors exist:

- Cylindrical
- Annular
- Torroidal

Single or multiple quantities of each can also be considered. Three methods of hydrazine injection exist:

- Axial
- Radial In
- Radial Out

The method of attachment of the reactors to the regenerative chamber manifold(s) and secondary injector can be welded or flanged.

The two primary candidate materials based on strength at elevated temperature and compatibility with the anticipated environment are columbium alloys and L-605. So, proper interface must be considered should unlike materials be desirable.

To realistically identify these reactor types and locations a summary of the major component combinations used for the tradeoff is shown in Figure 1. Selected layouts follow in subsequent sections including detailed description of each major component combination. An all-channeled regenerative chamber was assumed for the initial layouts.

5.1.4.2 Regenerative Chamber

The two major configurations of a regenerative chamber are:

- Integral (one piece or bonded)
- Free Standing (outer walls separate from inner wall)

The three major types of passages are:

- Channeled
- Drilled
- Annular

Various combinations of the above can be used for the "throat (nozzle)" region and the "barrel" region of the chamber. Seven major combinations are identified in Figure 2.

5.1.5 Thermal, Structural, Mass and Performance Analyses

Considerable analyses were conducted throughout this task to provide definition and guidance in the selection of a "preferred" regenerative thrust chamber design.

Heat transfer analyses included investigating the efficiency of various cooling passage geometries for both the throat station and chamber (barrel) region. These studies considered the effects of passage shape, height, number of passages, coolant flow area, material, combustion efficiency and ammonia dissociation on wall temperature. Analyses were also completed on the radiation-cooled nozzle extension for various area ratios and allowable interface temperature for different materials.

Structural analyses were made on the reactor designs for pressure loading, structural attachments and locations for the gimbal ring attachment, and the inner and outer chamber walls. Concern was given to both the elastic buckling and creep stresses in the chamber (barrel) and the divergent section. Thermal stresses were considered at all interface joints to compare the effects of different configurations on the loading of the joints (welded and bolted) and also the effects of reactor locations on the chamber. The nozzle extension buckling loads due to gimbal acceleration and accumulated thrust loads were also considered.

Various mass analyses were initially completed to present a relative comparison of a basic engine assembly with a variety of reactor designs located at the three major stations. Mass comparisons of the "preferred" regenerative chamber configurations were also made with appropriate passage type, gimbal provisions and valves. Common design rationale was used in the various configurations providing representative mass comparisons, not necessarily minimum mass. Further analyses were completed on two selected regenerative thrust chamber designs with concern for detailed mass reduction.

A preliminary system mass and performance tradeoff analysis was performed to determine initial effects of performance variations and engine mass on the total system. Assumptions were made that could be representative for a typical system using the Bimodal Engine.

5.1.6 Regenerative Chamber Configuration Rating and Selection

The ratings (tradeoff comparison) of the various regenerative chamber configurations were completed in accordance with the Task 1 Evaluation Plan. Two regeneratively cooled chamber configurations have been selected. Definition of these two basic configurations follow:

5.1.6.1 Reactor Location and Type

- Multiple (six) axial feed, cylindrical reactors at the secondary injector
- Annular, axial feed reactor at the nozzle/extension interface

5.1.6.2 Throat Passage Configurations

- Mini channel
- Annulus

The mini channel configuration allows about 627K (300°F) lower throat temperature and is, therefore, first preference.

5.1.6.3 Chamber (Barrel Configuration)

- Annulus

These selections have been based upon the tradeoff studies and include consideration for performance, durability/life, fabrication, risk, cost and mass. A more detailed discussion of these ratings and the rationale is given in the subsequent Technical Discussion Section.

5.1.7 Preliminary Regenerative Chamber Design Review

The Design Review was held at BAC on January 16, 1973 with these main items on the agenda:

- Regenerative chamber designs
- Film cooled chamber designs
- Related test results
- Initial system performance tradeoffs
- Future program plans

During the Design Review agreement was made between JPL and BAC to modify the technical effort for Phase I, since Phase II could not be funded due to budget restraints.

A Technical Direction Memorandum was issued with the following directions:

1. Eliminate the following per the program schedule:
 - a. Final design review of the regenerative chamber.
 - b. Alternate film-cooled configuration (i.e., Vortex)
 - c. Doublet injector pattern.
 - d. Related analyses of above.
2. Concentrate on the following (major emphasis):
 - a. Simplify Task 2 Evaluation Plan to compare only the ducted, film-cooled configuration with selected regenerative configurations.
 - b. Design (layout) ducted, film-cooled configuration with coaxial injector.
 - c. Layout drawings of two selected regenerative and ducted, film-cooled engine assemblies.

5.1.8 Regenerative Chamber Layout Design

Layout designs were completed for the two "preferred" regenerative configurations.

5.1.8.1 Configuration No. 1

1. Reactor and Location

Multiple (six) axial feed, cylindrical reactors at the secondary injector. Material selection is L-605

2. Chamber

Mini channel throat and annular chamber (barrel). Material selection is columbium.

3. Injector

Injectors with different methods of center cooling were considered for an all columbium injector and a columbium/L-605 combination as defined in Task 2.

5.1.8.2 Configuration No. 2

1. Reactor and Location

Annular, axial feed reactor at the nozzle/extension interface. Material selection is L-605.

2. Chamber

Mini channel throat and annular chamber (barrel). Material selection is columbium.

3. Injector

Same consideration as Configuration No. 1.

5.2 TASK 2 - BIMODAL ENGINE CONFIGURATION STUDY

The major activities accomplished in this task were:

- Design layouts of three different coaxial injectors
- Interface details between the reactor and the injector/chamber
- Ducted film-cooled designs for a pre-prototype and prototype engines
- Associated thermal, structural and mass analyses
- System mass/performance tradeoffs
- Rating and selection of the configuration
- Recommendations and conclusions
- Submittal of Final Report.

5.2.1 Design Layouts of Coaxial Injectors

Three basic coaxial injector designs were completed for the film-cooled chamber, including the following considerations:

5.2.1.1 Selection Criteria

The selection criteria for the injectors included performance, heat flux uniformity, ability to cool the face, and fabricability.

5.2.1.2 Material Combinations

The material combinations included:

- (1) All-columbium,
- (2) Columbium/L-605, and
- (3) All-L-605

All-Columbium Injector:

- (1) Welding to chamber and liner
- (2) An integral (one-piece) injector
- (3) Requires columbium oxidizer orifice stems (if welded)
- (4) Simplest design

A Columbium Face/L-605 Back Cover:

- (1) Compatible with a columbium liner and an L-605 cover
- (2) Allowance is required for thermal expansion differences
- (3) Oxidizer regenerative face cooling is not practical

All-L-605 Injector:

The all-L-605 injector is not practical with a columbium liner and chamber.

5.2.1.3 Methods of Face Cooling

Three methods of face cooling were considered:

- (1) Center combustion element
- (2) Oxidizer regenerative (100%)
- (3) Fuel regenerative (100% or partial)

The center combustion element can be designed for reduced mass flow, but sufficient flow to allow face cooling. It can also be designed for a "fuel-rich" mixture ratio to allow additional fuel for face cooling. The main concern with a center combustion element is the deviation from the present demonstrated injector pattern (12 versus 13 elements).

The oxidizer regeneratively cooled concept is compatible with an all-columbium injector but not practical with a columbium/L-605 injector due to interface and sealing requirements.

The fuel regeneratively cooled injector face is most compatible with all designs. The 100% regeneratively cooled concept requires supply of the fuel in the central region of the injector, resulting

in an increase in pressure drop and velocity due to the limited area available. It does provide, however, lowest injector center face temperature. The partial regeneratively cooled injector face is a practical design that can maintain the injector center face at a compatible temperature. This design requires bleed of the partial fuel regenerative gases into the chamber. A value of 6% of the fuel will maintain the injector center face temperature to approximately 1589K (2400°F). This amount of bleed into the chamber is expected to have little, if any, effect on the established combustion characteristics of the present injector.

Of the four methods of injector face cooling the partial regeneratively cooled injector face is preferred due to compatibility with overall design and minimum, if any, effects on the basic injector pattern and performance history.

5.2.2 Mechanical Interface Details

Various methods of attachment have been considered for the dissimilar material joints with columbium and L-605 using a hot mechanical joint. The basic methods considered are:

- (1) Nut and bolt
- (2) Stud and nut, with stud welded into parent material
- (3) Stud and nut with each locked in by local peening
- (4) Stud and nut, with stud locked in place with a pin
- (5) Bolt threaded directly into parent material.

The flange and bolt interface is critical due to the difference in thermal expansion of the two materials. The favored method of attachment for a mechanical joint is the use of columbium bolts and columbium washers in the L-605 flange. The columbium bolts are preferred for a flight-configuration engine due to the extended life required.

5.2.3 Ducted Film-Cooled Engine Designs

Depending upon the final design objectives and requirements, various ducted film-cooled configurations are practical and possible. To allow definition of the basic design features for a ducted film-cooled engine three designs were considered: (1) six individual cylindrical reactors with 6% fuel-cooled injector face, (2) six individual cylindrical reactors with 100% fuel-cooled injector face, and (3) six integral cylindrical reactors with 6% fuel-cooled injector face.

5.2.4 Thermal, Structural and Mass Analyses

Considerable analyses were also conducted in this task to define and guide the selection of the "preferred" ducted film-cooled thrust chamber design. Detailed results of these analyses are included in the subsequent sections. The test results of the ducted film-cooled chamber firings at JPL were used and compared with the thermal analyses completed on the various designs.

5.2.5 System Mass/Performance Tradeoffs

A preliminary system mass/performance tradeoff was completed based on assumptions for a representative system using the bimodal engine.

5.2.6 Rating and Selection of Final Configurations

Ratings and comparisons were made in this task for two regenerative configurations and three ducted film-cooled configurations. The rating methods are identical to that used for the Task 1 effort.

6.0 TECHNICAL DISCUSSION – TASK 1 (REGENERATIVE THRUST CHAMBER DESIGN STUDY)

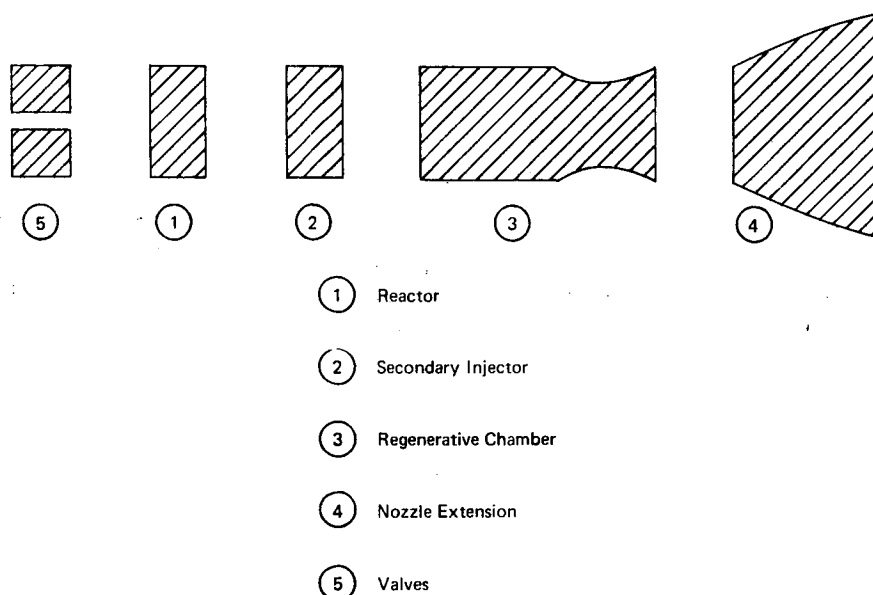
6.1 GENERAL

One of the concepts considered for a Bimodal engine is a regeneratively cooled engine. The selection of such an engine requires establishing a design which contains the most favorable characteristics to meet the overall goal. The optimum configuration shall be that which best meets the engine life cycle/durability requirements, with maximum performance, with least penalty in mass, pressure drop and cost. In addition, the engine must be configured to enable integration with the vehicle, with gimbal capability and no undesirable interaction effects.

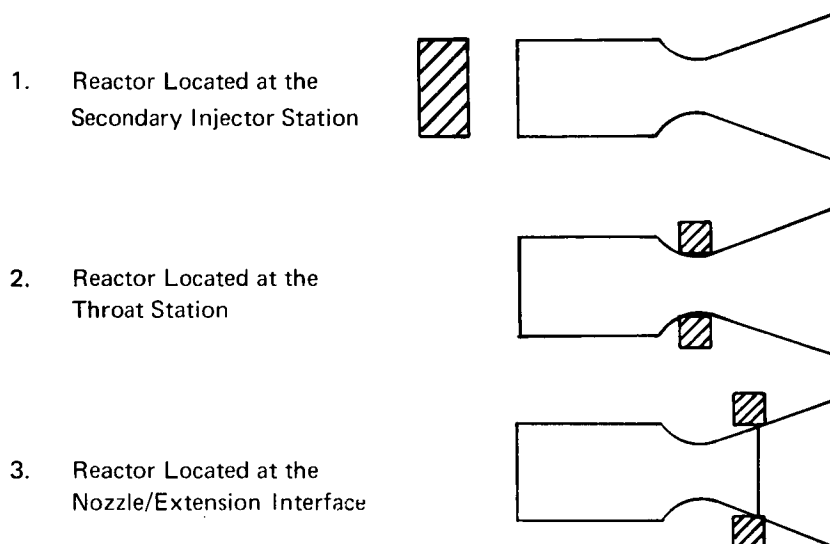
For final system application, four major parameters or features of the optimized engine can be identified:

- (1) **Life/Reliability** - The engine must be able to deliver its required thrust over the designated mission, repeatedly and reliably.
- (2) **System/Performance** - The engine must be able to deliver the required specific impulse with its mass kept to a minimum, with a minimum system pressure drop.
- (3) **System Integration** - The engine must be capable of integration to the vehicle with the capability of obtaining thrust vector control by gimbaling, with no problems of excessive heat transfer to the vehicle.
- (4) **Overall Cost** - The engine cost must be minimal, providing that the required engineering value is incorporated, to ensure that all anticipated operational requirements can be attained.

Due to the many possible "configurations" of hardware and "arrangements" of components, a rational or logical approach is required to determine an optimum design(s). Part of this rationale is to identify the five basic elements of a regeneratively cooled Bimodal engine:



Of these five basic elements, the reactor, secondary injector, and regenerative chamber are most significant in the overall study. The location of the gimbal ring is also a design factor that must be considered, but mainly for mass effects. Further classification of the design is beneficial by separating the configuration into the following three primary configurations:



Iterations of each exist, including the possibility of at least two basic materials: columbium alloys and L-605. Also, the possibility of all-welded, all-flanged, or partially welded/flanged configurations exists.

This technical section describes the detail of the tradeoff elements, including the Evaluation Plan, regenerative chamber conceptual layouts, all analyses, the rating and selection of the "preferred" regenerative designs, the Preliminary Design Review, and the final regenerative chamber design(s).

6.2 REGENERATIVELY COOLED ENGINE EVALUATION PLAN

Due to the many possible "arrangements" of components and "configurations" of hardware, a method of evaluation was needed to determine an optimum design. This Evaluation Plan has, therefore, been formulated to provide a method of selecting this optimum configuration. It is always difficult to establish a fair and all encompassing technique to select a "preferred" design. This is especially true with this study, due to the vast number of possible combinations. Many rating systems have been used in the past, and most if not all, have required improvement or adjustment with usage.

It was, therefore, the intent of this plan to approach the selection of an optimum regeneratively cooled engine with a combination of a numerical rating system and an "engineering logic and judgment" system.

As each major component is rated, the results are applied to a "total" engine configuration. Logic and judgment are used to establish the level of rating for each element of each major component. A weighting factor is then used for each major parameter based upon mutual agreement between JPL and BAC.

This Evaluation Plan model is formulated in the following manner:

- (1) Each of the five major components are rated on a separate basis, accounting for the variations of each component. Separate ratings are established for columbium alloys and L-605.
- (2) Each major component is rated against six major parameters:
 - (a) Performance
 - (b) Life/Durability
 - (c) Fabrication
 - (d) Risk
 - (e) Cost
 - (f) Weight

Secondary parameters are applied to performance and life/durability as applicable.

- (3) Weight factors for each of these six major parameters are used in conjunction with a value of rating (rating number). The rating number increases from 1 to 10, with 10 being the best rating.
- (4) The rating number is established by logic and judgment of many factors pertinent to each component.
- (5) Following iterative analyses of each component, a product of the weight factor and rating number is obtained and used for preliminary screening of the "favored" configurations of each component. Again, the highest number is the best rating.
- (6) The analysis to this point is considered only for an all-welded configuration. Adjustment is then made for an additional weight/complexity factor for a flanged joint, depending on material combinations. This allows a more direct and easier approach to differences of welded and flanged interfaces. Certainly all-welded configurations will be used except where dissimilar materials are desirable.
- (7) A preliminary selection of various combinations is made, followed by gimbaling considerations for the "favored" configurations.
- (8) The highest rated configurations are then compared and more detailed layout designs completed. Final selection is then made based on the final layout designs.

A descriptive "Flow Chart" of this plan is shown in Figure 3. An example of the "influencing factors" considered for rating the Regenerative Chamber is listed below:

- Size of passages
- Shape of passages
- Number of passages
- Method of "close out"
- Method of fabrication (EDM, drill, machine)
- Hot wall thickness
- Land-to-channel relationship
- Coatings
- Interface configurations
- Various columbium alloys for various portions of the chamber.

The weight factors for the major parameters are listed below:

Individual Component Rating Parameters

Performance		
Bipropellant	1.25	} 2.0
Monopropellant	0.75	
Durability/Life		2.5
Fabrication		1.0
Risk		2.0
Cost		1.0
Mass		1.5
		<hr/> 10.0

NOTE: When more than one element is used for performance or durability/life percentage weight factors for the sub-elements shall be used to keep the total weight factor constant.

Initially, final system ratings were to be repeated for the final "preferred" designs, but was considered redundant and, therefore, not conducted.

6.3 REGENERATIVE CHAMBER CONCEPTUAL LAYOUTS

Various layouts have been made to study the regenerative bimodal engine design. The various detailed configurations of components and their combinations have been identified and are described in the evaluation plan. The many arrangements of reactor location, reactor N_2H_4 supply and decomposed N_2H_4 supply manifolding are summarized in Figure 1. The intent of these layouts is to establish understanding of some of the typical arrangements and to address the critical interface or joint areas. The studies conducted considered reactors located at the secondary injector, throat, and nozzle/extension interface. All reactor designs shown are sized for a bed loading of $28.1 \text{ kg/m}^2\text{-sec}$, (0.04 lb/sec-in^2), except where noted.

The details of sealing arrangements, hydrazine injection and catalyst bed retention varied during the program, with consideration given to a large number of schemes. The variation in drawing details reflects the evolutionary nature of the design study. In each of the layouts, an all channelled chamber passage design was assumed. The layouts are described in the sequence in which they are presented in Figure 1.

6.3.1 Reactor at Secondary Injectors

The bimodal thrusters which have a single cylindrical reactor with a single feed tube to the coolant manifold and multiple cylindrical reactors with multiple feed tubes to the coolant manifold are not shown. Their equivalent configurations, which use an annular passage to transport the coolant gases from the reactor to the coolant manifold are shown in Figures 4 and 5.

Figure 4 shows a bimodal thrust chamber with a single cylindrical hydrazine reactor. For this concept the reactor has a double-layered bed of Shell 405 with a single injector fed from the single N_2H_4 inlet tube. The decomposed hydrazine gases from the bed feeds the regenerative cooling passages through an annulus in this all-welded configuration. It is also possible to provide a flanged version of this design, if the reactor or the reactor and secondary injector are fabricated from L-605 with the regenerative chamber and cooling jackets fabricated from a columbium alloy.

When multiple cylindrical reactors are used, a number of designs are possible. Figure 5 shows a typical all-welded assembly, while Figure 6 shows an L-605 reactor joined to the secondary injector, with metal O-rings used at the interface. Each of the six reactors is fed simultaneously from a distribution manifold located on the propellant valve outlet. The relative location and configuration of the distribution manifold and the reactor to secondary injector interface are discussed in detail for the final configuration tradeoffs in a subsequent section. If the individual reactors are arranged to flow radially inward, they become a very awkward configuration, which, therefore, is not shown.

When considering the use of multiple reactors joined at the secondary injector station, it becomes obvious that an annular bed is a potentially competitive arrangement. Figure 7 shows the all-welded annular bed assembly. Another version shows a flanged joint between the L-605 reactor and the secondary injector in Figure 6. This version has an excessive number of seals and would be modified in a final tradeoff. A representative radially in-fed annular reactor is shown in Figure 8. The hydrazine is injected radially inward, with the decomposed gases fed directly into the outer cooling annulus. The shell for this bed can be constructed completely prior to loading the catalyst. The catalyst can be added through ports in the reactor wall as indicated. Use of a vibrator and the multiple fill ports will ensure good packing of the reactor. This packing technique has been used with plexiglass models and proven to be satisfactory. This type of concept does require a large diameter which can interfere with a gimbal mount. The advantage is that this allows a short length chamber.

6.3.2 Reactors at Chamber Throat

An alternate location for the hydrazine reactors is the throat region or nozzle/extension interface. At either location all reactors require a common manifold at the hydrazine valve outlet and a "spider" type arrangement of hydrazine supply tubes to feed the annular type injectors. These "spider" feed lines, as well as the flexible line supplying the hydrazine valve, must be packaged without interfering with the gimbal activity.

In Figure 9 cylindrical reactors are packaged around the throat section along the divergent section of the nozzle. These cylindrical reactors are fabricated separately as are those located at the head end, however, the reactors are mounted closer to the entrance to the regenerative passage, minimizing the hot gas tubing required. The change in location of the reactors affects the gimbal mount arrangements and the forces needed in the gimbal actuators. All of the engine operating factors which are effected by locating the reactors in this new location are analyzed in the tradeoff study. The configuration which has individual hydrazine radial-in flow reactors at the throat is very complex and costly, and, therefore, is not shown.

Due to the problems of constructing reactors which are located at the chamber throat, the use of an annular, axial feed reactor was considered impractical. A radial-in flow annular reactor is shown in Figure 10. The overall packaging of this reactor provides a compact unit. The toroidal reactor shown in this figure would be assembled prior to mounting on the chamber. The assembly problems and costs are considered in the tradeoff study.

Figure 11 shows another radial-in flow concept, in which the outer jacket of the columbium thruster forms the entire inner shell for containing the 1/8-inch pellets. Although the radial length of the catalyst bed is shorter than the standard reactor, the unusual shape provides a smaller total volume. The reactor assembly must be performed in segments to form the annular shape. The relative complexity of this reactor assembly relating to the assembly of the components can be discerned from the notes on the figure.

Figure 12 shows a reactor which is formed from two "horseshoe" shaped parts. Each reactor operates as a semi-annulus and may consist of two 180° reactors or two reactors less than 180°, to allow weight reduction. By providing a "split" reactor the fabrication is greatly simplified and testing of the reactor can be accomplished prior to installation on the thrust chamber. The torus is mounted to the regenerative chamber as shown, however, the relation to the valve and distribution manifold is somewhat complex.

Flanged versions of each of these configurations can be fabricated; however, they will be heavier and contain seal joints which do not have the inherent reliability of welded interfaces. One of the primary decisions in the tradeoff is the use of L-605 reactors versus columbium alloy reactors.

6.3.3 Reactors at The Nozzle Extension Interface

When the reactor is located at the nozzle extension interface, one advantage is the ability to test it prior to installation on the chamber. Use of a single cylindrical reactor located at the throat or nozzle extension interface is not practical. Neither is the use of multiple radial-in fed reactors, because of packaging difficulty. Axial fed reactors for the nozzle extension interface location are very similar to those located at the throat, as shown in Figure 9.

The use of an annular reactor at the nozzle extension interface is a natural arrangement, because of reactor packaging. Since this location appeared to be a primary contender for final consideration, a number of variations were considered as shown in Figures 13 through 19.

Figure 13 shows an all-welded version of the annular reactor with two different bed loadings. The primary design is the 28.1 kg/sec m² (0.04 lb/sec-in²) configuration, with the heavier iteration for 21.1 kg/sec m² (0.03 lb/sec-in²) sketched in phantom. This reactor, and all others in this category can be pretested and then joined to the thrust chamber, after minor machining, to establish the dimensions at the weld or seal joints. Figure 14 shows an iteration of this design with the reactor shifted outward from an ϵ area ratio of 10 to 13. The finalized versions of this configuration have the reactor located at ϵ an area ratio of 5. Figure 15 shows an annular reactor fabricated from L-605 which is bolted to the columbium thruster, using 2 large metal O-rings. Figure 16 shows an alternate version of the same type of system with the fully separable reactor bolted to the bimodal thruster. Note that the reactor can be tested separately from the combustor, but machining is required to establish the critical sealing surfaces following reactor "checkout". Figure 17 shows the reactor configuration which forms the top part of the bed from L-605, with the remainder from columbium alloy. This configuration would be of interest if it was found that degradation of columbium would occur in the more active upstream bed section, allowing the downstream bed section to be made from a columbium alloy.

Figure 18 shows an L-605 reactor and shell. This configuration allows the use of only 1 seal; however, the unit is not repairable if the seal leaks and there may be problems of attaching the outer shell, depending on the secondary injector materials.

Figure 19 shows a bimodal engine with the reactor located at the nozzle extension joint, at an ϵ area ratio of 10. This reactor is a radial-in flow configuration, with a segmented annulus of catalyst around the thrust chamber. The closeout cover may be placed over the inner liner in 3 pieces and welded longitudinally. The inner liner has its channels EDM'd from the outside inward, except for the entrance section, which must be EDM'd through the parent material.

This type of reactor location and configuration circumvents the need for hot gas manifolding from a reactor at the secondary injector end to the regenerative cooling passages, and allows the catalyst bed to be fabricated from L-605. This can result in lower material cost with no coating requirement. With this

configuration, however, two seals must be compressed simultaneously, therefore, all dimensions and tolerances are critical. The differential thermal expansion between the liner and reactor may induce a gap to develop during the engine cool down and subsequent start-up cycle. Loading of the 1/8-inch catalyst pellets in the downstream bed can be accomplished by standing the thrust chamber with its nozzle down then loading the pellets while vibrating the assembly. After the pellets have completed their initial settling, a compression load can be placed on the downstream bed by the annular plate which forms the side of the assembled reactor. The top bed can be loaded separately as an annulus, with a loading force applied to the catalyst by the plate which forms a side of the top bed. The flanged joint enables the use of an L-605 reactor with a columbium alloy thrust chamber; however, an all-welded version of this design could be made if the reactor were fabricated from a columbium alloy.

No split reactor configurations were considered for the nozzle extension interface location, since the one piece annular reactors are simpler and easier to install.

6.4 THERMAL ANALYSES

Heat transfer studies have been directed toward investigating the thermal efficiency of various cooling passage geometries. These studies have included the effects of passage shape and height, number of passages, coolant flow area, choice of material, combustion efficiency and ammonia dissociation on wall temperature. The results of the analyses follow:

In the analysis of the regenerative chamber cooling methods, the following parameters must be established:

1. The gas driving temperature at the wall,
2. The effect of heat transfer coefficient from the gas to the wall,
3. The thermal resistance paths within the wall itself, and
4. The effective heat transfer coefficient from the wall to the coolant.

In the following studies the gas driving temperature is assumed to be the local turbulent flow recovery temperature, which depends on the local Mach number. The hot-gas side heat transfer coefficient has been computed, considering compressibility and recombination of the associated gas species, as well as variable transport properties in the boundary layer. At BAC the properties are evaluated at the Eckert reference enthalpy temperature. The transport properties of the combustion gases used in the heat transfer film coefficient equation assume equilibrium composition mixtures comprised of species corresponding to the mixture ratio adjacent to the wall. The heat transfer coefficient obtained by this method is $3245 \text{ j/m}^2 \text{ sec K}$ ($11 \times 10^{-4} \text{ BTU/in.}^2 \text{ sec}^\circ\text{F}$). Within the wall, the thermal resistance paths are computed automatically using a computer program wherein an arbitrary cross section is divided into thermal elements and the output of the program, consisting of thermal conductances, is used directly as an input to a multidimensional, steady-state heat transfer program. On the coolant side, the heat transfer coefficient is derived, using the usual turbulent flow form of the Colburn equation wherein the transport properties of the gas species are computed assuming equilibrium decomposition mixtures. The local pressure and Mach number within the cooling passage are determined, using a recently developed computer program wherein the local flow properties (that is, Mach number and pressure of the coolant) are computed by use of influence coefficients. The friction coefficient is computed by use of a Von Karman-Nikuradse expression. The temperature-dependent thermal conductivity of the wall material is employed in the studies. The thermal conductivity for pure columbium as well as selected columbium alloys and L-605 cobalt alloy is shown in Figure 20.

The design of a gas regeneratively cooled thrust chamber necessitates satisfying two criteria simultaneously: (1) the coolant passages must be sized to provide the mass flow adequate to cool the chamber walls, (2) the gas driving pressure must be high enough to force the required mass of gas through the passages. Since the gas is compressible, the normal relationship between velocity and flowrate does not apply. To account for the changes in gas density, the local gas pressure must be included in the calculations.

During bipropellant mode operation, the minimum flow area to pass the design flow rate of 0.684 kg/sec (1.51 lb/sec) is 10 cm^2 (1.55 in.^2). Larger passages are required to flow the same mass of decomposed hydrazine through the passages in the monopropellant mode when the density is lower due to reduced pressure. Figure 20 shows the minimum flow area required as a function of the inlet manifold total pressure and coolant Mach number for decomposed N_2H_4 at 50% ammonia dissociation. Even at the maximum coolant jacket inlet pressure allowed in the bimodal engine requirements (Table 2), for monomode operation 620 kN/m^2 (90 psia), the flow area would have to be greater than 14.5 cm^2 (2.25 in.^2). But, if the cooling passages were designed for some nominal Mach number (for example, $M = 0.65$ during the bipropellant mode of operation with flow area about 11.4 cm^2 (1.77 in.^2)) the flow would choke and the inlet manifold pressure would increase until the design coolant flow rate was passed. This pressure of about 793

kN/m^2 (115 psia) should not present any problem where the design of the chamber or reactor is concerned, since the thrust chamber will still run at about 320 kN/m^2 (46.4 psia) and the majority of the pressure head loss will manifest itself as shock losses downstream of the minimum cross section and during expansion into the secondary injector inlet manifold. To design the thrust chamber to operate in both monopropellant and bipropellant modes within the pressure drop limits specified, the passage minimum area must be sized to avoid choking in the monopropellant mode. However, the pressure drop limit specified for monomode operation is not meaningful since there are no corresponding engine input constraints.

6.4.1 Throat Station

The most critical point in the thermal design of a regeneratively cooled chamber is the region of the throat where the highest heat flux will occur. A slotted passage design reduces the wall temperature by two effects: the coolant coefficient is increased with the same total flow area over that of an annular passage and the lands act as fins to increase the effective cooling area.

Figure 22 shows the influence of cooling passage design parameters on the maximum temperatures experienced in the throat regions if the passage is designed to meet the maximum coolant jacket inlet pressure for monopropellant mode operation 620 kN/m^2 (90 psia) and the engine is presumed operating at 95% combustion efficiency. About 31 passages are needed to maintain the wall temperature less than 1755 K (2700°F) assuming the lands to be 25% of the circumferential area. A lower temperature could be obtained if either the flow area was decreased or the number of passages was increased with a major influence being that of increasing the number of passages.

The influence of designing the passage size, based on monopropellant mode operation coolant Mach number of passages, is shown in Figure 23. If the minimum cross section of the passage is sized for less than a choking condition, for example, $M = 0.65$, 37 passages are needed to maintain the wall at less than 1755 K (2700°F). The influence of designing the cooling passage on the basis of coolant Mach number and inlet manifold total pressure during monopropellant mode operation is shown in Figure 24. Maximum throat temperature is shown for a chamber cooled with 50 rectangular passages, having 25% land width, assuming 95% combustion efficiency and 50% ammonia dissociation. If such a chamber were designed to operate on the basis of maximum feed pressure for monopropellant mode operation, it would be more advantageous to design it for higher pressures than it would be to design it for higher Mach numbers. For example, with a 138 kN/m^2 (20 psi) increase in the coolant jacket inlet pressure, the wall temperature decreases about 20 K (36°F). Increasing the design Mach number from 0.65 to 1 decreases the maximum throat temperature 14 K (25°F).

The influence of land width on the maximum throat temperature, see Figure 25, indicates that the major thermal effect of slotted passages occurs with land widths greater than 15 or 20%. Increasing the percent land width further will continue to reduce the maximum wall temperature at an almost constant rate thereafter.

Of additional interest is the affect of an integral cover as opposed to a free-standing cover. This configuration was analyzed, and it was found that the maximum throat temperatures are not affected by the presence of the cover. At the land extremity the temperature was reduced approximately 2 K (4°F), showing that the thermal distribution is not significantly affected by the presence of the cover.

The influence of nonhomogeneous combustion is always of prime concern. All of the studies reported herein presumed homogeneous combustion at 95% combustion efficiency. If, as a result of injector design, streaking occurs and the local mixture ratio is increased close to stoichiometric, the possibility exists

that the wall could be overheated locally and the coating could fail. Such a case was analyzed for a chamber fabricated from SCB-291, having 50 coolant passages with 25% land width, designed for a monopropellant mode maximum coolant Mach number of 0.75. The study indicates an increase of about 100 K (180°F) in maximum wall temperatures will be experienced in the throat region, which suggests that the particular design examined is somewhat forgiving since the local gas recovery temperatures are increased by almost 330 K (600°F).

Figure 26 shows the effect of the land width and thermal conductivity on the throat temperature. The effect of the land width increases as the conductivity increases, and the temperature is reduced substantially when the conductivity is increased.

The foregoing analysis was performed, assuming the hot-gas heat transfer coefficient is that obtained theoretically. JPL Interoffice Memo, Kruger to Dodge, October 12, 1972 – Subject: "Heat Transfer Analysis of the Columbiun Bimodal Engine Without Film Cooling," presents experimental heat transfer coefficient data, using copper and columbiun laminarized throat contour chambers. Figure 27 shows three curves of heat transfer coefficients in the chamber section of the bimodal engine. Curve 1 is the theoretically calculated coefficient based on the equation that $h_g = h_{gt}/(A/A^*)^{0.8}$. Curve 2 is the upper limit of data obtained experimentally, using the copper chamber. Curve 3 shows that with the columbiun chamber, laminarized throat (with triplet injector), the film coefficient is further reduced.

To show the effect of the lower heat transfer coefficient resulting from the test data, the parametric analysis has been repeated, using a heat transfer coefficient of 1770 joule/m² sec K (6×10^{-4} BTU/in.² sec °F). Figures 28 to 31 show the same parameters for the lower coefficient as is shown in Figures 22 to 25 for the higher coefficient.

If 50 channels, 25% land and Mach number of 1.0 at 550 kN/m² (80 psia) are selected for comparison, the wall temperature for the theoretical (higher) coefficient is 1700 K (2605°F) (see Figure 23). With the experimental (lower) coefficient, the maximum throat wall temperature is 1540 K (2315°F) (see Figure 28), thus the wall temperature is reduced by 160 K (288°F). Similar reductions in maximum wall temperatures occur for other conditions. This reduction might allow one to design the chamber using C-103 columbiun.

Since the test data indicate a lower film coefficient on the combustion gas side, an annular passage design for the throat may be feasible. Figure 32 shows the variation of the maximum wall temperature as a function of annular flow area at the throat station for different values of h_g . It can be seen that the wall temperature is reduced by some 194 K (350°F) when the film coefficient is reduced from the theoretical value to the test value (Curve 2, Figure 27). If streaking occurs, the combustion gas temperature will be 3034 K (5002°F) and the resultant wall temperature will be 1770 K (2725°F). It is apparent that an annular design at the throat may be feasible.

6.4.2 Radiation Cooled Nozzle Temperatures

Figure 33 shows the temperature distribution as a function of expansion area ratio for the theoretical heat flux (3280 joule/m² sec K (11.1 BTU/in.² sec °F) at the throat) and for the test value (1770 joule/m² sec K (6.0 BTU/in.² sec °F) at the throat). The theoretical cutoff area ratio for a 1755 K (2700°F) equilibrium wall temperature is 4.2, and the cutoff point based on a lower heat flux at the throat is 2.5. For a temperature of 1589 K, (2400°F) the area ratios are 7.8 and 4.0, respectively.

6.4.3 Chamber Passage Design

Since the film heat transfer coefficient in the chamber section is lower than at the throat, it is probable that an annular passage is sufficient to keep the maximum wall temperature below 1755 K (2700°F). Figure 34 shows the comparison of the chamber wall temperature for both the theoretical and test heating rates assuming an annular passage. The maximum wall temperature using the test value of 1088 joule/m² sec K (3.7×10^{-4} BTU/in.² sec °F) is higher than the theoretical value and results in about 83 K (150°F) higher predicted wall temperature. If streaking occurs, the combustion driving gas temperatures increase from 2706 K (4411°F) to 3034 K (5002°F) and the resultant wall temperature increases by 100 K (180°F).

Figure 35 shows the maximum wall temperature as a function of flow area and land width for a drilled chamber design. The 40% land case result is almost identical to the annular design as shown in Figure 34. The heating film coefficient used in the analysis is the chamber theoretical value of 817 joule/m² sec K (2.77×10^{-4} BTU/in.² sec °F). The 25% land case shows about an 8 K (15°F) reduction in wall temperature compared to the annular design.

6.4.4 Typical Channel Design at Throat Station

Note: For ease of reading the following paragraphs have been prepared separately in S.I. and English units.

To compare the effects of various heat transfer coefficients at the throat station, a 50-passage design was selected, 25% land, 690 kN/m², $M = 1$ and wall thickness of 0.18 cm. For the theoretical heating coefficient of $h_g = 3245$ joule/m² sec K, 50% dissociation and 95% c^* , $T_g = 2706$ K, the predicted wall temperature is 1678 K. With the same conditions but with a lower coefficient, $h_g = 1770$ joule/m² sec K, the wall temperature is 1522 K, a reduction of 156 K. Again with a coefficient of 1180 joule/m² sec K (see Curve 3, Figure 27), the temperature is 1456 K, a further reduction of 66K. To determine the effect of ammonia dissociation, one case with 70% dissociation was analyzed and shows about 128 K reduction in maximum wall temperature. Figure 36 shows graphically the effect of heat transfer coefficient and percentage dissociation.

To compare the effects of various heat transfer coefficients at the throat station, a 50-passage design was selected, 25% land 100 psia, $M = 1$ and wall thickness of 0.07 in. For the theoretical heating coefficient of $h_g = 11 \times 10^{-4}$ BTU/in.² sec °F), 50% dissociation and 95% c^* , $T_g = 4411^\circ\text{F}$, the predicted wall temperature is 2560°F. With the same conditions but with a lower coefficient, $h_g = 6 \times 10^{-4}$ BTU/in.² sec °F, the wall temperature is 2280°F, a reduction of 280°F. Again with a coefficient of 4×10^{-4} BTU/in.² sec °F (see Curve 3, Figure 27), the temperature is 2160°F, a further reduction of 120°F. To determine the effect of ammonia dissociation, one case with 70% dissociation was analyzed and shows about 230°F reduction in maximum wall temperature. Figure 36 shows graphically the effect of heat transfer coefficient and percentage dissociation.

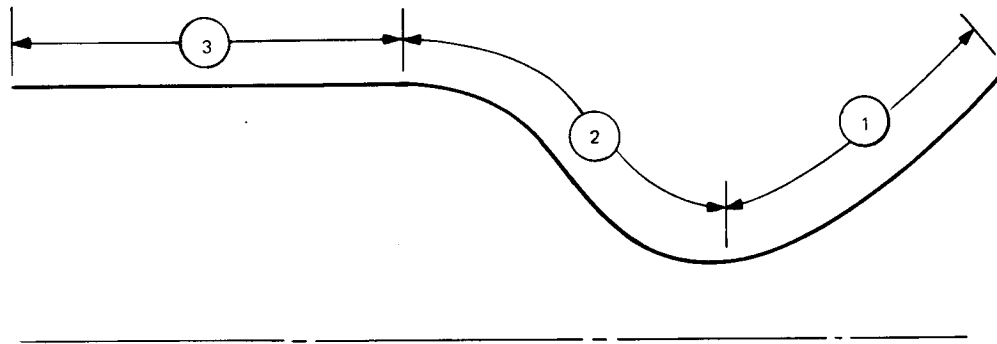
A summary of representative throat wall temperatures at the three heating coefficients, two pressure levels in the throat under monomode operations and channel versus annular type throat configurations is given in Table 3.

6.5 STRUCTURAL ANALYSIS

In the structural analysis of the bimodal engine assembly the primary loading consideration was that of operating pressures at maximum temperature conditions. Because of the many designs proposed only preliminary analyses were conducted on the various injector and generator-to-injector interfaces. So, particular attention was directed towards those components of the engine which needed intensive design investigations. These components included the regeneratively cooled chamber, film-cooled chamber and the six-cylindrical reactor design located at the secondary injector.

For the regenerative chamber, the hot inner liner was investigated for buckling due to external pressure loading. The material selected for the free standing liner was a columbium alloy designated SCb-291, which retains good strength properties at elevated temperatures. In the buckling analysis, it was assumed that the longitudinal lands did not contribute to the buckling stiffness of the structure, which is somewhat conservative, since the presence of these lands precludes any longitudinal buckling waves in the throat region. It was also assumed that a full pressure differential existed across the liner wall (no internal pressure) for the critical loading condition.

Due to the geometry of the liner, the structure was divided into three areas for analysis purposes:



where

- ① - Divergent Nozzle
- ② - Convergent Nozzle
- ③ - Chamber

A 1.5 safety factor was applied to the fuel coolant jacket pressure of 150 psia to arrive at a design pressure of 225 psia. The equation for determining the critical buckling pressure for each section is as follows:

$$P_{CR} = \frac{0.74 E}{\left(\frac{l}{\rho}\right) \left(\frac{\rho}{t}\right)^{5/2}}$$

where

- E - Elastic Modulus, kN/m² (psi)
- l - Total developed length for each section, m (in.)
- ρ - Average radius of section taken perpendicular to the shell, m (in.)
- t - Liner wall thickness, m (in.)

Ref. Weingarten, Morgan, and Seide, "Final Report on Development of Design Criteria for Elastic Stability of Thin Shell Structures," STL, AFBMD-TR-61-7, 31 Sept. 1960.

Two stability conditions were investigated; one was that of elastic buckling using the "short-time" modulus of elasticity, and the other was creep buckling for a 1000-sec maximum firing duration. Because of the axial temperature gradient which is developed in the liner during operation, it was decided to conduct a parametric buckling analysis, for wall temperatures of 1755 K (2700°F), 1700 K (2600°F), 1644 K (2500°F), and 1589 K (2400°F). The critical buckling pressure of the convergent nozzle is generally much higher than that of the chamber because of the associated double curvature, therefore, particular attention was focused on the divergent and chamber sections only.

For the elastic buckling portion of the analysis the sections were first sized for compression yield to ensure that the resultant stress distribution would remain elastic and thus would not require the use of tangent modulus theory. Figure 37 shows the effect of temperature on the tensile strength for SCb-291 material. It was assumed that the compressive yield was equal to the tensile yield for the investigation. A factor of safety of 1.5 was applied to the strength allowable to ensure that the resultant stress would be in the elastic region of the stress-strain diagram.

For the divergent nozzle the thickness was determined by

$$\text{Req. } t = \frac{pR}{\cos a (F_{cy}/1.5)}$$

where $R \sim$ maximum radius of divergent section, m (in.)

$a \sim$ wall slope at maximum radius location,

$p \sim$ coolant jacket pressure 1034 kN/m² (150 psia)

The maximum radius is 0.0762 m (3.0 in.) downstream of the throat and is:

$$R = 0.0685 \text{ m (2.70 in.)}, a = 32.5^\circ$$

Therefore the following thicknesses were determined for the four temperatures considered.

Temp	$F_{cy}/1.5$	Req t	Temp	$F_{cy}/1.5$	Req t
1755 K	41,380 kN/m ²	0.216 cm	2700°F	6,000 psi	0.085 in.
1700 K	50,621 kN/m ²	0.152 cm	2600°F	7,340 psi	0.060 in.
1644 K	59,793 kN/m ²	0.127 cm	2500°F	8,670 psi	0.050 in.
1589 K	68,966 kN/m ²	0.114 cm	2400°F	10,000 psi	0.045 in.

For the chamber section the thickness equation was

$$\text{Req } t = \frac{p R_c}{F_{cy}/1.5}$$

$R_c \sim$ chamber radius = 0.0737 m (2.90 in.)

$p \sim$ coolant jacket pressure = 1034 kN/m² (150 psia)

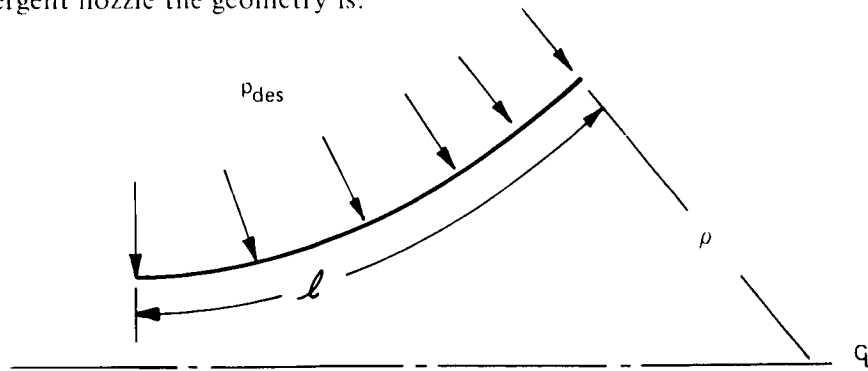
Therefore the calculated thicknesses were:

Temp	$F_{cy}/1.5$	Req t	Temp	$F_{cy}/1.5$	Req t
1755 K	41,380 kN/m ²	0.216 cm	2700°F	6,000 psi	0.075 in.
1700 K	50,621 kN/m ²	0.152 cm	2600°F	7,340 psi	0.060 in.
1644 K	59,793 kN/m ²	0.140 cm	2500°F	8,670 psi	0.055 in.
1589 K	68,966 kN/m ²	0.114 cm	2400°F	10,000 psi	0.045 in.

The modulus of elasticity of SCb-291 versus temperature is shown in Figure 38. This figure was generated through a test program which was conducted at Bell Aerospace. The moduli corresponding to the temperature range of the analysis were read from this figure and incorporated into the stability equation. It was decided to solve this equation for the required thicknesses for a design pressure of 225 psia and then compare the results with those determined previously for the elastic stress criteria. Thus, the buckling equation becomes:

$$\text{Req } t = \left[\frac{\left(\frac{1}{\rho}\right) p_{des}}{0.74 E} \right]^{2/5} \rho$$

For the divergent nozzle the geometry is:



$$\rho = \frac{0.0685}{\cos 32.5^\circ} = 0.0813 \text{ m (3.2 in.)}$$

$$l = 0.087 \text{ m (3.425 in.)} \quad \frac{l}{\rho} = 1.070$$

The divergent nozzle thicknesses are:

Temp	Modulus	Req t	Temp	Modulus	Req t
1755 K	$60.7 \times 10^6 \text{ kN/m}^2$	0.140 cm	2700°F	$8.8 \times 10^6 \text{ psi}$	0.055 in.
1700 K	$67.6 \times 10^6 \text{ kN/m}^2$	0.140 cm	2600°F	$9.8 \times 10^6 \text{ psi}$	0.055 in.
1644 K	$75.2 \times 10^6 \text{ kN/m}^2$	0.127 cm	2500°F	$10.9 \times 10^6 \text{ psi}$	0.050 in.
1589 K	$81.4 \times 10^6 \text{ kN/m}^2$	0.127 cm	2400°F	$11.8 \times 10^6 \text{ psi}$	0.050 in.

For the chamber section the geometry is:

$$\rho = 0.0736 \text{ m (2.90 in.)} \quad l = 0.0965 \text{ m (3.80 in.)} \quad \frac{l}{\rho} = 1.310$$

Since the above parameters are similar to the divergent section, the corresponding critical chamber buckling thicknesses are approximately the same as for the divergent nozzle.

The second phase of the analysis dealt with the determination of critical buckling of the liner due to creep effects. A maximum firing duration of 1000 sec was used as the time criteria for establishing the creep characteristics of the structure. Figures 39 and 40 reflect the general creep stress-strain-time relationships for those temperatures listed. The 0.05% creep strain curves shown in Figure 40 were determined from tests which were conducted at Bell Aerospace for temperatures of 1811 K (2800°F), 1977 K (3100°F) and 2144 K (3400°F). The creep curves shown in Figure 40 were generated from unpublished data quoted from the Fansteel Corp. This company is now conducting an in-house test program to substantiate and provide additional creep data for the SCb-291 material.

The method of analysis used to determine the critical creep buckling of the liner was to construct an equivalent creep stress-strain diagram which incorporates the effects of the 1000-second time element. From this diagram an equivalent modulus can be determined which then would be substituted back into the previously defined equation for p_{CR} . A description of the details of this method follows.

Since the temperatures shown in Figures 39 and 40 do not coincide with the investigated temperatures it was necessary to construct creep stress versus temperature curves keeping the strain and time constant. So, Figure 41 was constructed for the various creep strain levels for a constant applied time of 1000 seconds; as a result, the creep stress and strain could be read directly for any considered temperature level. The creep characteristic or equivalent stress-strain diagram can now be constructed from Figure 41 and plotted as shown in Figures 42 and 43. It can be concluded from these plots that there is an elastic region which will be used to define the critical buckling allowable for the structure. Besides obtaining the creep elastic modulus from the curve, the stress at the proportional limit will be used to define a thickness which will ensure that the applied stress distribution remains elastic. The following table lists the elastic moduli and limit stress for the temperatures in question.

Temp	Modulus	Limit Stress	Temp	Modulus	Limit Stress
1755 K	$27.58 \times 10^6 \text{ kN/m}^2$	$20.7 \times 10^3 \text{ kN/m}^2$	2700°F	$4.0 \times 10^6 \text{ psi}$	3000 psi
1700 K	$30.34 \times 10^6 \text{ kN/m}^2$	$27.24 \times 10^3 \text{ kN/m}^2$	2600°F	$4.4 \times 10^6 \text{ psi}$	3950 psi
1644 K	$38.62 \times 10^6 \text{ kN/m}^2$	$34.5 \times 10^3 \text{ kN/m}^2$	2500°F	$5.6 \times 10^6 \text{ psi}$	5000 psi
1589 K	$48.28 \times 10^6 \text{ kN/m}^2$	$43.4 \times 10^3 \text{ kN/m}^2$	2400°F	$7.0 \times 10^6 \text{ psi}$	6300 psi

The corresponding required thicknesses for the chamber and divergent nozzle can now be determined using the above tabulated values. Using the previously described thickness equations for the sections, the requirements are:

DIVERGENT NOZZLE THICKNESS REQUIREMENTS:

Temp. K	Elastic Creep Stress, cm	Elastic Creep Buckling, cm	Temp. °F	Elastic Creep Stress, in.	Elastic Creep Buckling, in.
1755	0.406	0.190	2700	0.160	0.075
1700	0.317	0.190	2600	0.125	0.075
1644	0.254	0.178	2500	0.100	0.070
1589	0.203	0.152	2400	0.080	0.060

CHAMBER THICKNESS REQUIREMENTS:

Temp. K	Elastic Creep Stress, cm	Elastic Creep Buckling, cm	Temp. °F	Elastic Creep Stress, in.	Elastic Creep Buckling, in.
1755	0.368	0.190	2700	0.145	0.075
1700	0.279	0.178	2600	0.110	0.070
1644	0.229	0.165	2500	0.090	0.065
1589	0.178	0.152	2400	0.070	0.060

Projected by the thermal analysis of the liner the design temperatures for the sections investigated are:

Divergent T = 1589 K (2400°F)
 Chamber T = 1644 K (2500°F)

Using the above temperatures the corresponding thickness requirements are:

Divergent t = 0.203 cm (0.080 in.)
 Chamber t = 0.229 cm (0.090 in.)

One more condition which was analyzed was the radial thermal growth of the liner relative to the middle shell. If the two shells were in intimate contact at ambient temperature then a circumferential compressive stress would be developed in the liner because of the differential growths. This additional load would be sufficient to develop a plastic stress in the liner and thus reduce the effective buckling modulus of elasticity. Therefore, it is necessary to start with a design gap at ambient conditions and allow the hot liner to

freely expand such that at steady-state temperatures the liner and middle shell would be in contact with each other without developing any load at their interface. So, assuming the worst thermal case of a 1755 K (2700°F) liner and 1255 K (1800°F) middle shell and using mean radii of 0.051 m (2.0 in.) and 0.058m (2.3 in.) for the liner and shell, the necessary gap must be:

$$\begin{aligned}\Delta R &= [\alpha (T - 294.3 \text{ K}) R]_{\text{Liner (SCb-291)}} - \\ &\quad [\alpha (T - 294.3 \text{ K}) R]_{\text{Middle Shell (C-103)}} \\ &= [8.91 \times 10^{-6} (1755 - 294.3) (0.051)] - \\ &\quad [7.74 \times 10^{-6} (1255 - 294.3) (0.058)] \\ &= 0.233 \times 10^{-3} \text{ m}\end{aligned}$$

The above is repeated in English units:

$$\begin{aligned}\Delta R &= [\alpha (T - 70) R]_{\text{Liner (SCb-291)}} - [\alpha (T - 70) R]_{\text{Middle Shell (C-103)}} \\ &= (4.95 \times 10^{-6}) (2700 - 70) (2.0) - (4.3 \times 10^{-6}) (1800 - 70) (2.3) \\ &= [4.95 \times 10^{-6}] [1755 - 294.3] [0.051] \\ &= 9.0 \times 10^{-3} \text{ in.}\end{aligned}$$

There is also a longitudinal differential thermal growth condition existing between the liner and outer closure shell, but this loading is not critical because of the mechanical expansion joint which is designed into the outer shell of the chamber.

6.6 MASS ANALYSES

Component mass analyses were made to present a relative comparison of a basic thrust chamber assembly with a variety of reactor designs located at the secondary injector, throat station and nozzle extension station. A summary of various configurations with the reactor located at either the secondary injector or throat station is given in Table 4. The inputs used for the mass analyses are shown in Table 5.

Preliminary analysis of early configurations indicated that a flexure type gimbaling system be included in the analyses to present a fair mass tradeoff study. The gimbal ring design in all cases includes the mounting pads for vehicle interface. The mass property effect of the gimbal ring positions for typical designs is presented in Tables 6, 7 and 8, and summarized as follows:

1. With the reactor located at the secondary injector, the gimbal ring will be positioned at the center of gravity of the engine assembly.
2. A choice of two gimbal locations is available when the reactor is located at the throat. The gimbal ring may be located at the secondary injector, which reduces mass but increases the actuator load; or near the throat, increasing mass but reducing the actuator loads.

Tables 6, 7 and 8 represent a detailed mass breakdown and center-of-gravity location of three different configurations using the same basic thrust chamber assembly and itemizing delta mass changes. These tables have been provided to be informative as well as to describe the extent of this analysis.

The mass analysis of each design was treated fairly with respect to changes peculiar to each design. Thermal type standoff mounts for the oxidizer and fuel valves are used for all secondary injector mounted reactors. With the reactor throat mounted and gimballed at the head end, thermal type standoff mounts for each valve are used at the head end and reactor. If the reactor is throat-mounted and gimballed near the throat, the valves are attached to the engine mount. Associated tubing is included with each design. A detailed analysis of the valve mounting and location is not mandatory at this time, but a mass estimate is necessary to complete the tradeoff study.

A complete engine assembly mass analysis has been made and represents a relative comparison of configurations using columbium material.

Table 9 shows engine mass as a function of various combinations of reactor assemblies with a head-mounted gimbal ring. The delta mass to change the gimbal position from the head-mounted configuration to a center-of-gravity-mounted configuration is estimated at +2.3 kg (+5.1 lb). All reactor beds considered are annular types. Table 10 summarizes the combinations included in Table 9.

Table 11 compares the mass of thrust chambers cooled with gases flowing through channels, drilled holes or an annular passage. The chamber assembly mass includes the downstream manifold and a constant mass injector, with the chamber ending at an area ratio of 11 in each case. Coolant passages for the channel configurations end at an area ratio of 8.9. For the drilled configurations, coolant passages end at an area ratio of 6.2, but the inside liner mass continues to area ratio of 11, the same as the channel configuration. A delta mass is shown to extend the drilled passages to an area ratio of 8.9 for a comparison with the channel design at the same area ratio. To define a minimum mass design, a configuration with the briefest length of cooling passages was considered, for both channeled and drilled designs. These configurations are called "mini-channel or mini-drilled passages." These configurations have a 0.0813 m (3.2 inch) long, controlled passage, throat section with an annulus upstream and downstream. The annular chamber portion is essentially an inner and outer liner separated by six webs or spaces.

Tables 12 and 13 are parametric studies showing the mass tradeoff for the chamber and nozzle extension as a function of coolant gas manifold position. These positions relate to maximum allowable radiation-cooled wall temperatures for three primary materials, SCb-291, C103 and L-605. Analysis showed that a radiation-cooled bimodal thruster with N_2O_4/N_2H_4 at $O/F = 1.5$ and $P_c = 900 \text{ kN/m}^2$ (130 psia), should cause the nozzle equilibrium wall temperatures, based on radiation cooling, to be 1755 K (2700°F), 1589 K (2400°F) and 1367 K (2000°F) at expansion area ratios of 4.2, 7.8 and 18.0, respectively.

Table 12 is a mass study with the reactor head-mounted and Table 13 shows the reactor throat-mounted. Other than the parametric tradeoffs within each table, the major difference between the throat-mounted reactor and the head-mounted reactor is that the head-mounted reactor position requires an outside coolant jacket around the chamber. The thickness of the outer liner (middle wall) can be 0.00102 m (0.040 in.) due to low pressure drop across the wall. The throat-mounted reactor eliminates the outer coolant jacket, but the outer liner must be 0.00178 m (0.070 in.). A mass estimate is provided for the head-mounted reactor configurations to show the effect of replacing the outer coolant jacket with six transfer tubes (welded). Manifolds starting at area ratio locations of $\epsilon = 4.2, 7.8$ and 18 show mass decreases of 0.32 kg (0.70 lb), 0.45 kg (1.0 lb) and 1.63 kg (3.6 lb).

A mass comparison of the "preferred" regenerative chamber configurations is listed in Table 14. These mass values include total engine mass (for mini channels) with gimbal provisions and valves, but no flexible tubing. All mass values are for welded configurations with various nozzle extension materials (SCb-291, C-103, and L-605). The effect of a bolted interface is identified separately.

It should be noted that the mass listed is representative for each configuration but not necessarily the minimum mass. In this tradeoff study common design rationale was applied to provide a trend in mass comparison. Final design of the selected configurations will incorporate more concern for detailed mass reduction.

The comparisons of these configurations are made for two heating coefficient assumptions at the throat :

- A. $hg = 3280 \text{ joule/m}^2 \text{ sec K}$ ($hg = 11 \times 10^{-4} \text{ BTU/in}^2 \text{ sec } ^\circ\text{F}$) with 95% c^* and
- B. $hg = 1770 \text{ joule/m}^2 \text{ sec K}$ ($hg = 6.0 \times 10^{-4} \text{ BTU/in}^2 \text{ sec } ^\circ\text{F}$) with 100% c^*

The lower heating coefficient is considered more representative of the actual hardware and is probably conservative since experimental data reveals heating coefficients as low as $1180 \text{ joule/m}^2 \text{ sec K}$ ($4.0 \times 10^{-4} \text{ BTU/in}^2 \text{ sec } ^\circ\text{F}$). Note that using the lower heating coefficient, $hg = 1770$ (6.0×10^{-4}) the C-103 Columbian alloy can be used at an area ratio of 5.0 with the temperature limit of 1589 K (2400°F). This area ratio selection is somewhat conservative, depending upon the configuration. The rationale follows:

Variations in interface area ratio also occur for an annular regenerative passage versus channeled regenerative passages, even a mini channel version. A practical length must exist between the manifold and the throat for an annular passage configuration and between the entrance to the rectangular passages and the throat for the channel configuration, to allow laminar type flow control to be established. An annular version is, therefore, more compatible with a low area ratio than a channel version. The channel configuration (mini channel) is preferred over the annular version however, since the throat temperature, convergent nozzle and divergent nozzle temperatures are lower. Stiffness is also provided in the divergent nozzle by use of the mini channel lands that reduce concern of buckling loads.

The nozzle extension is also subjected to buckling loads but is mainly due to gimbal acceleration loads and accumulated thrust loads. Although the internal pressure stresses are low in the nozzle extension

the above buckling conditions result in a practical temperature limitation of approximately 1589K (2400°F) for the C-103 nozzle extension.

Conservatism is inherent with the analyses to date since three dimensional effects have not been entirely considered. This is obvious in Figure 44 which shows the results of a two-dimensional analysis of the temperature distribution along the engine axis. Two analyses were completed, one for a heating coefficient of 1770 joule/m² sec K (6×10^{-4} BTU/in² sec °F) and the other for 1180 joule/m² sec K (4×10^{-4} BTU/in² sec °F). The temperature extremes that are shown from the analysis in the convergent nozzle and nozzle/extension interface are probably too high. The dotted lines are more representative of what can be expected. The convergent nozzle temperature peak is lowered due to three dimensional conduction effects and lower heating rates since streaking (100 c*) does not exist around the entire circumference of the chamber. The radiation extension temperature peak is lowered for the same reason plus the effect of cooling the nozzle extension interface by the decomposed N₂H₄ gases in the manifold, which is not included in the present thermal model.

6.7 REGENERATIVE CHAMBER CONFIGURATION RATING AND SELECTION

The Evaluation Ratings for the regenerative chamber configurations are listed in Table 15. This table consists of the ratings for the following three elements of the engine; reactors, regenerative chambers, and nozzle extensions. The secondary injector or valve rating does not apply at this time. Note that some of the reactor configurations have been eliminated prior to rating due to obvious bulkiness. The "Performance" parameter column includes an adjustment heading to allow more emphasis on the bipropellant performance versus monopropellant performance. The absence of any adjustment number infers equal importance of sub-parameters.

Personal judgment has a definite influence on the assignment of the rating number (between 1 to 10). However, due to the detailed selection of configurations and the wide range of major parameters we feel the resultant trends are fair and honest. The preferences of the various elements are circled in each Summary column. The last four items in the Regenerative Chamber (Table 3) rating sheet, i.e., Number of Passages, % Land Width, Mono Mach No., and Mono Total Pressure are included to indicate the effect of reasonable variations of each. The final selection for each are dependent upon the particular regenerative configuration.

To provide a quick comparison of the various regeneratively-cooled chamber design parameters and their effects on the throat temperature, a representative baseline design has been selected. This design is summarized in Table 16.

6.7.1 Rationale and Results

Certain design rationale have been applied to the regenerative chamber tradeoff. These rationale and a brief summary of the tradeoff results follow:

General

- (1) Prefer L-605 Reactor due to experience
- (2) Prefer Columbium Alloy (SCB-291 or C-103) for the regenerative chamber due to operating temperature. Therefore: Hot-gas joint(s) required - have minimum number of seals and smallest diameter seals.
- (3) Prefer capability of fire testing Reactor prior to installation on chamber - requires hot-gas joint or "cutoff and reweld" design.
- (4) Prefer C-103 - Nozzle Extension due to fabrication experience (spinning) and minimum regenerative chamber/nozzle extension area ratio ($\epsilon = 5.0$).
- (5) Either Coaxial or Triplet Secondary Injector acceptable. Performance and injector weights approximately the same. Coaxial design more compatible with additional element in center.
- (6) Valve tradeoff not addressed at this time since flight type oxidizer valve not available (off shelf). Fuel valve type demonstrated, flight type valve not available.

Tradeoff Results

I. Reactor Selection

- (a) Reactor at Secondary Injector
 - 1. Multiple Cylinders - with tubes
 - 2. Annular - with Annular Passage
- (b) Reactor at Throat
 - 1. Annular - 2 piece
- (c) Reactor at Nozzle/Ext.
 - 1. Annular - 1 piece

Reactor Material

L-605 preferred due to experience, but hot gas joint required.

Columbium Alloy requires demonstration of capability to withstand environment of decomposed $N_2 H_4$.

Reactor Fabrication

Machine from billet or roll cylinder and weld.

II. Regenerative Chamber Selection

- (a) Throat Passages
 - 1. Mini Channel
 - 2. Annulus
- (b) Chamber Passage
 - 1. Annulus

Chamber Material

Columbium Alloy SCB-291 or C-103 required dependent on final selection of concept.

	P = 690 kN/m ² (100 psia)		P = 550 kN/m ² (80 psia)	
	<u>c*=100%</u>	<u>c*=95%</u>	<u>c*=100%</u>	<u>c*=95%</u>
Throat (Channel)	C-103	C-103	291	C-103
Throat (Annulus)	291	291	-	291
Chamber (Channel)	C-103	C-103	C-103	C-103
Chamber (Annulus)	291	C-103	291	C-103

Chamber Fabrication

- (1) Mini Channel - Machine from billet - EDM or mill channels.
- (2) Annulus Inner Wall
 - (a) Hot spin
 - (b) 3 piece nozzle and chamber - weld
 - (c) 3 piece nozzle and weld; spin or roll and weld chamber.

(3) Cover "Close Outs"

- (a) 3 piece cover and weld
- (b) 3 piece cover and Hot Isostatic Press (HIP) (concern of throat shape and tooling).
- (c) Vapor deposit outer jacket (unalloyed material demonstrated only).

III. Nozzle Extension

- (1) C-103 Material, joint at $\epsilon = 5.0$, fabricate by cold spinning.
- (2) SCB-291 Material, joint at $\epsilon = 3.0$, fabricate by hot spinning or shape and weld.
(Impractical to have joint at low area ratio if channels are used or reactor located on a nozzle station.)
- (3) L-605 - Joint at $\epsilon = 11.5$, heavier than columbium extension.

IV. Injector

Fabricate front face from columbium and back cover from L-605, or fabricate both from columbium. Machine from billet.

6.8 Regenerative Chamber Layout Design

Two "preferred" regenerative concepts were initially studied during this task with final layout design completed during Task 2. The two "preferred" designs were: (1) Six individual cylindrical reactors at the secondary injector; (2) Annular reactor at the nozzle/extension interface.

7. TECHNICAL DISCUSSION - TASK 2 (BIMODAL ENGINE CONFIGURATION STUDY)

7.1 DESIGN LAYOUT OF COAXIAL INJECTORS

7.1.1 Selection Criteria and Combinations

The bipropellant injector selected for use with the bimodal thruster required consideration of the following factors:

- (1) Delivered performance
- (2) Heat flux uniformity
- (3) Ability to cool the injector face
- (4) Fabricability

Testing of the three types of injectors at JPL (doublet, triplet and coaxial) demonstrated high performance capability of the triplet and the coaxial, with the doublet being a lower performance injector. The heat flux at the throat is similar for the triplet and the coaxial injector. Figures 45 and 46 show cross sections of typical, all welded triplet injector configurations. Figure 47 reveals a coaxial type injector. It is apparent the coaxial injector allows better thermal isolation of the oxidizer circuit from the high temperature fuel circuit. Oxidizer flow variations may also exist between the outer and inner rows of oxidizer orifices on the triplet injector due to heating and probable vaporizing of the outer oxidizer circuit. Thermal insulation methods, such as sleeves, can be provided, but complicates the design. Agreement was made during the Design Review, therefore, that subsequent engine designs incorporate the coaxial injector.

Three basic material arrangements exist for the secondary injector:

- (1) All-columbium injector -- front face and back cover
- (2) Columbium front face -- L-605 back cover
- (3) All-L-605 injector -- front face and back cover

For the flight type injector a method of cooling the center face of the injector is preferred over use of an insulation piece. Three major types of cooling are practical:

- (1) Center combustion element
- (2) Oxidizer regenerative cooling
- (3) Fuel regenerative cooling

By combining these methods of cooling with the material arrangements all reasonable injector configurations can be considered. A design study of these combinations resulted in the following conclusions:

- (1) All-Columbium Injector
 - (a) Due to the need of a columbium chamber and inner liner (for film cooling) an all-columbium injector allows an all-welded assembly between the chamber and injector. A reasonable interface is possible also with an L-605 reactor.
 - (b) All three methods of injector face cooling are compatible with the all-columbium injector.

- (c) An integral (one piece) injector design is possible. (See Figure 47). Admittedly, more machining from a single billet is necessary, but weldments are reduced to a minimum with a sound structural design.
- (d) All-columbium oxidizer injector orifices are necessary with all columbium feed tubes for an all-welded design.

(2) Columbium Front Face – L-605 Back Cover

- (a) This injector design is most compatible with a chamber design using an L-605 middle and/or outer cover and a columbium inner wall.
- (b) Interface with the L-605 reactor located at the secondary injector can be made by welding, but a mechanical joint is required at the interface in the columbium divergent nozzle section. If the reactor is located at the nozzle/extension interface, welding can be accomplished on one side of the reactor with a mechanical joint on the outer side of the reactor.
- (c) Allowance must be made for the difference in thermal expansion between L-605 and columbium (approximately 2:1, L-605:columbium). To allow support of the columbium injector front face and also allow for difference of thermal expansion, one method is to provide a central post support in the L-605 back cover as shown in Figure 48. This design also provides for fuel regenerative cooling of the injector center with a fuel bleed into the chamber. This design compensates for both axial and radial growth differences between the two materials with majority of the bleed flow exiting into the chamber through 4 or 6 orifices. A center bleed orifice is also provided to prevent stagnation of gases due to leakage flow past the central post support. Approximately 6% of the fuel is required to maintain the injector at temperatures below 1589K (2400°F).

Since it is preferred to maintain the same injector pattern as presently tested at JPL, this method of face cooling would probably have minimum effect on the demonstrated performance.

Another design with an L-605 back cover and columbium injector face is shown in Figure 49. This design incorporates a central combustion element that would provide cooling of the injector center. The central (13th) element could be designed for less than the nominal flow rate for the other 12 elements to reduce the effect on the demonstrated performance. The element could also operate at an "off-mixture" ratio (fuel-rich) to allow sufficient fuel flow for cooling and have minimal effect on the established combustion pattern.

Oxidizer regenerative cooling is not as practical with these unlike materials used for the injector since the oxidizer circuit has to be separated from the hot-fuel circuit. This requires a mechanical seal and complicates the design.

(3) All L-605 Injector

The all L-605 injector design is not practical with the flight type columbium liner and chamber due to complex mechanical joints. Temperature limitation of the L-605 also requires additional fuel cooling of the center region of the injector.

7.1.2 Coaxial Injector Design Criteria

The following general criteria was used for the secondary injector designs:

- (1) Prefer use of present oxidizer orifice stem design.

- (2) Prefer retaining coaxial fuel orifice pattern if possible, including orifice diameter, orifice length, orifice entrance conditions, orifice angle and orifice circle diameter.
- (3) All metal seals shall be replaceable by disassembly at flanges; machining to allow seal replacement not desirable.
- (4) In most configurations using an L-605 reactor and L-605 injector back cover with a columbium injector face one of the following design options must be used:
 - (a) Replaceable (threaded) oxidizer orifice stems.
 - (b) Slotted or tapered inlets on fuel orifices to allow axial removal of oxidizer orifice stems.

The reason for requiring one of the above is to allow replacement capability of the metal O-ring or seal between the L-605 injector flange and columbium injector face flange. Certain designs provide for capability of initial installation of metal seal prior to welding of assembly, but should the seal leak or the flange joint be disassembled, the metal seal cannot be replaced.

7.1.2.1 Oxidizer Orifice Stem Installation

- (1) All Columbium Injector
 - (a) Threaded L-605 Oxidizer Orifice Stems
 - Requires hot gas seal, or liquid propellant seal, or both
 - Concern of "fine" threads in columbium, use "coarse" threads or helicoils
 - (b) Welded Columbium Oxidizer Orifice Stems
 - Requires columbium oxidizer orifice stems
- (2) Columbium Injector Face/L-605 Back Cover
 - (a) Welded L-605 Oxidizer Orifice Stems
 - (b) Threaded L-605 Oxidizer Orifice Stems
 - Requires hot gas seal, or liquid propellant seal, or both
 - "Fine" threads satisfactory
- (3) All-L-605 Injector - Same as (2) above

7.1.2.2 Fuel Orifice Variations

- (1) To utilize the present coaxial injector design as tested, fuel orifice overlap occurs at the exit. Minimum web thickness exists between orifices resulting in minimum structural support for the center of the injector. Sharp edges also result at the intersection of each fuel orifice on the exit side creating a high stress condition. To overcome the sharp edge at the overlap a

radius can be applied during fabrication. To radius this curved surface requires additional machining or hand finishing which is not desirable.

Two modifications may be made to the basic injector design to overcome this concern;

- (a) to decrease the fuel orifice diameter and therefore the area while maintaining the same circle diameter, (resulting in a velocity change).
 - (b) increase the fuel orifice circle diameter while maintaining the same orifice diameter. Of the two choices, the latter is preferred since it would be much less sensitive to performance change. Either change also provides a uniform cylindrical shape to each fuel orifice at the exit end as originally designed in the triplet injector configuration.
- (2) Due to the angle of the fuel orifices, it is not possible to install or remove the oxidizer orifice stems once installed in the back cover as a complete assembly. The major design configurations that permit disassembly consist of:
- (a) each oxidizer orifice stem must be installed individually and removed individually. This means each oxidizer orifice stem must be threaded and sealed with a metal seal, which is not preferred for a flight type engine.
 - (b) each fuel orifice must be modified to allow axial removal of the oxidizer orifice assembly. The three modifications are shown in Figure 50 and consists of:

Configuration A – Locally slot the entrance of each fuel orifice

Configuration B – Taper the entrance of each fuel orifice with an elliptical shaped cone

Configuration C – Taper the entrance of each fuel orifice with a circular cone

The effects of each configuration are described in the figure. Of the three configurations, the elliptical cone shaped entrance is preferred since it appears to be the best compromise by allowing maximum web thickness with less fuel flow maldistribution than the slotted configuration. Admittedly, the circular cone shaped entrance provides the most uniform flow path, but web thickness between fuel orifices is unsatisfactory.

7.2 MECHANICAL JOINTS

Various methods exist for bolting together the dissimilar materials, L-605 and columbium, for a hot gas mechanical joint. The most practical methods consist of:

- (1) Nut and bolt
- (2) Stud and nut, with stud welded into parent material
- (3) Stud and nut, with each locked in by local peening
- (4) Stud and nut, with stud locked in place with a pin
- (5) Bolt threaded directly into parent material

(a) Nut and Bolt

Figure 51 shows a reactor bolted to the flange from the columbium secondary injector, with dual O-rings being compressed. When using a mechanical joint for this application high temperature nuts and bolts are required, with thermal coefficients of expansion compatible with the parent materials. In addition the fastener must maintain its mechanical integrity at an operating temperature of 1255K (1800°F). Current candidates for nuts and bolts are columbium and L-605. The bolt heads or nuts could be shaped to a slide into a fixed notch on the L-605 reactor, to prevent the bolt or nut from turning while the nut or bolt is being torqued as shown in this figure. A standard nut and bolt is the preferred method whenever compatible with the design.

(b) Stud and Nut

Figure 52 shows this standard configuration. Replacement of the stud is possible but assurance of maintaining a torque between the stud and the base metal is questionable when subjected to the anticipated thermal cycling. Damage to the "female" thread can result in costly repair. It is possible to "peen" the stud in place as a method of locking or securing, but one may question this method for a flight type application. Another disadvantage of a stud and nut installation is the use of two sets of threads (one at each end of the stud). For high temperature, flight application, one set of threads is favored.

(c) Stud and Nut, Stud Welded Into Parent Material

Figure 53 shows a reactor bolted to the flange from the columbium secondary injector, with dual O-rings being compressed. The stud would be inserted into the columbium or the L-605, then welded to insure no loosening during operation. The inability to replace the welded studs due to damage or galling is a disadvantage of this method of attachment. Also, depending on the design, the weldment may be in the hot-gas manifold, as shown, which makes replacement more difficult.

(d) Stud and Nut, Locked with Pin

An alternate method of locking a stud is the use of a pin that can be welded in place after installation. This type of installation is more time consuming, more costly and again prevents easy replacement of a damaged stud.

(e) Bolt Threaded Into Parent Metal

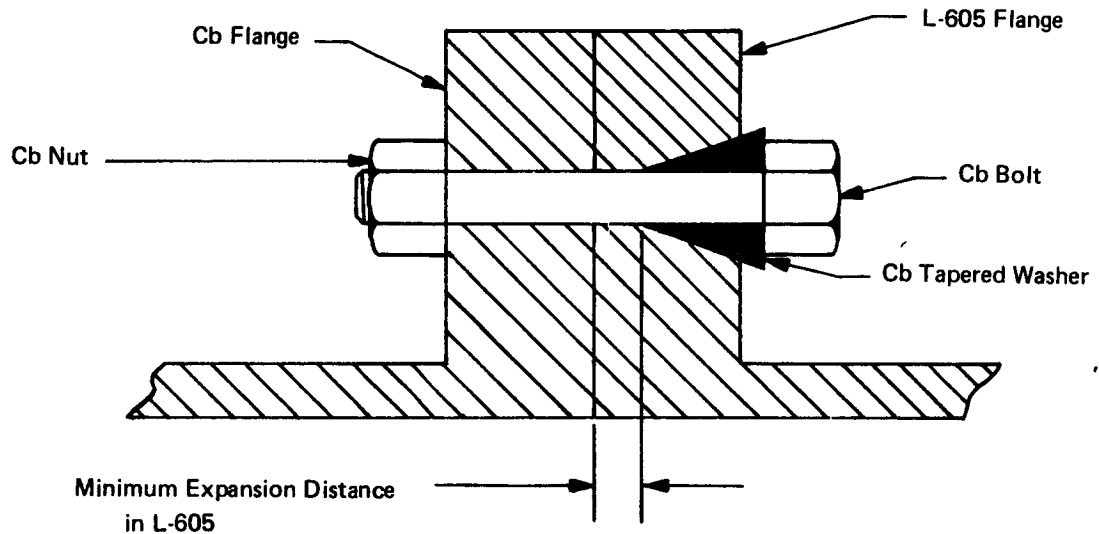
A similar concern exists for this installation method as for the stud installation previously mentioned, i.e., loss of torque and the difficulty of repairing a damaged thread in the parent metal. Depending on the columbium alloy used, threading in the parent metal may be risky due to the relative softness of some alloys. Helicoils would be required but thermal expansion differences cause concern.

(f) Flange/Bolt Interface Treatment

Whenever mechanical joints are made between injector and chamber components, proper design is critical. This is especially true when the two mating materials are different and have considerably different coefficients of thermal expansion. The L-605 expands approximately twice as much as columbium. Further concern must be given when the joint operates at high temperatures, such as 1255K (1800°F) in this application, during normal operation. The rationale applied to this type of joint includes the following:

- (1) Match the expansion of the bolt/nut assembly with the flanges, if possible.
- (2) If matching is not possible, reduce the mismatch to a minimum.

One method of accomplishing this is to reduce the thickness of the "foreign" flange material by counterboring the flange locally in the bolt region and insertion of a "tapered" or cylindrical sleeve of the bolt material. This method does not reduce the structural capability of the flange provided metal to metal contact is maintained. This method is shown below:



The reason expansion matching is so important is the need to maintain proper loading on the metal O-ring (or equivalent seal). At 1255K (1800°F) little mismatch is allowed before unloading the metal O-ring when using L-605 and columbium.

7.3 REACTOR/INJECTOR/CHAMBER INTERFACE

Many critical elements exist in the design of the interface between the reactor, injector, and chamber for a film-cooled chamber assembly. The following design rationale was established to aid in design definitions and selection. Consideration has been given for both a pre-prototype (with test flexibility) and a prototype (more flight type) design. In either case, flight type design practices were used wherever possible.

- (1) Minimize the number of seals
- (2) Use smallest diameter seals wherever possible
- (3) Locate seals as close as possible to bolt circle to assure maximum seal loading
- (4) Use welded interfaces wherever possible in place of seal joints
- (5) Allow for thermal coefficient of expansion differences of interface materials (columbium and L-605)
- (6) Provide for complete checkout of reactor prior to installation on chamber assembly
- (7) Allow replacement of all seals by flange disassembly for pre-prototype design (without machining requirements)
- (8) Provide orifice adjustment capability in film-coolant circuit for pre-prototype design, if possible
- (9) Allow adjustment of gap between liner and chamber by shim variation on chamber
- (10) Maintain low velocities in manifolds and passages to assure uniform flow distribution and low pressure drop.

7.4 DUCTED FILM-COOLED THRUST CHAMBER DESIGNS

Various film-cooled thrust chamber design layouts were completed to identify the proper combinations between the reactor, secondary injector, and chamber and liner. Two types of thrust chamber configurations were studied, (1) a pre-prototype and (2) a prototype.

The pre-prototype designs were made to allow for adjustment of liner/chamber gap to allow variation in film-coolant velocity. This was accomplished by providing shims between the chamber and injector. The liner is welded directly to the secondary injector, providing an all-welded, reliable joint identical to that used for the prototype (flight) configuration. The prototype configuration is identical except for removal of the shim capability and the area ratio of the nozzle extension. All pre-prototype designs were made for a nozzle exit area ratio of 25, whereas all prototype designs were made for an area ratio of 60.

The designs selected are shown in the subsequent Rating and Selection Section.

7.5 THERMAL ANALYSES

Various additional thermal analyses were completed for the injector configurations and the ducted film-cooled chamber. Results of these analyses follow, including comparison of the film-cooled analyses with data from a representative fire test conducted at JPL.

7.5.1 Partial Fuel Cooled Injector

Thermal analysis of the partial fuel cooled injector indicates the injector face temperature will be 1726 K (2646°F) (3% fuel flow) and 1593 K (2408°F) (6% fuel flow).

The predicted temperature rise of the oxidizer due to conduction through insulation is 2.8 K (5°F). An additional heat path through the birdcage bracket would not contribute more than an additional 5.6 K (10°F) maximum. Thus, during steady-state operation the propellant (oxidizer) temperature rise will be less than 8.4 K (15°F). The recesses and cavities can be filled with fibrous insulation.

7.5.2 Oxidizer Cooled Injector

A steady-state thermal analyses was made to determine the temperature rise of the oxidizer flowing behind the injector face, feed tubes and the oxidizer injector orifices.

The increase in temperature of the oxidizer flow is calculated to be 9.7 K (17.4°F). It is assumed that the feed tubes behind the injector are insulated with 3.2-mm (1/8-in.) insulation (thermal conductivity = 0.108 joule/m sec K (0.75 BTU in/hr ft² °F). A practical means of insulation application is to fill the recess behind and around the tubes with a fibrous insulation capable of long-term operation at 1256 K (1800°F).

7.5.3 Heat Gain by the Oxidizer Flow Through the Oxidizer Circuit

Table 17 shows the predicted temperature rise of the oxidizer as it passes through the various injector components during steady-state bimodal operation. The small increases in temperature rise will present no problem in the oxidizer flow. Also shown is the predicted maximum injector face temperatures for the three designs considered.

7.5.4 Chamber Wall Temperature

A parametric design study was conducted with the assumption that the outer chamber wall was free to radiate to a 311 K (100°F) sink temperature with an emissivity of 0.8. If the engine barrel section's ability to radiate is restricted by having to radiate to a much higher heat sink, or if the engine is buried in a cavity (equivalent to an emissivity = 0.1) the liner will increase in temperature. The peak will increase from 1438 K (2129°F) to 1584 K (2392°F). The corresponding liner temperature will increase from 1941 K (3034°F) to 1969 K (3084°F), an increase of 28 K (50°F).

7.5.5 Discussion of Bimodal Engine, DJ-339 Test Results (JPL - Edwards Test Station)

A sea level evaluation of the film cooled Bimodal engine (with liner) has been in process at JPL to determine the equilibrium columbium chamber wall temperature and performance with the coaxial injector. A test from this series was selected for comparison with the analytical model. This test, designated DJ 339, consisted of the following profile: 1) a series of monopropellant "warm up" firings, 2) 75 seconds of bimodal operation (35 seconds at 13.3% film coolant, 20 seconds at 11.6% film coolant, and 20 seconds at 10% film coolant), and 3) a short monopropellant "tailoff" prior to shutdown. The film coolant flow-rates ranged from 0.1043 kg/sec (0.23 lbs/sec) to 0.0771 kg/sec (0.17 lbs/sec). Ten thermocouples were attached at five axial stations from the injector end of the chamber to the nozzle exit. Seven thermocouples were used for comparison with the analytical model; two were located on the chamber cylinder near the injector, two were located on the chamber near the convergent section, one thermocouple was located in the middle of the convergent nozzle and two were located at the throat. At each axial location, one thermocouple was located "on pattern" and the other "between pattern" in reference to the injector coaxial elements. The chamber thermocouples near the injector were designated A-323 and A-37, respectively; those on the chamber were designated B-323 and B-37, and the one in the convergent nozzle was designated C-37, and those in the throat were designated D-323 and D-37.

A digital computer program was used to compare the theoretical results against the available test data. The test configuration geometry (gap size, wall thickness, chamber and liner radius) was used as input to the program and is represented by six axial stations in the liner film-cooled section. At each station a heat balance is written to calculate the inner and outer surface temperature of the liner and chamber wall temperatures. The inner liner receives heat from the combustion gases and conducts through the liner wall and then radiates to the chamber wall and convects to the film coolant stream. The radiation is a function of surface emissivities and radiation view factors. The fuel film convective heat transfer coefficient is based on the Coburn equation $h = 0.023 \times c_p \times w/a (RN)^{-0.2} PR^{-0.6}$. The cumulative addition of heat to the film coolant stream from station to station is accounted for in the program.

The geometry was such that a measured gap of 2.03 mm (0.080 in.) existed in the cold condition at the film discharge point. It is estimated that during equilibrium temperature operation this gap will decrease to 1.27 mm (0.050 in.). The thermal analysis is based on all annular passage sizes existing at steady-state temperatures. An auxiliary analysis was made for the film-cooled throat section based on the fuel film outlet temperature from the liner using a Hatch-Pappel solution.

Figure 54 shows the theoretical results for the chamber liner as a function of axial distance from the throat station for film fuel rates of 0.077 and 0.104 kg/sec (0.17 and 0.23 lb/sec). Also shown is the available test data points span of temperature measurements. It is apparent that the curve of $h_g = 1180$ joules/m² sec K (4×10^{-4} BTU/in.² sec °F) at the throat station (heating coefficient of 833 joules/m² sec K (2.83×10^{-4} BTU/in.² sec °F) in the chamber section), overpredicts the measured external chamber wall temperatures. Test data of thermocouple A323 does lie on the theoretical line. The other data points are below the theoretical results. The theoretical data are based on a constant inlet temperature of 1225 K (1745°F), whereas the test data indicates that there is considerable heat loss from the film coolant as it flows from the inlet and around the manifold.

The corresponding liner temperatures vary from 1700 K (2600°F) to 1811 K (2800°F).

Figure 55 shows the results of the throat section analysis. It is apparent that to match the peak test data for the throat temperatures a heating rate of greater than 1770 joules/m² sec K (6×10^{-4} BTU/in.² sec °F) is necessary. A heating rate of 1180 joules/m² sec K (4×10^{-4} BTU/in.² sec °F) would correspond to the D37 thermocouple test data.

The results of the test data would indicate that the curve for $h_g = 1180$ joules/m² sec K (4.0×10^{-4} BTU/in.² sec °F) is adequate for the chamber/liner section (h_g in the chamber equals 833 joules/m² sec K (2.83×10^{-4} BTU/in.² sec °F) but a heating rate of 1770 joules/m² sec K (6×10^{-4} BTU/in.² sec °F) is necessary at the throat section. Thus, the parametric design study with a heating rate equivalent to curve 2 appears conservative.

7.5.6 Parametric Thermal Study to Determine Influence of Engine variables on Wall Temperatures

A parametric study was conducted to determine the relative effects of changing dissociation, film coolant flow rate, annular gap and transfer coefficients.

Figure 56 shows the effect of changing the percentage dissociation from a nominal of 60%. A decrease to 50% dissociation (10% change) will result in 64 K (115°F) increase in liner temperature, 67 K (120°F) increase in throat wall temperature and 89 K (160°F) increase in the chamber wall temperature.

Figures 57 and 58 show the influence of film coolant flow rate and the gap between the liner and the chamber at the point where the coolant film mixes with the combustion gases in the chamber. The nominal gap of 0.203 cm (0.080 in.) cold changes to a lesser gap of 0.128 cm (0.0504 in.) when at operating

temperature. The gap at each station changes according to the vector summation of the axial and radial growth of chamber and liner at their respective operation temperatures.

Figure 59 shows the influence of heat transfer coefficient on the uninsulated throat temperature, and also the effect of efficiency upon throat temperature. A coefficient of 852 joules/m² sec K (2.89×10^{-4} BTU/in.² sec °F) was used in the chamber section and the cumulative effect of heat addition was included up to the throat station.

Figure 60 shows the variation of wall and liner temperature for heat transfer coefficients in the chamber section. The values of coefficients 3245, 1770 and 1180 joules/m² sec K (11×10^{-4} , 6×10^{-4} and 4×10^{-4} BTU/in.² sec °F) result in chamber heating coefficients of 852, 1147 and 821 joules/m² sec K (2.89×10^{-4} , 3.89×10^{-4} and 2.83×10^{-4} BTU/in.² sec °F), respectively. These are the data points at a contraction ratio of 5.2.

Figure 61 shows the complete data for the nominal design case of

$h_g = 1770$ joules/m² sec K (6×10^{-4} BTU/in.² sec °F) at Throat (Curve 2)

95% c*

w = 0.0907 kg/sec (0.20 lb/sec) Film Coolant Film Rate

60% Dissociation

0.203 cm (0.080 in.) Minimum Gap Cold 0.127 cm (=0.050 in. Hot)

7.6 STRUCTURAL ANALYSES

For the film-cooled design, which incorporates an inner liner to define the coolant passage, the critical loading is the pressure differential developed across this liner during engine operation. A parametric stability analysis was conducted on the liner for a Δp of 34.5 kN/m^2 (5 psia) and temperatures of 1700K (2600°F), 1811K (2800°F) and 1922K (3000°F). Elastic and creep buckling were investigated for long-term (1000 sec) effects. Also, a safety factor of two was applied to the pressure differential to arrive at a design loading of 69.0 kN/m^2 (10 psia) for the structure. Two candidate materials were selected for the liner design; these were C-103 and SCb-291 columbium alloys. The geometry of the inner liner used in the analysis is:

Radius $R = 0.0711 \text{ m}$ (2.8 in.)
Length $\ell = 0.159 \text{ m}$ (6.25 in.)

Using the same stability equation and analytical procedure described previously for the regenerative liner analysis, the table below lists the required thicknesses for the above temperatures and materials using an elastic buckling criteria:

SI Units

Inner Liner - Elastic Buckling (Steady State)

Temperature K	C-103		SCb-291	
	Elastic Modulus $\times 10^{-6}$ kN/m^2	Required Thickness cm	Elastic Modulus $\times 10^{-6}$ kN/m^2	Required Thickness cm
1700	33.1	0.0635	67.57	0.0508
1811	18.6	0.0762	55.16	0.0508
1922	10.3	0.1016	46.90	0.0635

English Units

Temperature °F	C-103		SCb-291	
	Elastic Modulus $\times 10^{-6}$ psi	Required Thickness in.	Elastic Modulus $\times 10^{-6}$ psi	Required Thickness in.
2600	4.8	0.025	9.8	0.020
2800	2.7	0.030	8.0	0.020
3000	1.5	0.040	6.8	0.025

As noted earlier, to ensure that the resultant stress distribution in the liner remains elastic, the structure must also be investigated using an allowable strength of compression yield divided by a safety factor of 1.5; that is, $F_{cy}/1.5$. Since little data are available on the compression properties for the materials, it was assumed that the compression yield was equal to the tensile yield strength of the material. So, the following table lists the allowables used and the required thicknesses for the temperatures in question.

SI Units

Inner Liner - Compression Yield (Steady State)

Temperature K	C-103		SCb-291	
	$F_{cy}/1.5$ kN/m ²	Required Thickness cm	$F_{cy}/1.5$ kN/m ²	Required Thickness cm
1700	34.5	0.0254	50.6	0.0127
1811	28.5	0.0254	36.8	0.0254
1922	15.6	0.0381	31.2	0.0254

English Units

Temperature °F	C-103		SCb-291	
	$F_{cy}/1.5$ psi	Required Thickness in.	$F_{cy}/1.5$ psi	Required Thickness in.
2600	5000	0.010	7340	0.005
2800	4130	0.010	5330	0.010
3000	2265	0.015	4530	0.010

For determining the required thicknesses for creep buckling of the liner, the same method used for the regenerative design will also be incorporated for the film-cooled concept. Figure 62 shows the Larson-Miller master plot for recrystallized C-103 columbium which relates time and temperature to creep stress and strain. These curves were generated from the Wah Chang Corporation Data Book on C-103 material.

As can be seen from this figure, the smallest creep strain noted was 0.2% which is still quite large for estimating the creep characteristic stress-strain curves; for the analysis, it was assumed that this strain (0.2%) defined the effective creep modulus at temperature. This modulus is generally much lower than the actual effective value based on the stress-strain curves shown in Figures 42 and 43 for SCb-291. Because of the conservatism associated with determining the creep modulus, it was assumed that the criteria of the elastic creep stress limit would not represent a worst-case design allowable for the thickness analysis of the

C-103 liner. Figure 63 shows the characteristic stress-strain diagrams as determined from the data of Figure 62 and the above assumptions.

Figure 64 shows the creep characteristic stress-strain curves determined from Figure 41 for the SCb-291 material at temperature. The effective creep modulus and limit stress can be ascertained directly from these diagrams. The following table lists the properties and thickness requirements for both the C-103 and SCb-291 columbium alloys.

For the C-103 Material:

Inner Liner - Creep (Steady State)

Temperature K	Creep Modulus $\times 10^{-6}$ kN/m ²	Required Thickness cm	Temperature °F	Creep Modulus $\times 10^{-6}$ psi	Required Thickness in.
1700	8.0	0.114	2600	1.16	0.045
1811	5.2	0.127	2800	0.75	0.050
1922	3.4	0.152	3000	0.495	0.060

For the SCb-291 Material:

SI Units

Temperature K	Buckling		Elastic Stress	
	Creep Modulus $\times 10^{-6}$ kN/m ²	Required Thickness cm	Limit Stress kN/m ²	Required Thickness cm
1700	30.3	0.0635	27.2	0.0254
1811	22.8	0.0762	15.2	0.0381
1922	15.2	0.0889	9.0	0.0635

English Units

Temperature °F	Buckling		Elastic Stress	
	Creep Modulus $\times 10^{-6}$ psi	Required Thickness in.	Limit Stress psi	Required Thickness in.
2600	4.4	0.025	3950	0.010
2800	3.3	0.030	2200	0.015
3000	2.2	0.035	1300	0.025

Besides the steady-state loading of the liner, there are also start transients which must be investigated. One transient state is a monomode start at peak bimode temperatures. Now there is only pressure in the coolant passage with no chamber pressure, so the design loading on the liner would be an external pressure of 353.8 kN/m^2 (which is $P_C + 34.4 \text{ kN/m}^2$) (51.3 psia, which is $P_C + 5 \text{ psia}$). Because of the relatively short duration of this loading a safety factor of 1.5 will be used to define the critical design pressure; that is,

$$p_{\text{des}} = 1.5 p_{\text{ex}} = 531 \text{ kN/m}^2 (77 \text{ psia}).$$

The following table reflects the required thicknesses for the candidate materials using the elastic modulus criteria.

SI Units

Inner Liner - Elastic Buckling (Monomode Transient)

Temperature K	C-103		SCb-291	
	Elastic Modulus $\times 10^{-6}$ kN/m^2	Required Thickness cm	Elastic Modulus $\times 10^{-6}$ kN/m^2	Required Thickness cm
1700	33.1	0.140	67.57	0.102
1811	18.6	0.178	55.16	0.114
1922	10.3	0.216	46.90	0.127

English Units

Temperature °F	C-103		SCb-291	
	Elastic Modulus $\times 10^{-6}$ psi	Required Thickness in.	Elastic Modulus $\times 10^{-6}$ psi	Required Thickness in.
2600	4.8	0.055	9.8	0.040
2800	2.7	0.070	8.0	0.045
3000	1.5	0.085	6.8	0.050

The other start transient is a bimode start at peak monomode temperatures. From the thermal analysis of the structure, it was found that the maximum temperature of the liner was 1255K (1800°F). Again it was assumed that there is no chamber pressure during start but only an external load of 930 kN/m^2 (135 psia). A safety factor of 1.5 was applied to this pressure to arrive at a design loading of:

$$p_{\text{des}} = 1397 \text{ kN/m}^2 (202.5 \text{ psia})$$

Therefore, the following thicknesses would be required for buckling at 1255K (1800°F).

C-103	Elastic Modulus	$E = 91.0 \times 10^6 \text{ kN/m}^2 (13.2 \times 10^6 \text{ psi})$
	Required Thickness	$t = 0.1397 \text{ cm (0.055 in.)}$
SCb-291	Elastic Modulus	$E = 106.2 \times 10^6 \text{ kN/m}^2 (15.4 \times 10^6 \text{ psi})$
	Required Thickness	$t = 0.1397 \text{ cm (0.055 in.)}$

An analysis was also conducted on the bolted interface joints of the reactors to chamber/injector assembly to determine the required bolt material and joint configuration. Since these joints are bimetallic, that is, L-605 to columbium, there is a problem of differential thermal growths which could be detrimental to the pressure sealing capability of the structure. The maximum temperature at all bolted joints was considered to be the fuel gas temperature of 1255K (1800°F). At this temperature, the relative coefficients of thermal expansion for the L-605 and columbium (C-103) materials are:

$$\text{L-605} \quad \alpha = 5.39 \times 10^{-6} \text{ m/m/K (9.7} \times 10^{-6} \text{ in./in./}^\circ\text{F)}$$

$$\text{C-103} \quad \alpha = 2.39 \times 10^{-6} \text{ m/m/K (4.3} \times 10^{-6} \text{ in./in./}^\circ\text{F)}$$

As can be seen from the above values the L-605 possesses an expansion of over twice that of the columbium, so a bolt material must be selected which will have a thermal expansion somewhere inbetween and also retain a reasonable yield strength at 1255K (1800°F). It should be noted that a L-605 bolt would not be feasible for the bimetallic-joint concept because the large expansion of the bolt would precipitate a relaxation of the initial torque with the result that the precompression on the seal would be lost and the gases would leak.

The material selected for the bolt and nut design was a coated columbium alloy designated F-48 (D-40) which has an element composition – Cb-15W-5Mo-1Zr. The following material data for this alloy was taken from DMIC Report 188, "The Engineering Properties of Columbium and Columbium Alloys," 6 September 1963. At 1255K (1800°F), F-48 bar material possesses the following properties:

$$\alpha = 2.71 \times 10^{-6} \text{ m/m/K (4.88} \times 10^{-6} \text{ in./in./}^\circ\text{F)}$$

$$E = 134.6 \times 10^6 \text{ kN/m}^2 (19.45 \times 10^6 \text{ psi})$$

$$F_{tu} = 500.0 \times 10^3 \text{ kN/m}^2 (72.5 \times 10^3 \text{ psi})$$

$$F_{ty} = 348.3 \times 10^3 \text{ kN/m}^2 (50.5 \times 10^3 \text{ psi})$$

The primary design criteria for the joint design is that the summation of all applied loads (initial tension and thermal) in the bolt were not to exceed the proportional limit of the F-48 material. Since this value was not quoted in the reference, the analysis uses a factor of 1.25 divided into the tension yield as defining this limit stress allowable; that is:

$$F_{P/L} = F_{ty}/1.25 = 275.9 \times 10^3 \text{ kN/m}^2 (40 \times 10^3 \text{ psi})$$

Because of the additional load developed in the bolt due to the differential expansion of the attachment flanges relative to the bolt, a joint design must be incorporated such that this loading, when combined with torquing, will not exceed the limit stress noted above. Generally, the flange thicknesses are defined for either pressure, thermal or vibrational loading conditions; so, the overall flange designs cannot be altered to minimize the thermal stresses in the bolt. One concept available for reducing the effect of the large expansion of the L-605 is to locally decrease the thickness of the flange at the bolt location by using thick columbium spacers or washers. Each joint configuration would have to be investigated separately to determine the optimum width of the columbium washer for thermal loading of the bolt.

7.7 MASS ANALYSES

Additional mass analyses were completed for the final "preferred" regenerative and ducted film-cooled configurations. These analyses are summarized in Table 18.

7.8 SYSTEM MASS/PERFORMANCE TRADEOFF

A preliminary system mass tradeoff analysis was performed to obtain initial effects of performance variations and engine mass on the total system. Assumptions were made that could be representative for a typical system using the bimodal engine.

Objective

Define relative merit of engine mass to delivered specific impulse over total impulse range of 0 to 8.34×10^6 Newton-seconds (0 to 1.875×10^6 pound seconds) (design for propulsion system).

Approach

Estimate mass of all propulsion system elements which are sensitive to engine specific impulse and engine mass on common baseline for direct comparison.

Parametric evaluation over the following range was used to enable alternate designs to be compared.

I_{sp}	2940 to 3140 N-s/kg (300 to 320 $lb_f\text{-sec}/lb_m$)
Engine Mass	18.14 to 45.36 kilograms (40 to 100 pounds)
I_t	0 to 8.9×10^6 Newton-seconds (0 to 2×10^6 pound seconds)

Figures 65 through 67 show the system mass comparison versus total impulse and system mass versus specific impulse, respectively. Figures 68 through 70 reveal the computer output for three specific impulse values.

7.9 RATING AND SELECTION OF FINAL BIMODAL THRUSTER CONFIGURATIONS

The final selection of the preferred bimodal thruster requires a decision between the regeneratively-cooled and the film-cooled designs. The two primary contenders for the regeneratively-cooled designs were derived from the tradeoff analysis in Task 1. The designs are basically a bimodal thruster with either multiple cylindrical reactors at the secondary injector station or an annular reactor at the nozzle extension interface. Each of these designs could have regeneratively-cooled passages which have min-channels or an

annulus at the throat. The only part needed to complete the basic thruster is the secondary injector. All activities during Task 1 were concerned with all-welded reactors and undefined interfaces. In Task 2 a similar rating system is used for choosing the preferred regeneratively-cooled configuration, considering all the primary alternatives. Selection of the preferred film-cooled design requires the same secondary injector considerations as the regeneratively-cooled thruster. In addition, the hydrazine reactor must be located at the secondary injector station, so any selections made for the regeneratively-cooled thrusters for these components would be used for both cases. Bimodal thruster designs, however, with the reactor located at the nozzle extension interface, are significantly different from the secondary injector stationed configurations and therefore analyzed separately.

The tradeoff analysis between the film-cooled and two regeneratively-cooled configurations is performed according to the method used in Task 1. The tradeoff includes: (1) secondary injectors, (2) reactor/injector combinations at secondary injector, and (3) reactor/liner/secondary injectors, reactor at nozzle/extension interface. These are shown in Tables 19, 20 and 21.

The logic or decision charts are given in Figures 71 and 72.

7.9.1 Ratings of Secondary Injectors

7.9.1.1 All-Columbium Injector

- (1) N_2O_4 Regeneratively-Cooled
- (2) N_2H_4 Regeneratively-Cooled (100%)
- (3) N_2H_4 Partial Regeneratively Cooled - 6% (Dump Cooled)

There is not a competitive design available for the all-columbium injector which uses 100% of the hydrazine for cooling the secondary injector face. The problem arises at the joint between the reactors and the secondary injector. Any flanged configuration will require complex mating arrangements and be difficult to assemble because of the inaccessibility of the bolts and nuts.

(a) Transient Mono I_{sp}

More injector surface area is subjected to the hydrazine gases with the 100% regeneratively-cooled injector than with the 6% cooled injector. Therefore, the former will have more of the mono-propellant heat lost to the hardware. The heat loss from the monopropellant means a decrease in available performance.

(b) Transient Bipropellant I_{sp}

The N_2O_4 -cooled injector will lose performance because of two-phase flow for N_2O_4 and less than optimum combustion. Relative heat masses are the same.

(c) Durability/Life

The N_2O_4 and N_2H_4 100% regeneratively-cooled designs will provide lower injector face temperatures than the configuration using 6% of the N_2H_4 gases. Therefore, the temperature capability

of the two injectors is rated higher than the third. Since the N_2O_4 coolant provides a lower temperature at the secondary injector face there is a large thermal differential between the center of the injector and the remaining portion of the injector. The N_2O_4 -cooled injector therefore has higher thermal stresses.

(d) Ease of Fabrication

The N_2O_4 -cooled injector has extra EB welding because of the coolant passages and manifold needed to pass the N_2O_4 along the back of the injector face. This increases the fabrication cost and difficulty of this injector. The injector configuration which utilizes all the hydrazine to cool the injector requires complex welding and fixturing for assembly. Thus, the relative ratings are as shown.

(e) Risk

The risk of using each of the injectors is a function of their durability and complexity. The more durable the configuration, the lower the risk. The fewer parts and welds, the lower the risk.

(f) Cost

The relative cost of each of the injectors is proportional to their fabricability, since material costs will not vary significantly between configurations.

(g) The mass ratings are based on the relative masses calculated from the geometry and density considerations.

7.9.1.2 Columbium Injector Face/L-605 Back Cover

1. N_2O_4 Regeneratively-Cooled
2. N_2H_4 Regeneratively-Cooled (100%)
3. N_2H_4 Partial Regeneratively Cooled - 6% (Dump Cooled)

Any design which has an L-605 back cover and a columbium secondary injector face will have an inter-propellant sealing problem if cooled by N_2O_4 . Therefore, this type of design was eliminated from consideration. However, an L-605 back cover, columbium secondary injector face lends itself well to the 100% hydrazine-cooled injector face design. Therefore, this design is competitive with the 6% hydrazine dump cooled secondary injector except for being slightly more costly because of welding difficulties at the hydrazine reactor joint. These basic differences are noted in the evaluation plan ratings.

7.9.2 Ratings of Reactor/Injector Combinations with the Reactor at the Secondary Injection Station

7.9.2.1 Columbium Secondary Injector

- (1) Columbium reactor welded to secondary injector.
- (2) L-605 reactor bolted to secondary injector.

Basic Characteristics

- (a) The L-605 bolted to the columbium injector is a heavier unit than the all-welded columbium reactor and secondary injector.
- (b) The columbium reactor configuration has no demonstrated experience and presents potential compatibility problems with decomposed hydrazine.
- (c) The all-welded columbium assembly would provide higher reliability than a bolted assembly of different materials.

(1) Performance

Columbium reactor assembly has lower thermal mass, therefore, higher monopropellant performance.

Bipropellant performance is about the same.

(2) Durability/Life

Columbium reactor all-welded assembly has the same basic temperature capability (within the expected limits); less thermal stress, because of similar materials; the same mechanical stress, but greater reliability because of no potential seal leakage problem.

There is a potential compatibility problem with decomposed hydrazine

(3) Ease of Fabrication

Both should be about the same since installation of the bolts is faster than welding an assembly, but flanges have to be machined for the seal surfaces.

(4) Low Risk

The all-welded columbium assembly has a higher risk because of the question of compatibility between the hydrazine decomposition gases and the coated columbium in the reactor.

(5) Cost

The all-columbium assembly will be about the same price as the L-605 reactor/columbium injector assembly because of the cost of metal O-rings and columbium bolts with the latter and the high material costs for the former.

(6) Mass

The all-welded columbium assembly has a lower mass than the L-605 back cover, secondary injector. Both the flanges and bolts between the reactor and secondary injector makes the L-605 reactor/columbium injector configuration heavier.

7.9.2.2 Columbium Secondary Injector with L-605 Back Cover

- (1) L-605 reactor welded to injector back cover
- (2) L-605 reactor bolted to injector back cover
- (a) There is at least one flanged joint required between the L-605 back cover and the columbium injector. Therefore, if the L-605 reactor is bolted to the L-605 back cover, a second flange and setoff seals will be needed. This extra flange adds mass, complexity and cost to the configuration.
- (b) The columbium/L-605 secondary injector is heavier than the all-welded columbium secondary injector. In addition, it has extra seals which degrade its reliability.

(1) Performance

Transient mono performance is lower than an all-columbium injector due to greater mass. Bipropellant performance are comparable.

(2) High Durability/Life

The designs have lower reliability than the all-columbium injector because of fewer seals, however, the compatibility problem between the decomposed N_2/H_4 and the columbium reactor is uncertain.

The all-columbium configurations have less thermal stress because of fewer points of contact between the dissimilar materials and fewer flanges with their associated thermal gradients. The all-welded L-605 joint has fewer thermal stresses, than the bolted joint of one less seal joint and flange.

(3) Ease of Fabrication

Little difference exists for fabrication of either configurations.

(4) Risk

The design with the highest rating in durability/life is modified by the ease of fabrication. The case of highly stressed or difficult to inspect areas provide the relative risk ratings.

(5) Cost

The cost of each design was directly related to the fabrication cost plus the cost of seals and bolts, since the relative cost of materials is a minor part of the difference.

7.9.3 Ratings of Preferred Reactor/Liner/Secondary Injector With Reactor at The Nozzle Extension Interface

7.9.3.1 All Columbium Secondary Injector

1. Columbium reactor welded to columbium outer shell
2. L-605 reactor bolted to columbium outer shell and inner liner.

General Description

When an all-columbium secondary injector is used, it is not practical to use anything but a columbium outer shell to avoid a seal joint at the injector end of the thruster. The primary differences between the configurations of A1 and A2 are discussed for each rating category.

(1) Performance

Analysis of the mass associated with each configuration shows that configuration A2 is heavier than A1. Therefore, the transient monopropellant performance is higher for A1 and A2. The bipropellant performance should be about the same since it is not as sensitive to the reactor/thruster joint configuration.

(2) Durability Life

The all-welded columbium configuration will have a lower probability of failure than a metallic seal, however, the redundancy of the seal should reduce the leakage probability. Therefore, A1 and A2 have equal ratings. All of these designs have joint problems due to the large diameter at which the seal is made. The thermal stresses will be higher in A2 because of the material differences at the interface joints. The overall configuration will have very high thermal stresses because of the large amount of thermal growth at the nozzle/extension interface station and the thermal differences in the hardware. There is a potential chemical compatibility problem with the columbium reactor which causes the A1 to have a significantly lower rating than A2. Although the SCb-291 columbium alloy coated with silicide 512E has been shown to be capable of withstanding the gases, the coating becomes a critical part of the reactor rating.

(3) Fabrication

Fabrication of the flanged assembly, using the L-605 reactor, requires expensive machining setups because of the large number of tolerances which are required for proper sealing of the metal O-rings. Thus, configuration A2 is rated lower than A1 because of the machining effort required. In general, the effort required to setup and machine the material at the nozzle/extension interface is expensive. In addition, the feed tube structure for the hydrazine reactor is large and requires extra care in handling during all operations.

(4) Risk

The use of an all-welded columbium reactor assembly has a high risk because of the compatibility question between the hydrazine decomposition gases and the coated columbium in the reactor. The sensitivity to free H^+ and N^+ ions released during the N_2H_4 initial decomposition has yet to be defined. In addition, the use of coatings entails the concern of porosity and formation of a continuous barrier to the ions.

(5) Cost

(1) The cost of each design is a function of the machining, welding and assembly costs, plus the raw materials and nuts and bolts. Configuration 1 has a series of EB welds not required in configuration 2. The seals needed in Configuration A2 will require columbium bolts and metal O-rings which add substantial costs to the final assembly, (\$27 per bolt and nut and \$21 per seal). Thus, configuration A2 has a relatively higher cost than configuration A1.

7.9.3.2 Columbium Secondary Injector with L-605 Back Cover

(1) L-605 reactor welded to L-605 outer shell, bolted to columbium inner liner, L-605 outer shell is welded to L-605 back cover.

(2) L-605 reactor bolted to columbium outer shell and inner liner. Columbium outer shell and inner liner welded to columbium injector face. L-605 back cover bolted to columbium secondary injector face.

(3) L-605 reactor bolted to L-605 over liner and columbium inner liner. Outer cover welded to L-605 back cover.

Configuration B1 consists of an L-605 reactor located at the nozzle extension interface. The coolant passage outer cover is L-605, which is welded to the reactor. This outer cover is also welded to the L-605 secondary injector back cover, with the columbium injector trapped in place. The reactor to columbium inner liner joint is made with the columbium bolts and nuts, with pressurized metal O-rings used to make the hot-gas seal.

Configuration B2 has an L-605 reactor bolted to a columbium (C-103) outer shell and inner liner at the nozzle extension interface. The columbium inner liner and outer shell are welded to the columbium injector face. The L-605 back cover must be bolted to the columbium injector face with high temperature bolts and sealed with pressurized metal O-rings. Thus, this configuration requires three sets of metal O-rings and the related tight toleranced seal surfaces.

Configuration B3 employs an L-605 reactor bolted to an L-605 outer shell and an SCB-291 inner liner. The L-605 outer shell is welded to the L-605 secondary injector back cover, with the columbium injector plate trapped in place, as in Configuration B1.

Analysis of these three configurations shows that only configuration B2 has a fully removable reactor, but it requires three separate sets of hot-gas seals. Thus, it is apparent that each of these configurations has fabrication and operational drawbacks not encountered with configuration A2. The differences are reflected in each of the elements considered in the ratings.

(4) Ease of Fabrication

Each of the three configurations requires the establishment of carefully machined seal joints in series with other seal joints or EB welds. The machining tolerances required, the assembly fixturing, the handling of the large reactor assemblies, because of their diameter, entails extra costs. In addition, all of the components are made from larger diameter stock, providing an immediate cost penalty. If any problems with the seals develop, extra costs are entailed for disassembly of configurations B1 and B3. Thus, the fabrication costs of this type of reactor/thruster assembly is higher than for the reactor at the secondary injector station.

(5) Risk

The risk associated with each of the configurations is related to the durability/life considerations, plus the fabricability considerations. Configuration B2 presents potential problems in fabrication which makes potential schedule problems. Configuration B1, with its difficulty in seal maintenance also provides risk in fabrication and assembly. The relative effect of each of these factors is inputted to the ratings.

(6) Cost

Considerations of schedule, machining, raw materials, seals and bolts defined the relative costs of each configuration. For reasons discussed previously, and considering the number of joints, the relative costs of the assemblies were proportional to the number of seals involved.

(7) Mass

The mass of the configurations is proportional to the number of seals because of the flanges and bolts involved. Varying materials have little effect on the relative masses. The need for these additional seals and flange assemblies detracts from the attractiveness of the assembly with the reactor at the nozzle extension interface, as seen in the final rating sheets.

7.10 FINAL DESIGNS

As a result of the rating tradeoff, the following configurations were selected for layout design:

Regenerative Cooled (see Figures 73 and 74)

Configuration No. 1 - Six individual cylindrical reactors at the secondary injector.

Configuration No. 2 - An annular reactor at the nozzle/extension interface.

Film Cooled (All Reactors at Secondary Injector) (see Figures 75 through 77)

Configuration No. 1 - Six individual cylindrical reactors with injector face 6% fuel cooled.

Configuration No. 2 - Six individual cylindrical reactors with injector face 100% fuel cooled.

Configuration No. 3 - Six integral cylindrical reactors with injector face 6% fuel cooled.

Note that both regenerative configurations and the film-cooled configuration No. 1 are for prototype (flight) designs. Film-cooled configurations No. 2 and No. 3 are shown as a pre-prototype with an insert for the prototype configuration.

7.11 RECOMMENDATIONS AND CONCLUSIONS

As a result of the regeneratively-cooled and ducted film-cooled thrust chamber studies and tradeoffs, the following recommendations and conclusions are made for a prototype (flight) configuration engine:

- (1) The ducted film-cooled chamber is preferred due to demonstrated feasibility, lower cost, simplicity, and lower mass.
- (2) An all-columbium chamber and liner are required.
- (3) Six L-605 individual cylindrical reactors are preferred.
- (4) Axial oriented reactors with six small diameter seals are preferred (or angled reactors with two large diameter seals).
- (5) Redundant hot-gas seals are recommended.
- (6) An all-columbium injector is preferred.
- (7) A fuel partial regeneratively (or dump-) cooled injector (6%) is preferred.
- (8) Slightly larger (1/4 in.) circle diameter fuel injector orifice pattern is preferred to allow sufficient spacing between fuel orifices to accommodate coaxial pattern.
- (9) Gusset supported reactor bottom plate recommended.
- (10) "Contained" upper reactor bed recommended.
- (11) C.G. mounted gimbal ring with flexure pivots preferred.

NOTE: An all columbium reactor/injector/chamber preferred if compatibility of coated columbium reactor is demonstrated.

Valve development required to obtain a flight rated valve capability.

7.12 NEW TECHNOLOGY

1. Hot Gas Regeneratively Cooled Columbium Chamber;
2. Innovators - Nelson Roth and Neil Safeer;
3. Information identified in Monthly, Quarterly and Final Report for this contract; and
4. New Technology Report submitted in June 1973.

TABLES S.I.

TABLE 1 SI AND I
BIMODAL REGENERATIVE THRUST CHAMBER REQUIREMENTS

	Bipropellant Mode	Monopropellant Mode	Either Mode
A. Design Parameters Thrust, Steady-State Nominal at Standard Conditions*, N(lb _f) Propellants Mixture Ratio, Nominal at Standard Conditions* (O/F) Hydrazine Flow Ratio, Bipropellant Mode: Monopropellant Mode Chamber Pressure, Nominal Nozzle Stagnation, kN/m ² (psia) Pressure Drop, Maximum through Regenerative Cooling Jacket, kN/m ² (psid) Cooling Gas Composition Cooling Velocity in Regenerative Cooling Jacket Cooling Gas Inlet, Temperature K (°F) Combustion Length, Bipropellant Impingement-to-Throat, m (in.) Expansion Area Ratio Nozzle Contour Area Ratio at Start of Uncooled Extension Operating Duration Capability Minimum Total(s) Maximum Continuous(s) Minimum Continuous(s) Duty Cycle Restrictions*** B. Performance Goal Specific Impulse, Minimum Steady-State at Standard Conditions* N-s/kg, (lb _f -s/lb _m)	4500.0 (1010.0) N ₂ O ₄ /N ₂ H ₄ 1.15 900.0 (130.0) --- Subsonic 1500.0 1000.0 10.0 3050.0 (311.0)	1600.0 (360.0), approx. N ₂ H ₄ 0 320.0 (46.3), approx. 300.0 (43.5) Subsonic 1000.0 500.0 1.0 2300.0 (234.0)	1.0 (Venturi Controlled) N ₂ H ₄ Decomposition Products at an NH ₃ Disassociation = 50 ± 5% 1250 ± 50 (1800 ± 90) 0.21 (8.25) 60:1 80% Bell TBD** None

* Standard Conditions ≡ 295K (71.6° F) propellant temperatures, 0 kN/m² (0 psia) ambient pressure

** TBD ≡ to be determined (by Contractor)

*** Other than that a bipropellant mode firing is always started with a 300 ms monopropellant lead and terminated with a (TBD) ms monopropellant lag

TABLE 2 SI AND 2
FLIGHT-TYPE BIMODAL ENGINE REQUIREMENTS

	Bipropellant Mode	Monopropellant Mode	Either Mode
A. Engine Characteristics			
Oxidizer	N_2O_4	---	
Fuel	N_2H_4	N_2H_4	
Mixture Ratio, Nominal at Standard Conditions (1) (O/F)	1.15	0.0	
Thrust, Steady-State Nominal at Standard Conditions ⁽¹⁾ , N(lb _f)	4500.0 (1010.0)	1600.0 (360.0) approx.	
Specific-Impulse, Steady-State Minimum at Standard Conditions, (1), N-s/kg (lb _f -s/lb _m)	3050.0 (311.0)	2300.0 (234.0)	
Impulse Repeatability, 3σ Intermodal Decay Transient, N-s (lb _f -s)	300.0 (67.3)		
Shutdown, N-s (lb _f -s)		22.0 (4.9)	
Propellant Supply Pressures at Engine Inlets, kN/m ² (psia)			TBD ⁽²⁾ in the range 1400-2100.0 (203 - 305)
Fuel Metering			Cavitating Venturi
Gaseous Helium Propellant Saturation Acceptance (%)			up to 100.0
Mass, Maximum, kg (lb _m)			27.0 (59.5)
Operating Duration Capability			
Minimum Total (3) _s	1500.0	1000.0	
Maximum Continuous, (3) _s	1000.0	500.0	
Minimum Continuous, s	10.0	1.0	
Duty Cycle Restrictions			none ⁽⁴⁾
Propellant Manifold Purges			none
Thrust Vector Misalignment, Maximum Relative to Geometric Thrust Vector			
Angular (deg)			±0.5
Offset, mm (in.)			1.3 (0.051)
TVC Gimbal Angle, in Two Orthogonal Planes (deg)			±8.0
Gimbal Torque, Maximum at 960 deg./sec ² , m-N (in-lb _f)			17.0 (149.0)
B. Thrust Chamber Characteristics			
Type			all-metallic; radiation-cooled (outer) wall
Chamber Pressure, Nominal			
Nozzle Stagnation, kN/m ² (psia)	900.0 (130.0)	TBD ⁽²⁾ 320.0 (46.3), approx.	
Expansion Area Ratio			60:1
Combustion Length, Minimum, m (in.) Bipropellant Impingement-to-Throat			0.21 (8.25)
Nozzle Contour			80% Bell
C. Reactor Characteristics			
Type	Spontaneous Catalytic		
Catalyst	Shell 405 ABSG (or mixed Shell 405 ABSG/HA-3)		
Startup Temperature Capability, Bed, K (°F)	272.0 (32.0) to steady-state thermal equilibrium		
Fuel, K (°F)	278.0 to 311.0 (40.0 to 100.0)		

TABLE 3 SI
SUMMARY OF REGENERATIVE THROAT WALL TEMPERATURES
FOR VARIOUS CONFIGURATIONS

Analysis Constants: 25% Land

Mach No. = 1.0 Monomode 95% c*

No. of Passages	Throat Pressure (Monomode) kN/m ²	Film Coefficient h_g	Throat Wall Temp.
		joules/m ² sec K	K
50	551.7	3245	1703
50	689.7	3245	1678
50	551.7	1770	1542
50	689.7	1770	1522
50	689.7	1180	1456
Annulus	689.7	1770	1689

TABLE 4 SI
BIMODAL ENGINE CONFIGURATIONS MASS ANALYSIS

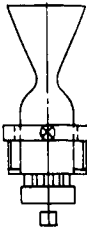
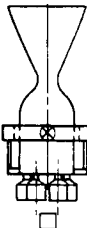
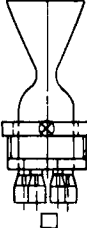
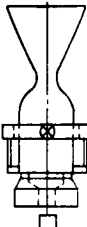
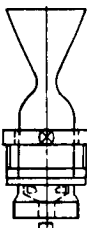
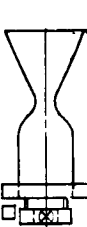
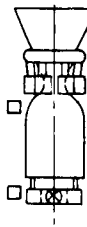
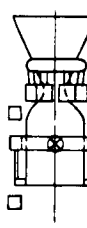
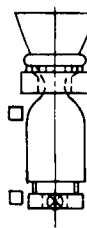
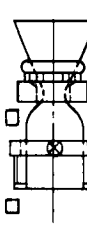
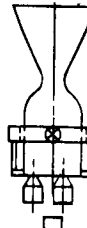
	Figure A Secondary Inj. Station Single Reactor Welded Interface	Figure B Secondary Inj. Station 6 Cylindrical Reactors Welded Interface (Typical)	Figure C Secondary Inj. Station 6 Cylindrical Reactors Flanged Interface (Typical)	Figure D Secondary Inj. Station Annular Reactor Welded Interface	Figure E Secondary Inj. Station Annular Reactor Flanged Interface	Figure F Secondary Inj. Station Radial Inflow Annular Reactor
Thrust = 4500 Newtons Chamber Pressure = 900 kN/m ² c = 60, 80% Ball N ₂ O ₄ /N ₂ H ₄ Propellants						
	Mass - Kilograms	Mass - Kilograms	Mass - Kilograms	Mass - Kilograms	Mass - Kilograms	Mass - Kilograms
Reactor	4.2	4.0	4.9	5.3	5.0	7.7
Secondary Injector	9.3	7.4	7.4	7.4	12.7	5.7
Chamber	15.3	15.3	15.3	15.3	19.6	15.3
Nozzle Extension	4.8	4.8	4.8	4.8	4.8	4.8
TCA	33.6	31.5	32.4	32.8	(42.1)	(33.5)
Oxidizer Valve	2.0	2.0	2.0	2.0	2.0	2.0
Fuel Valve	1.7	1.7	1.7	1.7	1.7	1.7
Valve Mounts and Feed Tubes	1.1	1.1	1.1	1.1	1.1	1.1
Gimbal Ring Flexure	2.1	2.3	2.3	2.3	2.3	1.6
Pivot	2.0	2.3	2.3	2.3	2.3	...
Engine Mount	42.5	40.9	41.8	42.2	51.5	39.9
Engine Assembly						
	Figure G Throat Station 6 Cylindrical Reactors Welded Head Mounted Gimbal	Figure H Throat Station 6 Cylindrical Reactors Welded Throat Mounted Gimbal	Figure I Throat Station Annular Reactor Welded Head Mounted Gimbal	Figure J Throat Station 2 Section Annular Re- actor - Welded Throat Mounted Gimbal	Figure K Secondary Inj. Station 3 Cylindrical Re- actors Welded Interface Throat Mounted Gimbal	
						
	Mass - Kilograms	Mass - Kilograms	Mass - Kilograms	Mass - Kilograms	Mass - Kilograms	
Reactor	4.9	4.9	5.2	5.2	3.9	
Secondary Injector	5.7	6.0	5.7	6.0	4.9	
Chamber	14.3	14.3	14.3	14.3	15.3	
Nozzle Extension	4.8	4.8	4.8	4.8	4.8	
TCA	(29.7)	(30.0)	(30.0)	(30.3)	(28.9)	
Oxidizer Valve	2.0	2.0	2.0	2.0	2.0	
Fuel Valve	1.7	1.7	1.7	1.7	1.7	
Valve Mount - Feed Tube Reactor Supports	1.8	1.1	1.8	1.1	1.1	
Gimbal Ring Flexure	1.6	1.9	1.6	1.9	2.3	
Pivot	...	2.2	...	2.2	2.3	
Engine Mount	36.8	38.9	37.1	39.2	38.3	
Engine Assembly						

TABLE 5 SI
REGENERATIVELY COOLED BIMODAL ENGINE MASS ANALYSIS INPUTS

Operation Requirements

Thrust = 4500 Newtons

Chamber Pressure = 900 kN/m²

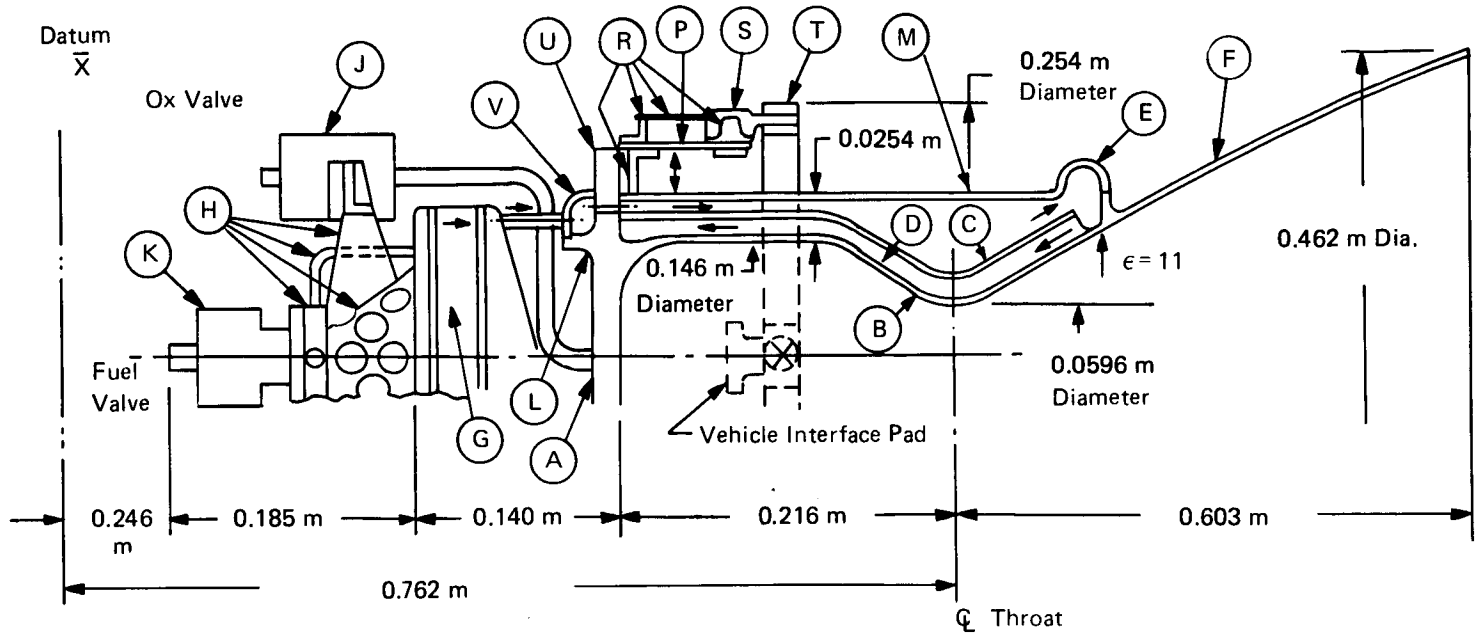
ϵ = 60, 80% Bell

N₂O₄/N₂H₄ Propellants

Material Used	Density kg/m ³
Columbium Alloy	
C103	8.86 x 10 ³
Scb291	9.695 x 10 ³
Titanium Alloy	
6Al-4V	4.43 x 10 ³
Shell 405	
20-30 Mesh	1.55 x 10 ³
1/8 in. Pellets	1.16 x 10 ³

<u>Item</u>	<u>Input</u>
A	Secondary injector 80% solid
D	Coolant Passages - 30 required
	Chamber 1.0 cm Wide x 1.01 cm High
	Throat 0.493 cm Wide x 1.27 cm High
	Manifold 1.0 cm Wide x 1.27 cm High
E	Torus manifold Diameter = 3.56 cm
F	Divergent nozzle extension tapered from 0.153 cm to 0.051 cm thickness
G	Catalyst bed volume = 0.0012 m ³
J	Oxidizer valve - torque motor
K	Fuel valve - solenoid
L	Outer coolant jacket length - 35.6 cm
M	Manifold torus at secondary injector - 3.18 cm

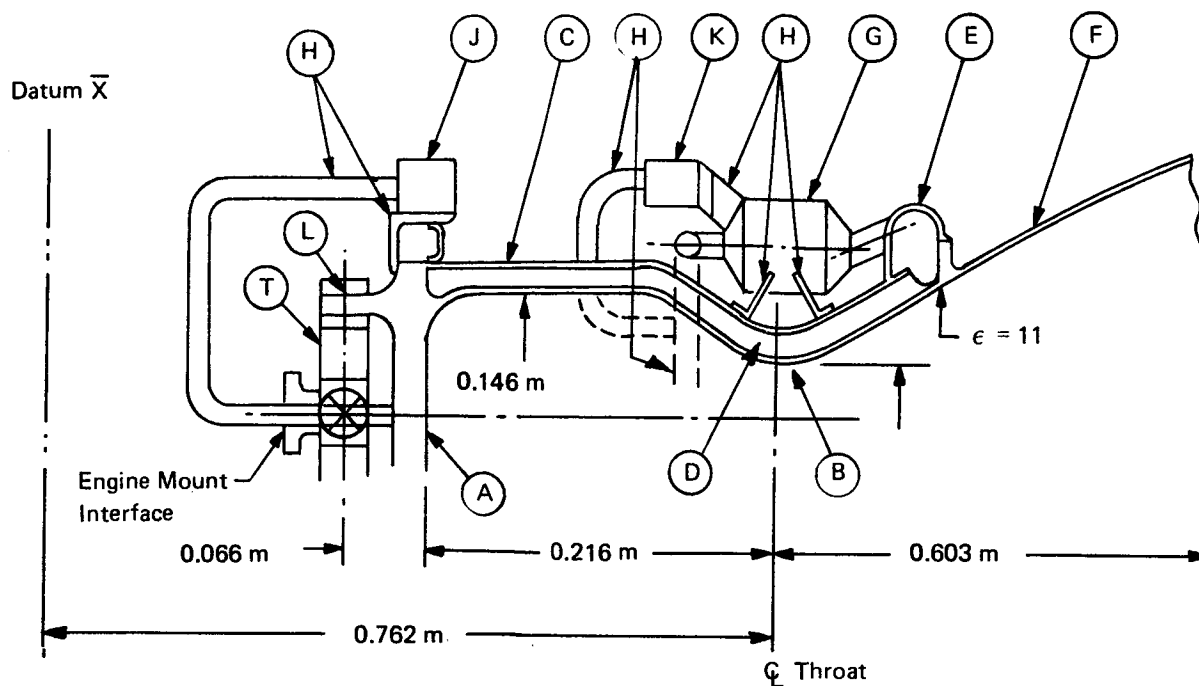
TABLE 6 SI
BIMODAL ENGINE SINGLE BED REACTOR
THROAT MOUNTED GIMBAL RING



Item		Thick (m)	Material	Mass. (kg)			\bar{X} (m)
G	Reactor - Single Can		C103		4.173		0.457
	Secondary Injector				9.344		0.528
A	Basic Injector	0.0286	C103	5.035			0.533
L	Δ Mass.		C103	1.905			0.533
U	Δ Mass. Inj. for Eng. Mt.		C103	1.814			0.521
V	Δ Mass. Manif. Inj.	0.00127	C103	0.590			0.503
	Chamber				15.290		0.699
B	Inner Liner	0.00178	Scb291	3.084			0.528
C	Outer Liner	0.00178	C103	1.724			0.770
D	Channel Walls			6.76			0.700
E	Torus Manifold	0.00178	C103	1.36			0.739
M	Outer Coolant Jacket	0.00127	C103	2.36			0.871
F	Nozzle Extension $\epsilon=11$ to $\epsilon=60$	0.00152 to 0.0005	C103		4.76		0.747
	TCA					33.56	0.699
J	Ox Valve		St.		2.04		0.355
K	Fuel Valve		St.		1.72		0.305
H	Valve Mts. and Feed Tubes		C103		1.13		0.381
T	Gimbal Ring-Flexure Pivot	0.00254	Ti		2.13		0.643
	Engine Mount				2.00		0.610
P	Cylinder	0.00127	Ti	0.499			0.607
R	Rings and Stringers	0.00102 to 0.00076	Ti	0.862			0.601
S	Gimbal Lugs		Ti	0.635			0.610
Engine Assy.						42.60	0.650

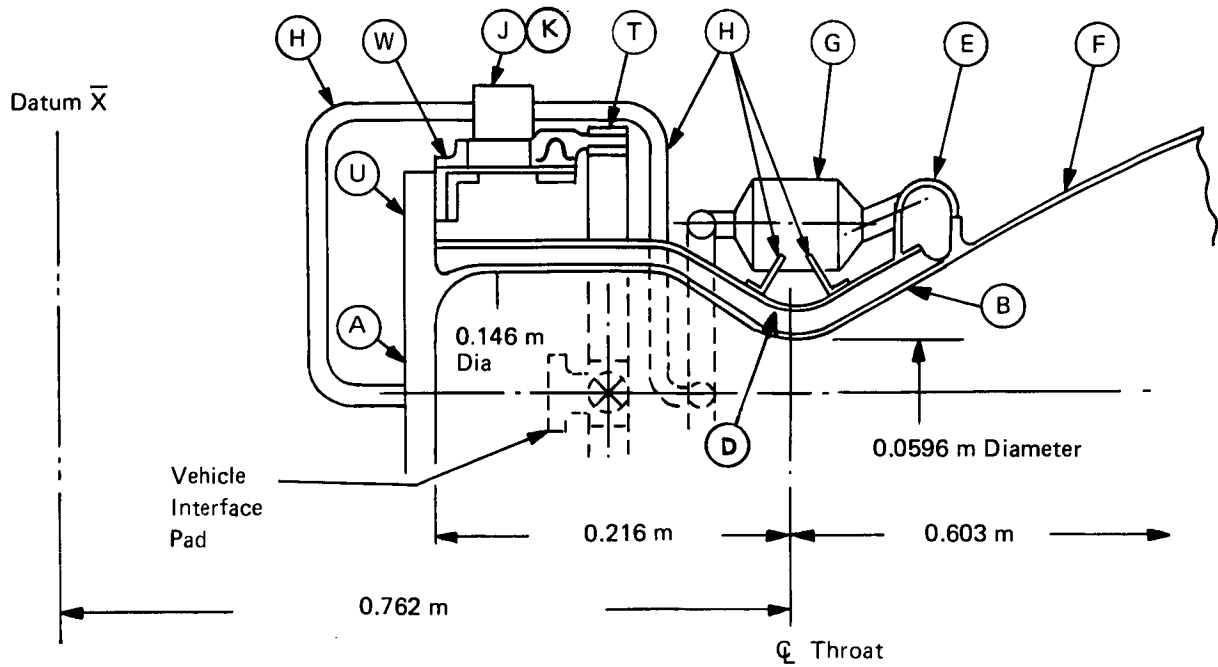
Note: Δ Mass. Tradeoff-tubes in lieu of outer coolant jacket - 0.4536 kg.

TABLE 7 SI
BIMODAL ENGINE 6 CYLINDRICAL REACTORS
HEAD MOUNTED GIMBAL RING



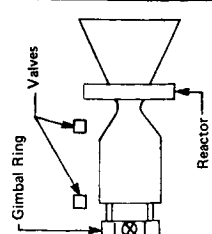
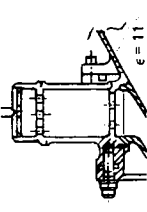
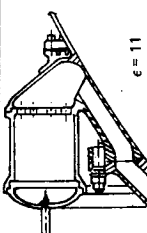
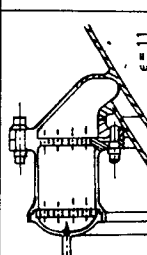
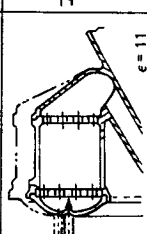
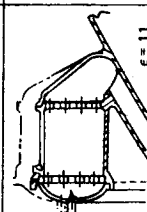
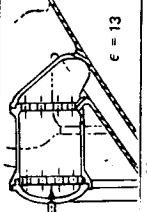
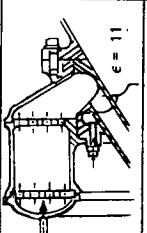
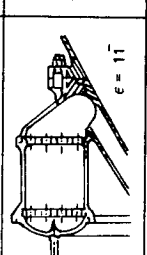
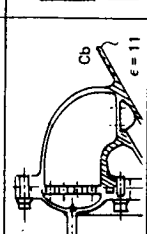
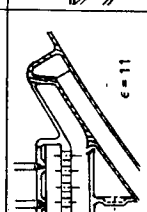
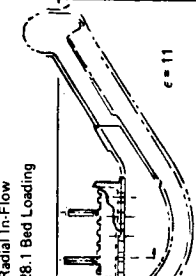
Item		Thick (m)	Material	Mass (kg)			\bar{X} (m)
G	Reactor - Cluster (6)				4.840		0.772
A	Secondary Injector				5.674		0.532
L	Basic Injector	0.0286	C103	5.030			0.533
	Δ Mass Injector for Gimbal Ring			0.644			0.518
	Chamber				14.300		0.750
B	Inner Liner	0.00178	Scb291	3.100			0.768
C	Outer Liner	0.00178	C103	3.08			0.699
D	Channel Walls		Scb291	6.76			0.739
E	Torus Manifold	0.00178	C103	1.36			0.871
F	Nozzle Extension $\epsilon-11$ to $\epsilon-60$	0.00152 to 0.0005	C103		4.749		1.092
	TCA					29.563	0.766
J	Oxidizer Valve		St.		2.041		0.533
K	Fuel Valve		St.		1.701		0.762
H	Valve Mount Feed Tube, Reactor Supports		C103		1.814		0.749
T	Gimbal Ring		Ti		1.588		0.508
Engine Assembly					36.71		0.742

TABLE 8 SI
BIMODAL ENGINE 6 CYLINDRICAL REACTORS
THROAT MOUNTED GIMBAL RING



Item		Thickness (m)	Mat'l	Mass. (kg)		\bar{X} (m)
G	Reactor-Cluster (6)			4.840		0.772
	Secondary Injector			5.983		0.532
A	Basic Injector	0.0286	C103	5.030		0.533
U	Δ Mass. Inj. for Engine Mount			0.952		0.533
	Chamber				14.297	0.750
B	Inner Liner	0.00178	Scb291	3.098		0.768
C	Outer Liner	0.00178	C103	3.080		0.699
D	Channel Walls		Scb291	6.759		0.739
E	Torus Manifold	0.00178	C103	1.361		0.871
F	Nozzle Extension ϵ -11 to ϵ -60	0.00152	C103		4.749	1.092
	TCA				29.856	0.764
J	Ox Valve		St.		2.041	0.635
K	Fuel Valve		St.		1.701	0.635
H	Valve Mounts, Feed Tubes, Reactor Supports		Ti		1.134	0.749
T	Gimbal Ring		C103		1.905	0.642
W	Engine Mount		Ti		2.223	0.608
Engine Assy.					38.874	0.737

TABLE 9 SI
BIMODAL ENGINE CONFIGURATION MASS ANALYSIS

<p>Bed Loading: 28.1 kg/m²s 21.1 kg/m²s</p> 	<p>Figure A L605 Reactor C103 Bolted Nozzle Ext. Div. Nozzle Station Radial Inflow Reactor Bolted Joint 28.1 Bed Loading</p>  <p>Mass = kg</p>	<p>Figure B L605 Reactor C103 Bolted Nozzle Ext. Div. Nozzle Station Axial Flow Reactor Bolted Joint 28.1 Bed Loading</p>  <p>Mass = kg</p>	<p>Figure C L605 Reactor C103 Bolted Nozzle Ext. Div. Nozzle Station Axial Flow Reactor Bolted Joint 28.1 Bed Loading</p>  <p>Mass = kg</p>	<p>Figure D C103 Reactor - Welded C103 Welded Nozzle Ext. Div. Nozzle Station Axial Flow Reactor 28.1 Bed Loading</p>  <p>Mass = kg</p>	<p>Figure E C103 Reactor - Welded C103 Welded Nozzle Ext. Div. Nozzle Station Axial Flow Reactor 21.1 Bed Loading</p>  <p>Mass = kg</p>	<p>Figure F C103 Reactor - Welded C103 Welded Nozzle Ext. Div. Nozzle Station $\epsilon=13$ Axial Flow Reactor 28.1 Bed Loading Div. Nozzle Sta. $\epsilon=10$ Same as D</p>  <p>Mass = kg</p>	<p>Figure G L605 Reactor - Bolted C103 Bolted Nozzle Extension Div. Nozzle Station Axial Flow Reactor 28.1 Bed Loading</p>  <p>Mass = kg</p>	<p>Figure H C103 Reactor - Bolted C103 Bolted Nozzle Ext. Div. Nozzle Station Axial Flow Reactor 28.1 Bed Loading</p>  <p>Mass = kg</p>	<p>Figure I L605/C103 Reactor - Bolted C103 Welded Nozzle Ext. Div. Nozzle Station Axial Flow Reactor 28.1 Bed Loading</p>  <p>Mass = kg</p>	<p>Figure J C103 Reactor - Welded C103 Welded Nozzle Extension Div. Nozzle Station Radial In-Flow 28.1 Bed Loading</p>  <p>Mass = kg</p>	<p>Figure K C103 Reactor - Welded C103 Welded Nozzle Extension Throat Station Radial In-Flow 28.1 Bed Loading</p>  <p>Mass = kg</p>
<p>Reactor Secondary Injector Chamber Nozzle Extension TCA Ox. Valve Fuel Valve Valve Mounts and Feed Tubes Gimbal Ring Engine Assembly</p>	<p>Reactor Secondary Injector Chamber Nozzle Extension TCA Ox. Valve Fuel Valve Valve Mounts and Feed Tubes Gimbal Ring Engine Assembly</p>	<p>Reactor Secondary Injector Chamber Nozzle Extension TCA Ox. Valve Fuel Valve Valve Mounts and Feed Tubes Gimbal Ring Engine Assembly</p>	<p>Reactor Secondary Injector Chamber Nozzle Extension TCA Ox. Valve Fuel Valve Valve Mounts and Feed Tubes Gimbal Ring Engine Assembly</p>	<p>Reactor Secondary Injector Chamber Nozzle Extension TCA Ox. Valve Fuel Valve Valve Mounts and Feed Tubes Gimbal Ring Engine Assembly</p>	<p>Reactor Secondary Injector Chamber Nozzle Extension TCA Ox. Valve Fuel Valve Valve Mounts and Feed Tubes Gimbal Ring Engine Assembly</p>	<p>Reactor Secondary Injector Chamber Nozzle Extension TCA Ox. Valve Fuel Valve Valve Mounts and Feed Tubes Gimbal Ring Engine Assembly</p>	<p>Reactor Secondary Injector Chamber Nozzle Extension TCA Ox. Valve Fuel Valve Valve Mounts and Feed Tubes Gimbal Ring Engine Assembly</p>	<p>Reactor Secondary Injector Chamber Nozzle Extension TCA Ox. Valve Fuel Valve Valve Mounts and Feed Tubes Gimbal Ring Engine Assembly</p>	<p>Reactor Secondary Injector Chamber Nozzle Extension TCA Ox. Valve Fuel Valve Valve Mounts and Feed Tubes Gimbal Ring Engine Assembly</p>	<p>Reactor Secondary Injector Chamber Nozzle Extension TCA Ox. Valve Fuel Valve Valve Mounts and Feed Tubes Gimbal Ring Engine Assembly</p>	<p>Reactor Secondary Injector Chamber Nozzle Extension TCA Ox. Valve Fuel Valve Valve Mounts and Feed Tubes Gimbal Ring Engine Assembly</p>

Note: The engine assembly configuration positions the gimbal ring at the secondary injector. The Δ mass change for a c.g. mounted gimbal ring using an engine mount shell is +2.31 kg.

TABLE 10 SI
SUMMARY OF TABLE 9

Fig. No.	Bed Loading $\frac{\text{kg}}{\text{m}^2 \text{ sec}}$	Area Ratio at End of Reactor	Material of Reactor Ass'y	Bolted or Welded	Hydrazine Injection Type	Diverg. Nozzle Ext. Material	TCA	
							kg	lb
A	28.1 *	$\epsilon = 10$	L605	Bolted	Radial - in	C103	32.5	71.7
B	28.1	$\epsilon = 10$	L605	Bolted	Axial	C103	30.1	66.4
C	28.1	$\epsilon = 10$	L605/C103	Bolted	Axial	C103	30.5	67.3
D	20.2 **	$\epsilon = 10$	C103	Welded	Axial	C103	27.4	60.5
E	28.1	$\epsilon = 10$	C103	Welded	Axial	C103	29.1	64.2
F	20.2	$\epsilon = 13$	C103	Welded	Axial	C103	29.9	66.0
G	28.1	$\epsilon = 10$	L605/C103	Bolted	Axial	C103	31.2	68.8
H	↓	↓	C103	Bolted	Axial	C103	29.5	65.1
I		↓	L605/C103	Bolted	Axial	C103	30.3	66.9
J		Throat	C103	Welded	Radial - in	C103	26.6	58.7
K		Throat	C103		Radial - in	C103	26.0	57.4

* 0.04 lb/sec in²

** 0.03 lb/sec in²

TABLE 11 SI
BIMODAL CHAMBER ASSEMBLY CONFIGURATIONS
CHANNEL, DRILLED, ANNULAR

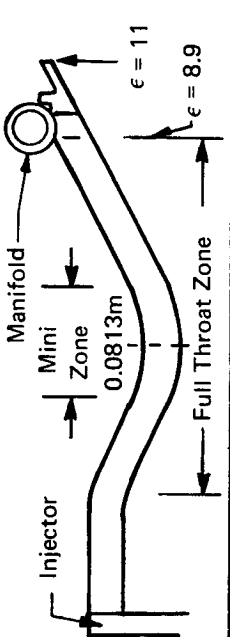
Typical Channel Design 	All Channel $\epsilon = 8.9$	Throat Full Channel $\epsilon = 8.9$	Throat Mini Channel	All Annular	All Drilled $\epsilon = 6.2$	Throat Full Drill $\epsilon = 6.2$	Throat Mini Drill
	kg	kg	kg	kg	kg	kg	kg
Injector	5.03	5.03	5.03	5.03	5.03	5.03	5.03
Chamber	[14.30]	[12.31]	[8.19]	[8.00]	[14.21]	[12.49]	[8.82]
Barrel Zone	(4.16)	(2.17)	(2.17)	(2.30)	(3.89)	(2.17)	(2.17)
Inner Liner	0.82	0.82	0.82	0.82		0.82	0.82
Outer Liner	1.34	1.25	1.25	1.34		1.25	1.25
Channel Lands	2.00	0.10	0.10	0.14		0.10	0.10
Throat and Manifold	(10.14)	(10.14)	(6.02)	(5.70)	(10.32)	(10.32)	(6.65)
Inner Liner	2.28	2.28	2.28	2.28			2.28
Outer Liner	1.74	1.74	1.74	1.74			1.74
Channel Lands	4.76	4.76	0.64	0.32			1.27
Torus Manifold	1.36	1.36	1.36	1.36			1.36
Δ Mass to Extend Drill Passages (to $\epsilon = 8.9$)	—	—	—	—	+2.99	+2.99	—
Total Chamber Assembly (Mass Cutoff at $\epsilon = 11$)	19.33	17.34	13.22	13.03	22.23	20.51	13.85

TABLE 12 SI
BIMODAL CONFIGURATION CHANGES, HEAD - MOUNTED REACTOR (6)

	Baseline		Head Mounted Reactor					
	$\epsilon = 8.9$		$\epsilon = 4.2$ (1755K)		$\epsilon = 7.8$ (1589K)		$\epsilon = 18$ (1366K)	
	Material	kg	Material	kg	Material	kg	Material	kg
Chamber Assembly		(15.28)		(12.05)		(14.17)		(23.40)
Inner Liner	Scb291	3.08		2.48		3.02		4.37
Outer Liner	C103	1.72		1.50		1.72		4.06
Channel Walls	Scb291	6.76		5.14		6.23		9.69
Torus Manifold	C103	1.36		1.00		1.32		2.06
Outer Coolant Jacket	C103	2.36		1.93		1.88		3.22
Diverg. Nozzle Extension	C103	(4.76)	C103	(5.08)	C103	(4.80)	L605	(4.13)
Δ Mass to Chamber Assembly if Transfer Tubes used in Lieu of Outer Coolant Jacket		-0.45		-0.32		-0.45		-1.63

TABLE 13 SI
BIMODAL CONFIGURATION CHANGES, THROAT - MOUNTED REACTOR (6)

	Baseline		Throat Mounted Reactor					
	$\epsilon = 8.9$		$\epsilon = 4.2$ (1755K)		$\epsilon = 7.8$ (1589K)		$\epsilon = 18$ (1366K)	
	Material	kg	Material	kg	Material	kg	Material	kg
Chamber Assy		(14.30)		(11.24)		(13.54)		(20.18)
Inner Liner	Scb291	3.10		2.48		3.03		4.37
Outer Liner	C103	3.08		2.63		2.97		4.06
Channel Walls	Scb291	6.76		5.13		6.23		9.69
Torus Manifold	C103	1.36		1.00		1.31		2.06
Div. Nozzle Extension	ϵ -11 to -60	(4.75)	C103	(5.08)	C103	(4.81)	L605	(4.13)

TABLE 14 SI AND 14

	Hg = 3280 (Hg - 11) (95% c*)				Hg = 1770 (Hg - 6) (100% c*)			
	$\epsilon = 4.2$		$\epsilon = 7.8$		$\epsilon = 5.0$		$\epsilon = 11.0$	
	Scb-291 Noz. Ext. 1755K at $\epsilon = 4.2$ (2700°F)		Cb-103 Noz. Ext. 1589K at $\epsilon = 7.8$ (2400°F)		Cb-103 Noz. Ext. 1589K at $\epsilon = 5.0$ (2400°F)		L-605 Noz. Ext 1367K at $\epsilon = 11.0$ (2000°F)	
	Mass kg	(lb)	Mass kg	(lb)	Mass kg	(lb)	Mass kg	(lb)
A. Reactor at Sec. Inj. (cg Gimbal)	34.0	(75.0)	34.4	(75.9)	33.6	(74.0)	34.7	(76.6)
	35.3	(77.9)	35.9	(79.1)	34.7	(76.6)	36.0	(79.4)
B. Reactor at Throat	30.4	(67.0)	30.8	(68.0)	29.8	(65.7)	31.0	(68.4)
	32.6	(71.8)	33.0	(72.8)	32.0	(70.5)	33.2	(73.2)
C. Reactor at Noz/Ext Joint	27.4	(60.4)	27.6	(60.8)	26.8	(59.1)	27.7	(61.1)
	29.6	(65.2)	29.8	(65.6)	29.0	(63.9)	29.9	(65.9)

TABLE 15 SI AND 15
EVALUATION RATINGS FOR REGENERATIVE CHAMBERS,
REACTORS AND NOZZLE EXTENSIONS
REGENERATIVE CHAMBER

Major Parameter		Performance										High Durability/Life										Ease of Fabrication		Low Risk		Low Cost		Low Mass		Summary
Weight Factor		2.0										2.5										1.0		2.0		1.0		1.5		
Element	Adjustment % (If Any)	Transient Mono Isp		Transient Biprop Isp		γp	Total Rating No.	Wt. Factor	Total Rating No. X	Low Wall Temp	Thermal Stress	Mech. Stress	Total Rating No.	Total Rating No. X	Rating No.		Total	Rating No.		Total	Rating No.		Total	Rating No.		Total				
		Full	0.75	Full	1.25										Full	5		4	3		Full	1		2	Full		1	2	Full	1
Column Number		1	2	3	4	5	2 + 4 + 5 3		A	6	7	8	6 + 7 + 8 3		B	C		D		E	F		A + B + C + D + E + F							
A. Throat Passages		8	60	10	12.5	9	9.2	18.4	9.3	10	9	9	9.3	23.2	8	8.0	9	18.0	8	8.0	9	9.0	3	4.5	80.1					
A.1 All Channel		8	60	10	12.5	9	9.2	18.4	9.3	10	9	9	9.3	23.2	8	8.0	9	18.0	8	8.0	9	9.0	3	4.5	80.1					
A.2 Mini Channel		9	67.5	10	12.5	9	9.4	18.6	9.0	9	9	9	9.0	22.5	9	9.0	9	18.0	9	9.0	9	9.0	1	1.5	80.6					
A.3 All Drilled		7	5.25	10	12.5	7	8.2	16.4	8.7	8	8	10	8.7	21.8	5	5.0	10	20.0	5	5.0	10	5.0	1	1.5	80.6					
A.4 Mini Drilled		8	60	10	12.5	8	8.8	17.6	8.3	8	8	9	8.3	20.8	7	7.0	10	20.0	7	7.0	10	7.0	7	7.0	85.9					
A.5 Annulus		10	7.5	10	12.5	10	9.9	19.8	8.0	6	10	8	8.0	20.0	10	10.0	8	16.0	10	10.0	10	10.0	10	15.0	90.8					
B. Chamber (Barrel)		8	60	10	12.5	9	9.2	18.4	9.3	10	9	9	9.3	23.2	9	9.0	9	18.0	9	9.0	2	3.0	80.6							
B.1 All Channel		8	60	10	12.5	9	9.2	18.4	9.3	10	9	9	9.3	23.2	9	9.0	9	18.0	9	9.0	2	3.0	80.6							
B.2 All Drilled		7	5.25	10	12.5	9	8.9	17.8	8.7	8	8	10	8.7	21.8	7	7.0	10	20.0	7	7.0	1	1.5	75.1							
B.3 Annulus		10	7.5	10	12.5	10	9.8	19.6	9.3	9	10	9	9.3	23.2	10	10.0	8	16.0	10	10.0	10	10.0	10	15.0	93.8					
C. Number of Passages		10	7.5	10	12.5	10	10.0	20.0	10.0	10	10	10	10.0	25.0	8	8.0	10	20.0	9	9.0	10	15.0	97.0							
C.1 50		10	7.5	10	12.5	10	10.0	20.0	10.0	9	9	9	10.0	25.0	9	9.0	9	18.0	10	10.0	10	15.0	94.5							
C.2 30		10	7.5	10	12.5	10	10.0	20.0	10.0	9	9	9	10.0	25.0	8	8.0	10	20.0	9	9.0	10	15.0	94.5							
D. % Land Width		10	7.5	10	12.5	10	10.0	20.0	9.7	9	10	10	9.7	24.2	9	9.0	9	18.0	10	10.0	10	15.0	96.2							
D.1 25%		10	7.5	10	12.5	10	10.0	20.0	9.7	9	10	10	9.7	24.2	9	9.0	9	18.0	10	10.0	10	15.0	96.2							
D.2 50%		9	6.75	10	12.5	10	9.75	19.5	9.3	10	8	10	9.3	23.2	8	8.0	10	20.0	9	9.0	8	12.0	91.7							
E. Mono Mach No.		10	7.5	10	12.5	9	9.7	19.4	9.3	10	9	9	9.3	23.2	10	10.0	10	20.0	10	10.0	10	15.0	97.6							
E.1 1.0		10	7.5	10	12.5	9	9.7	19.4	9.3	10	9	9	9.3	23.2	10	10.0	10	20.0	10	10.0	10	15.0	97.6							
E.2 0.65		10	7.5	10	12.5	10	10.0	20.0	9.7	9	10	10	9.7	24.2	10	10.0	9	18.0	10	10.0	9	13.5	95.7							
F. Mono Total Pressure		10	7.5	10	12.5	9	9.7	19.4	9.7	10	10	9	9.7	24.2	10	10.0	10	20.0	10	10.0	10	15.0	98.6							
F.1 100		10	7.5	10	12.5	9	9.7	19.4	9.7	10	10	10	9.7	24.2	10	10.0	10	20.0	10	10.0	10	15.0	98.6							
F.2 80		10	7.5	10	12.5	10	10.0	20.0	9.7	9	10	10	9.7	24.2	10	10.0	9	18.0	10	10.0	10	15.0	95.7							

TABLE 15 SI AND 15 (CONT)
REACTOR

Major Parameter		Performance						Durability/Life (High)						Ease of Fabrication		Low Risk		Low Cost		Low Mass		Summary
Weight Factor		2.0						2.5						1.0		2.0		1.0		1.5		
Element	Trans- ient Mono	Trans- ient Riprop	UP	Total Rating (TR)	T.R. x W.F.	Welds	Stress	Reactor/ Chamber Joint	Total Rating (TR)	T.R. x W.F.	Rating No.	Total	Rating No.	Total	Rating No.	Total	Rating No.	Total				
Adjustment %	0.75	1.25	1	$\frac{(1)+(2)+(3)}{3}$	(A)	(4)	(5)	(6)	$\frac{(4)+(5)+(6)}{3}$	(B)	(C)	(D)	(E)	(F)	(A)+(B)+(C)+(D)+(E)+(F)							
Column No.	(1)	(2)	(3)																			
Configuration																						
A. Reactor at Secondary Station																						
A-1 Single Cyl. (Axial) - Tube	Eliminated - Too Bulky																			83.1		
A-2 Multiple Cyl. (Axial) - Tubes	8/6	10/12.5	10	9.5	18.6	4	10	10	8.0	20.0	9	9.0	8	16.0	9	9.0	7	10.5				
A-3 Multiple Cyl. (Radial-in) - Tubes	Eliminated - Too Bulky																					
A-4 Single Cyl. (Axial) - Annular Passages	8/6	10/12.5	10	9.5	18.6	5	5	8	6.0	15.0	8	8.0	6	12.0	8	8.0	6	9.0		70.6		
A-5 Multiple Cyl. (Axial) - Annular Passages	8/6	10/12.5	10	9.5	18.6	4	10	8	7.3	18.3	6	6.0	7	14.0	6	6.0	6	9.0		71.9		
A-6 Multiple Cyl. (Radial-in) - Annular Passages	Eliminated - Too Bulky																			81.6		
A-7 Annular (Axial) - Annular Passages	8/6	10/12.5	10	9.5	18.6	10	6	8	8.0	20.0	9	9.0	8	16.0	9	9.0	6	9.0				
A-8 Annular (Radial) - Annular Passages	8/6	10/12.5	10	9.5	18.6	10	4	6	6.6	16.5	5	5.0	5	10.0	5	5.0	7	10.5				
B. Reactor at Throat																						
B-1 Single Cyl. (Axial) - Tube	Eliminated - Too Bulky																			65.7		
B-2 Multiple Cyl. (Axial) - Tubes	9/6.75	10/12.5	10	9.75	19.2	2	5	8	5.0	12.5	6	6.0	5	10.0	6	6.0	8	12.0				
B-3 Multiple Cyl. (Radial-in) - Tubes	Eliminated - Too Bulky																					
B-4 Annular (Axial) - One Piece	Eliminated - Too Bulky																			63.0		
B-5 Annular (Radial-in) - One Piece	9/6.75	10/12.5	10	9.75	19.2	8	4	4	5.3	13.3	5	5.0	5	10.0	5	5.0	7	10.5				
B-6 Annular (Axial) - Two Piece	9/6.75	10/12.5	10	9.75	19.2	7	5	8	6.6	16.5	7	7.0	6	12.0	7	7.0	7	10.5				
B-7 Annular (Radial-in) - Two Piece	9/6.75	10/12.5	10	9.75	19.2	4	5	6	5.0	12.5	5	5.0	5	10.0	5	5.0	10	15.0		72.2		
C. Reactor at Nozzle/Extension Interface																						
C-1 Single Cyl. (Axial) - Tube	Eliminated - Too Bulky																			89.0		
C-2 Multiple Cyl. (Axial) - Tubes	Same as Configuration B-2																					
C-3 Multiple Cyl. (Radial-in) - Tubes	Eliminated - Too Bulky																					
C-4 Annular (Axial) - One Piece	10/7.5	10/12.5	10	10.0	20.0	10	5	8	7.6	19.0	10	10.0	7.5	15.0	10	10.0	10	15.0		85.0		
C-5 Annular (Radial-in) - One Piece	10/7.5	10/12.5	10	10.0	20.0	10	5	8	7.6	19.0	10	10.0	7.5	15.0	10	10.0	8	12.0		62.8		
C-6 Annular (Axial) - Two Piece	10/7.5	10/12.5	10	10.0	20.0	9	5	8	7.3	18.3	7	7.0	7.0	14.0	7	7.0	9	13.5				
C-7 Annular (Radial-in) - Two Piece	10/7.5	10/12.5	10	10.0	20.0	7	5	8	6.6	16.5	7	7.0	6.5	13.0	7	7.0	10	12.0			75.5	

*First Number is Full Rating - Second Number is Adjusted Rating

TABLE 15 SI AND 15 (CONT)
NOZZLE EXTENSION

Major Parameter	Performance					High Durability/Life					Ease of Fabrication		Low Risk		Low Cost		Low Mass		Summary
	2.0					2.5					1.0		2.0		1.0		1.5		
Weight Factor (W.F.)																			
Element	High Mono I _{sp}	High Biprop I _{sp}	Total Rating No.	T.R. x W.F.	Low Wall Temp	Low Thermal Stress	High Thermal Margin	Total Rating No.	T.R. x W.F.	Rating No.	T.R. x W.F.	Rating No.	T.R. x W.F.	Rating No.	T.R. x W.F.	Rating No.	T.R. x W.F.	Rating No.	
Adjustment % (if Any)	Full	0.75	1.25	Full	①	②	③	④	⑤	⑥	⑦	⑧	⑨	⑩	⑪	⑫	⑬	⑭	
Column No.	①	②	③	④	⑤	⑥	⑦	⑧	⑨	⑩	⑪	⑫	⑬	⑭	⑮	⑯	⑰	⑱	⑲
A Extension SCB-291 Interface with Regen Chamber at ε = 4.2 or 2.5 (Temp = 2700°) Exit C = 60	10	7.5	10	12.5	20.0	8	8	8.3	20.8	8	8.0	10	20.0	8	8.0	10	15.0	91.8	
B Extension C-103 Interface with Regen Chamber at ε = 7.8 or 5.0 (Temp = 2400 F) Exit C = 60	9	6.8	10	12.5	19.2	9	3	9.3	23.3	10	10.0	10	20.0	10	10.0	9	13.5	96.0	
C Extension L-605 Interface with Regen Chamber at ε = 18 or 11.0 Exit C = 60	8	6.0	10	12.5	18.4	10	10	9.7	24.2	9	9.0	8	16.0	8	8.0	5	7.5	83.1	

TABLE 16 SI AND 16
SUMMARY — REGENERATIVE CHAMBER DESIGN PARAMETER EFFECT
ON THROAT TEMPERATURE

Assumptions for Baseline

1. Material SCB 291
2. No. of Passages 50
3. % Land Width 25%
4. %c* 100%
5. NH₃ Dissociation 50%
6. Cooling Enhancement None
7. hg (Hot Gas Film Coefficient) 1770 joule/m² sec K (6.0 x 10⁻⁴ BTU/in.² sec °F)
8. Mono Mach No. 1.0
9. Mono Total Pressure 690 KN/m² (100 psia)
10. Throat Hot Wall Thick 0.18 cm (0.070 in.)
11. Type of Passages Rect. Channels
12. Throat Temperatures Channel 1580K (2385°F), Annulus 1775K (2735°F)

1. Material Conductivity: SCB 291 Nominal
C-103, 274.8K (35°F) incr.

2. No. of Passages: 50 - Nominal
30 - 291.5K (65°F) incr.

3. % Land Width: 25 - Nominal
50 - 280.4K (45°F) decr.

S.I. Units			English Units		
Channel		Annulus	Channel		Annulus
4. % c*			4. %c*		
100% 3034K	Nominal 1580K	Nominal 1775K	100% 5002°F	Nominal 2385°F	Nominal 2735°F
95% 2706K	1525K, 311K decr.	1683K, 347K dcr	95% 4411°F	2885°F, 100°F decr.	2570°F, 165°F decr
5. NH ₃ Dissociation			5. NH ₃ Dissociation		
50%	Nominal 1580K	Nominal 1775K	50%	Nominal 2385°F	Nominal 2735°F
70%	1450K, 386K, decr.	1658K, 372K dcr	70%	2150, 235°F decr	2525, 210°F decr
6. Cooling Enhancement			6. Cooling Enhancement		
None	Nominal 1580K	Nominal 1775K	None	Nominal 2385°F	Nominal 2735°F
50%	1536K	1666K	50%	2305°F	2540°F
100%	1508K	1608K	100%	2255°F	2435°F
7. Hot Gas Film Coefficient (hg)			7. Hot Gas Film Coefficient (hg)		
1770	Nominal 1580K	Nominal 1775K	6.0	Nominal 2385°F	Nominal 2735°F
3280	1761K	1666K	11.0	2710°F	2540°F
1180	1508K	1608K	4.0	2225°F	2435°F
8. Mono Mach No.			8. Mono Mach No.		
1.0	Nominal	Nominal	1.0	Nominal	Nominal
0.65	266K incr.	255K incr.	0.65	20°F incr.	75°F incr.
9. Mono Total Pressure			9. Mono Total Pressure		
690	Nominal	Nominal	100	Nominal	Nominal
550	277K incr.	319K incr.	80	40°F incr.	115°F incr.
10. Throat Inner Hot Wall Thickness			10. Throat Inner Hot Wall Thickness		
0.18	Nominal	Same	0.070	Nominal	Same
0.229	272K incr.	Same	0.090	30°F incr.	Same
11. Throat Temperatures	100% c*	95% c*	11. Throat Temperatures	100% c*	95% c*
Full Channel	1580K	1522K	Full Channel	2385°F	2280°F
Full Drilled	1636K	1577K	Full Drilled	2485°F	2380°F
Mini Channel	1580K	1522K	Mini Channel	2385°F	2280°F
Annulus	1775K	1683K	Annulus	2735°F	2570°F
12. Barrel Temperatures	100%	95% c*	12. Barrel Temperatures	100%	95% c*
Full Channel	1539K	1486K	Full Channel	2310°F	2215°F
Full Drilled	1589K	1530K	Full Drilled	2400°F	2295°F
Annulus	1586K	1528K	Annulus	2395°F	2290°F

TABLE 17 SI AND 17
OXIDIZER TEMPERATURE RISE AND INJECTOR FACE TEMPERATURE

Component	Oxidizer Cooled Injector	Fuel Cooled Injector (6%)	Fuel Cooled Injector (100%)
Temperature Rise of Oxidizer in Injector Stem	1.1 K (2.0°)	1.1 K (2.0°F)	1.1 K (2.0°F)
Temperature Rise of Oxidizer in Feed Tubes	1.1 K (2.0°F)	1.1 K (2.0°F)	1.1 K (2.0°F)
Temperature Rise of Oxidizer in Injector Manifold	7.2 K (13.0°F)	—	—
Temperature Rise of Oxidizer in Center Feed Tube	0.55 K (1.0°F)	0.55 K (1.0°F)	0.55 K (1.0°F)
Temperature Rise of Oxidizer due to Conduction through Support	0.55 K (1.0°F)	0.55 K (1.0°F)	0.55 K (1.0°F)
Injector Face Temperature	506 K (450°F)	1593 K (2408°F)	1489 K (2220°F)

TABLE 18 SI AND 18
FINAL MASS ANALYSES

		<u>MASS</u> <u>Kg</u>	<u>lb</u>
<u>REGENERATIVE COOLED</u>			
CONFIGURATION NO. 1	SIX INDIVIDUAL CYLINDRICAL REACTORS AT INJECTOR	32.5	71.8
CONFIGURATION NO. 2	ANNULAR REACTOR AT NOZZLE/EXTENSION	28.2	62.2
<u>FILM COOLED</u>			
CONFIGURATION NO. 1	SIX INDIVIDUAL CYLINDRICAL REACTORS INJECTOR FACE 6% FUEL COOLED	25.4	56.1
CONFIGURATION NO. 2	SIX INDIVIDUAL CYLINDRICAL REACTORS INJECTOR FACE 100% FUEL COOLED	24.5	54.1
CONFIGURATION NO. 3	INTEGRAL SIX CYLINDRICAL REACTORS INJECTOR FACE 6% FUEL COOLED	27.9	61.6

TABLE 19 SI AND 19
SECONDARY INJECTORS

Major Parameter		Performance										High Durability/Life				Ease of Fabrication		Low Risk		Low Cost		Low Mass		Summary
Weight Factor		2.0					2.5					1.0		2.0		1.0		1.5						
Element	Adjustment % (If Any)	Transient Mono I _{sp}	Transient Biprop I _{sp}	ΔP	Total Rating No.	Total Rating No. X Wt. Factor	Temp. Capability	Thermal Stress	Mech. Stress	Total Rating No.	Total Rating No. X Wt. Factor	Rating No.	Total	Rating No.	Total	Rating No.	Total	Rating No.	Total					
		Full	0.75	Full	1.25	1.00	-	-	-	-	-	-	-	-	-	-	-	-	-					
Column Number		1	2	3	4	5	$\frac{2+4+5}{3}$	A	6	7	8	$\frac{6+7+8}{3}$	B		C		E		F					
A. All Columbium		10	7.5	6	7.5	10	8.3	16.7	10	9	10	9.7	24.2	8	8	7	14	8	8	9	13.5	84.4		
1. N ₂ O ₄ Regeneratively Cooled																								
2. N ₂ H ₄ Regeneratively Cooled																								
3. N ₂ H ₄ Dump Cooled																								
NOT COMPETITIVE BECAUSE OF SEALING PROBLEMS		10	7.5	9	11.3	10	9.6	19.2	9	10	10	9.6	24.0	9	9	10	20	9	9	8	12	93.2		
B. Columbium Injector/Face L-605 Back Cover																								
1. N ₂ O ₄ Regeneratively Cooled																								
2. N ₂ H ₄ Regeneratively Cooled																								
3. N ₂ H ₄ Dump Cooled		9	6.8	9	11.3	10	9.4	18.7	10	8.5	9.5	9.1	22.8	7	7	9	18	7	7	6	9	82.5		
All L-605 Injector		10	7.5	9	11.3	10	9.6	19.2	10	9.5	9.5	9.5	23.8	8	8	9	18	8	8	6	9	86.0		
1. N ₂ O ₄ Regeneratively Cooled																								
2. N ₂ H ₄ Regeneratively Cooled																								
3. N ₂ H ₄ Dump Cooled																								
Capability to Meet Operating Requirements is Marginal																								

TABLE 20 SI AND 20
REACTOR/INJECTOR COMBINATIONS – REACTOR AT
SECONDARY INJECTOR STATION

Major Parameter		Performance										High Durability/Life						Ease of Fabrication		Low Risk		Low Cost		Low Mass		Summary
Weight Factor		2.0										2.5						1.0		2.0		1.0		1.5		
Element	Adjustment% (If Any)	Transient Mono I _{sp}		Transient Biprop I _{sp}		ΔP	Total Rating No.	Total Rating No. X Wt Factor	Joint Between Parts	Stress Capabil- ity	Chemical Compat- ability	Total Rating No.	Total Rating No. X Wt Factor	Rating No.	Total	Rating No.	Total	Rating No.	Total	Rating No.	Total	Rating No.	Total	A+B+C +D+E+F		
		Full	0.75	Full	1.25																				Full	5
Column Number		1	2	3	4	5	— 3	A	6	7	8	6+7+8 3	B	—	—	—	—	—	—	—	—	—	—	A+B+C +D+E+F		
A.	All Welded Columbiu Secondary Injector																									
	1. Columbiu Reactor Welded To Secondary Injector	10	7.5	10	12.5	10	10.0	20	10	10	5	8.3	20.8	9	4	8	9	9	9	9	9	9	13.5	80.3		
	2. L-605 Reactor Bolted To Injector	9	6.8	10	12.5	10	9.8	19.6	9	10	10	9.7	24.2	9	9	18	8	8	8	8	8	8	12.0	90.8		
B.	Columbiu Secondary Injector With L-605 Back Cover																									
	1. L-605 Reactor Welded To Injector	8	6	10	12.5	10	9.5	19.0	8	10	10	9.3	23.3	9	9	18	8	8	8	8	8	8	12.0	89.3		
	2. L-605 Reactor Bolted To Injector	7	5.3	10	12.5	10	9.3	18.6	7	10	10	9	22.5	9	8	16	6	6	6	6	7	10.5	82.6			
C.	L-605 Secondary Injector																									
	1. L-605 Reactor Welded To Injector	Capability to Meet Operating Requirements is Marginal																								
	2. L-605 Reactor Bolted To Injector																									

TABLE 21 SI AND 21
REACTOR/LINER/SECONDARY INJECTORS - REACTOR AT
NOZZLE EXTENSION INTERFACE

Major Parameter		Performance										High Durability/Life					Ease of Fabrication		Low Risk		Low Cost		Low Mass		Summary
Weight Factor		2.0					2.5					1.0		2.0		1.0		1.5							
Element	Adjustment % (If Any)	Transient Mono I _{sp}		Transient Biprop I _{sp}		ΔP	Total Rating No.	Total Rating No. X Wt. Factor	Seal Joints	Stress	Chemical Compat-ability	Total Rating No.	Total Rating No. X Wt. Factor	Rating No.	Total	Rating No.	Total	Rating No.	Total	Rating No.	Total				
		Full	0.75	Full	1.25	1.00	2 + 4 + 5 3	A	6	7	8	6 + 7 + 8 3	B								A + B + C + D + E + F				
A.	All Columbium Secondary Injector																								
	1. Columbium Reactor Welded to Columbium Outer Shell	10	7.5	10	12.5	10	10	20	8	5	5	6.0	15.0	9	5	10	9	9	9	9	13.5				
	2. L-605 Reactor Bolted to Columbium Outer Shell and Inner Liner	8	6	10	12.5	10	9.5	19.0	8	4	10	7.3	18.3	8	7	14	8	8	7	10.5	77.8				
B.	Columbium Secondary Injector With L-605 Back Cover																								
	1. L-605 Reactor Welded To L-605 Outer Shell, Bolted to Inner Liner	9	6.8	10	12.5	10	9.8	19.6	8	4	10	7.3	18.3	7	7	14	7	8	12	77.9					
	2. L-605 Reactor Bolted To Columbium Outer Shell and Inner Liner, Bolted to Secondary Injector	7	5.3	10	12.5	10	9.3	18.6	6	3	10	6.3	15.8	6	6	12	6	5	7.5	65.9					
C.	L-605 Reactor Bolted To L-605 Outer Shell and Columbium Liner	8	6	10	12.5	10	9.5	19.0	8	4	10	7.3	18.3	8	7	14	8	8	10.5	77.8					
	All L-605 Secondary Injector	Eliminated Due to Inability To Meet Operating Requirements																							

TABLES ENGLISH

TABLE 1 SI AND I
BIMODAL REGENERATIVE THRUST CHAMBER REQUIREMENTS

	Bipropellant Mode	Monopropellant Mode	Either Mode
A. Design Parameters			
Thrust, Steady-State Nominal at Standard Conditions*, N(lb _f)	4500.0 (1010.0)	1600.0 (360.0), approx.	
Propellants	N ₂ O ₄ /N ₂ H ₄	N ₂ H ₄	
Mixture Ratio, Nominal at Standard Conditions* (O/F)	1.15	0	
Hydrazine Flow Ratio, Bipropel- lent Mode: Monopropellant Mode			1.0 (Venturi Controlled)
Chamber Pressure, Nominal Nozzle Stagnation, kN/m ² (psia)	900.0 (130.0)	320.0 (46.3), approx.	
Pressure Drop, Maximum through Regenerative Cooling Jacket, kN/m ² (psid)	---	300.0 (43.5)	
Cooling Gas Composition			N ₂ H ₄ Decomposition Products at an NH ₃ Dis- association = 50 ± 5%
Cooling Velocity in Regenerative Cooling Jacket	Subsonic	Subsonic	
Cooling Gas Inlet, Temperature K (°F)			1250 ± 50 (1800 ± 90)
Combustion Length, Bipropellant Impingement-to-Throat, m (in.)			0.21 (8.25)
Expansion Area Ratio			60:1
Nozzle Contour			80% Bell
Area Ratio at Start of Uncooled Extension			TBD**
Operating Duration Capability			
Minimum Total(s)	1500.0	1000.0	
Maximum Continuous(s)	1000.0	500.0	
Minimum Continuous(s)	10.0	1.0	
Duty Cycle Restrictions***			None
B. Performance Goal			
Specific Impulse, Minimum Steady-State at Standard Conditions* N-s/kg, (lb _f -s/lb _m)	3050.0 (311.0)	2300.0 (234.0)	

* Standard Conditions ≡ 295K (71.6° F) propellant temperatures, 0 kN/m² (0 psia) ambient pressure

** TBD ≡ to be determined (by Contractor)

*** Other than that a bipropellant mode firing is always started with a 300 ms monopropellant lead and terminated with a (TBD) ms monopropellant lag

**TABLE 2 SI AND 2
FLIGHT-TYPE BIMODAL ENGINE REQUIREMENTS**

	Bipropellant Mode	Monopropellant Mode	Either Mode
A. Engine Characteristics			
Oxidizer	N_2O_4	---	
Fuel	N_2H_4	N_2H_4	
Mixture Ratio, Nominal at Standard Conditions (1) (O/F)	1.15	0.0	
Thrust, Steady-State Nominal at Standard Conditions ⁽¹⁾ , N(lb _f)	4500.0 (1010.0)	1600.0 (360.0) approx.	
Specific-Impulse, Steady-State Minimum at Standard Conditions, (1), N-s/kg (lb _f -s/lb _m)	3050.0 (311.0)	2300.0 (234.0)	
Impulse Repeatability, 3σ Intermodal Decay Transient, N-s (lb _f -s)	300.0 (67.3)		
Shutdown, N-s (lb _f -s)		22.0 (4.9)	
Propellant Supply Pressures at Engine Inlets, kN/m ² (psia)			TBD ⁽²⁾ in the range 1400-2100.0 (203 - 305)
Fuel Metering			Cavitating Venturi
Gaseous Helium Propellant Saturation Acceptance (%)			up to 100.0
Mass, Maximum, kg (lb _m)			27.0 (59.5)
Operating Duration Capability			
Minimum Total (3) _s	1500.0	1000.0	
Maximum Continuous, (3) _s	1000.0	500.0	
Minimum Continuous, s	10.0	1.0	
Duty Cycle Restrictions			none ⁽⁴⁾
Propellant Manifold Purges			none
Thrust Vector Misalignment, Maximum Relative to Geometric Thrust Vector			
Angular (deg)			±0.5
Offset, mm (in.)			1.3 (0.051)
TVC Gimbal Angle, in Two Orthogonal Planes (deg)			±8.0
Gimbal Torque, Maximum at 960 deg./sec ² , m-N (in-lb _f)			17.0 (149.0)
B. Thrust Chamber Characteristics			
Type			all-metallic; radiation- cooled (outer) wall
Chamber Pressure, Nominal Nozzle Stagnation, kN/m ² (psia)	900.0 (130.0)	TBD ⁽²⁾ 320.0 (46.3), approx.	
Expansion Area Ratio			60:1
Combustion Length, Minimum, m (in.) Bipropellant Impingement- to-Throat			0.21 (8.25)
Nozzle Contour			80% Bell
C. Reactor Characteristics			
Type	Spontaneous Catalytic		
Catalyst	Shell 405 ABSG (or mixed Shell 405 ABSG/HA-3)		
Startup Temperature Capability, Bed, K (°F)	272.0 (32.0) to steady-state thermal equilibrium		
Fuel, K (°F)	278.0 to 311.0 (40.0 to 100.0)		

TABLE 3
SUMMARY OF REGENERATIVE THROAT WALL TEMPERATURES
FOR VARIOUS CONFIGURATIONS

Analysis Constants: 25% Land

Mach No. = 1.0 Monomode 95% c*

No. of Passages	Throat Pressure (Monomode) psia	Film Coefficient h_g	Throat Wall Temp.
		BTU/in ² sec°F	°F
50	80	11×10^{-4}	2605
50	100	11×10^{-4}	2560
50	80	6×10^{-4}	2315
50	100	6×10^{-4}	2280
50	100	4×10^{-4}	2160
Annulus	100	6×10^{-4}	2580

TABLE 4
BIMODAL ENGINE CONFIGURATIONS MASS ANALYSIS

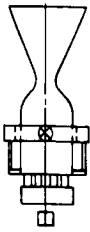
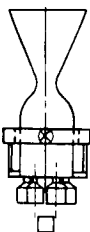
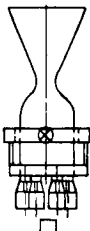
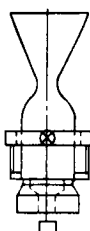
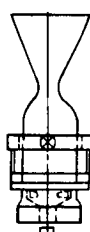
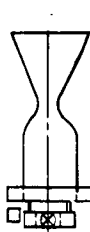
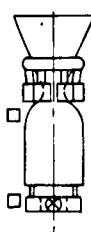
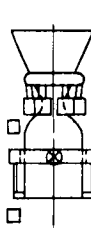
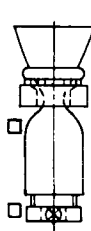
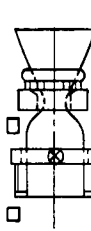
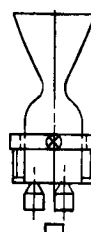
Thrust = 1010 lbf Chamber Pressure = 130 psia $\epsilon = 60, 80\%$ Bell N_2O_4, N_2H_4 Propellants	Figure A Secondary Inj. Station Single Reactor Welded Interface	Figure B Secondary Inj. Station 6 Cylindrical Reactors Welded Interface (Typical)	Figure C Secondary Inj. Station 6 Cylindrical Reactors Flanged Interface (Typical)	Figure D Secondary Inj. Station Annular Reactor Welded Interface	Figure E Secondary Inj. Station Annular Reactor Flanged Interface	Figure F Secondary Inj. Station Radial Inflow Annular Reactor
						
	Mass = lb	Mass = lb	Mass = lb	Mass = lb	Mass = lb	Mass = lb
Reactor	9.2	8.9	10.9	11.7	11.1	17.0
Secondary Injector	20.6	16.4	16.4	16.4	27.9	12.5
Chamber	33.7	33.7	33.7	33.7	43.2	33.7
Nozzle Extension	10.5	10.5	10.5	10.5	10.5	10.5
TCA	(74.0)	(69.5)	(71.5)	(72.3)	(92.7)	(73.7)
Oxidizer Valve	4.5	4.5	4.5	4.5	4.5	4.5
Fuel Valve	3.8	3.8	3.8	3.8	3.8	3.8
Valve Mounts and Feed	2.5	2.5	2.5	2.5	2.5	2.5
Tubes	4.7	5.1	5.1	5.1	5.1	3.5
Gimbal Ring Flexure	4.5	5.0	5.0	5.0	5.0	...
Pivot	94.0	90.4	92.4	93.2	113.6	88.0
Engine Mount						
Engine Assembly						
	Figure G Throat Station 6 Cylindrical Reactors Welded Head Mounted Gimbal	Figure H Throat Station 6 Cylindrical Reactors Welded Throat Mounted Gimbal	Figure I Throat Station Annular Reactor Welded Head Mounted Gimbal	Figure J Throat Station 2 Section Annular Re- actor - Welded Throat Mounted Gimbal	Figure K Secondary Inj. Station 3 Cylindrical Re- actors Welded Interface Throat Mounted Gimbal	
						
	Mass = lb	Mass = lb	Mass = lb	Mass = lb	Mass = lb	
Reactor	10.7	10.7	11.4	11.4	8.6	
Secondary Injector	12.5	13.2	12.5	13.2	10.9	
Chamber	31.5	31.5	31.5	31.5	33.7	
Nozzle Extension	10.5	10.5	10.5	10.5	10.5	
TCA	(65.2)	(65.9)	(65.9)	(66.6)	(63.7)	
Oxidizer Valve	4.5	4.5	4.5	4.5	4.5	
Fuel Valve	3.8	3.8	3.8	3.8	3.8	
Valve Mounts and Feed	4.0	2.5	4.0	2.5	2.5	
Tubes	3.5	4.2	3.5	4.2	5.1	
Gimbal Ring Flexure	...	4.9	...	4.9	5.0	
Pivot	81.0	85.8	81.7	86.5	84.6	
Engine Mount						
Engine Assembly						

TABLE 5
REGENERATIVELY COOLED BIMODAL ENGINE MASS ANALYSIS INPUTS

Operation Requirements

Thrust = (1010 lb_f)

Chamber Pressure = (130 psia)

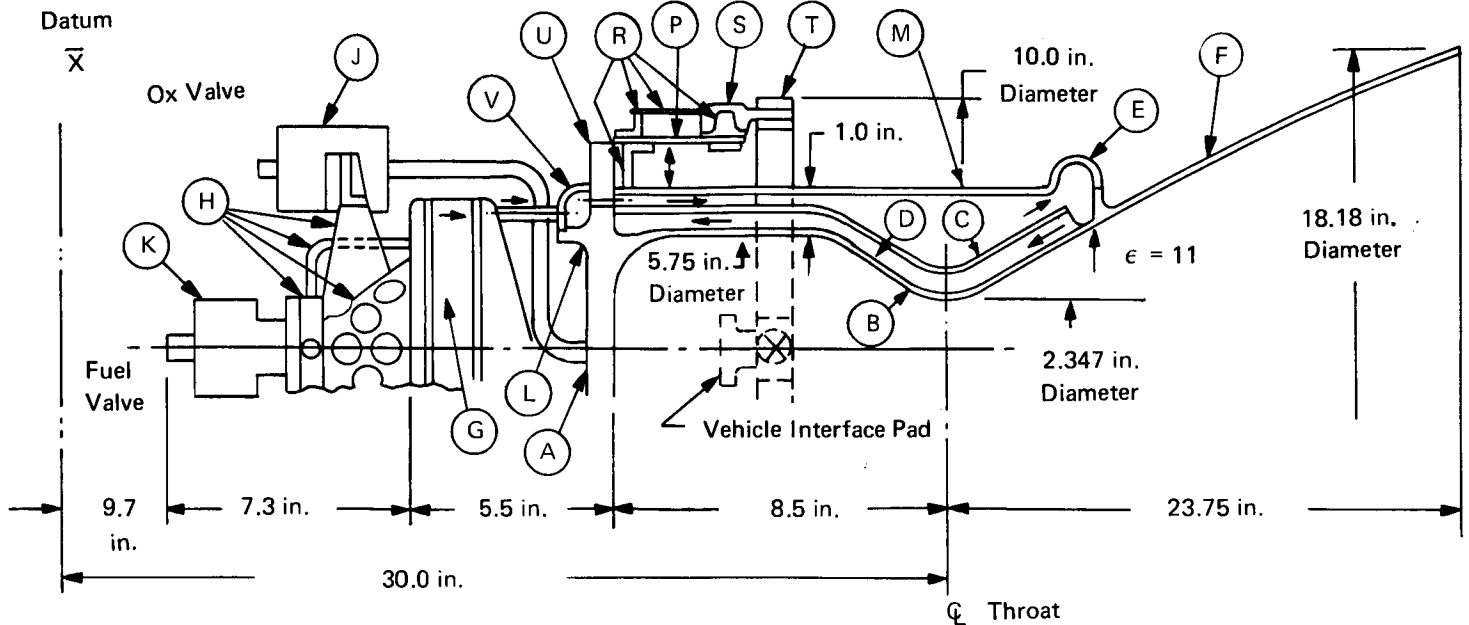
ϵ = 60, 80% Bell

N₂O₄/N₂ H₄ Propellants

Materials Used	Density lb/in. ³
Columbium Alloy	
C103	0.32
Scb291	0.35
Titanium Alloy	
6Al-4V	0.16
Shell 405	
20-30 Mesh	0.056
1/8 in. Pellets	0.042

<u>Item</u>	<u>Input</u>
A	Secondary injector 80% solid
D	Coolant Passages - 30 required
	Chamber (0.394 in.) Wide x (0.4 in.) High
	Throat (0.194 in.) Wide x (0.5 in.) High
	Manifold (0.394 in.) Wide x (0.5 in.) High
E	Torus manifold Diameter = (1.4 in.)
F	Divergent nozzle extension tapered from 0.06 to 0.02 in. thickness
G	Catalyst bed volume = (74.8 in. ³)
J	Oxidizer valve - torque motor
K	Fuel valve - solenoid
L	Outer coolant jacket length (14 in.)
M	Manifold torus at secondary injector - (1.25 in.)

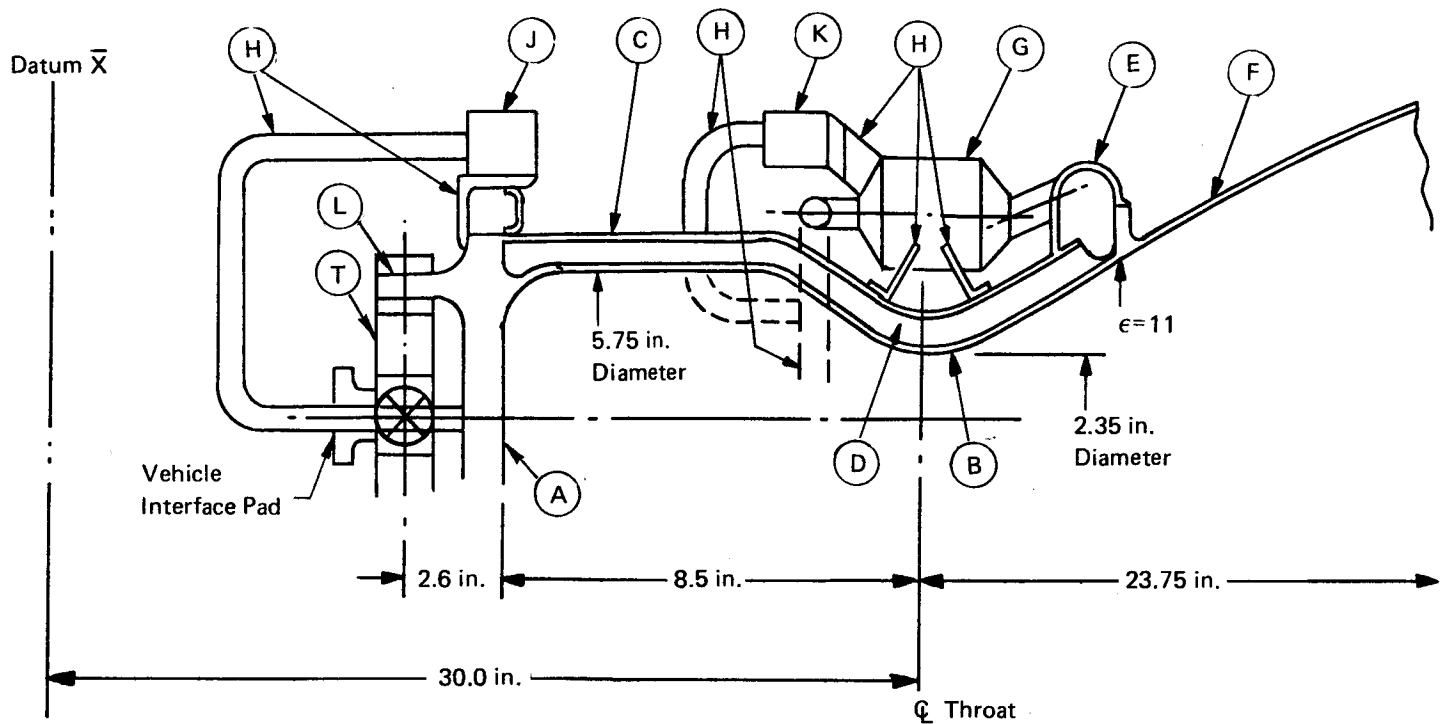
TABLE 6
BIMODAL ENGINE, SINGLE-BED REACTOR,
THROAT-MOUNTED GIMBAL RING



Item		Thick (in.)	Mat'l	Mass. (lbs)			\bar{X} (in.)
G	Reactor - Single Can		C103		9.2		18.0
	Secondary Injector				20.6		20.8
A	Basic Injector	1.125	C103	11.1			21.0
L	Δ Mass.		C103	4.2			21.0
U	Δ Mass. Inj. for Engine						
	Mount		C103	4.00			20.5
V	Δ Mass. Manifold						
	Injector	0.050	C103	1.3			19.8
	Chamber				33.7		29.4
B	Inner Liner	0.070	Scb291	6.8			30.25
C	Outer Liner	0.040	C103	3.8			27.5
D	Channel Walls		Scb291	14.90			29.1
E	Torus Manifold	0.070	C103	3.00			34.3
M	Outer Coolant Jacket	0.050	C103	5.20			27.5
F	Nozzle Extension $\epsilon = 11$ to $\epsilon = 60$	0.060/ 0.020	C103	10.5			43.0
	TCA					74.0	27.5
J	Ox Valve		St.		4.50		14.0
K	Fuel Valve		St.		3.8		12.0
H	Valve Mounts and Feed						
	Tubes		C103		2.5		15.0
T	Gimbal Ring—Flexure Pivot	0.10	Ti		4.7		25.3
	Engine Mount				4.5		23.95
P	Cylinder	0.050	Ti	1.1			23.9
R	Rings and Stringers	0.040	Ti	1.9			23.9
S	Gimbal Lugs		Ti	1.4			24.0
Engine Assy.					93.90		25.63

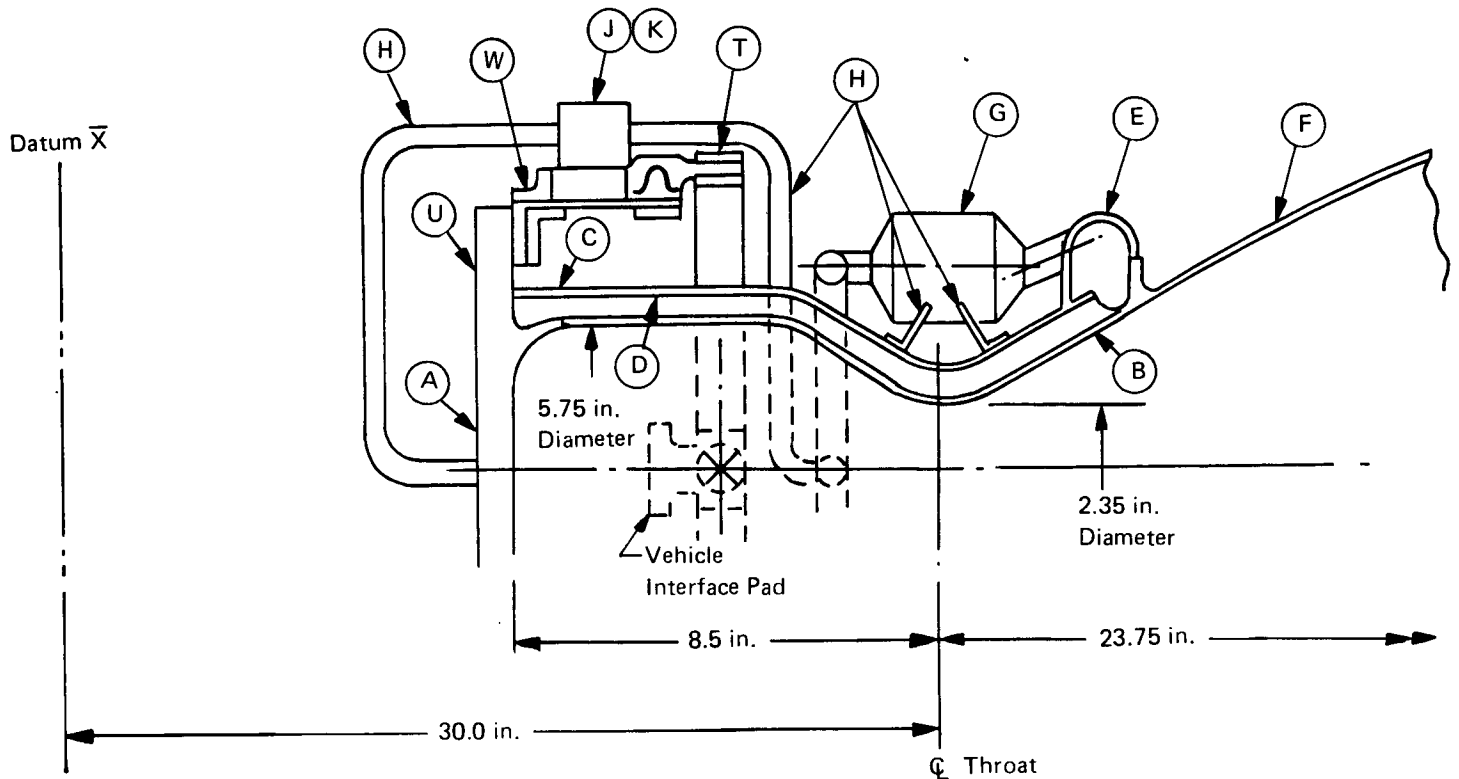
Note: Δ Mass. tradeoff-tubes in lieu of outer coolant jacket — 1.0 lb.

TABLE 7
BIMODAL ENGINE 6 CYLINDRICAL REACTORS
HEAD MOUNTED GIMBAL RING



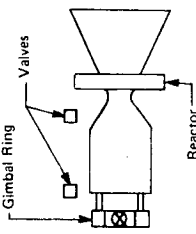
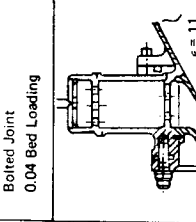
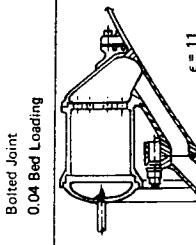
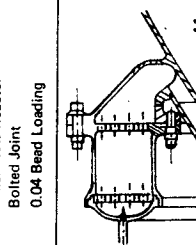
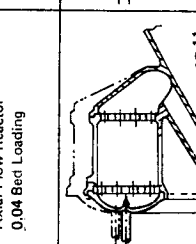
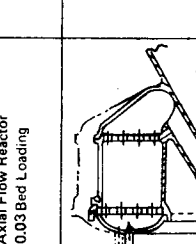
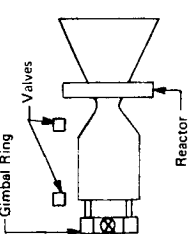
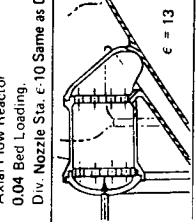
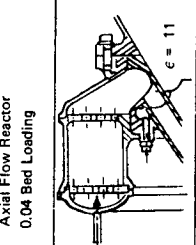
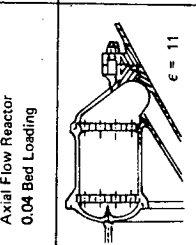
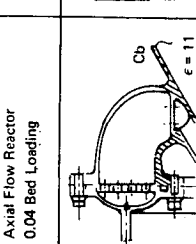
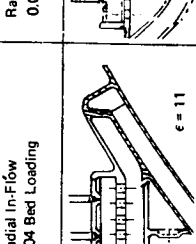
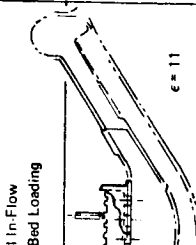
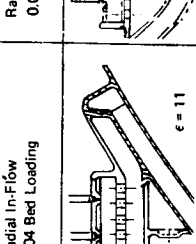
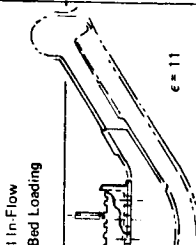
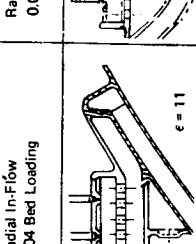
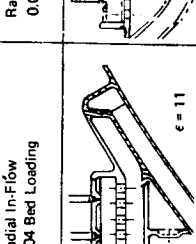
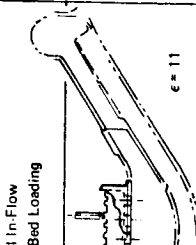
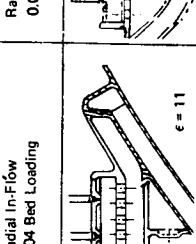
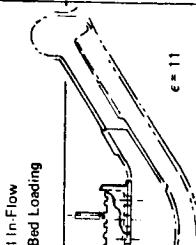
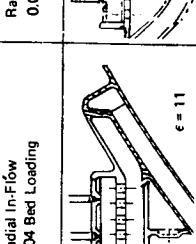
Item		Thick in.	Mat'l	Mass - lb			\bar{X} in.
G	Reactor - Cluster (6)				10.67		30.40
	Secondary Injector				12.51		20.94
A	Basic Injector	1.125	C103	11.09			21.0
L	Δ Mass. Inj. for Gimbal Ring			1.42			20.4
	Chamber				31.52		29.53
B	Inner Liner	0.070	Scb 291	6.83			30.25
C	Outer Liner	0.070	C103	6.79			27.50
D	Channel Walls		Scb291	14.90			29.1
E	Torus Manifold	0.070	C103	3.00			34.3
F	Nozzle Extension ϵ -11 to ϵ -60	0.060/ 0.020	C103		10.47		43.0
	TCA					65.17	30.18
J	Ox Valve		St.		4.50		21.0
K	Fuel Valve		St.		3.75		30.0
H	Valve Mount, Feed Tube, Reactor Supts.		C103		4.00		29.5
T	Gimbal Ring		Ti		3.50		20.0
Engine Assy					80.92		29.20

TABLE 8
BIMODAL ENGINE 6 CYLINDRICAL REACTORS
THROAT MOUNTED GIMBAL RING



Item		Thick (in.)	Mat'l	Mass. (lb.)			\bar{X} (in.)
G	Reactor-Cluster (6)				10.67		30.4
A	Secondary Injector				13.19		21.0
U	Basic Injector	1.125	C103	11.09			21.0
	Δ Mass. Inj. for		C103	2.10			21.0
	Engine Mount						21.0
	Chamber				31.52		29.53
B	Inner Liner	0.070	Scb291	6.83			30.25
C	Outer Liner	0.070	C103	6.79			27.5
D	Channel Walls		Scb291	14.90			29.1
E	Torus Manifold	0.070	C103	3.00			34.3
F	Nozzle Extension	0.060/					
	e-11 to e-60	0.020	C103		10.47		43.0
	TCA					65.85	30.10
J	Ox Valve		St.			4.50	25.0
K	Fuel Valve		St.			3.75	25.0
H	Valve Mounts, Feed						
	Tubes, Reactor						
	Supts.		C103			2.50	29.5
T	Gimbal Ring		Ti			4.20	25.3
W	Engine Mount		Ti			4.90	23.94
Engine Assy.						85.70	29.01

TABLE 9
BIMODAL ENGINE CONFIGURATION MASS ANALYSIS

	Figure A L605 Reactor C103 Bolted Nozzle Ext. Div. Nozzle Station Radial Inflow Reactor Bolted Joint 0.04 Bed Loading	Figure B L605 Reactor C103 Bolted Nozzle Ext. Div. Nozzle Station Axial Flow Reactor Bolted Joint 0.04 Bed Loading	Figure C L605 Reactor C103 Bolted Nozzle Ext. Div. Nozzle Station Axial Flow Reactor Bolted Joint 0.04 Bed Loading	Figure D C103 Reactor - Welded C103 Welded Nozzle Ext. Div. Nozzle Station Axial Flow Reactor 0.03 Bed Loading	Figure E C103 Reactor - Welded C103 Welded Nozzle Ext. Div. Nozzle Station Axial Flow Reactor 0.03 Bed Loading
					
Reactor Secondary Injector Chamber Nozzle Extension TCA Ox. Valve Fuel Valve Valve Mounts and Feed Tubes Gimbal Ring Engine Assembly	Mass = lb 17.9 57.4 in. ³ 12.5 28.5 12.8 71.7 4.5 3.8 2.1 3.5 85.6	Mass = lb 13.5 61.4 in. ³ 12.5 28.5 11.9 66.4 4.5 3.8 2.1 3.5 80.3	Mass = lb 17.6 65.6 in. ³ 12.5 28.5 12.4 71.0 4.5 3.8 2.1 3.5 84.9	Mass = lb 9.0 61.4 in. ³ 12.5 28.5 10.5 60.5 4.5 3.8 2.1 3.5 74.4	Mass = lb 12.7 82.3 in. ³ 12.5 28.5 10.5 64.2 4.5 3.8 2.1 3.5 78.1
					
Reactor Secondary Injector Chamber Nozzle Extension TCA Ox. Valve Fuel Valve Valve Mounts and Feed Tubes Gimbal Ring Engine Assembly	Mass = lb 10.4 69.3 in. ³ 12.5 32.6 10.5 66.0 4.5 3.8 2.1 3.5 79.9	Mass = lb 15.4 65.6 in. ³ 12.5 28.5 12.4 68.8 4.5 3.8 2.1 3.5 82.7	Mass = lb 11.7 65.6 in. ³ 12.5 28.5 12.4 65.1 4.5 3.8 2.1 3.5 79.0	Mass = lb 15.4 83.9 in. ³ 12.5 28.5 10.5 66.9 4.5 3.8 2.1 3.5 80.8	Mass = lb 7.5 38.2 in. ³ 12.5 28.2 10.5 58.7 4.5 3.8 2.1 3.5 72.6
					
Reactor Secondary Injector Chamber Nozzle Extension TCA Ox. Valve Fuel Valve Valve Mounts and Feed Tubes Gimbal Ring Engine Assembly	Mass = lb 10.4 69.3 in. ³ 12.5 32.6 10.5 66.0 4.5 3.8 2.1 3.5 79.9	Mass = lb 15.4 65.6 in. ³ 12.5 28.5 12.4 68.8 4.5 3.8 2.1 3.5 82.7	Mass = lb 11.7 65.6 in. ³ 12.5 28.5 12.4 65.1 4.5 3.8 2.1 3.5 79.0	Mass = lb 15.4 83.9 in. ³ 12.5 28.5 10.5 66.9 4.5 3.8 2.1 3.5 80.8	Mass = lb 7.5 38.2 in. ³ 12.5 28.2 10.5 58.7 4.5 3.8 2.1 3.5 72.6
					

Note: The engine assembly configuration positions the gimbal ring at the secondary injector. The Δ mass change for a c.g. mounted gimbal ring using an engine mount shell is +5.08 lb.

TABLE 10
SUMMARY OF TABLE 9

Figure No.	Bed Loading lb/in. ² sec	Area Ratio at End of Reactor	Material of Reactor Assembly	Bolted or Welded	Hydrazine Injection Type	Diverg. Nozzle Ext. Material	TCA
							lb
A	0.04	$\epsilon = 10$	L605	Bolted	Radial - in	C103	71.7
B	0.04	↓	L605	Bolted	Axial	↓	66.4
C	0.04	↓	L605/C103	Bolted	Axial	↓	67.3
D	0.03	↓	C103	Welded	Axial	↓	60.5
E	↓	↓	C103	Welded	Axial	↓	64.2
F	↓	$\epsilon = 13$	C103	Welded	Axial	↓	66.0
G	↓	$\epsilon = 10$	L605/C103	Bolted	Axial	↓	68.8
H	↓	↓	C103	Bolted	Axial	↓	65.1
I	↓	↓	L605/C103	Bolted	Axial	↓	66.9
J	↓	Throat	C103	Welded	Radial - in	↓	58.7
K	↓	Throat	C103		Radial - in	↓	57.4

TABLE 11
BIMODE CHAMBER ASSEMBLY CONFIGURATIONS
CHANNEL, DRILLED, ANNULAR

Typical Channel Design	All Channel $\epsilon = 8.9$	Throat Full Channel $\epsilon = 8.9$	Throat Mini Channel	All Annular	All Drilled $\epsilon = 6.2$	Throat Full Drill $\epsilon = 6.2$	Throat Mini Drill
	(lb)	(lb)	(lb)	(lb)	(lb)	(lb)	(lb)
Injector Chamber	11.09 [31.52]	11.09 [27.13]	11.09 [18.04]	11.09 [17.62]	11.09 [31.32]	11.09 [27.53]	11.09 [19.44]
Barrel Zone	(9.17)	(4.78)	(4.78)	(5.06)	(8.57)	(4.78)	(4.78)
Inner Liner	1.81	1.81	1.81	1.81		1.81	1.81
Outer Liner	2.95	2.76	2.76	2.95		2.76	2.76
Channel Lands	4.41	0.21	0.21	0.30		0.21	0.21
Throat and Manifold	(22.35)	(22.35)	(13.26)	(12.56)	(22.75)	(22.75)	(14.66)
Inner Liner	5.02	5.02	5.02	5.02			5.02
Outer Liner	3.84	3.84	3.84	3.84			3.84
Channel Lands	10.49	10.49	1.40	0.70			2.80
Torus Manifold	3.00	3.00	3.00	3.00			3.00
Δ Weight to Extend Drill Passages (to $\epsilon = 8.9$)	—	—	—	—	+6.60	+6.60	—
Total Chamber Assembly (Weight Cutoff at $\epsilon = 11$)	42.61	38.22	29.13	28.71	49.01	45.22	30.52

TABLE 12
BI MODAL CONFIGURATION CHANGES HEAD MOUNTED REACTOR (6)

	Baseline		Head Mounted Reactor					
	$\epsilon = 8.9$		$\epsilon = 4.2 (2700^{\circ}\text{F})$		$\epsilon = 7.8 (2400^{\circ}\text{F})$		$\epsilon = 18 (2000^{\circ}\text{F})$	
	Material	lb	Material	lb	Material	lb	Material	lb
Chamber Assy		(33.70)		(26.56)		(31.25)		(51.60)
Inner Liner	Scb291	6.8		5.46		6.65		9.63
Outer Liner	C103	3.8		3.30		3.80		8.96
Channel Walls	Scb291	14.9		11.34		13.74		21.36
Torus Manifold	C103	3.0		2.20		2.90		4.55
Outer Coolant Jacket	C103	5.2		4.26		4.16		7.10
Div. Noz. Ext.	C103	(10.5)	C103	(11.21)	C103	(10.60)	L605	(9.10)
Δ Mass to Chamber Assembly if Transfer Tubes used in lieu of Outer Collant Jacket		-1.0		-0.70		-1.0		-3.60

TABLE 13
BIMODAL CONFIGURATION CHANGES THROAT MOUNT REACTOR (6)

	Baseline		Throat Mounted Reactor					
	$\epsilon = 8.9$		$\epsilon = 4.2$ (2700°F)		$\epsilon = 7.8$ (2400°F)		$\epsilon = 18$ (2000°F)	
	Material	lb	Material	lb	Material	lb	Material	lb
Chamber Assy		(31.52)		(24.79)		(29.85)		(44.50)
Inner Liner	Scb291	6.83		5.46		6.68		9.63
Outer Liner	C103	6.79		5.79		6.54		8.96
Channel Walls	Scb291	14.90		11.34		13.73		21.36
Torus Manifold	C103	3.00		2.20		2.90		4.55
Div. Noz. Extension	$\epsilon - 11$ to 60	(10.47)	C103	(11.21)	C103	(10.60)	L605	9.1

TABLE 14 SI AND 14
REGENERATIVE CHAMBER MASS COMPARISON

	Hg = 3280 (Hg - 11) (95% c*)		Hg = 1770 (Hg - 6) (100% c*)	
	$\epsilon = 4.2$ Scb-291 Noz. Ext. 1755K at $\epsilon = 4.2$ (2700°F)		$\epsilon = 5.0$ Cb-103 Noz. Ext. 1589K at $\epsilon = 5.0$ (2400°F)	
	Mass kg	(lb)	Mass kg	(lb)
Note: All Engine Assy Masses Include Mini Channels in Throat				
A. Reactor at Sec. Inj. (cg Gimbal) 1. (6) Mult. Cyl. Tubular Passage (Weld)	34.0	(75.0)	33.6	(74.0)
				34.7 (76.6)
2. Annular, Annular Passage (Welded) Bolted - Add 1.1 kg for Mult. Cyl.	35.3	(77.9)	34.7	(76.6)
				36.0 (79.4)
B. Reactor at Throat 1. Annular (Hd. Mtd. Gimbal) (Welded)	30.4	(67.0)	29.8	(65.7)
				31.0 (68.4)
2. Annular (cg Mtd. Gimbal) (Welded)	32.6	(71.8)	32.0	(70.5)
				33.2 (73.2)
C. Reactor at Noz/Ext Joint 1. Annular (Hd. Mtd. Gimbal) (Welded)	27.4	(60.4)	26.8	(59.1)
				27.7 (61.1)
2. Annular (cg Mtd. Gimbal) (Welded) Bolted - Add 2.09 kg	29.6	(65.2)	29.0	(63.9)
				29.9 (65.9)

TABLE 15 SI AND 15
EVALUATION RATINGS FOR REGENERATIVE CHAMBERS,
REACTORS AND NOZZLE EXTENSIONS
REGENERATIVE CHAMBER

Major Parameter		Performance										High Durability/Life										Ease of Fabrication		Low Risk		Low Cost		Low Mass		Summary																																																																																																																																																																																																																																																																																																																																																																																																																													
Weight Factor		2.0										2.5										1.0		2.0		1.0		1.5																																																																																																																																																																																																																																																																																																																																																																																																																															
Element	Adjustment % (If Any)	Transient Mono I _{sp}		Transient Biprop I _{sp}		Δp	Total Rating No.	Total Rating No. X	Low Wall Temp	Thermal Stress	Mech. Stress	Total Rating No.	Total Rating No. X	Rating No.	Total	Rating No.	Total	Rating No.	Total	Rating No.	Total	Rating No.	Total	Rating No.	Total	Rating No.	Total	Rating No.	Total	Rating No.	Total	Rating No.	Total	Rating No.	Total	Rating No.	Total	Rating No.	Total	Rating No.	Total	Rating No.	Total	Rating No.	Total	Rating No.	Total	Rating No.	Total	Rating No.	Total	Rating No.	Total	Rating No.	Total	Rating No.	Total	Rating No.	Total	Rating No.	Total	Rating No.	Total	Rating No.	Total	Rating No.	Total	Rating No.	Total	Rating No.	Total	Rating No.	Total	Rating No.	Total	Rating No.	Total	Rating No.	Total	Rating No.	Total	Rating No.	Total	Rating No.	Total	Rating No.	Total	Rating No.	Total	Rating No.	Total	Rating No.	Total	Rating No.	Total	Rating No.	Total	Rating No.	Total	Rating No.	Total	Rating No.	Total	Rating No.	Total	Rating No.	Total	Rating No.	Total	Rating No.	Total	Rating No.	Total	Rating No.	Total	Rating No.	Total	Rating No.	Total	Rating No.	Total	Rating No.	Total	Rating No.	Total	Rating No.	Total	Rating No.	Total	Rating No.	Total	Rating No.	Total	Rating No.	Total	Rating No.	Total	Rating No.	Total	Rating No.	Total	Rating No.	Total	Rating No.	Total	Rating No.	Total	Rating No.	Total	Rating No.	Total	Rating No.	Total	Rating No.	Total	Rating No.	Total	Rating No.	Total	Rating No.	Total	Rating No.	Total	Rating No.	Total	Rating No.	Total	Rating No.	Total	Rating No.	Total	Rating No.	Total	Rating No.	Total	Rating No.	Total	Rating No.	Total	Rating No.	Total	Rating No.	Total	Rating No.	Total	Rating No.	Total	Rating No.	Total	Rating No.	Total	Rating No.	Total	Rating No.	Total	Rating No.	Total	Rating No.	Total	Rating No.	Total	Rating No.	Total	Rating No.	Total	Rating No.	Total	Rating No.	Total	Rating No.	Total	Rating No.	Total	Rating No.	Total	Rating No.	Total	Rating No.	Total	Rating No.	Total	Rating No.	Total	Rating No.	Total	Rating No.	Total	Rating No.	Total	Rating No.	Total	Rating No.	Total	Rating No.	Total	Rating No.	Total	Rating No.	Total	Rating No.	Total	Rating No.	Total	Rating No.	Total	Rating No.	Total	Rating No.	Total	Rating No.	Total	Rating No.	Total	Rating No.	Total	Rating No.	Total	Rating No.	Total	Rating No.	Total	Rating No.	Total	Rating No.	Total	Rating No.	Total	Rating No.	Total	Rating No.	Total	Rating No.	Total	Rating No.	Total	Rating No.	Total	Rating No.	Total	Rating No.	Total	Rating No.	Total	Rating No.	Total	Rating No.	Total	Rating No.	Total	Rating No.	Total	Rating No.	Total	Rating No.	Total	Rating No.	Total	Rating No.	Total	Rating No.	Total	Rating No.	Total	Rating No.	Total	Rating No.	Total	Rating No.	Total	Rating No.	Total	Rating No.	Total	Rating No.	Total	Rating No.	Total	Rating No.	Total	Rating No.	Total	Rating No.	Total	Rating No.	Total	Rating No.	Total	Rating No.	Total	Rating No.	Total	Rating No.	Total	Rating No.	Total	Rating No.	Total	Rating No.	Total	Rating No.	Total	Rating No.	Total	Rating No.	Total	Rating No.	Total	Rating No.	Total	Rating No.	Total	Rating No.	Total	Rating No.	Total	Rating No.	Total	Rating No.	Total	Rating No.	Total	Rating No.	Total	Rating No.	Total	Rating No.	Total	Rating No.	Total	Rating No.	Total	Rating No.	Total	Rating No.	Total	Rating No.	Total	Rating No.	Total	Rating No.	Total	Rating No.	Total	Rating No.	Total	Rating No.	Total	Rating No.	Total	Rating No.	Total	Rating No.	Total	Rating No.	Total	Rating No.	Total	Rating No.	Total	Rating No.	Total	Rating No.	Total	Rating No.	Total	Rating No.	Total	Rating No.	Total	Rating No.	Total	Rating No.	Total	Rating No.	Total	Rating No.	Total	Rating No.	Total	Rating No.	Total	Rating No.	Total	Rating No.	Total	Rating No.	Total	Rating No.	Total	Rating No.	Total	Rating No.	Total	Rating No.	Total	Rating No.	Total	Rating No.	Total	Rating No.	Total	Rating No.	Total

TABLE 15 SI AND 15 (CONT)
REACTOR

Major Parameter		Performance						Durability/Life (High)						Ease of Fabrication		Low Risk		Low Cost		Low Mass		Summary
Weight Factor		2.0						2.5						1.0		2.0		1.0		1.5		
Element	Trans- ient Mono	Trans- ient Riprop	UP	Total Rating (TR)	T.R. x W.F.	Welds	Stress	Reactor/ Chamber Joint	Total Rating (TR)	T.R. W.F.	Rating No.	Total	Rating No.	Total	Rating No.	Total	Rating No.	Total				
Adjustment %	0.75	1.25	1																			
Column No.	①	②	③	$\frac{①+②+③}{3}$	④	⑤	⑥	⑥	$\frac{④+⑤+⑥}{3}$	⑦	⑧	⑨	⑩	⑪	⑫	⑬	⑭	⑮	⑯	⑰		
Configuration																						
A. Reactor at Secondary Station																						
A.1 Single Cyl. (Axial) - Tube	Eliminated - Too Bulky																					
A.2 Multiple Cyl. (Axial) - Tubes	8/6	10/12.5	10	9.5	18.6	4	10	10	8.0	20.0	9	9.0	8	16.0	9	9.0	7	10.5	83.1			
A.3 Multiple Cyl. (Radial-in) - Tubes	Eliminated - Too Bulky																					
A.4 Single Cyl. (Axial) - Annular Passages	8/6	10/12.5	10	9.5	18.6	5	5	8	6.0	15.0	8	8.0	6	12.0	8	8.0	6	9.0	70.6			
A.5 Multiple Cyl. (Axial) - Annular Passages	8/6	10/12.5	10	9.5	18.6	4	10	8	7.3	18.3	6	6.0	7	14.0	6	6.0	6	9.0	71.9			
A.6 Multiple Cyl. (Radial-in) - Annular Passages	Eliminated - Too Bulky																					
A.7 Annular (Axial) - Annular Passages	8/6	10/12.5	10	9.5	18.6	10	6	8	8.0	20.0	9	9.0	8	16.0	9	9.0	6	9.0	81.6			
A.8 Annular (Radial) - Annular Passages	8/6	10/12.5	10	9.5	18.6	10	4	6	6.6	16.5	5	5.0	5	10.0	5	5.0	7	10.5	65.6			
B. Reactor at Throat																						
B.1 Single Cyl. (Axial) - Tube	Eliminated - Too Bulky																					
B.2 Multiple Cyl. (Axial) - Tubes	9/6.75	10/12.5	10	9.75	19.2	2	5	8	5.0	12.5	6	6.0	5	10.0	6	6.0	8	12.0	65.7			
B.3 Multiple Cyl. (Radial-in) - Tubes	Eliminated - Too Bulky																					
B.4 Annular (Axial) - One Piece	Eliminated - Too Bulky																					
B.5 Annular (Radial-in) - One Piece	9/6.75	10/12.5	10	9.75	19.2	8	4	4	5.3	13.3	5	5.0	5	10.0	5	5.0	7	10.5	63.0			
B.6 Annular (Axial) - Two Piece	9/6.75	10/12.5	10	9.75	19.2	7	5	8	6.6	16.5	7	7.0	6	12.0	7	7.0	7	10.5	72.2			
B.7 Annular (Radial-in) - Two Piece	9/6.75	10/12.5	10	9.75	19.2	4	5	6	5.0	12.5	5	5.0	5	10.0	5	5.0	10	15.0	66.7			
C. Reactor at Nozzle Extension Interface																						
C.1 Single Cyl. (Axial) - Tube	Eliminated - Too Bulky																					
C.2 Multiple Cyl. (Axial) - Tubes	Same as Configuration B.2																					
C.3 Multiple Cyl. (Radial-in) - Tubes	Eliminated - Too Bulky																					
C.4 Annular (Axial) - One Piece	10/7.5	10/12.5	10	10.0	20.0	10	5	8	7.6	19.0	10	10.0	7.5	15.0	10	10.0	10	15.0	89.0			
C.5 Annular (Radial-in) - One Piece	10/7.5	10/12.5	10	10.0	20.0	10	5	8	7.6	19.0	10	10.0	7.5	15.0	10	10.0	8	12.0	86.0			
C.6 Annular (Axial) - Two Piece	10/7.5	10/12.5	10	10.0	20.0	9	5	8	7.3	18.3	7	7.0	7.0	14.0	7	7.0	9	13.5	62.8			
C.7 Annular (Radial-in) - Two Piece	10/7.5	10/12.5	10	10.0	20.0	7	5	8	6.6	16.5	7	7.0	6.5	13.0	7	7.0	10	12.0	75.5			

*First Number is Full Rating - Second Number is Adjusted Rating

TABLE 15 SI AND 15 (CONT)
NOZZLE EXTENSION

Major Parameter	Performance										High Durability/Life					Ease of Fabrication		Low Risk		Low Cost		Low Mass		Summary
	2.0										2.5					1.0		2.0		1.0		1.5		
	High Mono 1 sp		High Biprop 1 sp		Total Rating No.		T.R. x W.F.		Low Wall Temp		Low Thermal Stress		High Thermal Margin		Total Rating No.		T.R. x W.F.		Rating No.		T.R. x W.F.			
Element	Full	0.75	Full	1.25	Full	0.75	Full	1.25	Full	0.75	Full	1.25	Full	0.75	Full	1.25	Full	0.75	Full	1.25	Full	0.75		
Adjustment % (If Any)	①	②	③	④	⑤	⑥	⑦	⑧	⑨	⑩	⑪	⑫	⑬	⑭	⑮	⑯	⑰	⑱	⑲	⑳	㉑	㉒		
Column No.	①	②	③	④	⑤	⑥	⑦	⑧	⑨	⑩	⑪	⑫	⑬	⑭	⑮	⑯	⑰	⑱	⑲	⑳	㉑	㉒		
A. Extension SCB-291 Interface with Regen Chamber at ε = 4.2 or 2.5 (Temp = 2700°) Exit ε = 60	10	7.5	10	12.5	10	20.0	8	8	9	8.3	20.8	8	8.0	10	20.0	8	8.0	10	15.0	91.8				
B. Extension C-103 Interface with Regen Chamber at ε = 7.8 or 5.0 (Temp = 2400°F) Exit ε = 60	9	6.8	10	12.5	9.6	19.2	9	9	10	9.3	23.3	10	10.0	10	20.0	10	10.0	9	13.5	96.0				
C. Extension L-605 Interface with Regen Chamber at ε = 18 or 11.0 Exit ε = 60	8	6.0	10	12.5	9.2	18.4	10	10	9	9.7	24.2	9	9.0	8	16.0	8	8.0	5	7.5	83.1				

TABLE 16 SI AND 16
SUMMARY – REGENERATIVE CHAMBER DESIGN PARAMETER EFFECT
ON THROAT TEMPERATURE

Assumptions for Baseline

- | | | |
|-----|-------------------------------|--|
| 1. | Material | SCB 291 |
| 2. | No. of Passages | 50 |
| 3. | % Land Width | 25% |
| 4. | %c* | 100% |
| 5. | NH ₃ Dissociation | 50% |
| 6. | Cooling Enhancement | None |
| 7. | hg (Hot Gas Film Coefficient) | 1770 joule/m ² sec K (6.0 x 10 ⁻⁴ BTU/in. ² sec °F) |
| 8. | Mono Mach No. | 1.0 |
| 9. | Mono Total Pressure | 690 KN/m ² (100 psia) |
| 10. | Throat Hot Wall Thick | 0.18 cm (0.070 in.) |
| 11. | Type of Passages Rect. | Channels |
| 12. | Throat Temperatures | Channel 1580K (2385°F), Annulus 1775K (2735°F) |

- | | | |
|----|------------------------|---|
| 1. | Material Conductivity: | SCB 291 Nominal
C-103, 274.8K (35°F) incr. |
| 2. | No. of Passages: | 50 - Nominal
30 - 291.5K (65°F) incr. |
| 3. | % Land Width: | 25 - Nominal
50 - 280.4K (45°F) decr. |

S.I. Units			English Units		
Channel		Annulus	Channel		Annulus
4.	% c*		4.	%c*	
	100% 3034K	Nominal 1580K		100% 5002°F	Nominal 2385°F
	95% 2706K	1525K, 311K decr.		95% 4411°F	2885°F, 100°F decr.
5.	NH ₃ Dissociation		5.	NH ₃ Dissociation	
	50%	Nominal 1580K		50%	Nominal 2385°F
	70%	1450K, 386K, decr.		70%	2150, 235°F decr
6.	Cooling Enhancement		6.	Cooling Enhancement	
	None	Nominal 1580K		None	Nominal 2385°F
	50%	1536K		50%	2305°F
	100%	1508K		100%	2255°F
7.	Hot Gas Film Coefficient (hg)		7.	Hot Gas Film Coefficient (hg)	
	1770	Nominal 1580K		6.0	Nominal 2385°F
	3280	1761K		11.0	2710°F
	1180	1508K		4.0	2225°F
8.	Mono Mach No.		8.	Mono Mach No.	
	1.0	Nominal		1.0	Nominal
	0.65	266K incr.		0.65	20°F incr.
9.	Mono Total Pressure		9.	Mono Total Pressure	
	690	Nominal		100	Nominal
	550	277K incr.		80	40°F incr.
10.	Throat Inner Hot Wall Thickness		10.	Throat Inner Hot Wall Thickness	
	0.18	Nominal		0.070	Nominal
	0.229	272K incr.		0.090	30°F incr.
11.	Throat Temperatures	100% c*	11.	Throat Temperatures	100% c*
	Full Channel	1580K		Full Channel	2385°F
	Full Drilled	1636K		Full Drilled	2485°F
	Mini Channel	1580K		Mini Channel	2385°F
	Annulus	1775K		Annulus	2735°F
12.	Barrel Temperatures	100%	12.	Barrel Temperatures	100%
	Full Channel	1539K		Full Channel	2310°F
	Full Drilled	1589K		Full Drilled	2400°F
	Annulus	1586K		Annulus	2395°F

TABLE 17 SI AND 17
OXIDIZER TEMPERATURE RISE AND INJECTOR FACE TEMPERATURE

Component	Oxidizer Cooled Injector	Fuel Cooled Injector (6%)	Fuel Cooled Injector (100%)
Temperature Rise of Oxidizer in Injector Stem	1.1 K (2.0° F)	1.1 K (2.0° F)	1.1 K (2.0° F)
Temperature Rise of Oxidizer in Feed Tubes	1.1 K (2.0° F)	1.1 K (2.0° F)	1.1 K (2.0° F)
Temperature Rise of Oxidizer in Injector Manifold	7.2 K (13.0° F)	—	—
Temperature Rise of Oxidizer in Center Feed Tube	0.55 K (1.0° F)	0.55 K (1.0° F)	0.55 K (1.0° F)
Temperature Rise of Oxidizer due to Conduction through Support	0.55 K (1.0° F)	0.55 K (1.0° F)	0.55 K (1.0° F)
Injector Face Temperature	506 K (450° F)	1593 K (2408° F)	1489 K (2220° F)

TABLE 18 SI AND 18
FINAL MASS ANALYSES

<u>REGENERATIVE COOLED</u>		<u>MASS</u> <u>Kg</u>	<u>lb</u>
CONFIGURATION NO. 1	SIX INDIVIDUAL CYLINDRICAL REACTORS AT INJECTOR	32.5	71.8
CONFIGURATION NO. 2	ANNULAR REACTOR AT NOZZLE/EXTENSION	28.2	62.2
<u>FILM COOLED</u>			
CONFIGURATION NO. 1	SIX INDIVIDUAL CYLINDRICAL REACTORS INJECTOR FACE 6% FUEL COOLED	25.4	56.1
CONFIGURATION NO. 2	SIX INDIVIDUAL CYLINDRICAL REACTORS INJECTOR FACE 100% FUEL COOLED	24.5	54.1
CONFIGURATION NO. 3	INTEGRAL SIX CYLINDRICAL REACTORS INJECTOR FACE 6% FUEL COOLED	27.9	61.6

Major Parameter		Performance										High Durability/Life				Ease of Fabrication		Low Risk		Low Cost		Low Mass		Summary
Weight Factor		2.0										2.5				1.0		2.0		1.0		1.5		
Element	Adjustment % (If Any)	Transient Mono I _{sp}		Transient Biprop I _{sp}		ΔP	Total Rating No.	Total Rating Wt. Factor	Temp. Capability	Thermal Stress	Mech. Stress	Total Rating No.	Total Rating Wt. Factor	Rating No.	Total	Rating No.	Total	Rating No.	Total	Rating No.	Total			
A.	All Columbium	Full	0.75	Full	1.25	1.00	—	—	—	—	—	—	—	—	—	—	—	—	—	—	—	A+B+C +D+E+F		
	1. N ₂ O ₄ Regeneratively Cooled	1	2	3	4	5	$\frac{2+4+5}{3}$	A	6	7	8	$\frac{8+7+8}{3}$	B	—	C	D	—	E	—	F	—			
	2. N ₂ H ₄ Regeneratively Cooled																							
	3. N ₂ H ₄ Dump Cooled																							
B.	Columbium Injector/Face L-605 Back Cover	10	7.5	6	7.5	10	8.3	16.7	10	9	10	9.7	24.2	8	8	7	14	8	8	9	13.5	84.4		
	1. N ₂ O ₄ Regeneratively Cooled	10	7.5	9	11.3	10	9.6	19.2	9	10	10	9.6	24.0	9	9	10	20	9	9	8	12	93.2		
	2. N ₂ H ₄ Regeneratively Cooled																							
	3. N ₂ H ₄ Dump Cooled	9	6.8	9	11.3	10	9.4	18.7	10	8.5	9.5	9.1	22.8	7	7	9	18	7	7	6	9	82.5		
C.	All L-605 Injector	10	7.5	9	11.3	10	9.6	19.2	10	9.5	9.5	9.5	23.8	8	8	9	18	8	8	6	9	86.0		
	1. N ₂ O ₄ Regeneratively Cooled	Capability to Meet Operating Requirements is Marginal																						
	2. N ₂ H ₄ Regeneratively Cooled																							
	3. N ₂ H ₄ Dump Cooled																							

TABLE 20 SI AND 20
REACTOR/INJECTOR COMBINATIONS -- REACTOR AT
SECONDARY INJECTOR STATION

Major Parameter		Performance										High Durability/Life					Ease of Fabrication		Low Risk		Low Cost		Low Mass		Summary
Weight Factor		2.0						2.5				1.0		2.0		1.0		1.5							
Element	Adjustment% (If Any)	Transient Mono I _{sp}		Transient Biprop I _{sp}		ΔP	Total Rating No.	Total Rating No. X Wt Factor	Joint Between Parts	Stress Capabil- ity	Chemical Compat- ability	Total Rating No.	Total Rating No. X Wt Factor	Rating No.	Total	Rating No.	Total	Rating No.	Total	Rating No.	Total	A+B+C +D+E+F			
		Full	0.75	Full	1.25	Full	—	$\frac{2+4+5}{3}$	A	6	7	8	$\frac{6+7+8}{3}$	B	—	—	—	—	—	—	—				
A.	All Welded Columbium Secondary Injector																								
	1. Columbium Reactor Welded To Secondary Injector	10	7.5	10	12.5	10	10.0	20	10	10	5	8.3	20.8	9	4	8	9	9	9	13.5	80.3				
	2. L-605 Reactor Bolted To Injector	9	6.8	10	12.5	10	9.8	19.6	9	10	10	9.7	24.2	9	9	8	8	8	12.0	90.8					
B.	Columbium Secondary Injector With L-605 Back Cover																								
	1. L-605 Reactor Welded To Injector	8	6	10	12.5	10	9.5	19.0	8	10	10	9.3	23.3	9	9	8	8	8	12.0	89.3					
	2. L-605 Reactor Bolted To Injector	7	5.3	10	12.5	10	9.3	18.6	7	10	10	9	22.5	9	8	6	6	7	10.5	82.6					
C.	L-605 Secondary Injector																								
	1. L-605 Reactor Welded To Injector	Capability to Meet Operating Requirements is Marginal																							
	2. L-605 Reactor Bolted To Injector																								

TABLE 21 SI AND 21
REACTOR/LINER/SECONDARY INJECTORS - REACTOR AT
NOZZLE EXTENSION INTERFACE

Major Parameter	Performance										High Durability/Life					Ease of Fabrication		Low Risk		Low Cost		Low Mass		Summary
Weight Factor	2.0										2.5					1.0		2.0		1.0		1.5		
	Transient Mono I _{sp}		Transient Biprop I _{sp}		ΔP	Total Rating No.	Total Rating No. X Wt. Factor	Seal Joints	Stress	Chemical Compat-ability	Total Rating No.	Total Rating No. X Wt. Factor	Rating No.	Total	Rating No.	Total	Rating No.	Total	Rating No.	Total				
	Full	0.75	Full	1.25																	3	4	5	
Element Adjustment % (If Any)	1	2	3	4	5	1.00	2+4+5 3	A	6	7	8	6+7+8 3	B	Rating No.	Total	Rating No.	Total	Rating No.	Total	Rating No.	Total			
Column Number	1	2	3	4	5	1.00	2+4+5 3	A	6	7	8	6+7+8 3	B								A + B + C + D + E + F			
A. All Columbium Secondary Injector																								
1. Columbium Reactor Welded to Columbium Outer Shell	10	7.5	10	12.5	10	10	10	20	8	5	5	6.0	15.0	9	9	5	10	9	9	9	13.5	76.5		
2. L-605 Reactor Bolted to Columbium Outer Shell and Inner Liner	8	6	10	12.5	10	10	9.5	19.0	8	4	10	7.3	18.3	8	7	14	8	8	7	10.5	77.8			
B. Columbium Secondary Injector With L-605 Back Cover																								
1. L-605 Reactor Welded To L-605 Outer Shell, Bolted to Inner Liner	9	6.8	10	12.5	10	10	9.8	19.6	8	4	10	7.3	18.3	7	7	14	7		8	12	77.9			
2. L-605 Reactor Bolted To Columbium Outer Shell and Inner Liner, Bolted to Secondary Injector	7	5.3	10	12.5	10	10	9.3	18.6	6	3	10	6.3	15.8	6	6	6	12	6	6	5	7.5	66.9		
3. L-605 Reactor Bolted To L-605 Outer Shell and Columbium Liner	8	6	10	12.5	10	10	9.5	19.0	8	4	10	7.3	18.3	8	7	14	8	8	8	7	10.5	77.8		
C. All L-605 Secondary Injector																								
Eliminated Due to Inability To Meet Operating Requirements																								

FIGURES S.I.

A. Reactor at Secondary Injector

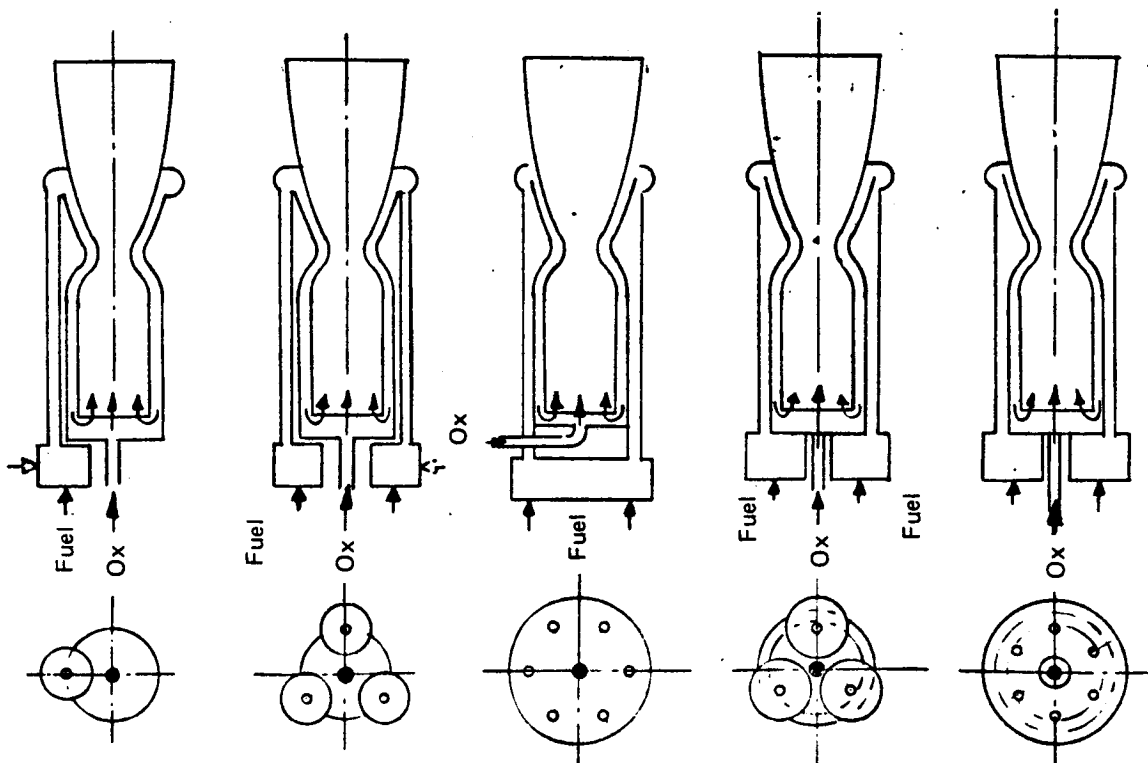
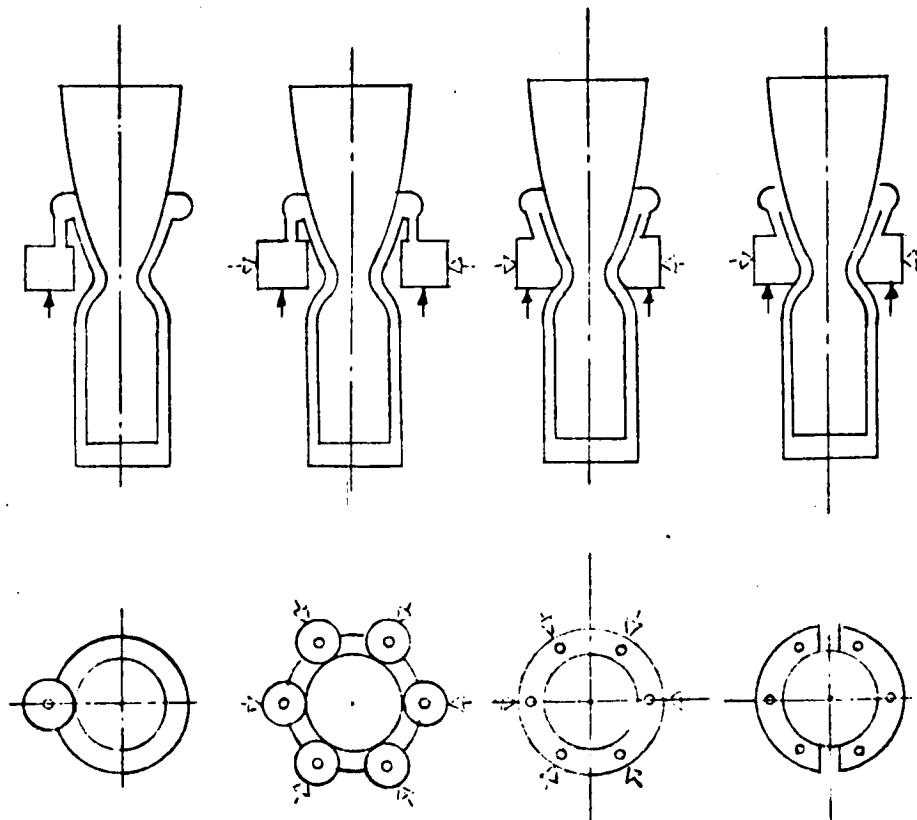


Figure 1 SI. Major Component Combinations

B. Reactor at Throat



1. Single Cylindrical Reactor - Single Feed Tube

a. Axial Feed Only

2. Multiple Cylindrical Reactor - Multiple Feed Tube

a. Axial Feed

b. Radial In Feed

3. Annular Reactor - One-Piece Toroidal

a. Axial Feed

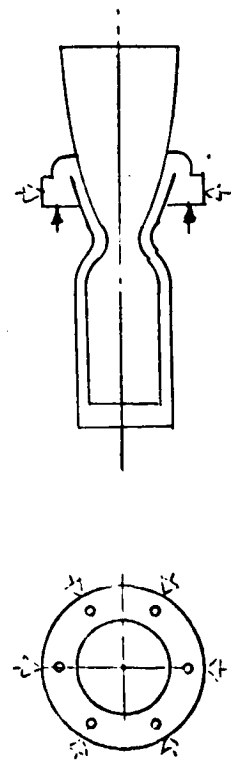
b. Radial In Feed

4. Annular Reactor - Two Split Sections

a. Axial Feed

b. Radial In Feed

C. Reactor at Nozzle/Extension Interface



1. Same Basic
2. Configurations as
3. Shown for Reactor
4. At Throat

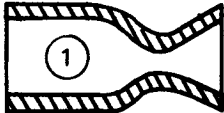
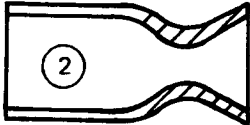
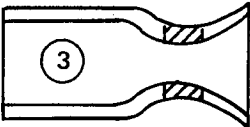
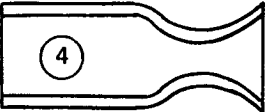
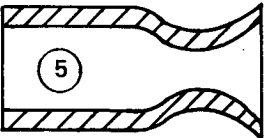
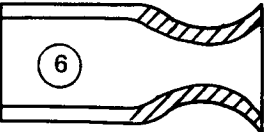
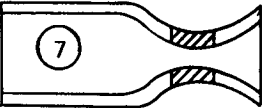
<u>Type</u>	<u>Throat (Nozzle)</u>	<u>Barrel</u>
	Channel	Channel
	Channel	Annular
	"Mini" Channel	Annular
	Annular	Annular
	Drilled	Drilled
	Drilled	Annular
	"Mini" Drilled	Annular

Figure 2 SI. Regenerative Chamber Passage Combinations

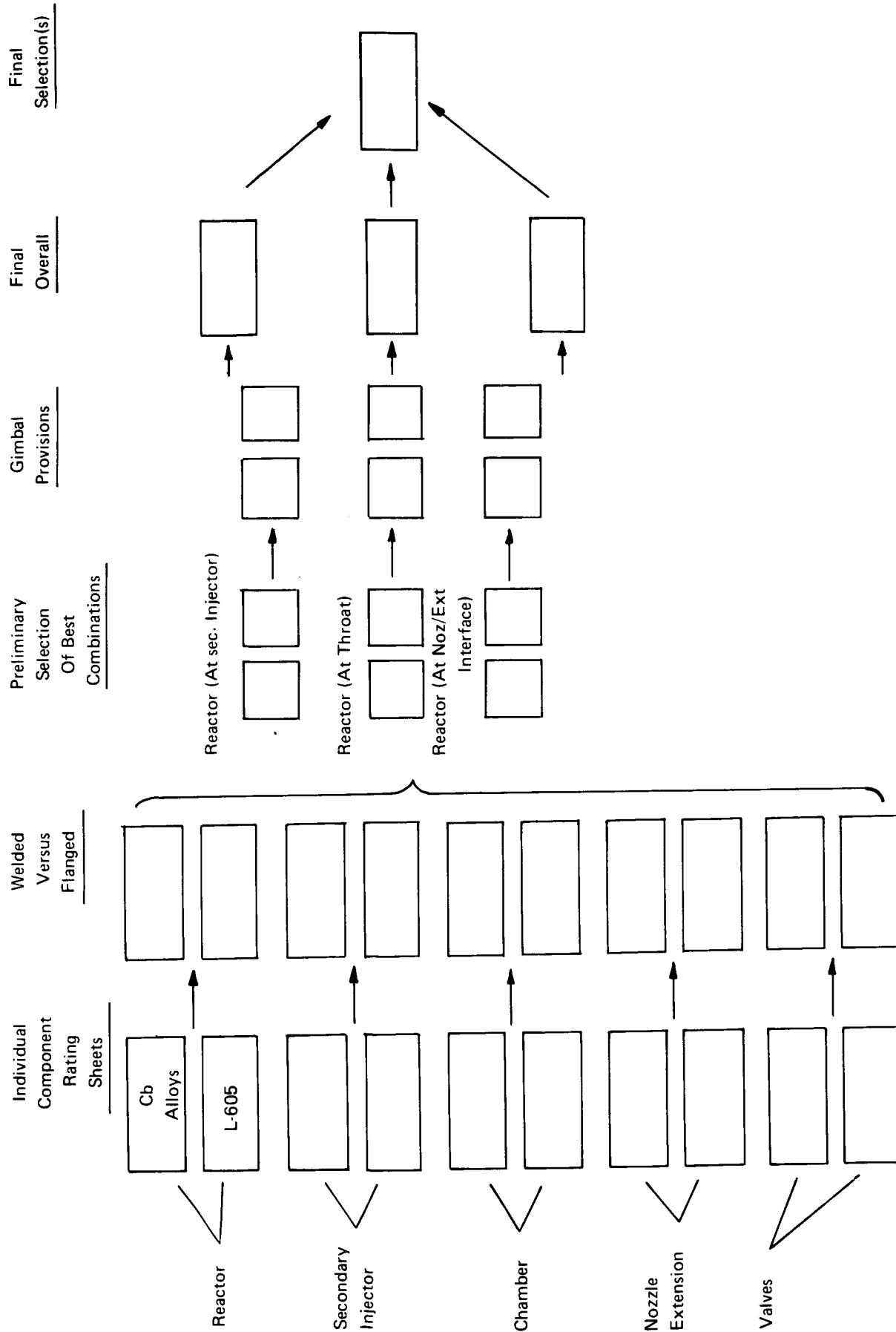


Figure 3 Sl. Flow Chart

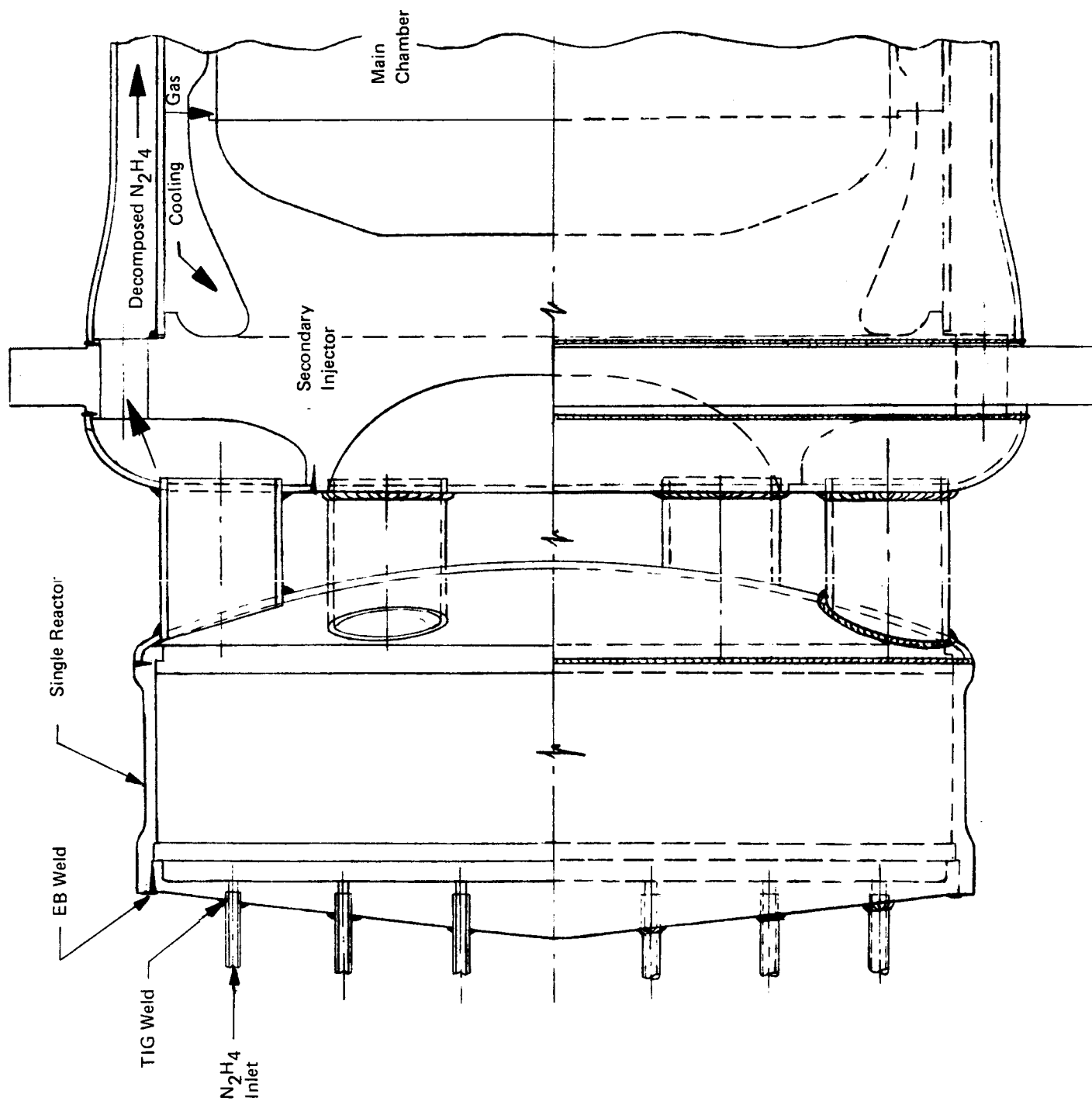


Figure 4 SI. Secondary Injector Station, Single Cylinder Reactor – Annular Passage Welded Interface

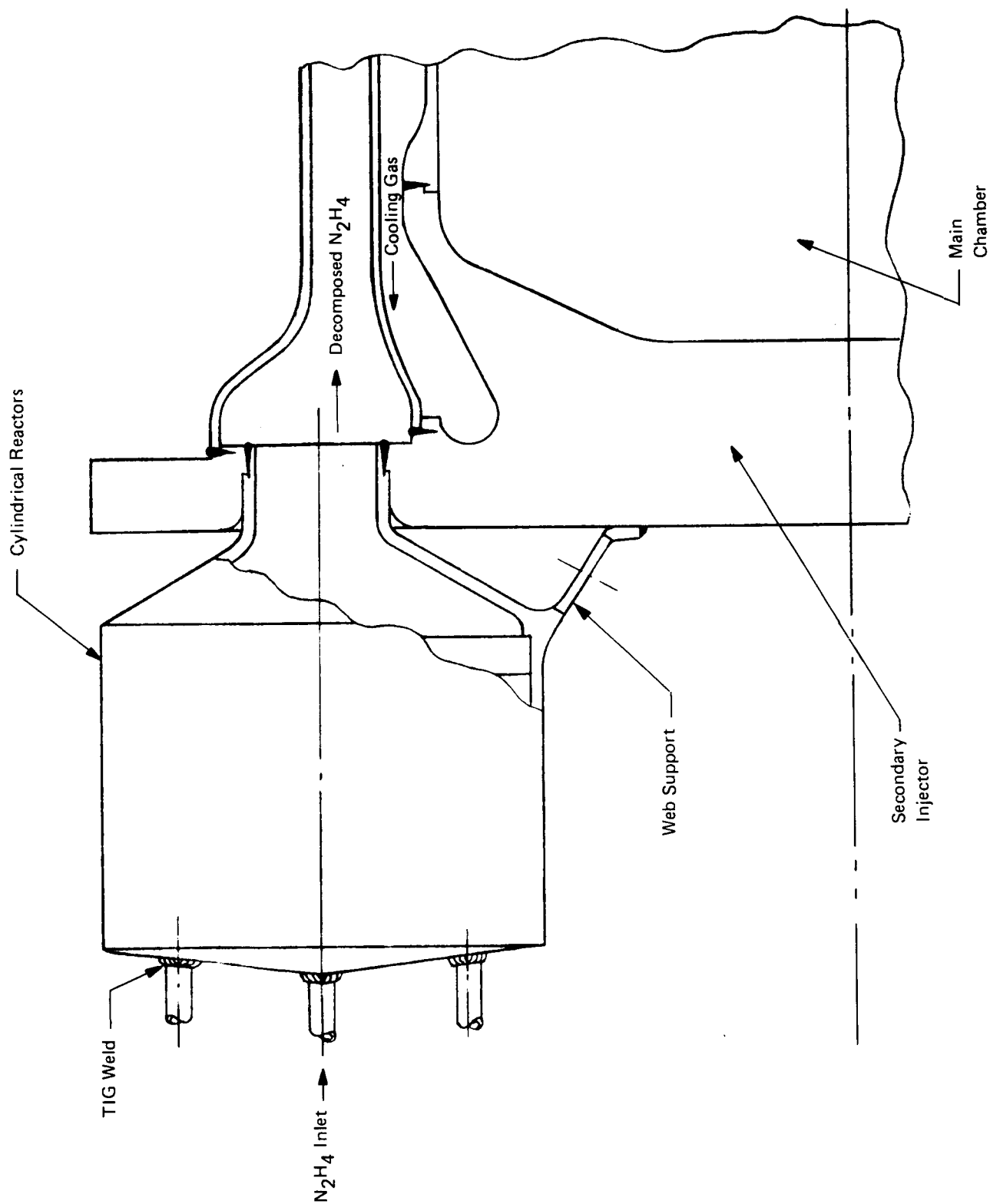


Figure 5 SI. Secondary Injector Station, Multiple Cylindrical Reactors - Annular Passage Welded Interface Cluster of 6 (Typical)

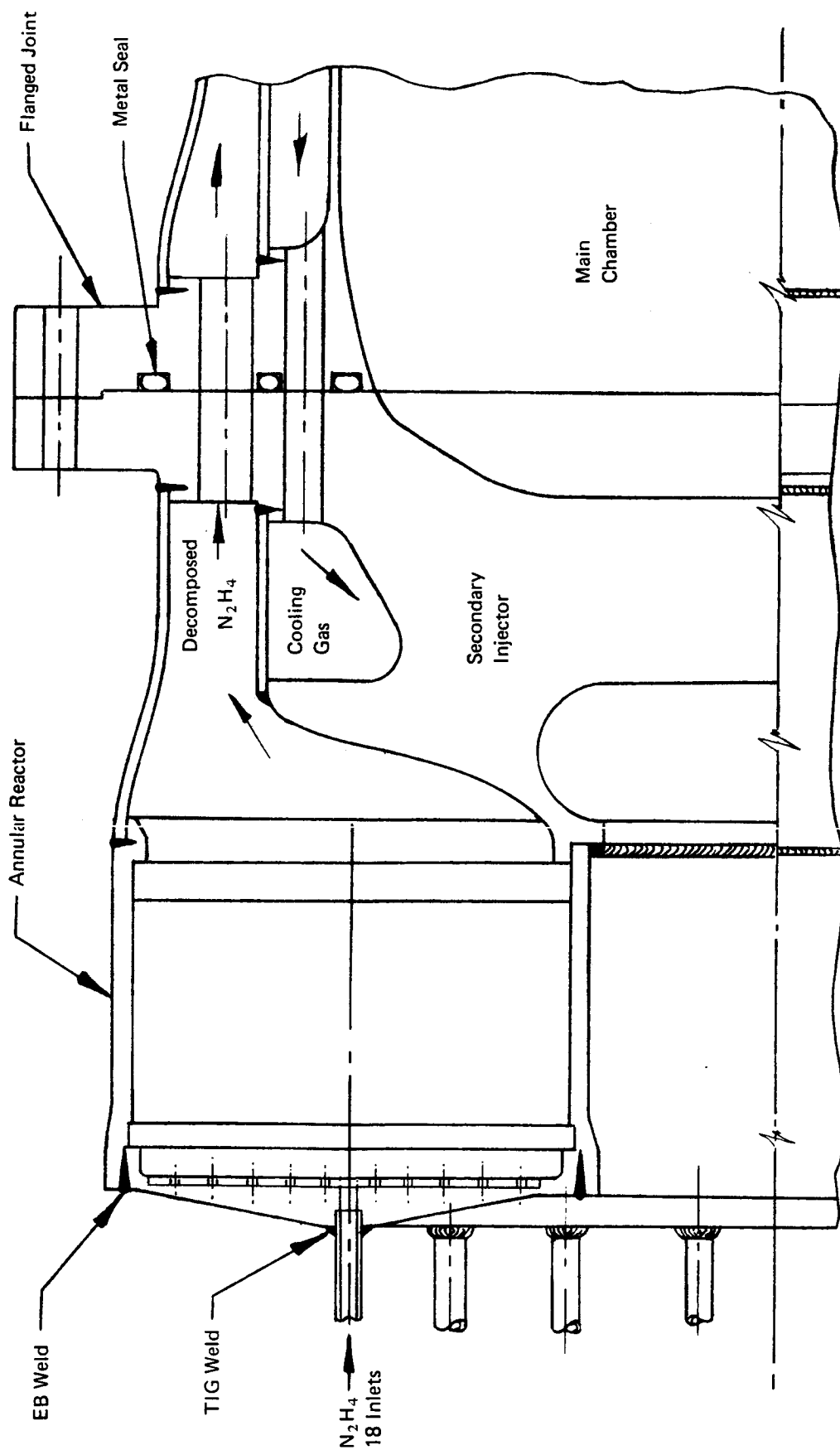


Figure 6 SI. Secondary Injector Station, Annular Reactor,
Flanged Interface

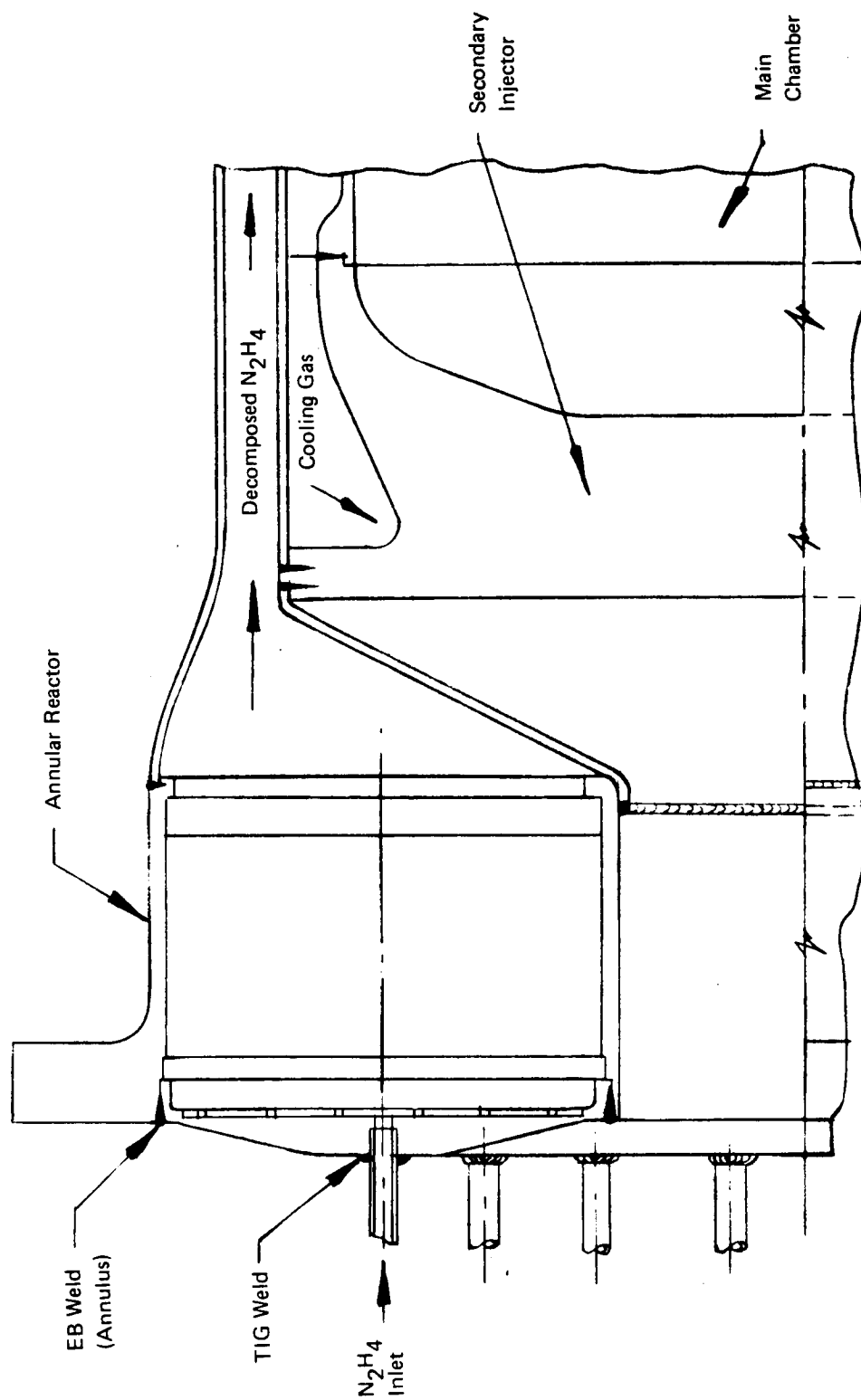


Figure 7 SI. Secondary Injector Station - Annular Reactor - Annular Passage,
Welded Interface

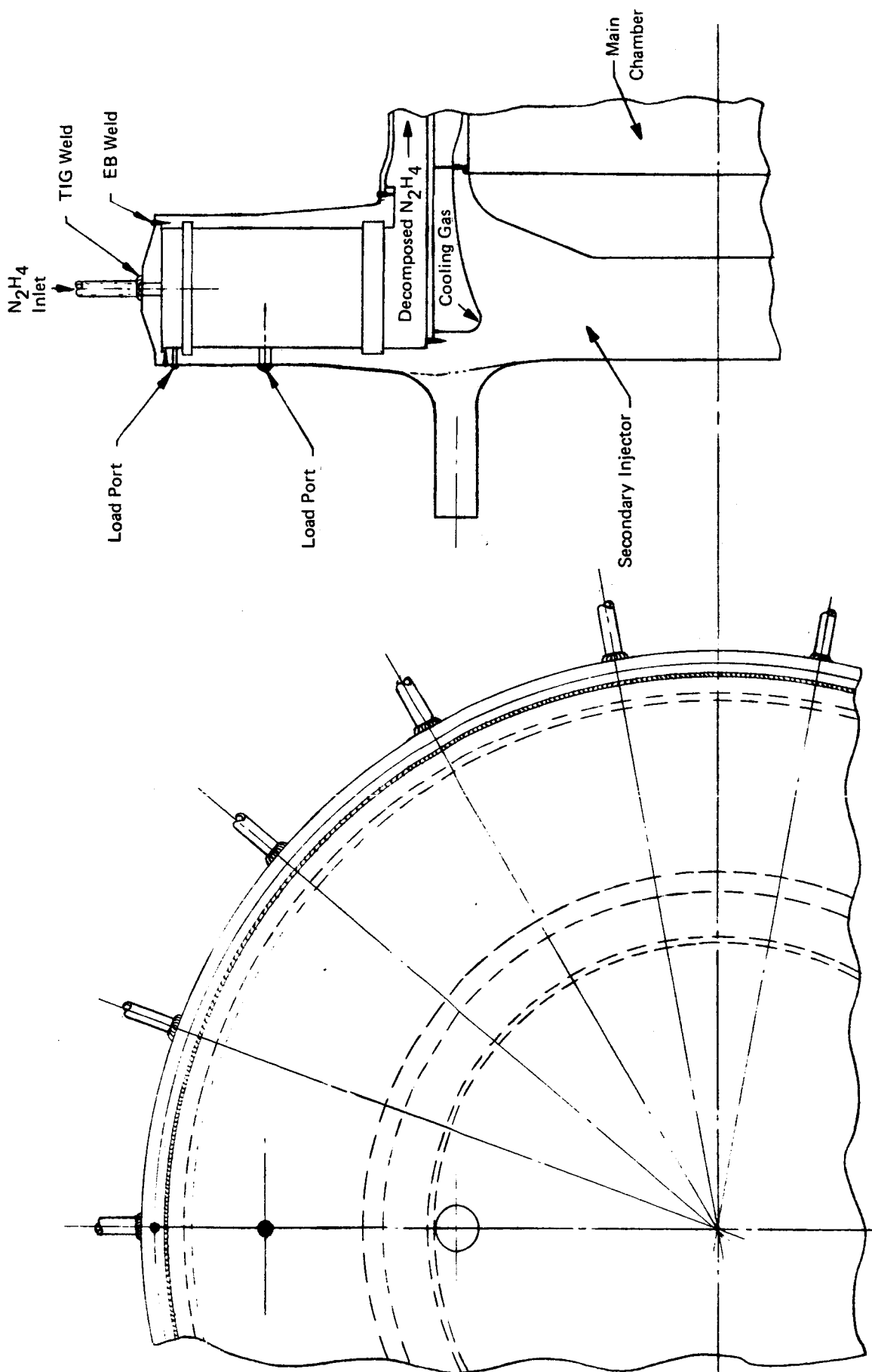


Figure 8 Sl. Secondary Injector Station Radial in Feed - Annular Reactor -
Annular Passage

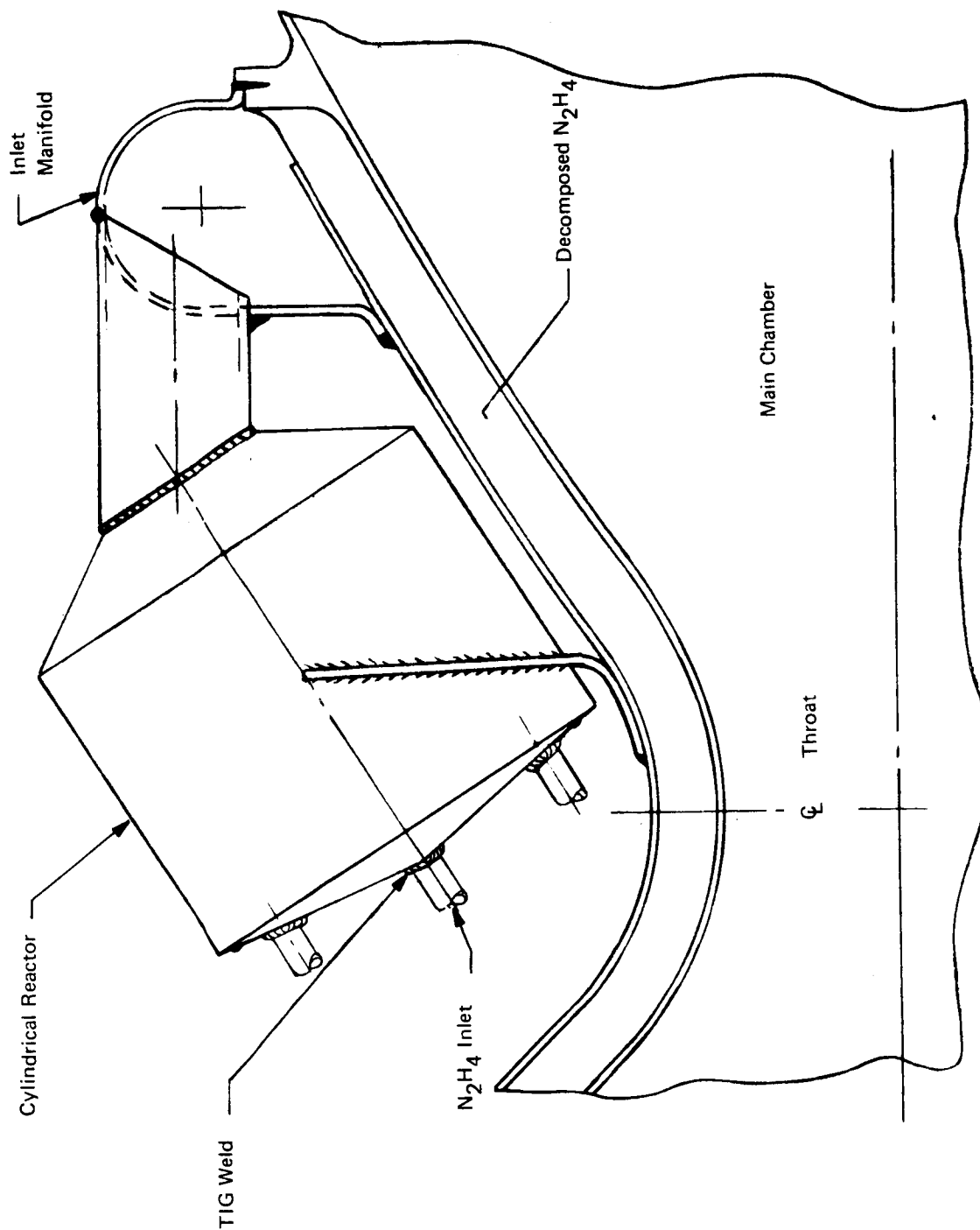


Figure 9 SI. Throat Station, Multiple Cylindrical, Welded Reactors
Cluster of 6 (Typical)

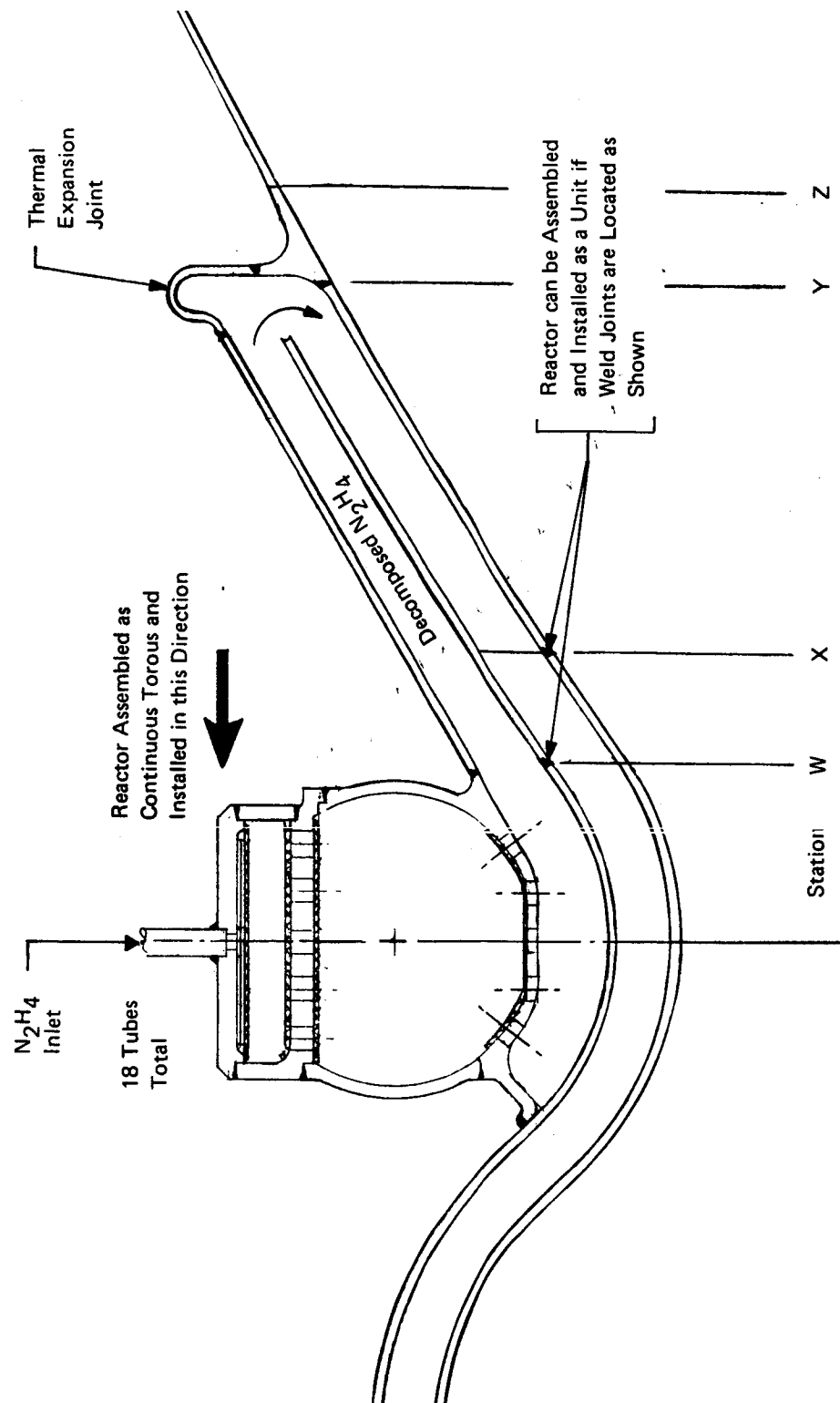


Figure 10 SI. Throat Station, Radial in Feed Toroidal Reactor

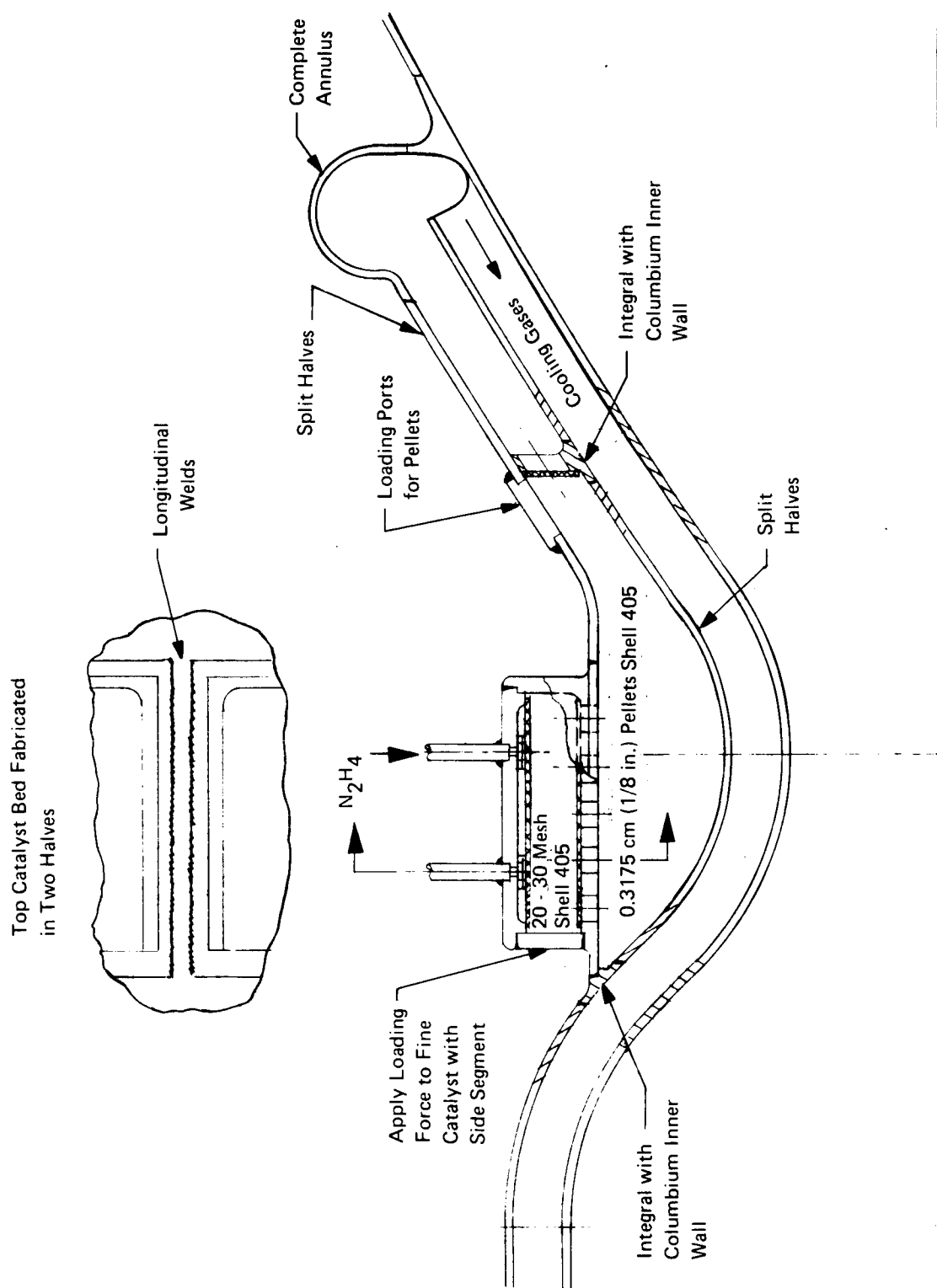


Figure 11 SI. Throat Station, Radial In-Feed, Annular Reactor, Split Section
All-Welded Columbium Alloy Design

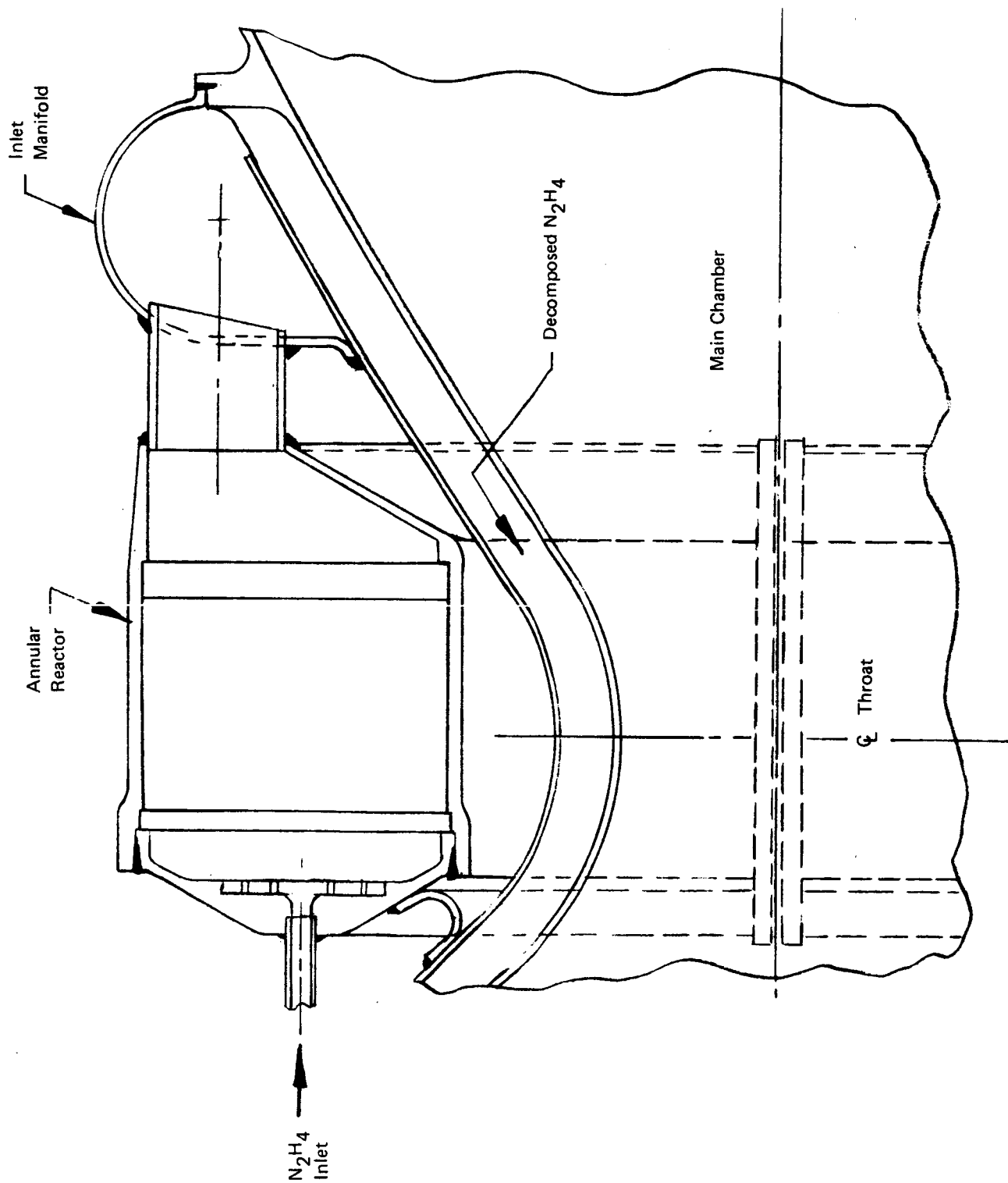


Figure 12 SL. Throat Station, Axial Feed Annular Reactor - Split Sections
All Welded

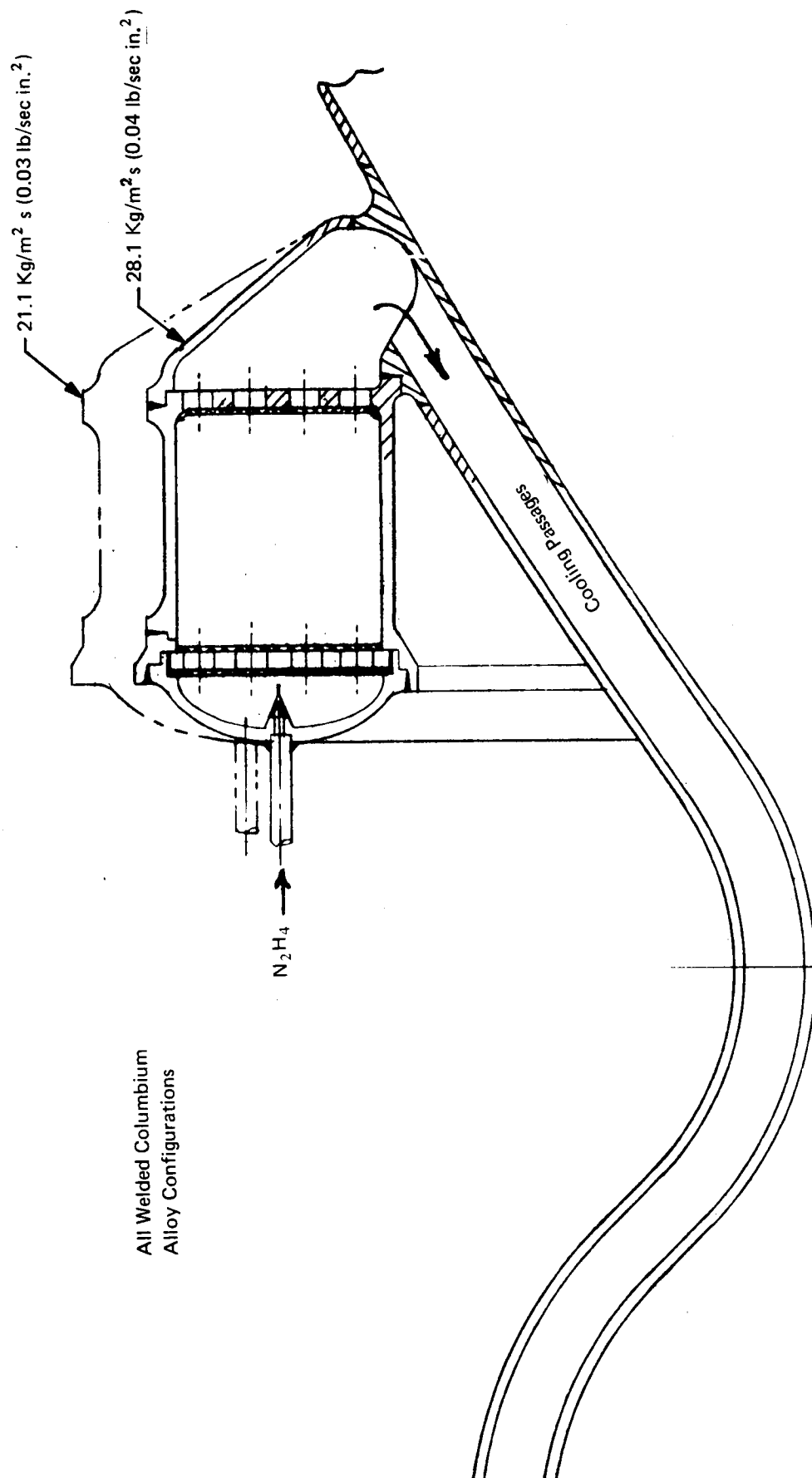


Figure 13 SI. Divergent Nozzle Station. Axial Flow Reactor
Bed Loading Comparison

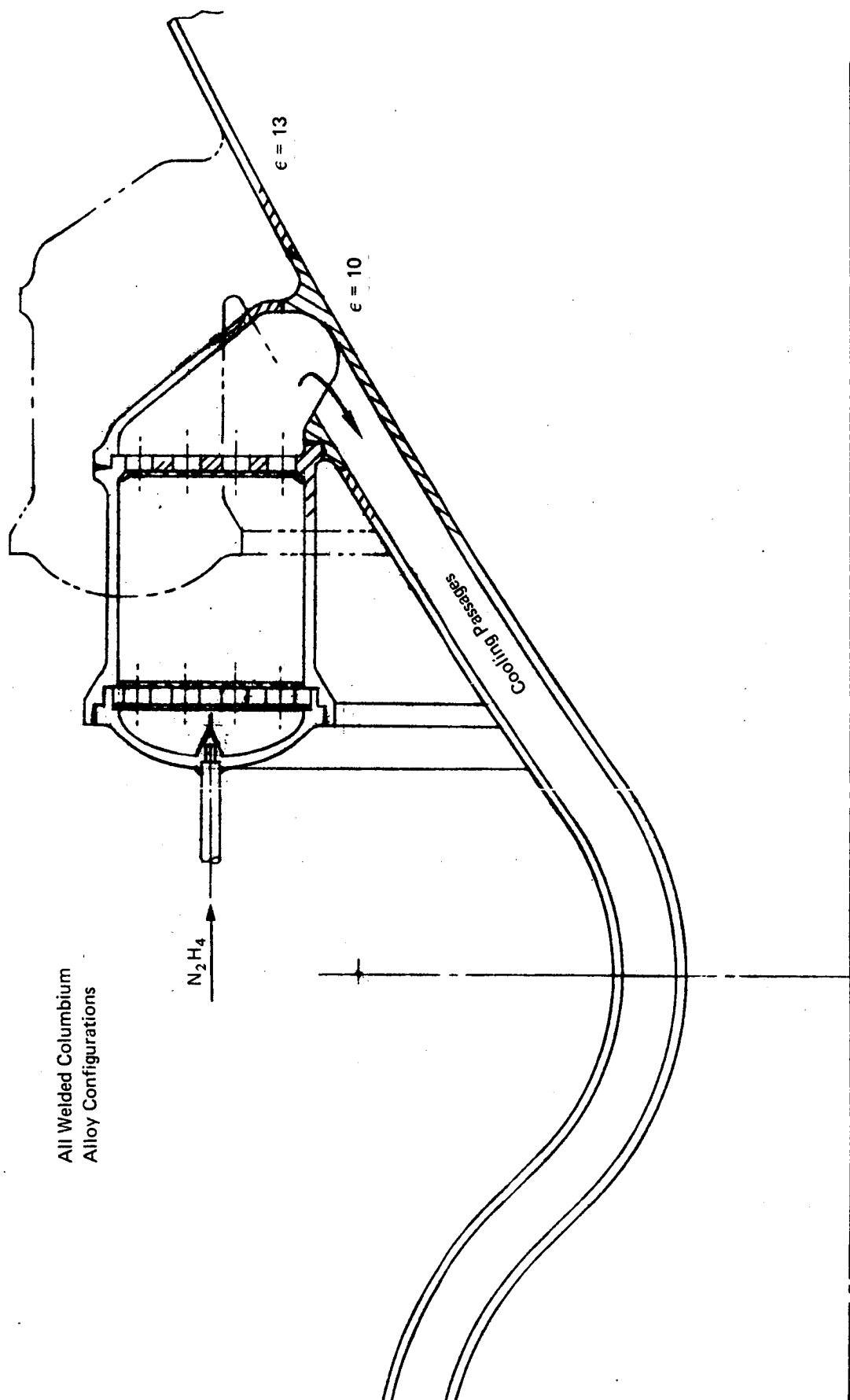


Figure 14 SI. Divergent Nozzle Stations, $\epsilon = 10$ and $\epsilon = 13$ Axial Flow Reactor, Welded Joints

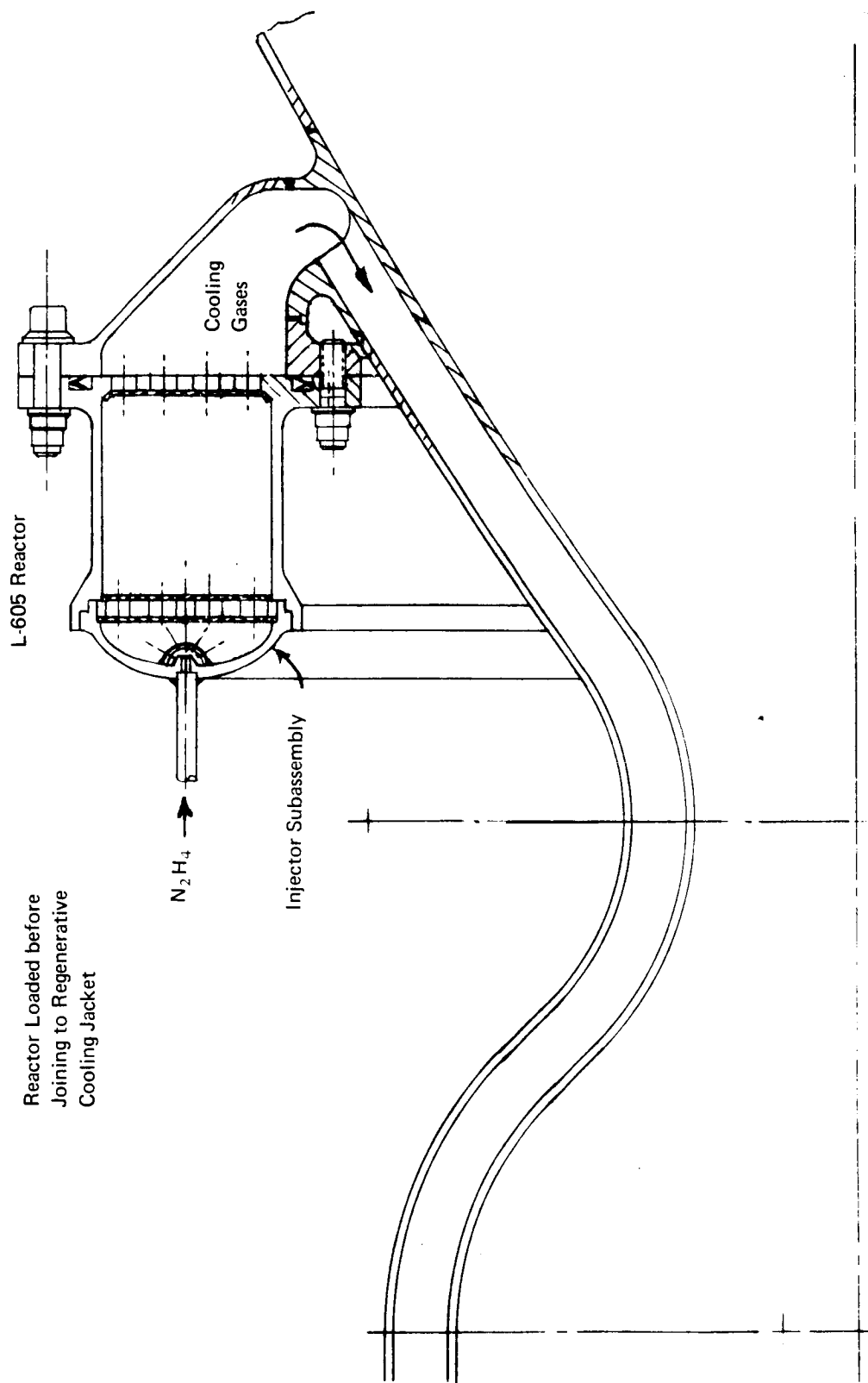


Figure 15 SL. Nozzle/Extension Station, Annular Reactor Axial Feed
Reactor Bolted to Thrust Chamber

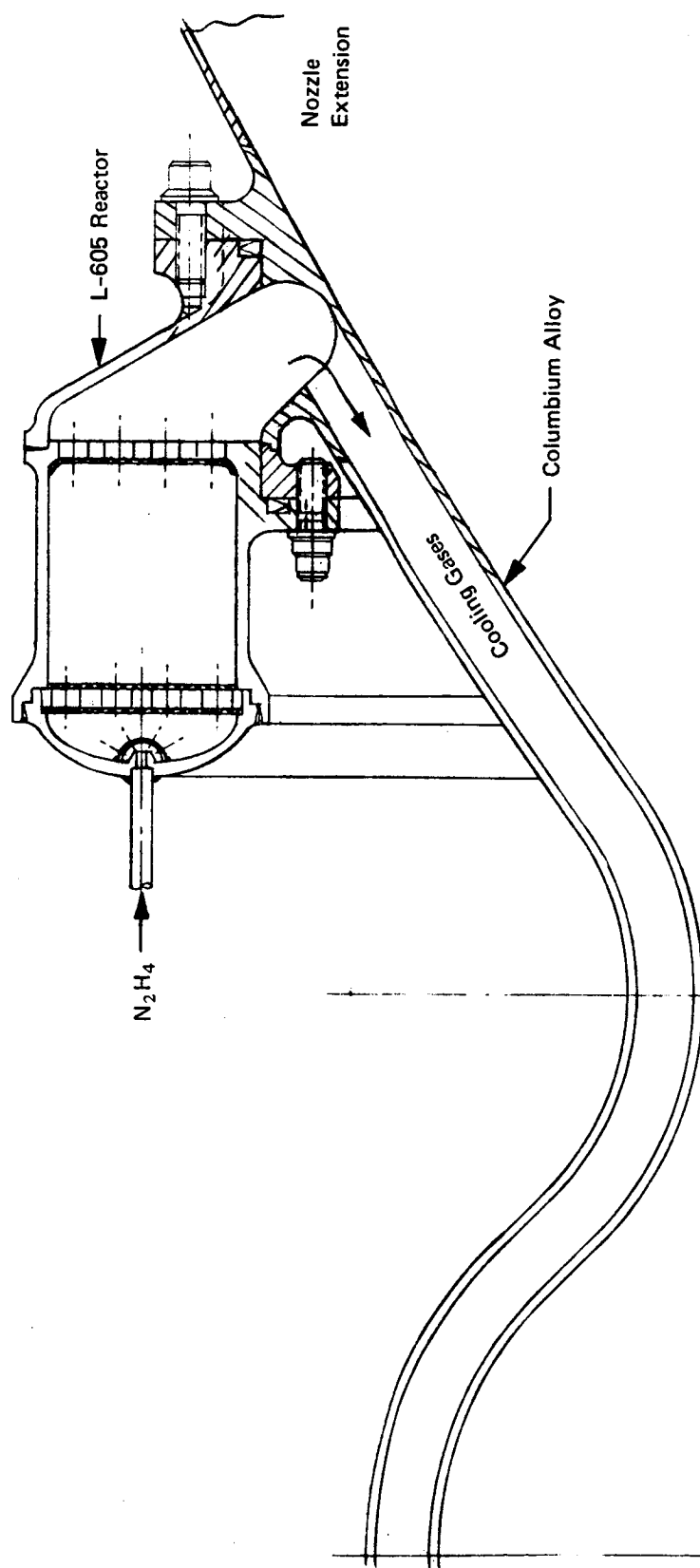


Figure 16 SL. Nozzle/Extension Station, Axial Flow Reactor
L-605 Annular Reactor

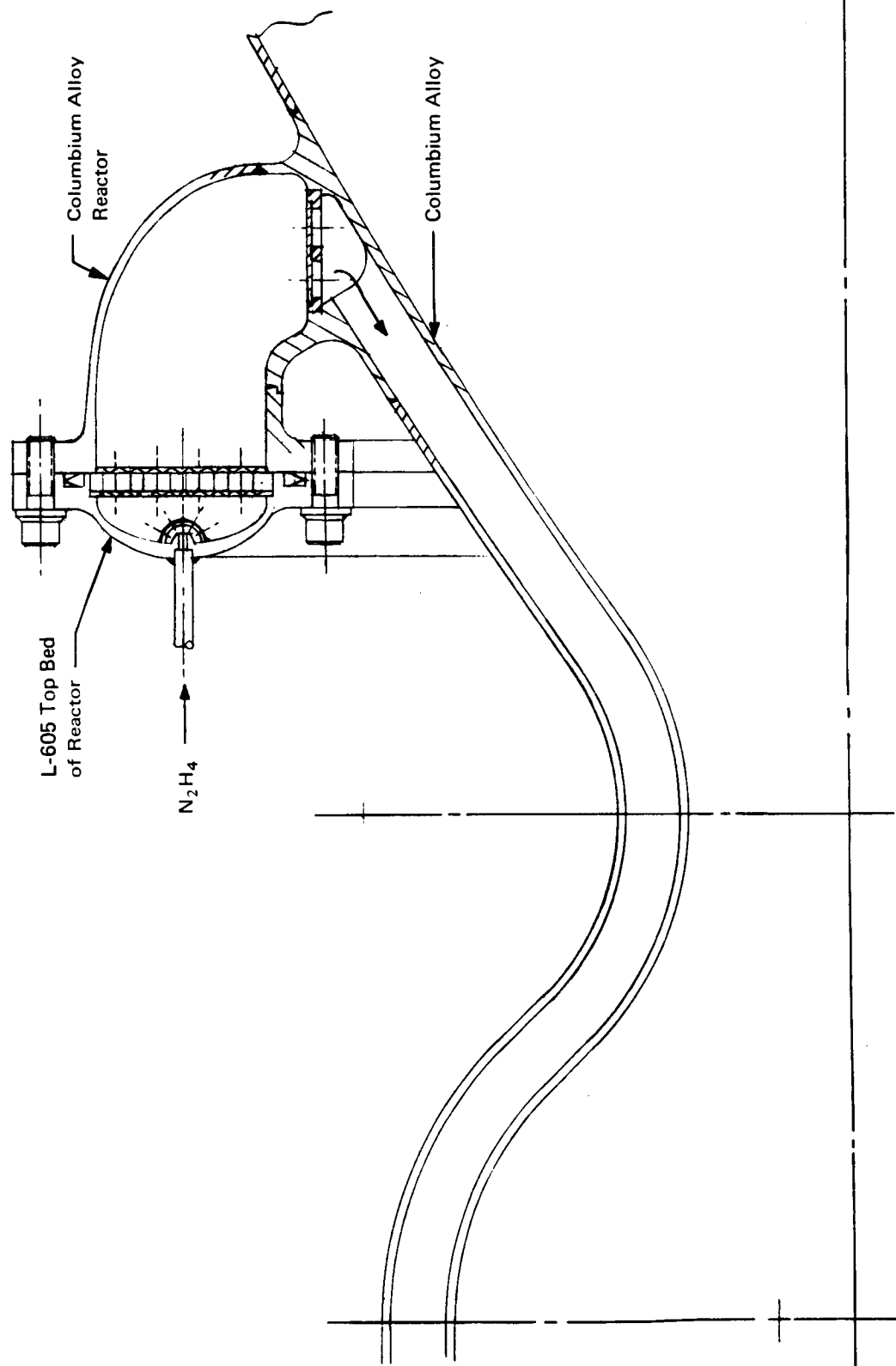


Figure 17 SI. Nozzle/Extension Station, Annular Reactor Axial Feed
Top Bed Bolted Configuration

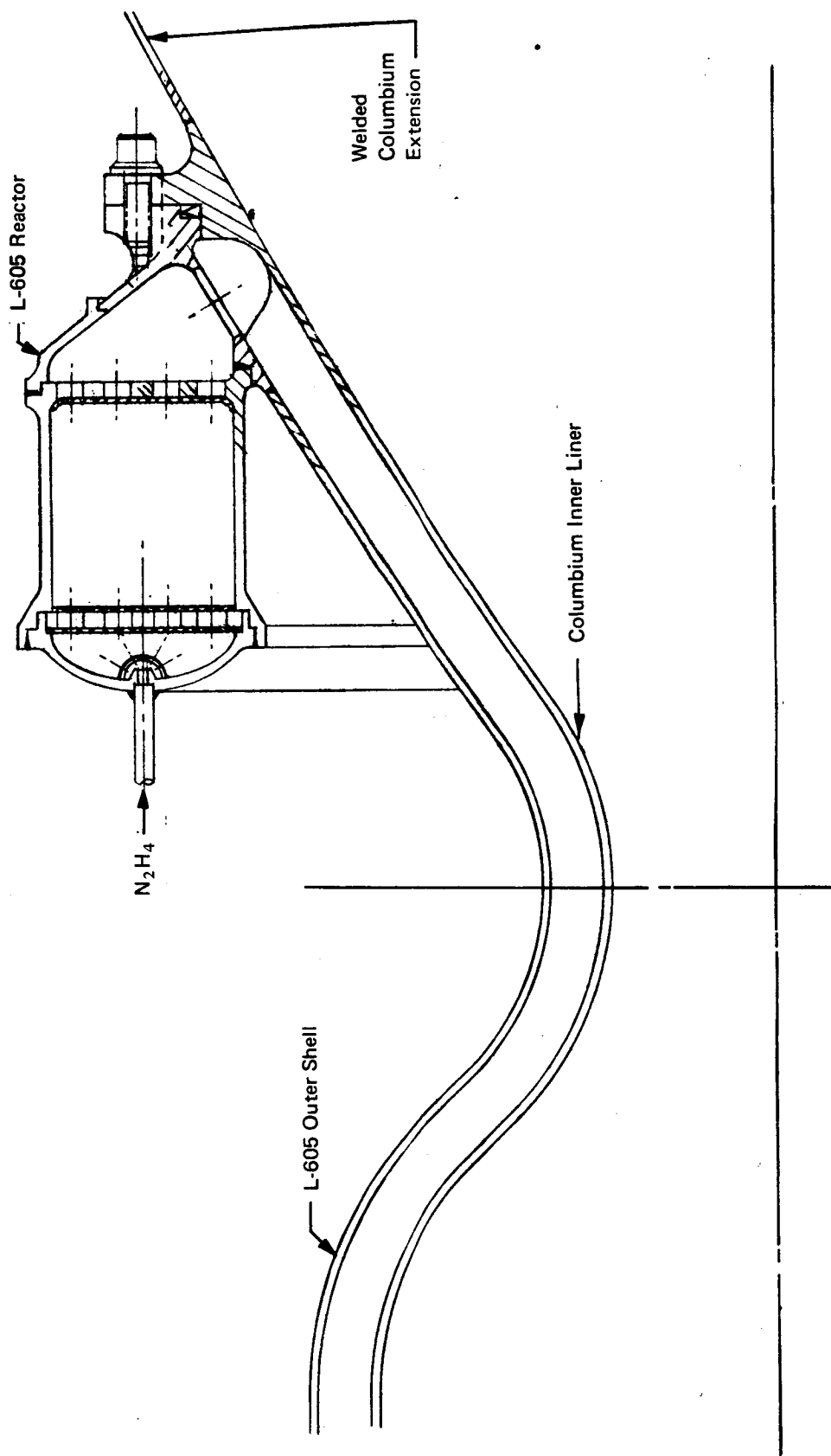


Figure 18 SI. Nozzle/Extension Station Axial Flow Injector, Annular Chamber
Only Inner Liner and Injector Face Fabricated from Columbian Alloy

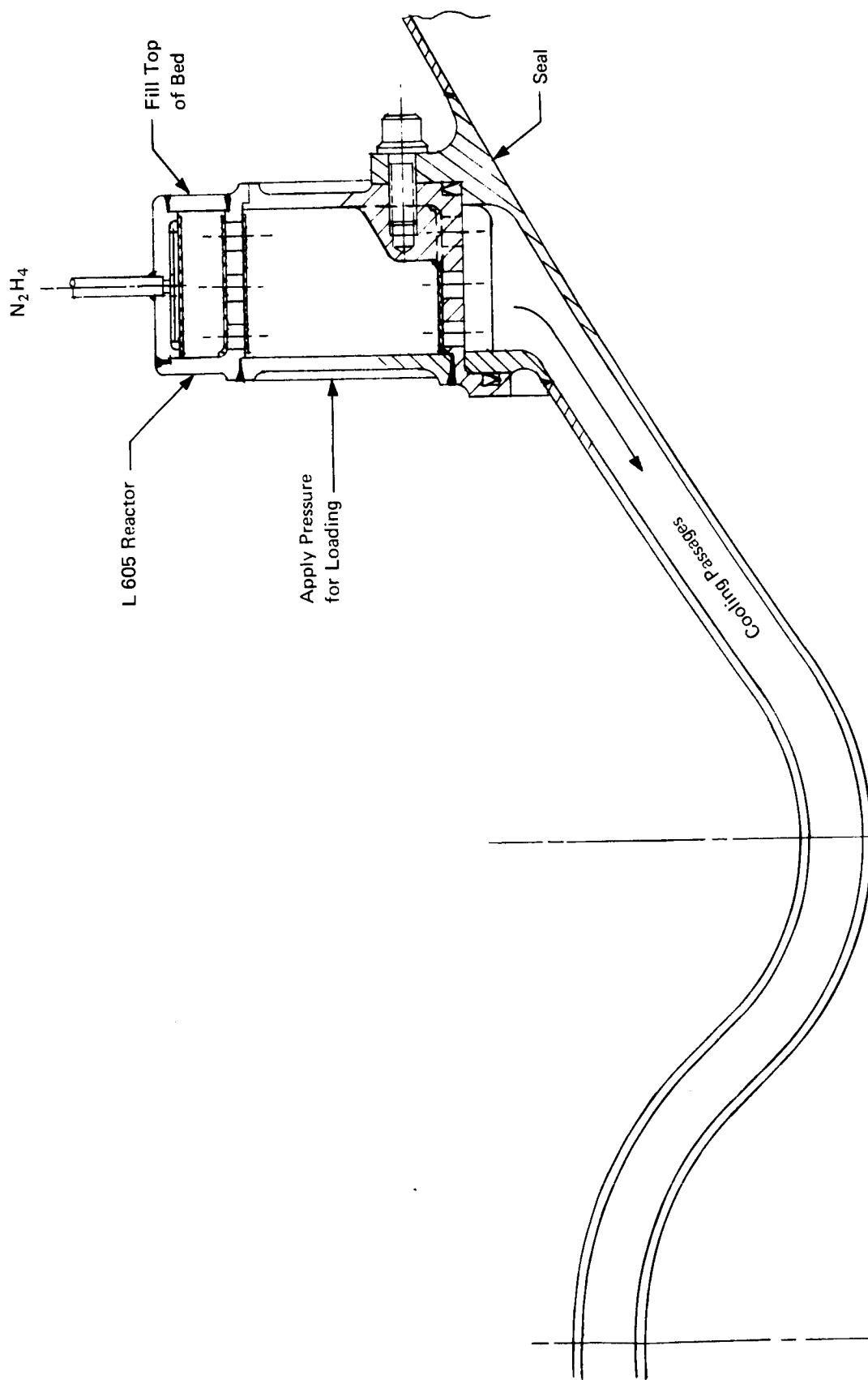


Figure 19 SI. Nozzle Extension Station Annular Configuration Radial in Feed Reactor Bolted Joint

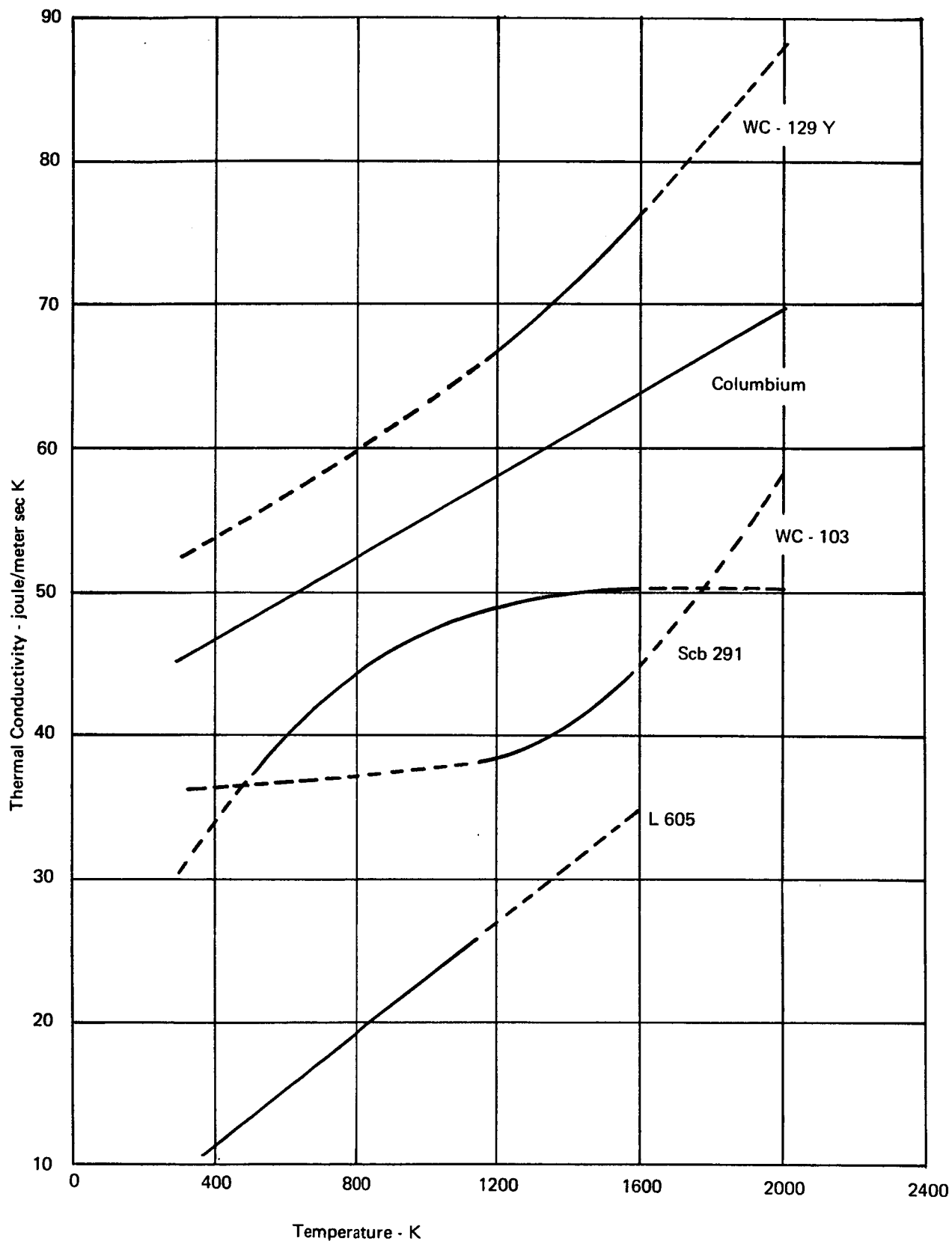


Figure 20 SI. Thermal Conductivity

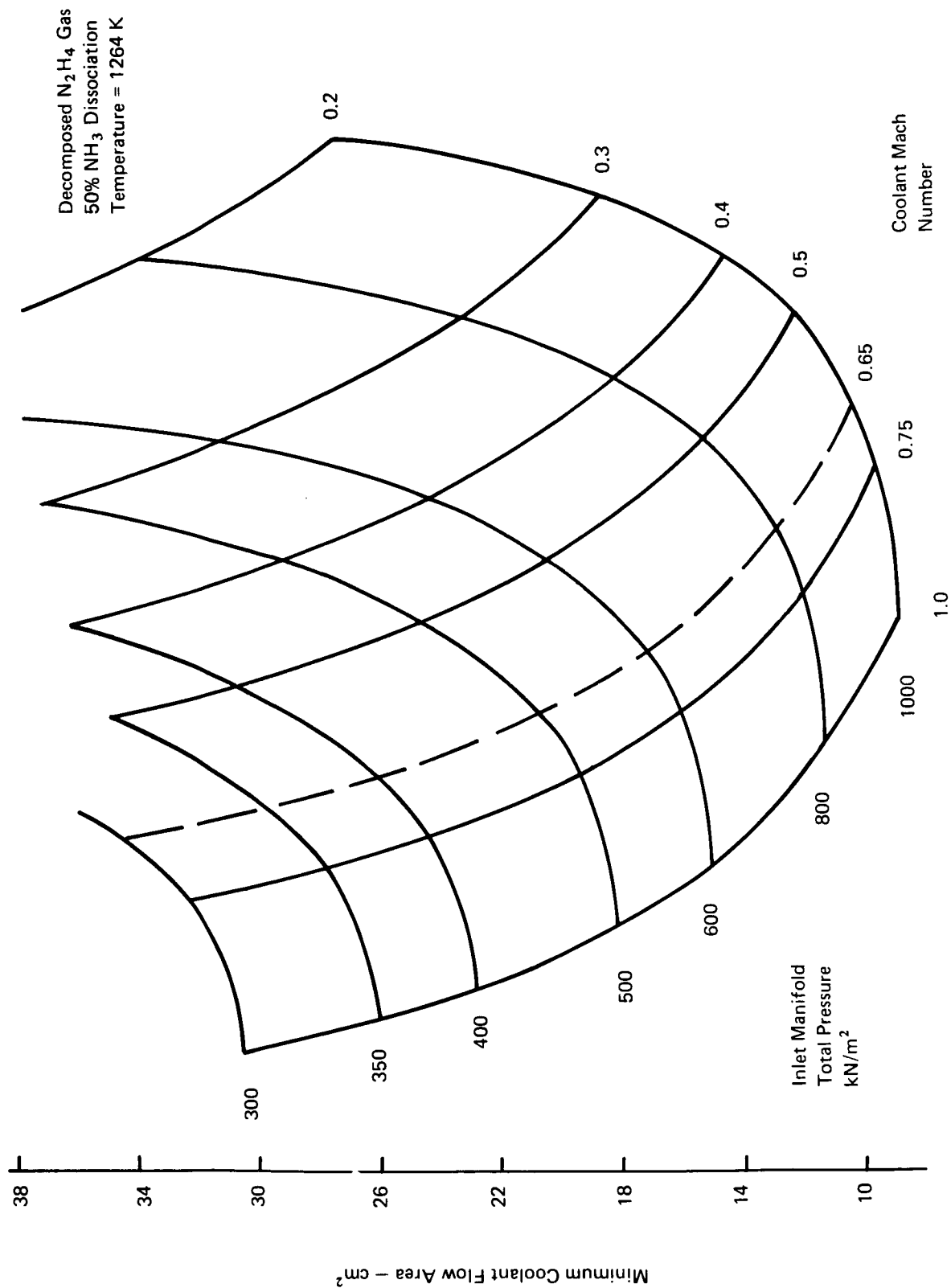


Figure 21 SI. Influence of Inlet Manifold Pressure on Cooling Passage Design Variables

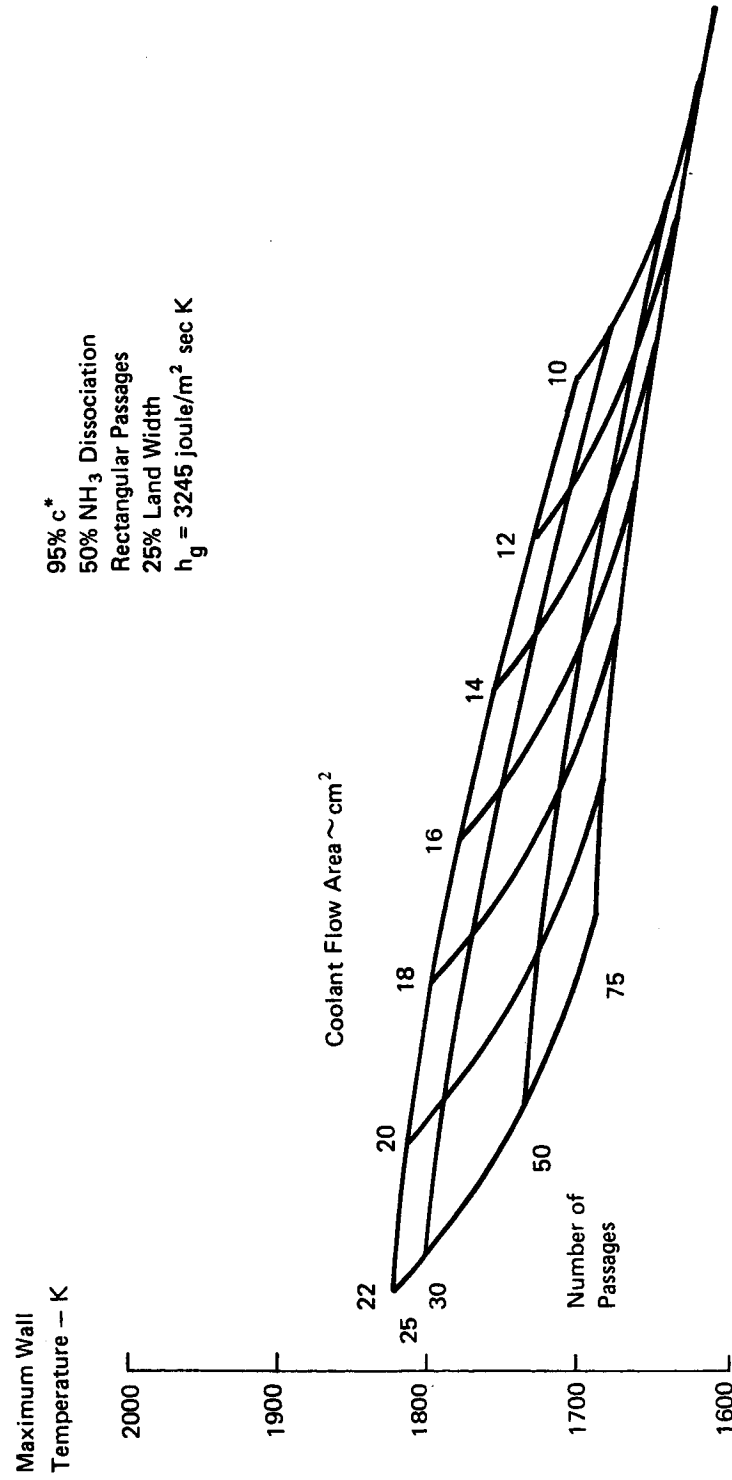


Figure 22 SI. Influence of Coolant Passage Design Parameters on Maximum Throat Temperature

95% c*
 50% NH₃ Dissociation
 Rectangular Passages
 Total Pressure = 550 kN/m² (Monomode)
 25% Land Width
 h_g = 3245 joules/m² sec K

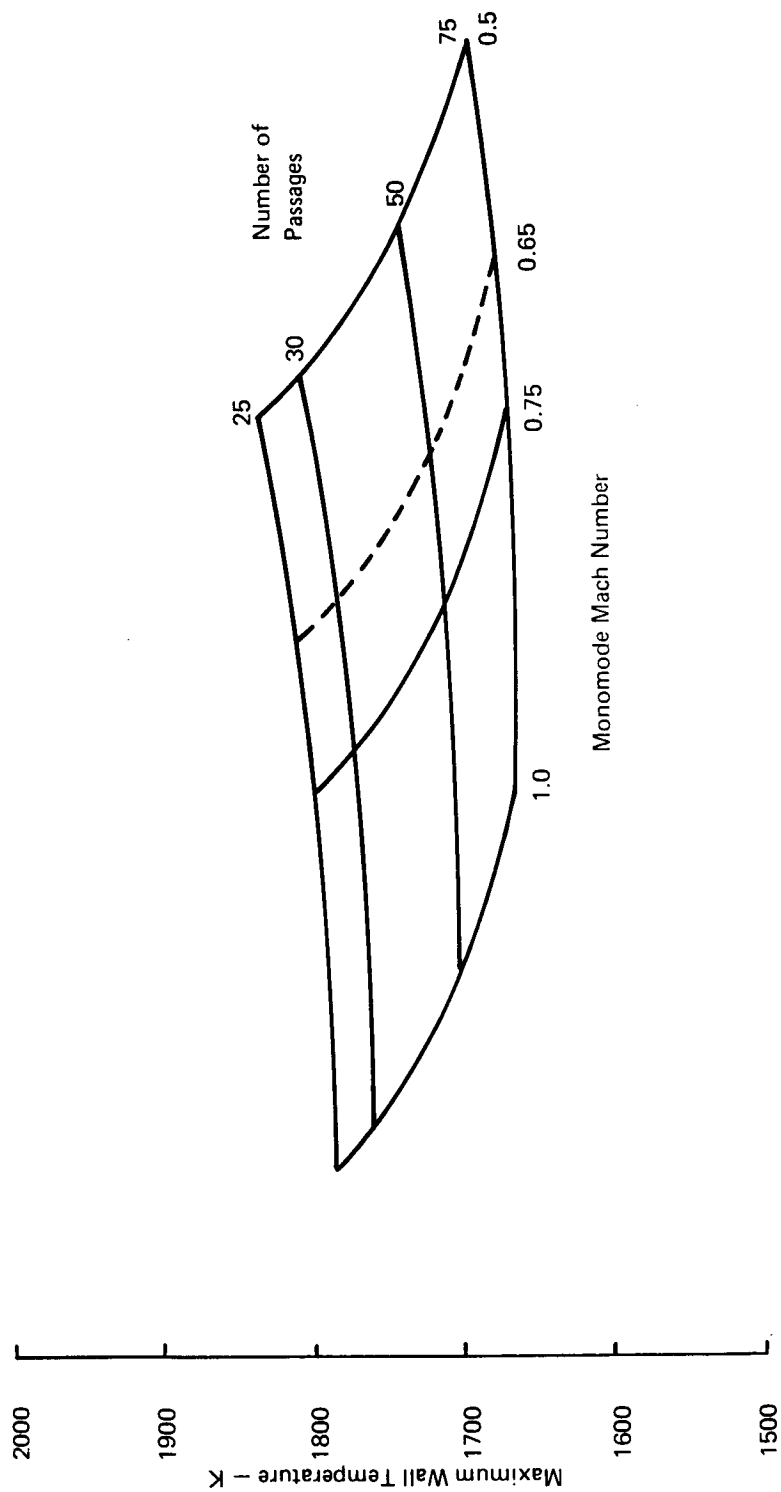


Figure 23 SI. Influence of Coolant Passage Design Parameters on Maximum Throat Temperature

95% c*
 50% NH₃ Dissociation
 50 Rectangular Passages
 25% Land Width
 $h_g = 3245 \text{ joules/sec m}^2 \text{ K}$

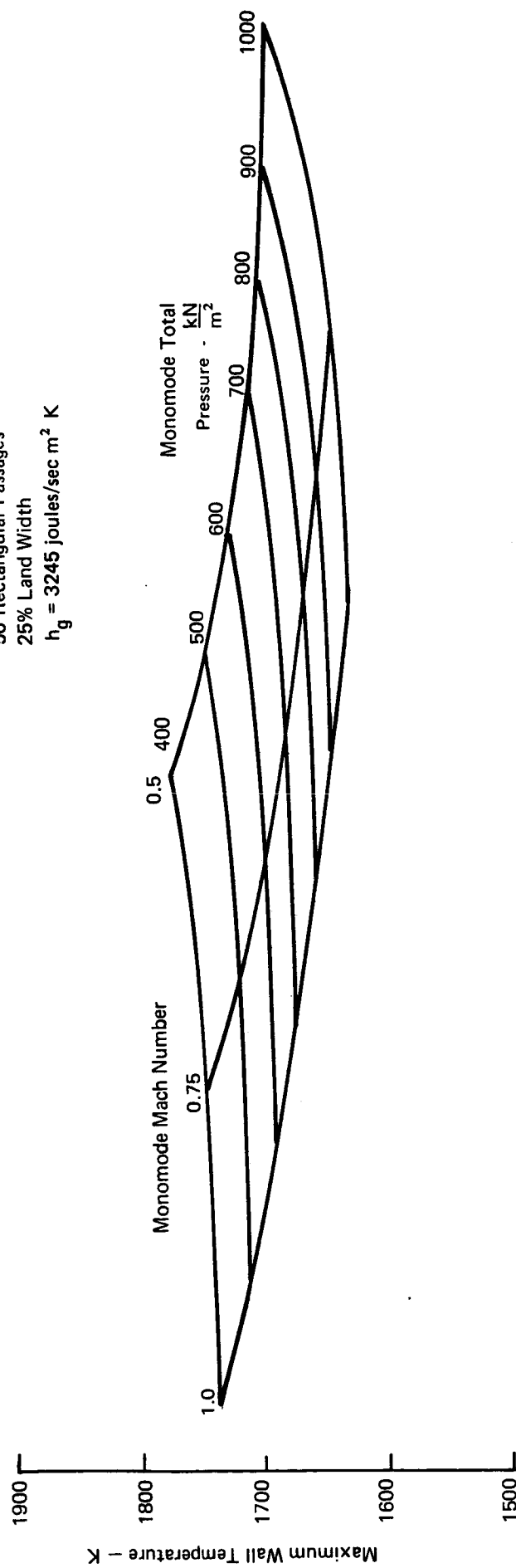


Figure 24 SI. Influence of Coolant Passage Design Parameters on Maximum Throat Temperature

95% c^*
 50% NH_3 Dissociation
 50 Rectangular Passages
 Mach number = 0.75
 Total Pressure = 550 kN/m^2
 $h_g = 3245 \text{ joules/m}^2 \text{ sec K}$

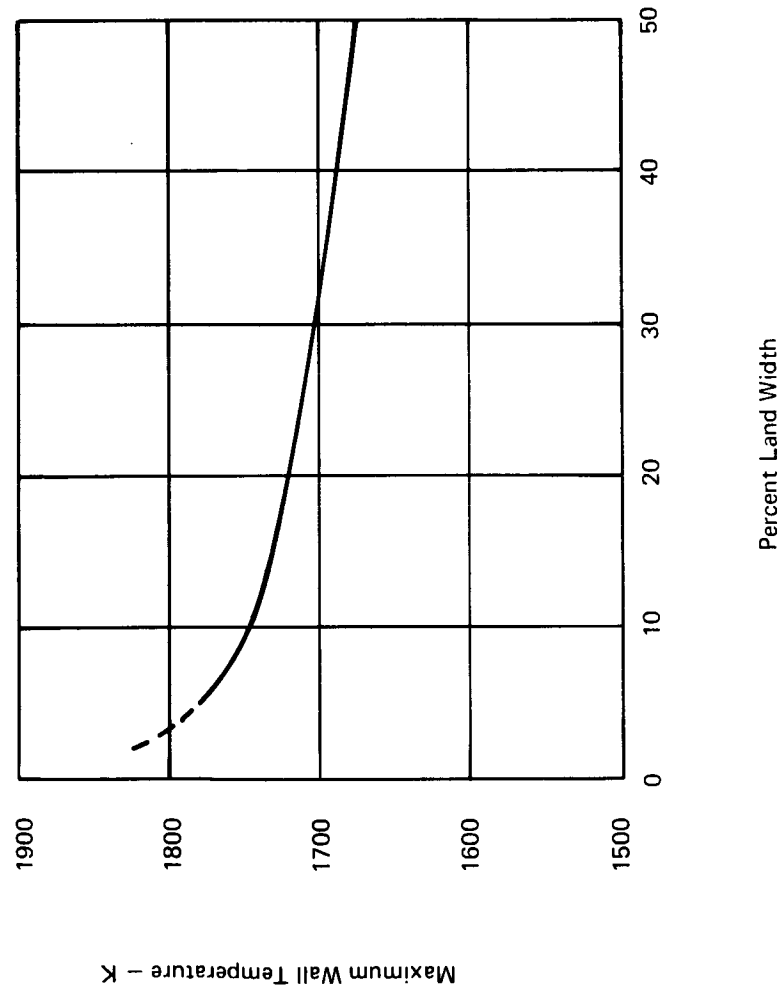


Figure 25 SI. Influence of Percent Land Width on Maximum Throat Temperature

95% c*
 50% NH₃ Dissociation
 50 Rectangular Passages
 $H_g = 3245 \text{ joule/m}^2 \text{ sec K}$

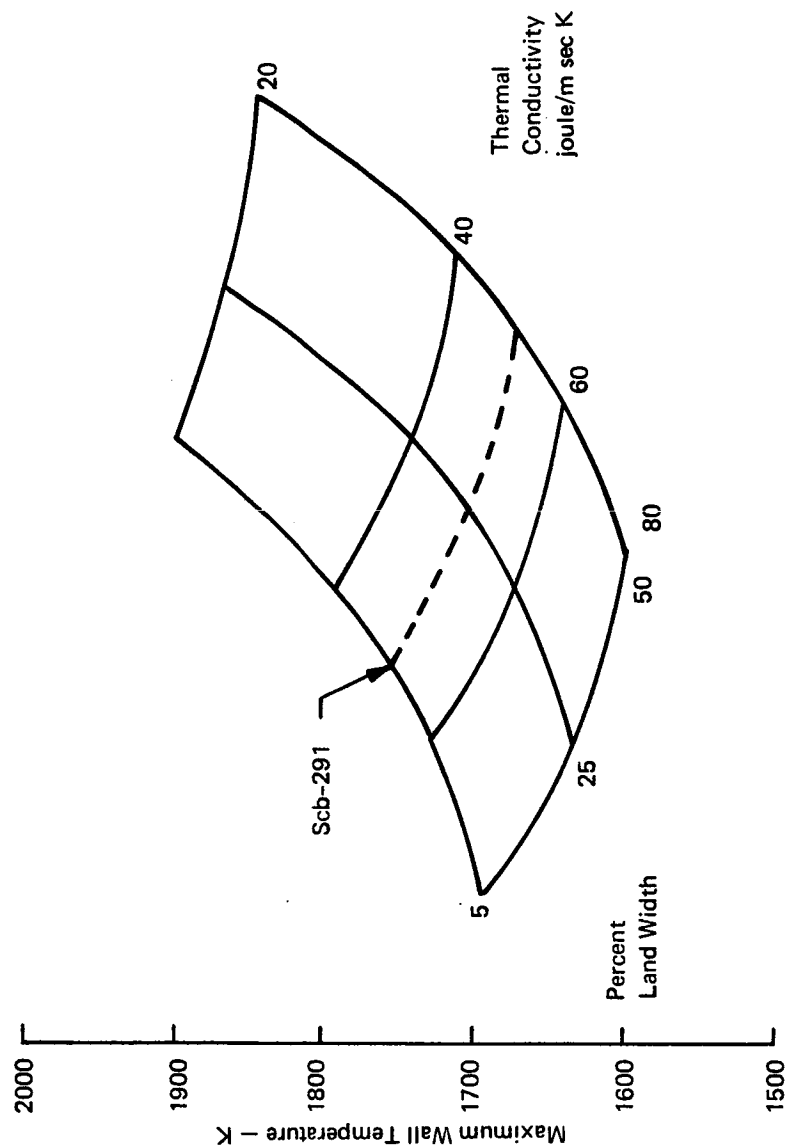


Figure 26 SI. Influence of Wall Thermal Conductivity and Land Width on Maximum Throat Temperature

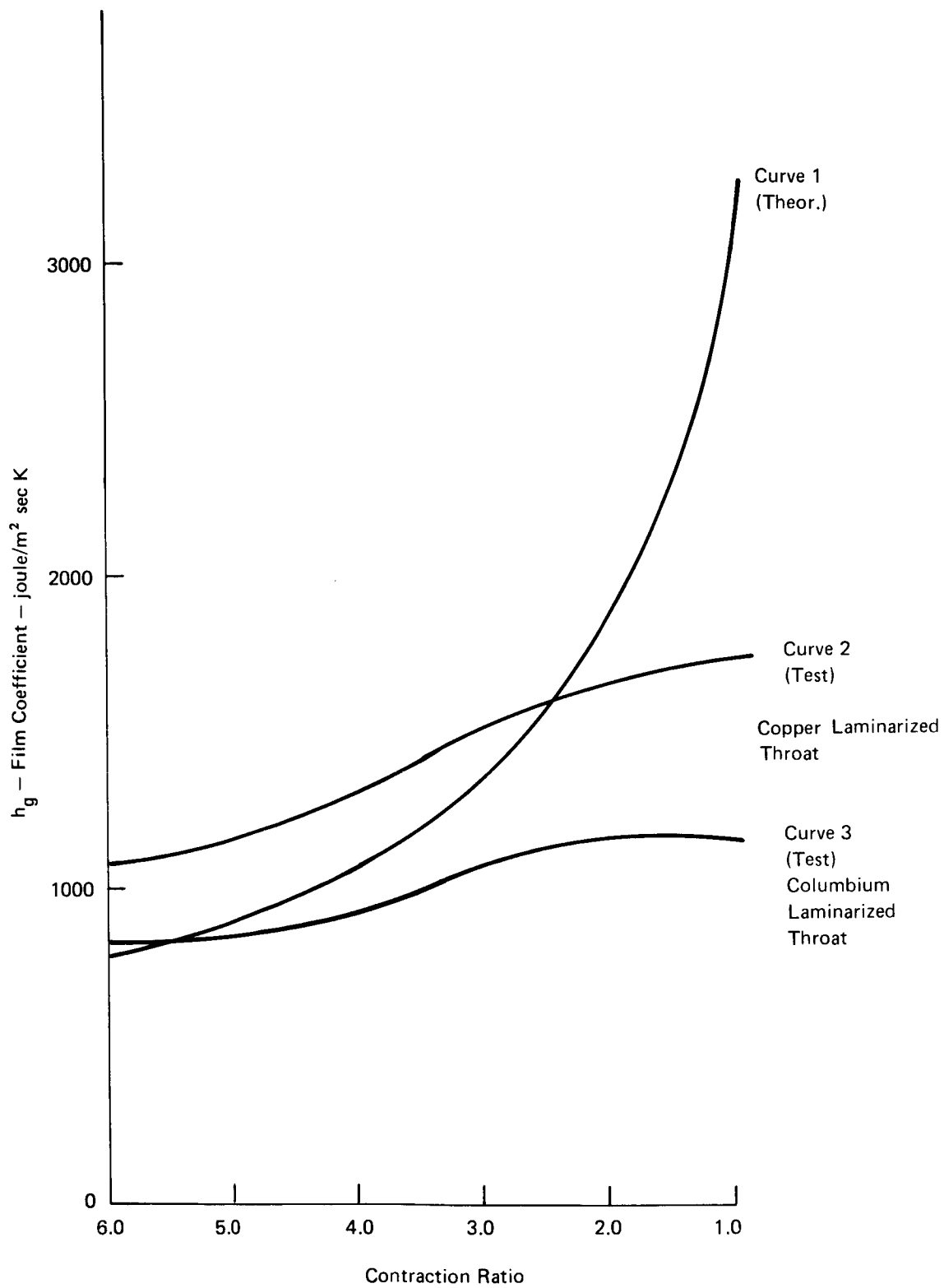


Figure 27 SI. Hot Gas Film Coefficient versus Contraction Ratio

95% c*
 50% NH₃ Dissociation
 Rectangular Passages
 25% Land Width
 $h_g = 1770 \text{ joule/m}^2 \text{ sec K}$

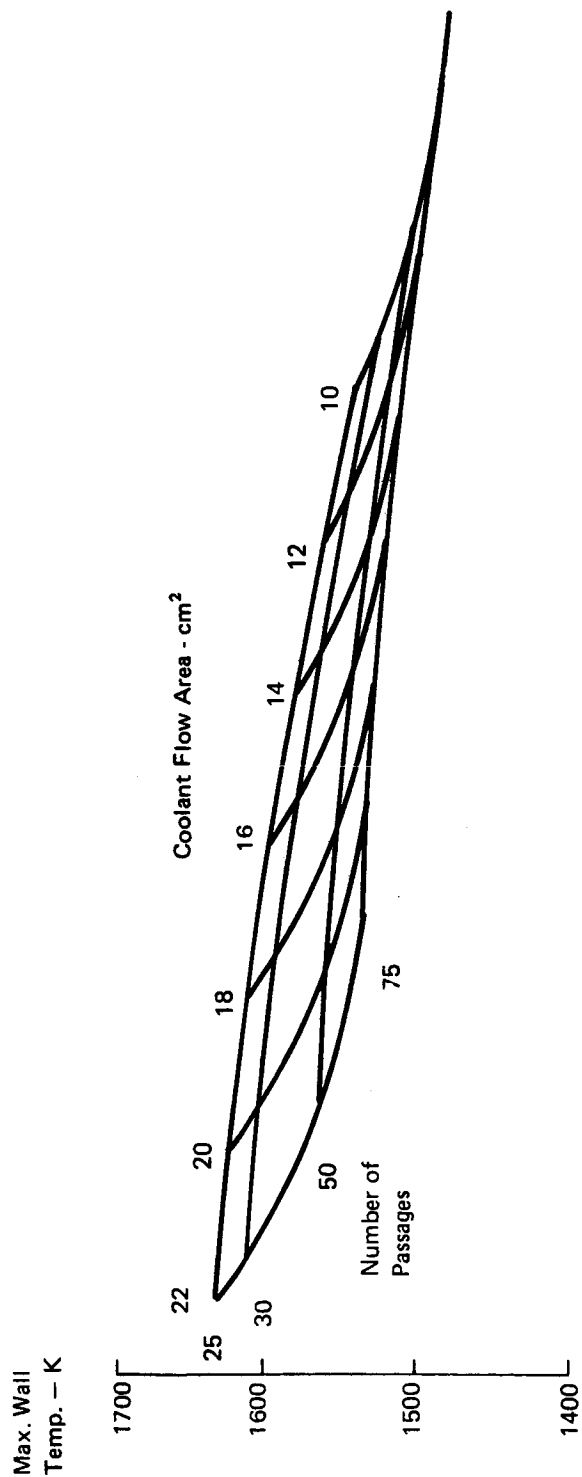


Figure 28 Sl. Influence of Coolant Passage Design Parameters on Maximum Throat Temperature

95% c*
 50% NH₃ Dissociation
 Rectangular Passages
 Total Pressure = 550 kN/m² (Monomode)
 25% Land Width
 h_g = 1770 joule/m² sec K

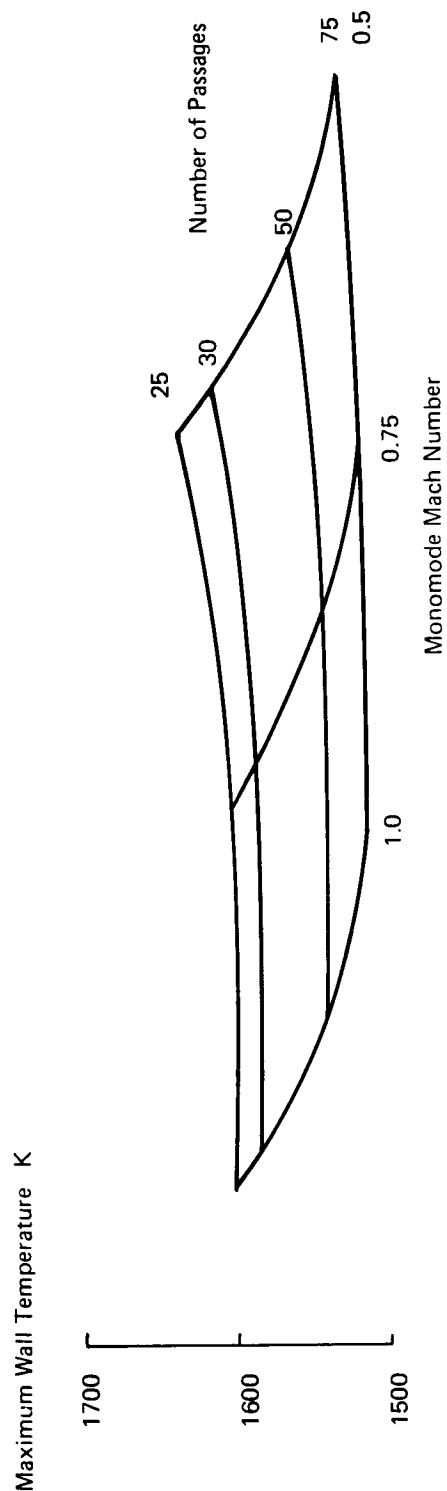


Figure 29 Sl. Influence of Coolant Passage Design Parameters on Maximum Throat Temperature

95% c*
 50% NH₃ Dissociation
 50 Rectangular Passages
 25% Land Width
 $h_g = 1770 \text{ joules/m}^2 \text{ sec K}$

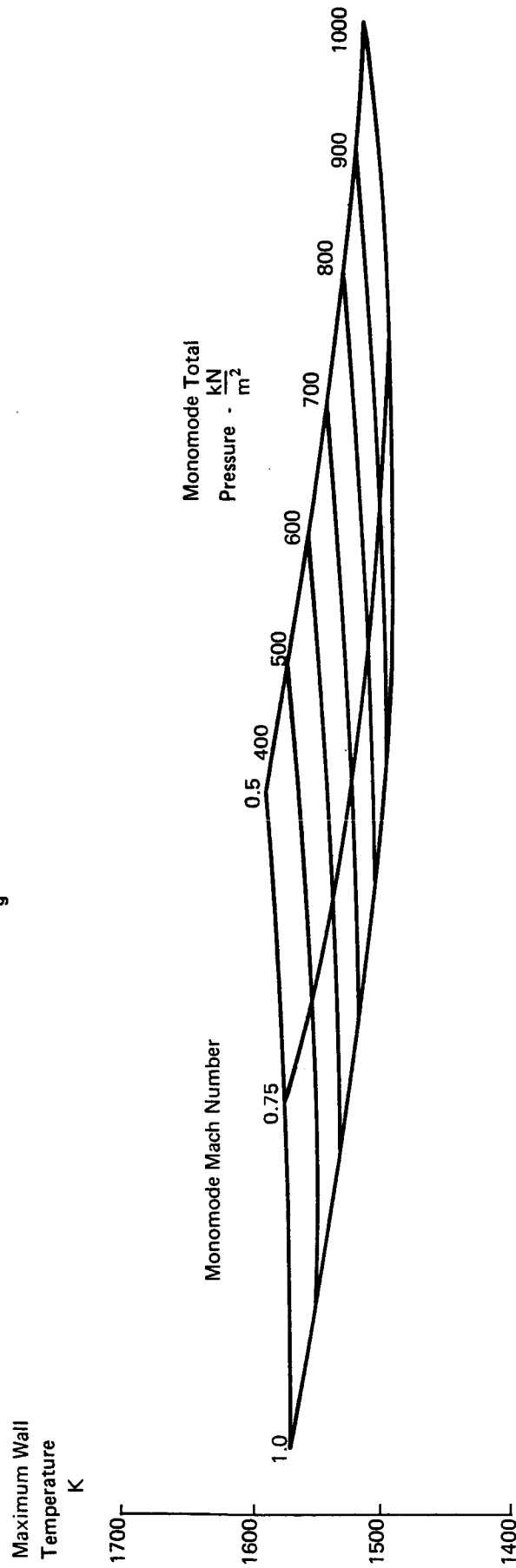


Figure 30 SI. Influence of Coolant Passage Design Parameters on Maximum Throat Temperature

95% c*
50% NH₃ Dissociation
50 Rectangular Passages
Mach Number = 0.75
Total Pressure = 500 kN/m²
 $h_g = 1770 \text{ joules/m}^2 \text{ sec K}$

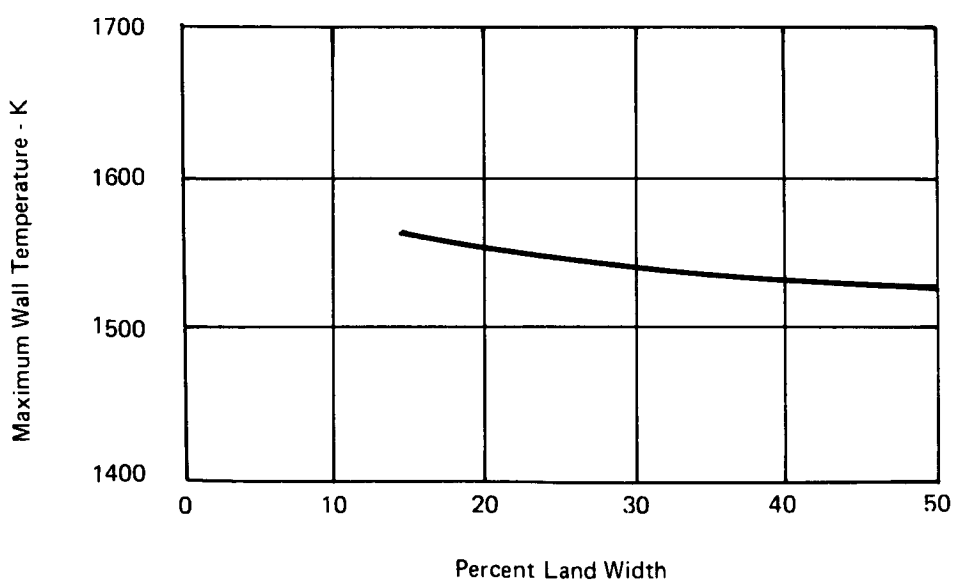


Figure 31 SI. Influence of Percent Land Width on Maximum Throat Temperature

Max. Wall Temp. -K

Wall Thickness = 0.00178 m

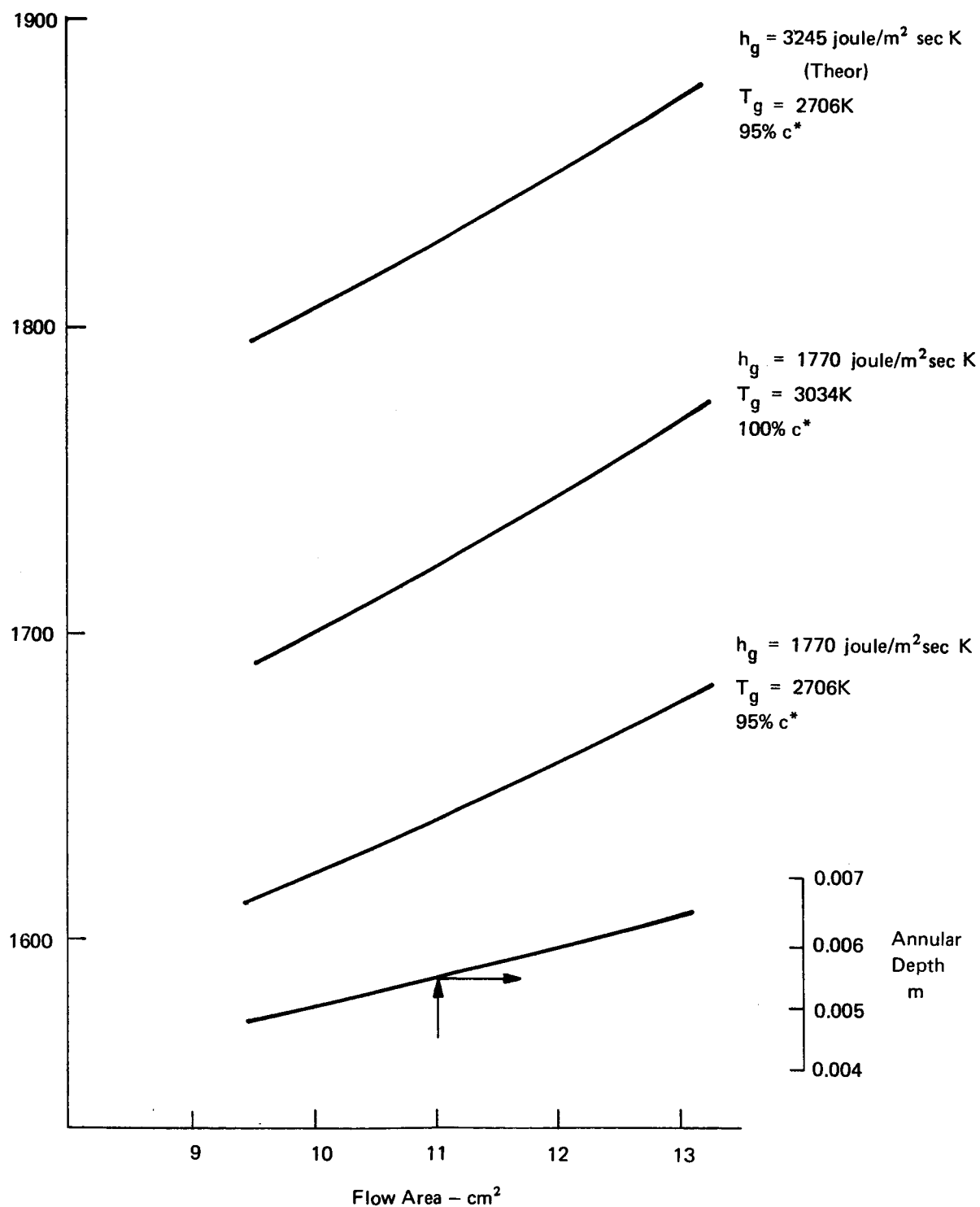


Figure 32 SI. Annular Passage Wall Temperature at the Throat

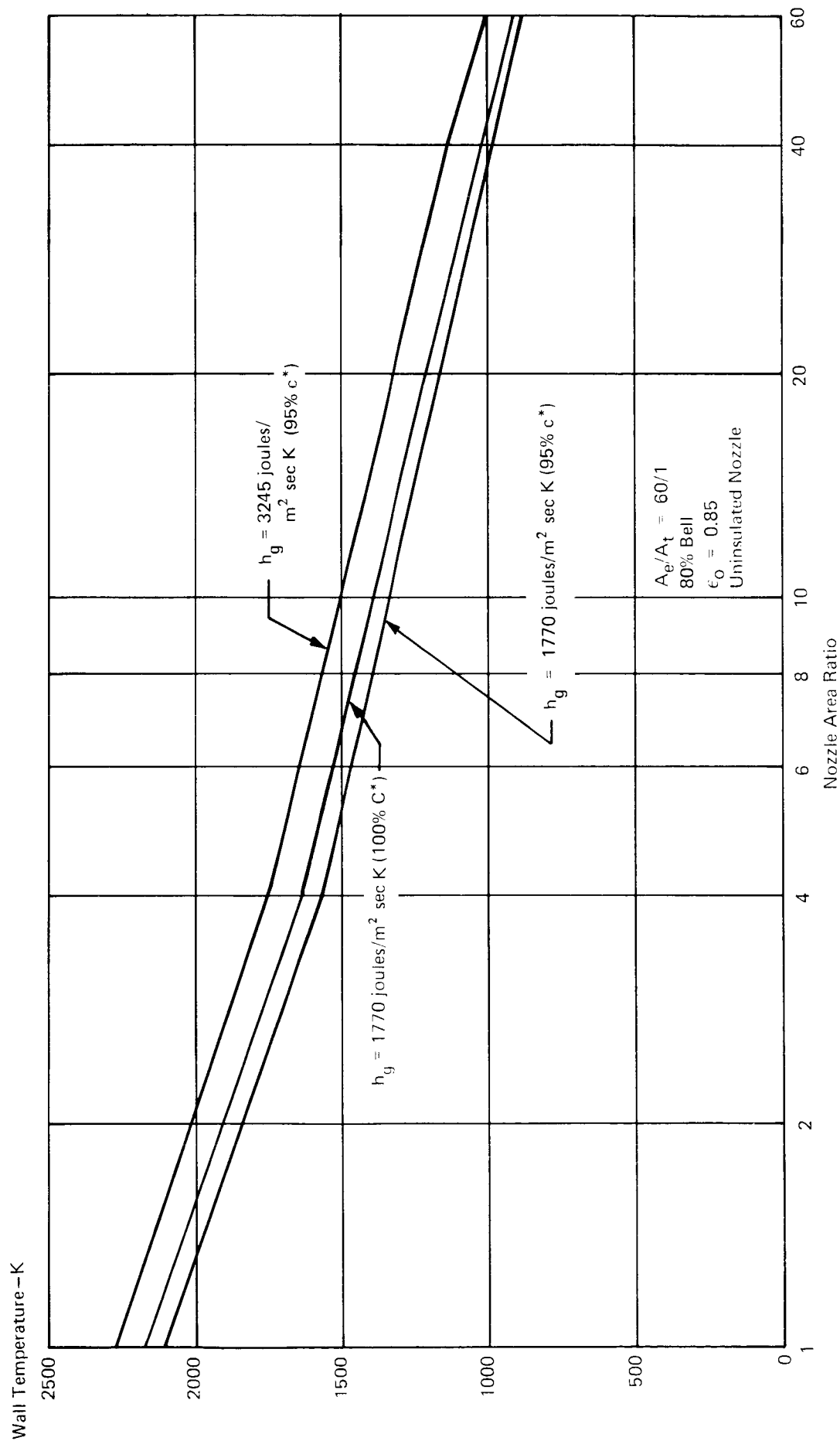


Figure 33 SL. Nozzle Extension Temperature versus Area Ratio

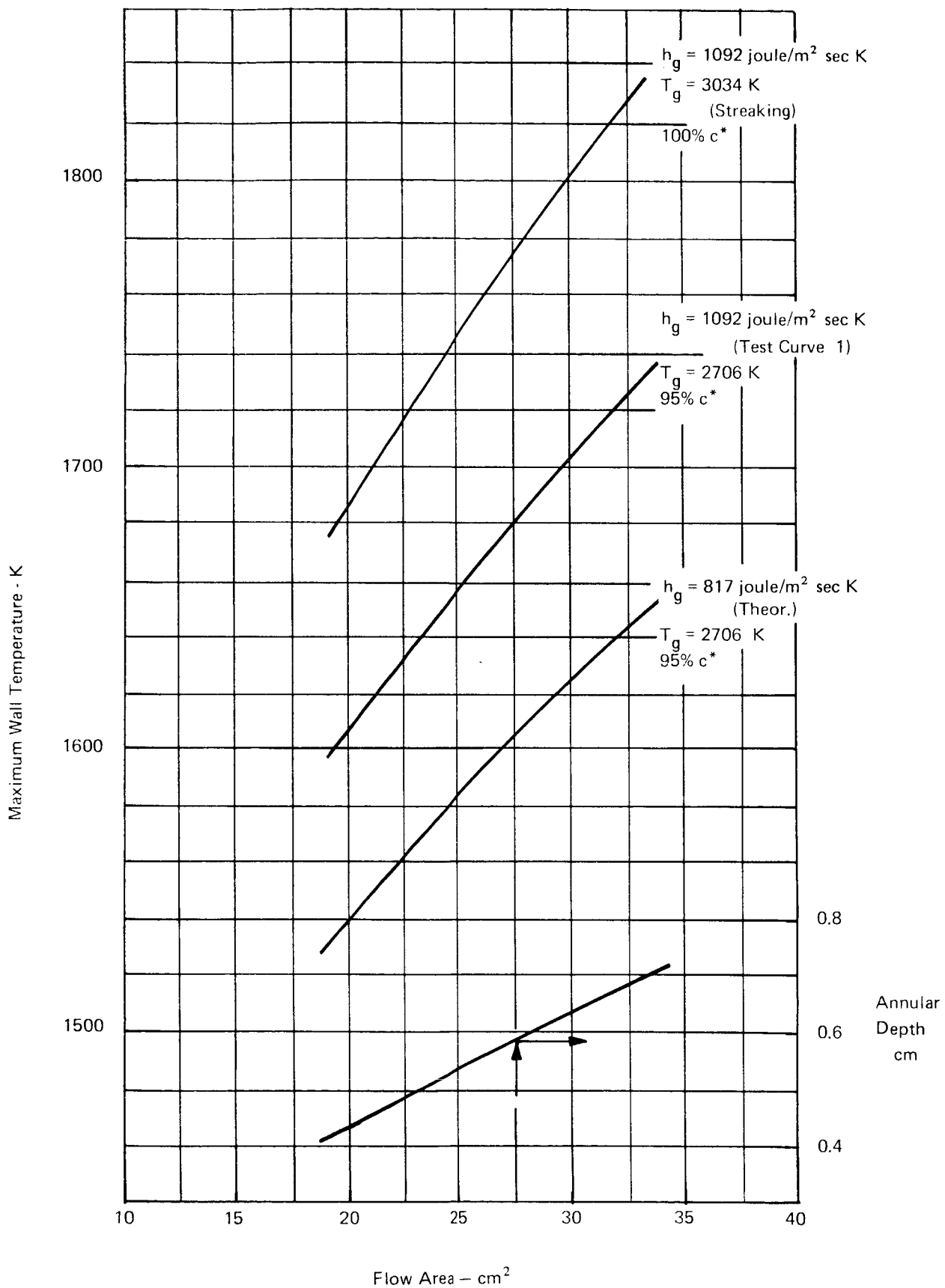


Figure 34 SI. Annular Passage Wall Temperature - Chamber

$$h_g = 817 \text{ joule/m}^2 \text{ sec K (Theor.)}$$

$$T_g = 2706 \text{ K}$$

95% c*

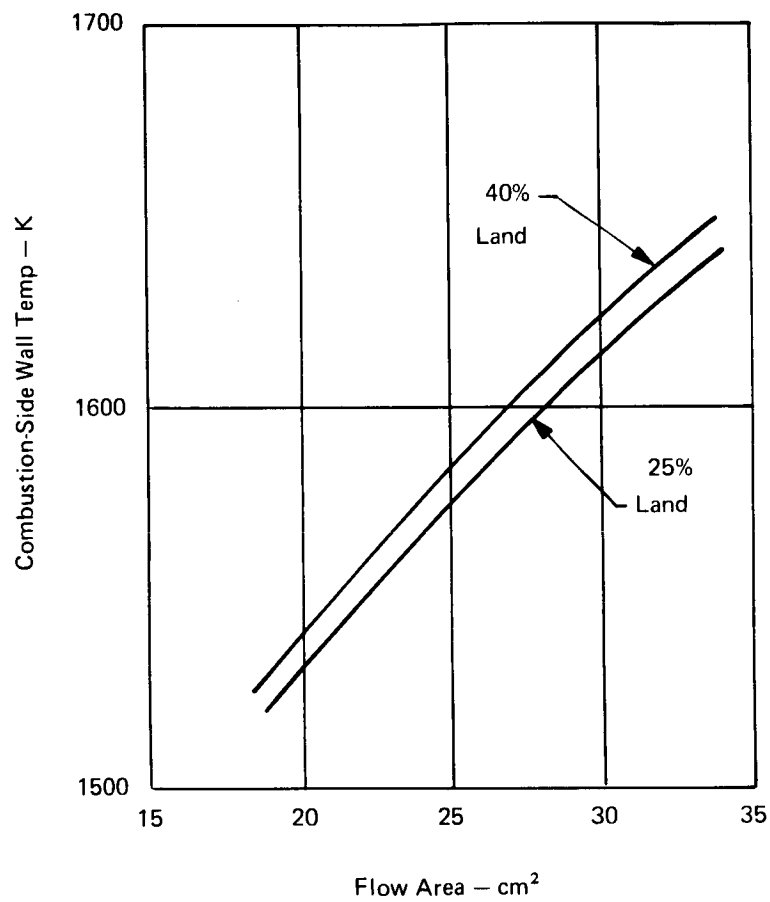


Figure 35 SI. Drilled Passages - Wall Temperature - Chamber

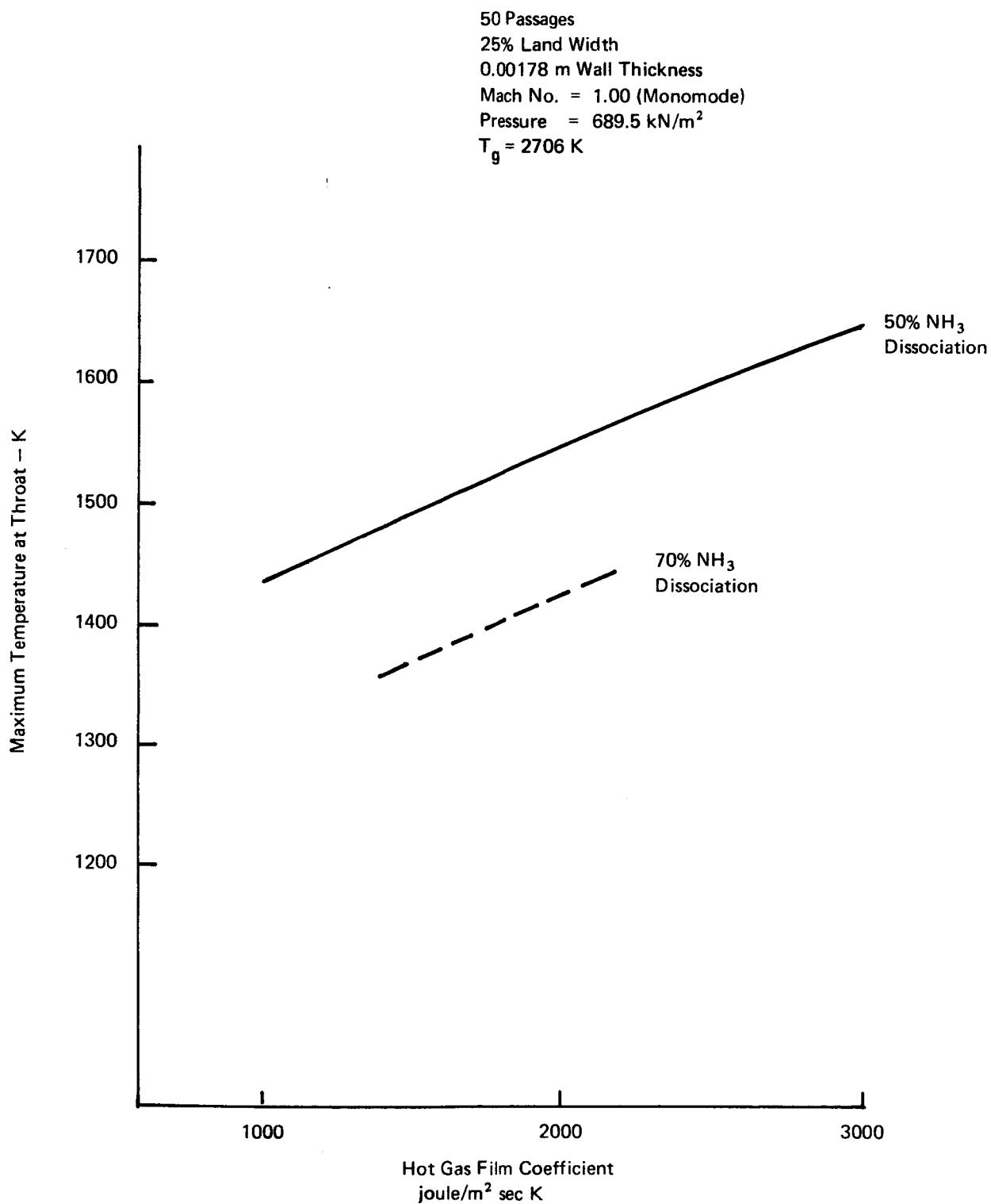


Figure 36 SI. Wall Temperature at Throat Station versus Hot Gas Film Coefficient

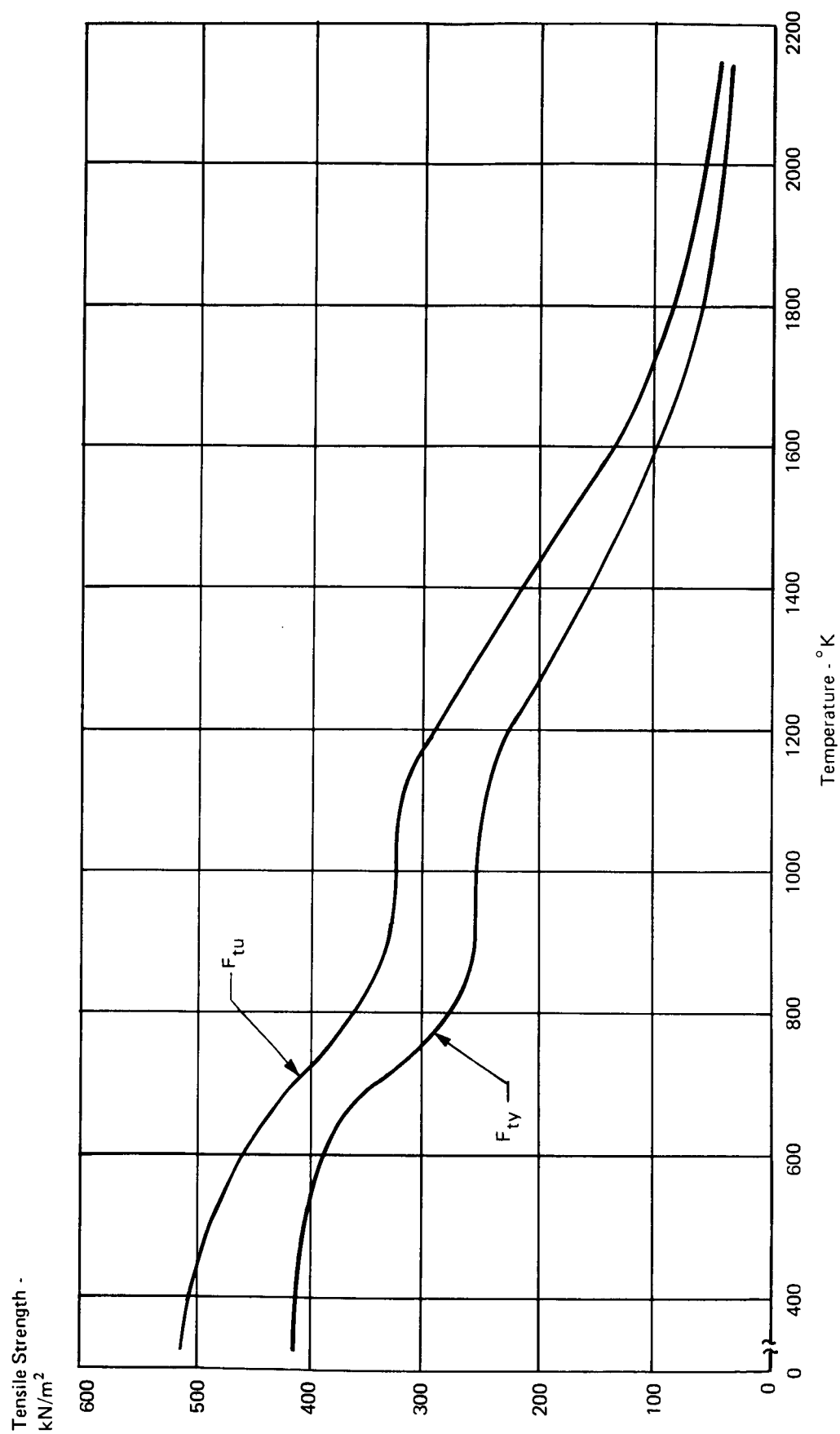


Figure 37 SI. Tensile Strength versus Temperature SCb-291 Columbium

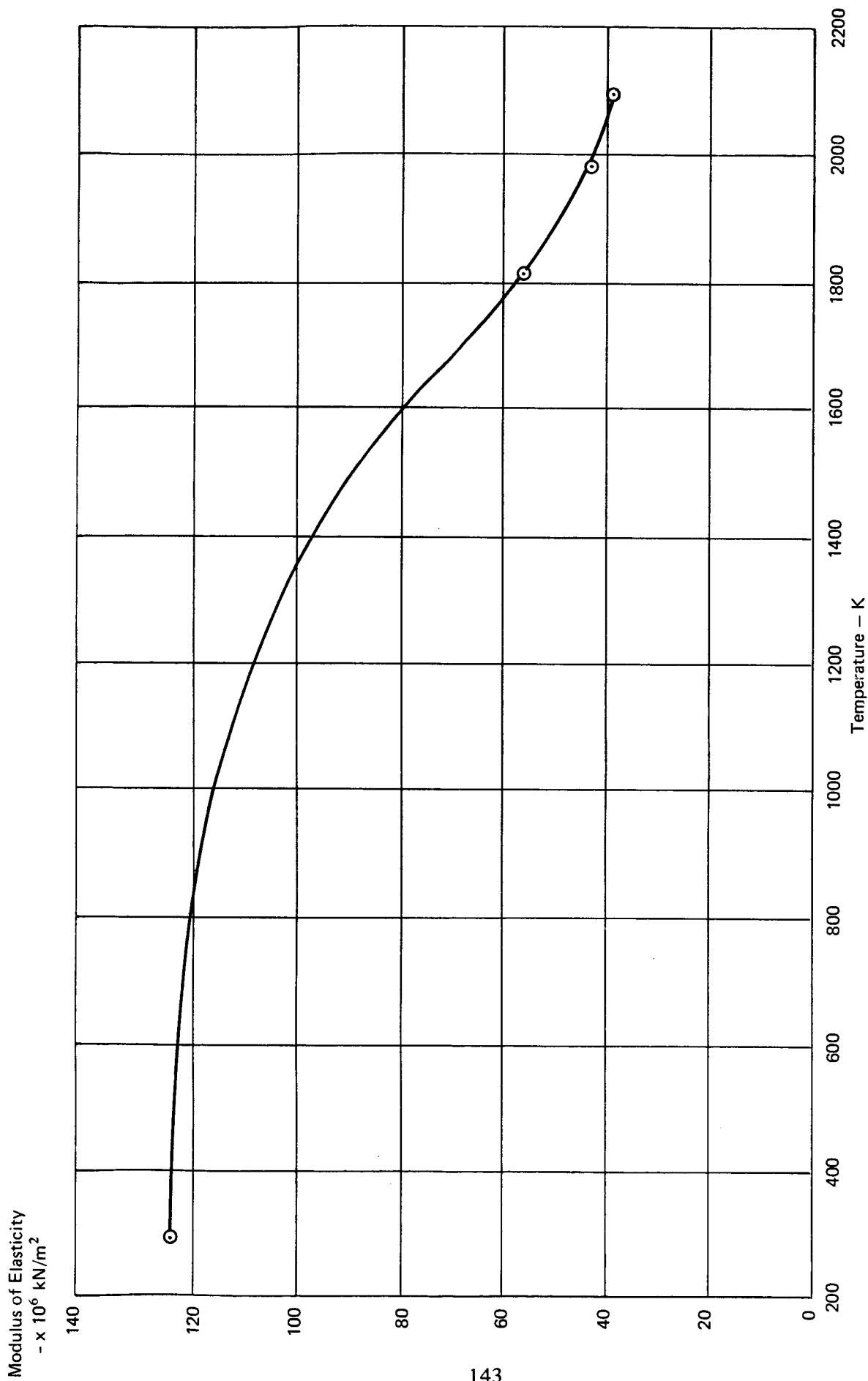


Figure 38 SI. Effect of Temperature on Modulus of Elasticity for SCb-291 Columbium

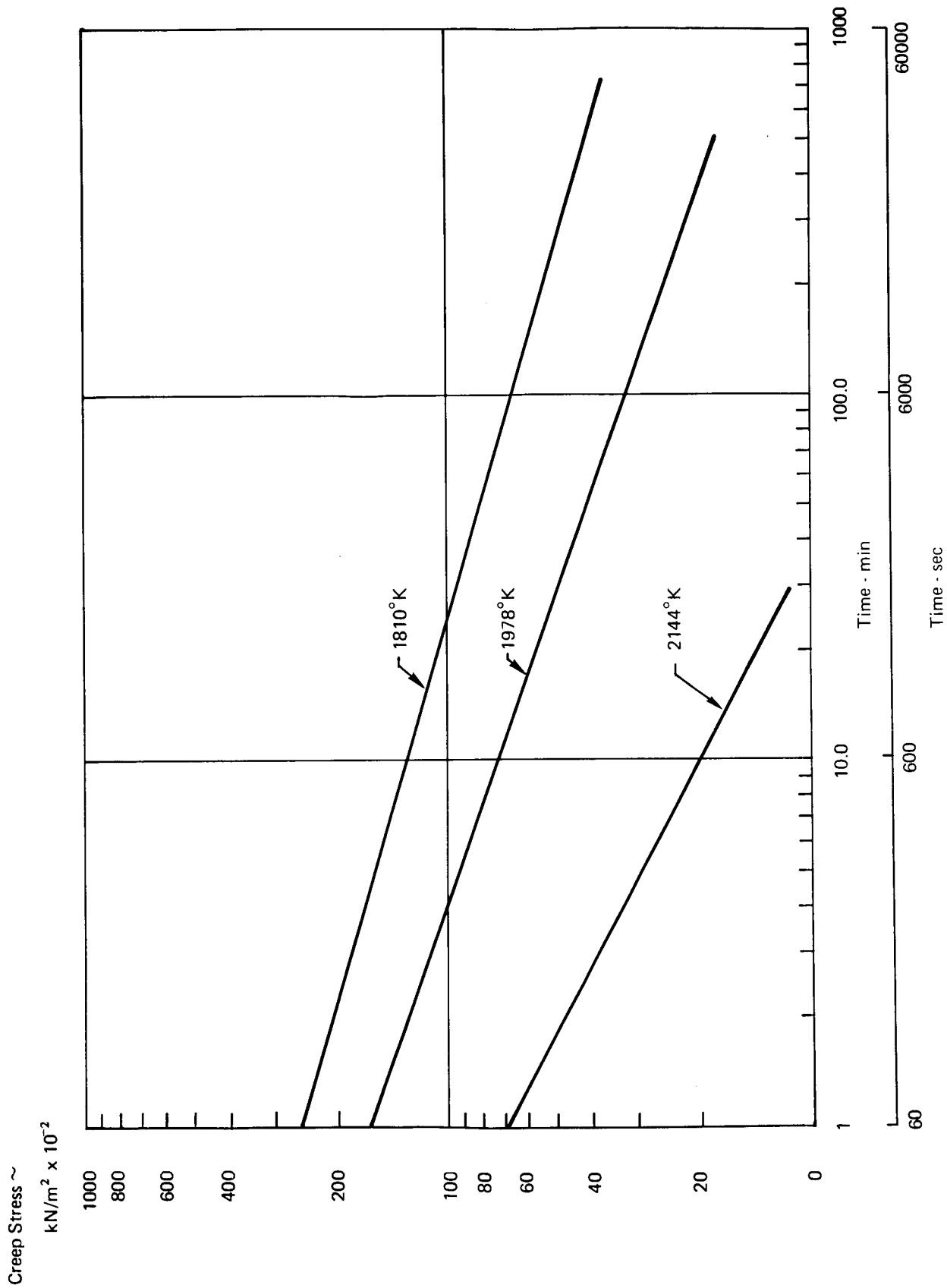


Figure 39 SI. Stress Necessary to Produce a Creep Strain of 0.05% in SCb-291

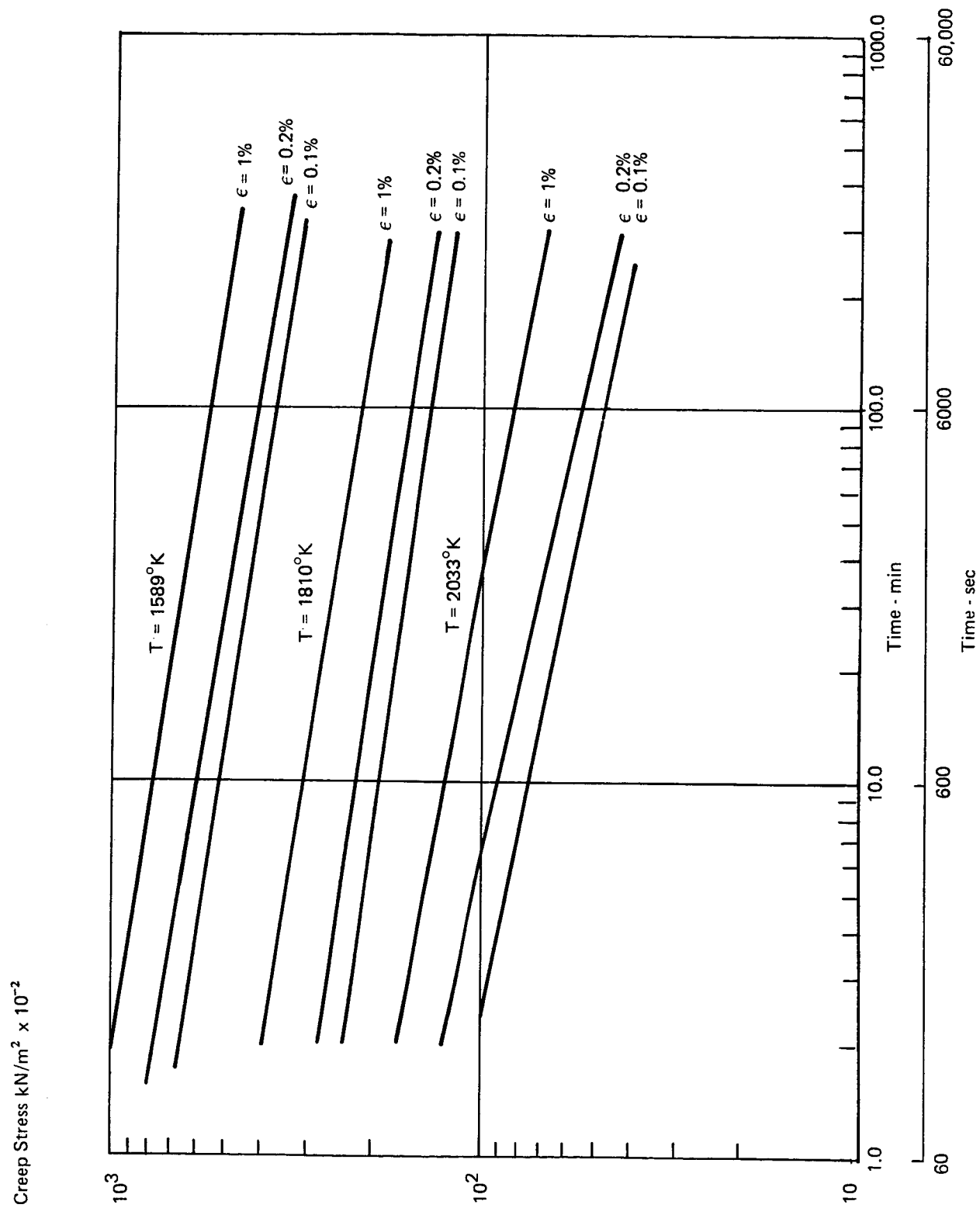


Figure 40 SI. Material SCb-291 Stress Necessary to Produce Indicated Creep Strain at Temperature

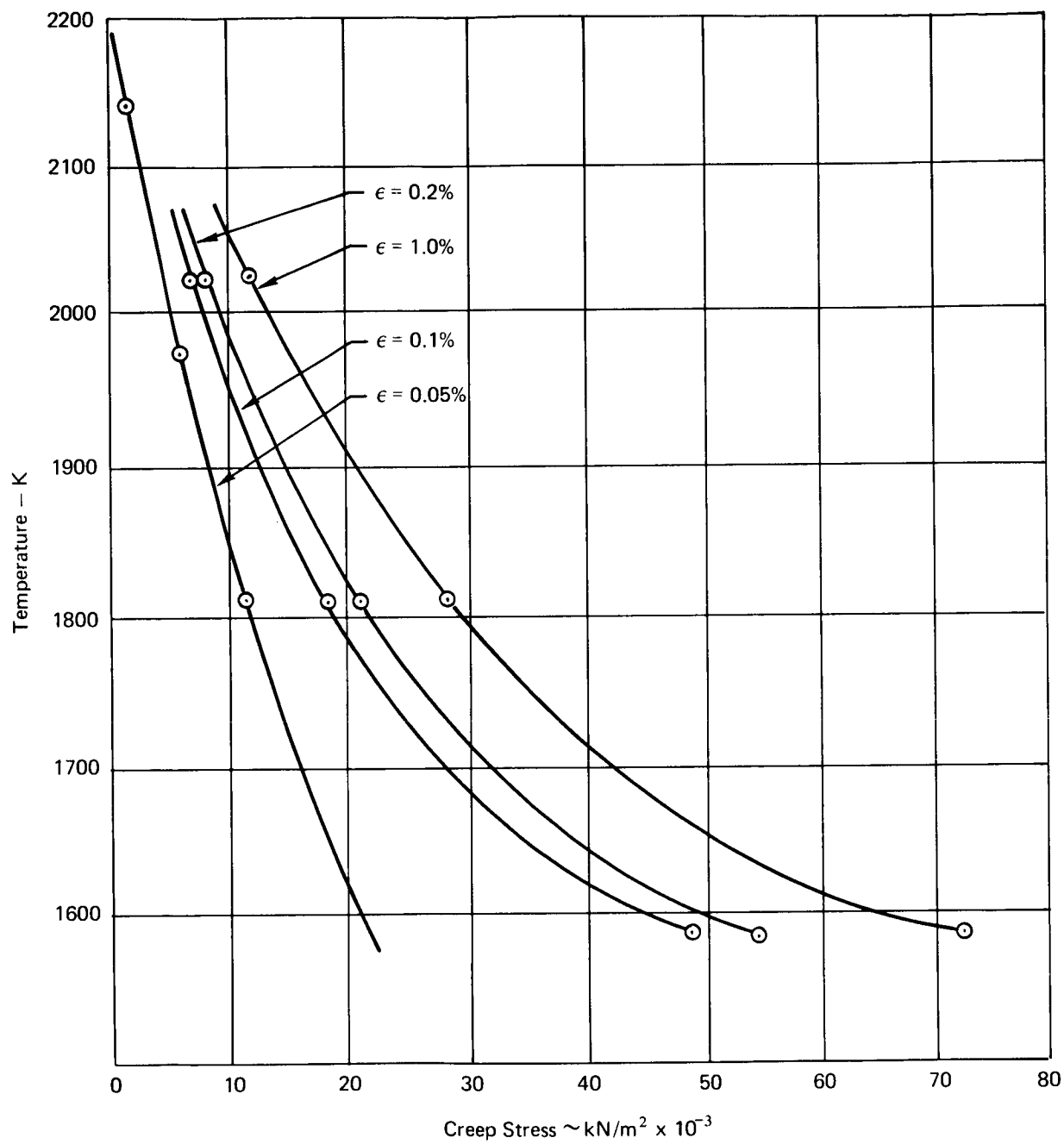


Figure 41 SI. Material SCb-291 Stress versus Temperature for Indicated Creep Strain at $t = 1000$ sec

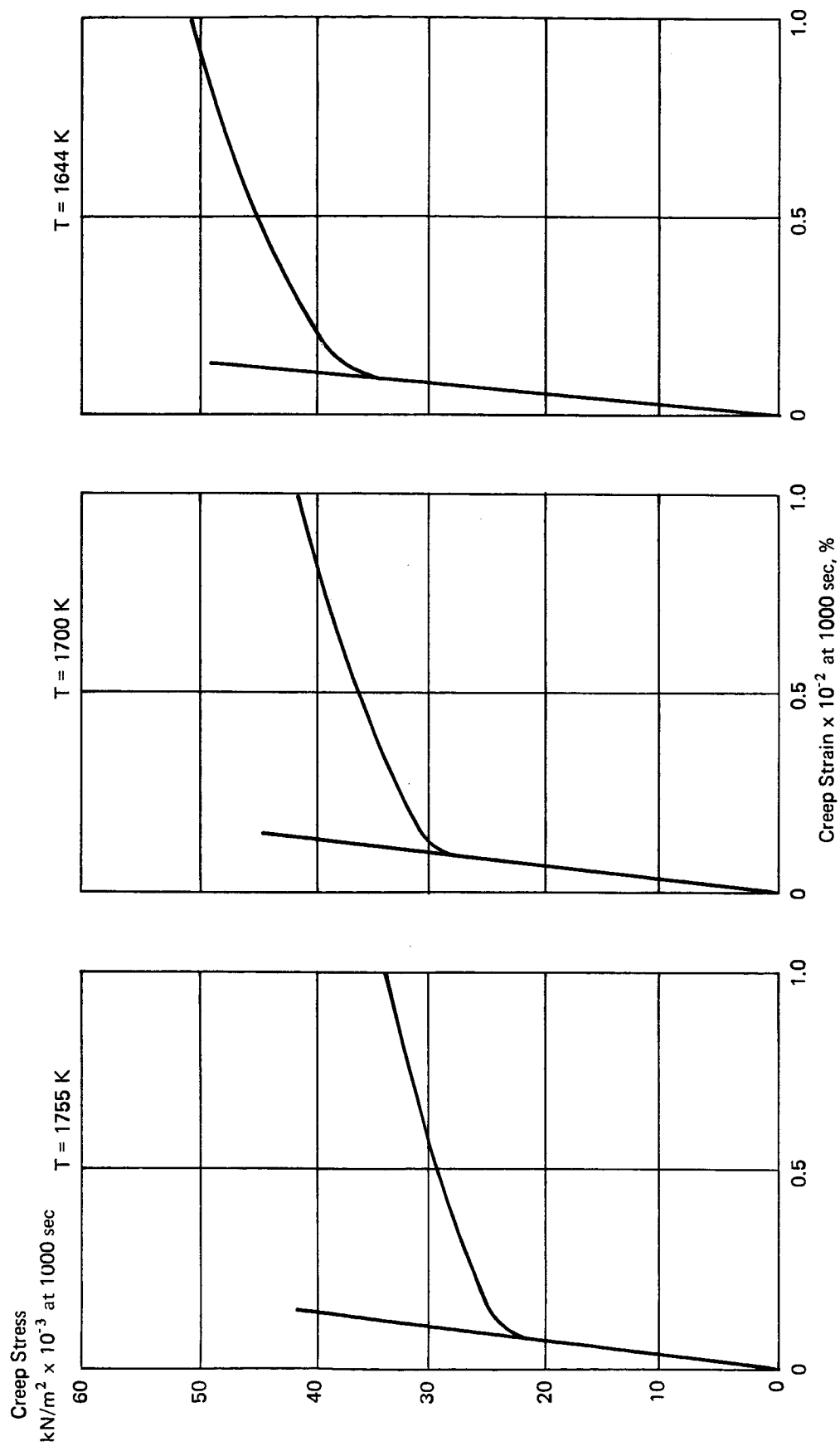


Figure 42 SI. Material - SCb-291 Creep Characteristic Stress - Strain Diagrams at $t = 1000\text{ sec}$

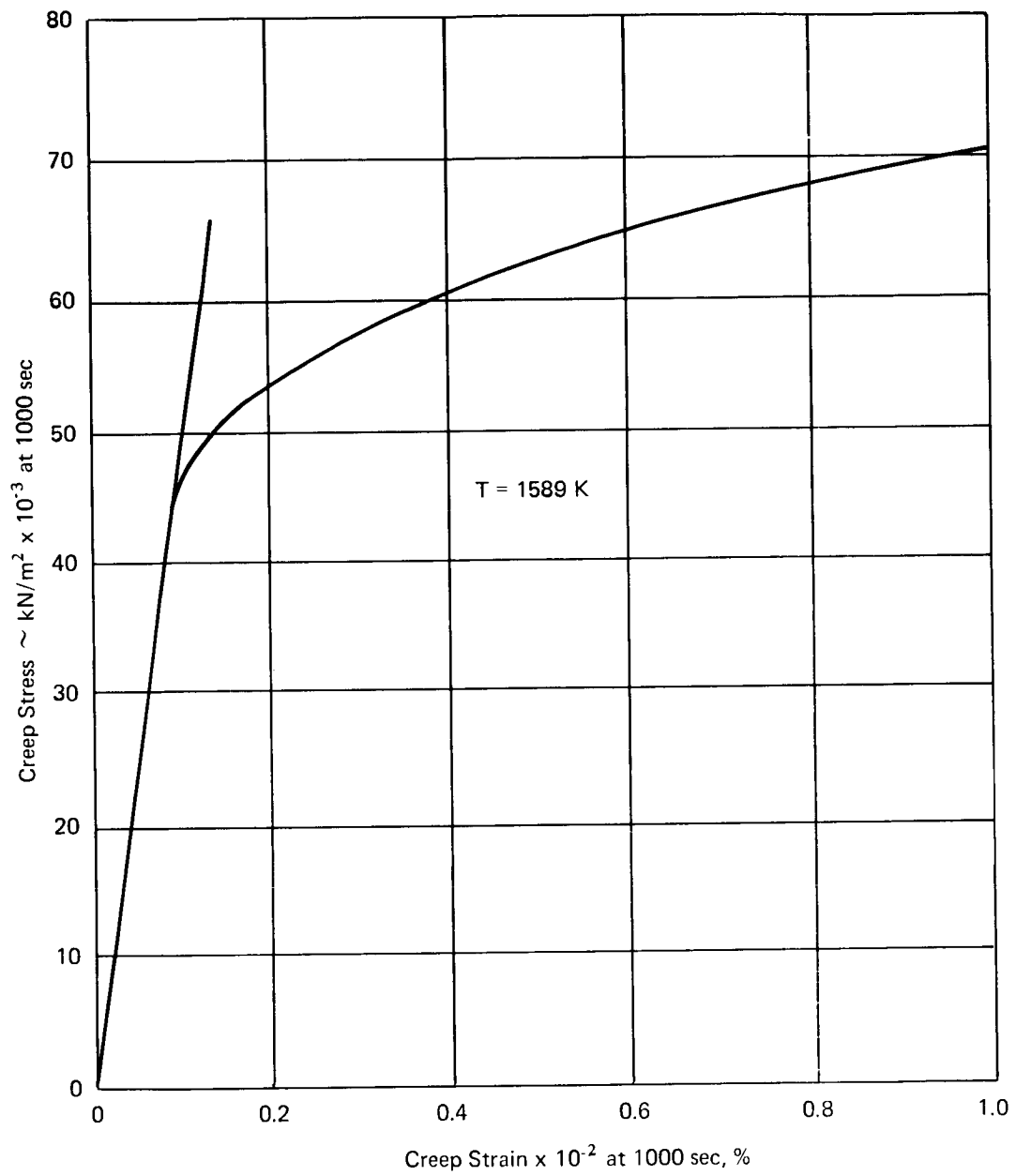


Figure 43 SI. Material - SCb-291 Creep Characteristic Stress - Strain Diagram at $t = 1000 \text{ sec}$

$F = 4500N$
 $T_g = 3034K$ (100% c*)

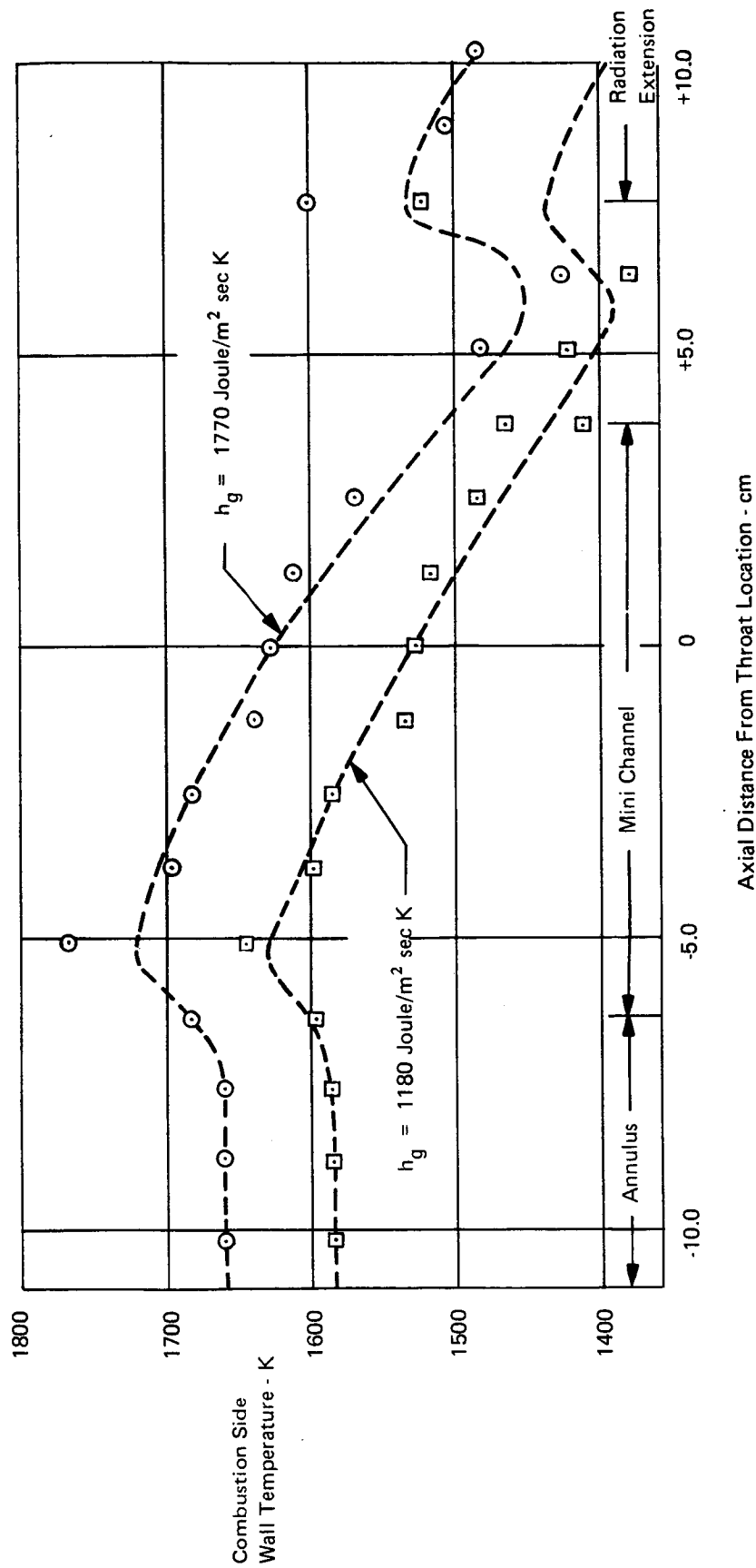


Figure 44 SI. Bimode Engine Axial Temperature versus Distance

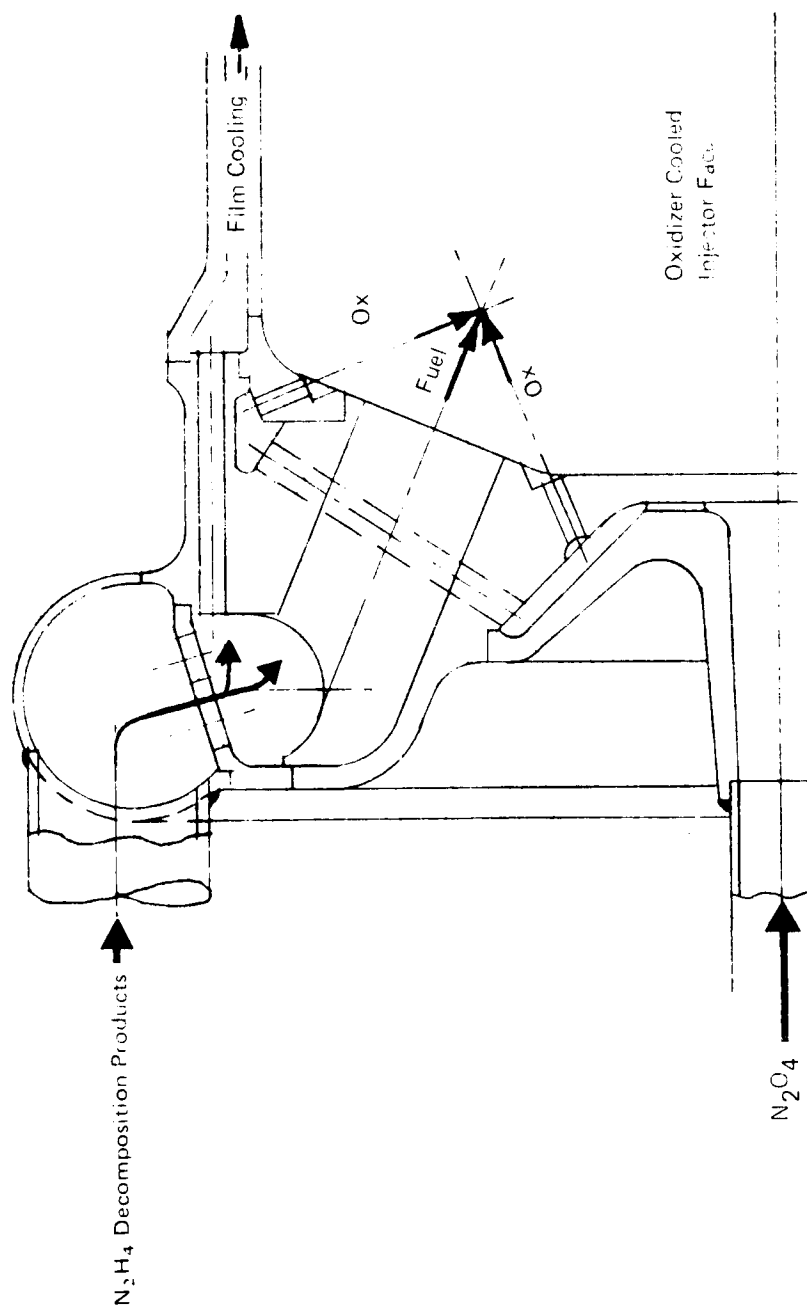


Figure 45 Sl. Bimodal Engine, Film Cooled Triplet Injector Reactor Mounted at Secondary Injector Station

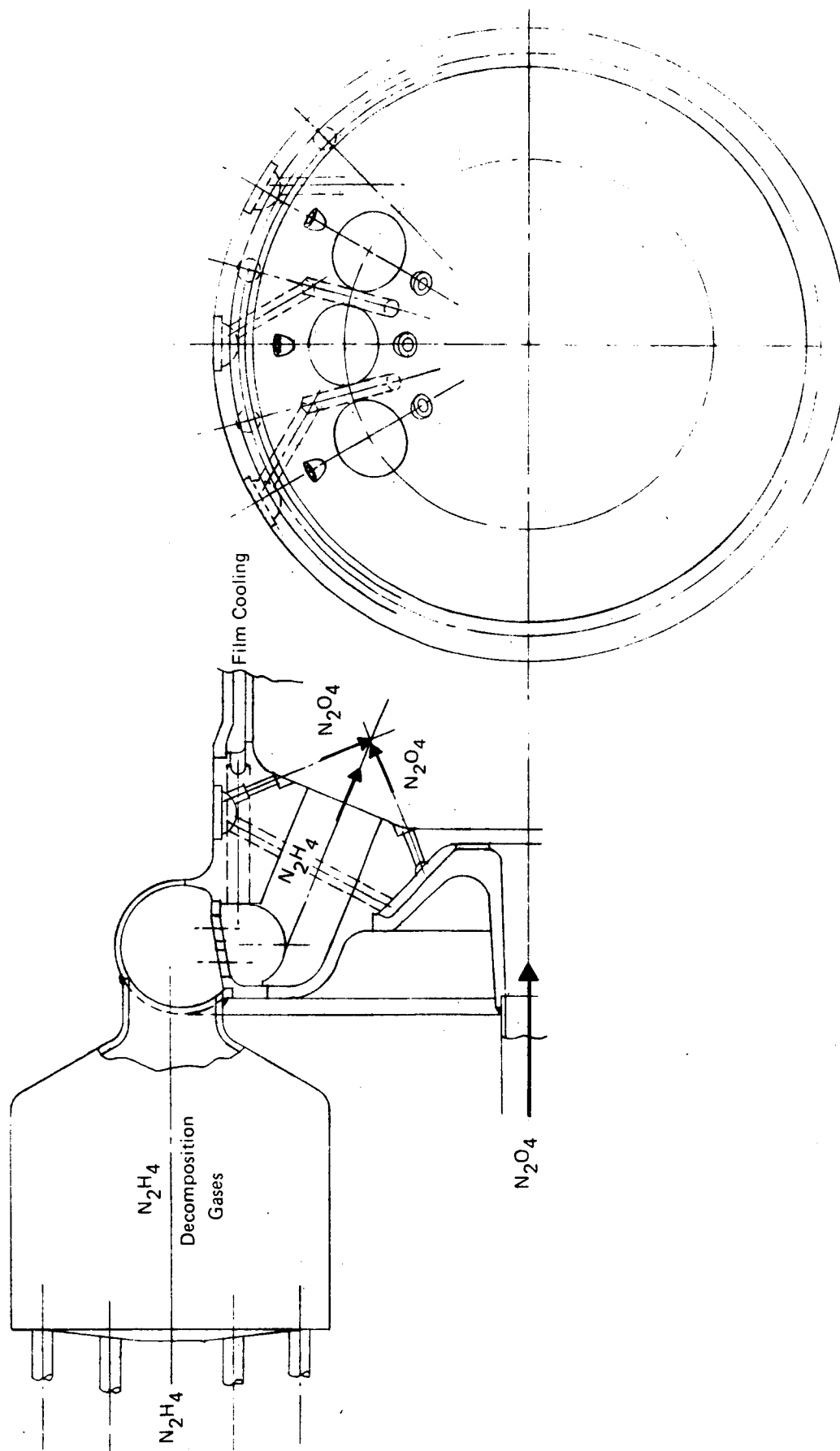


Figure 46 SI. Bimodal Engine, Film Cooled Triplet Injector Reactor Mounted
at Secondary Injector Station

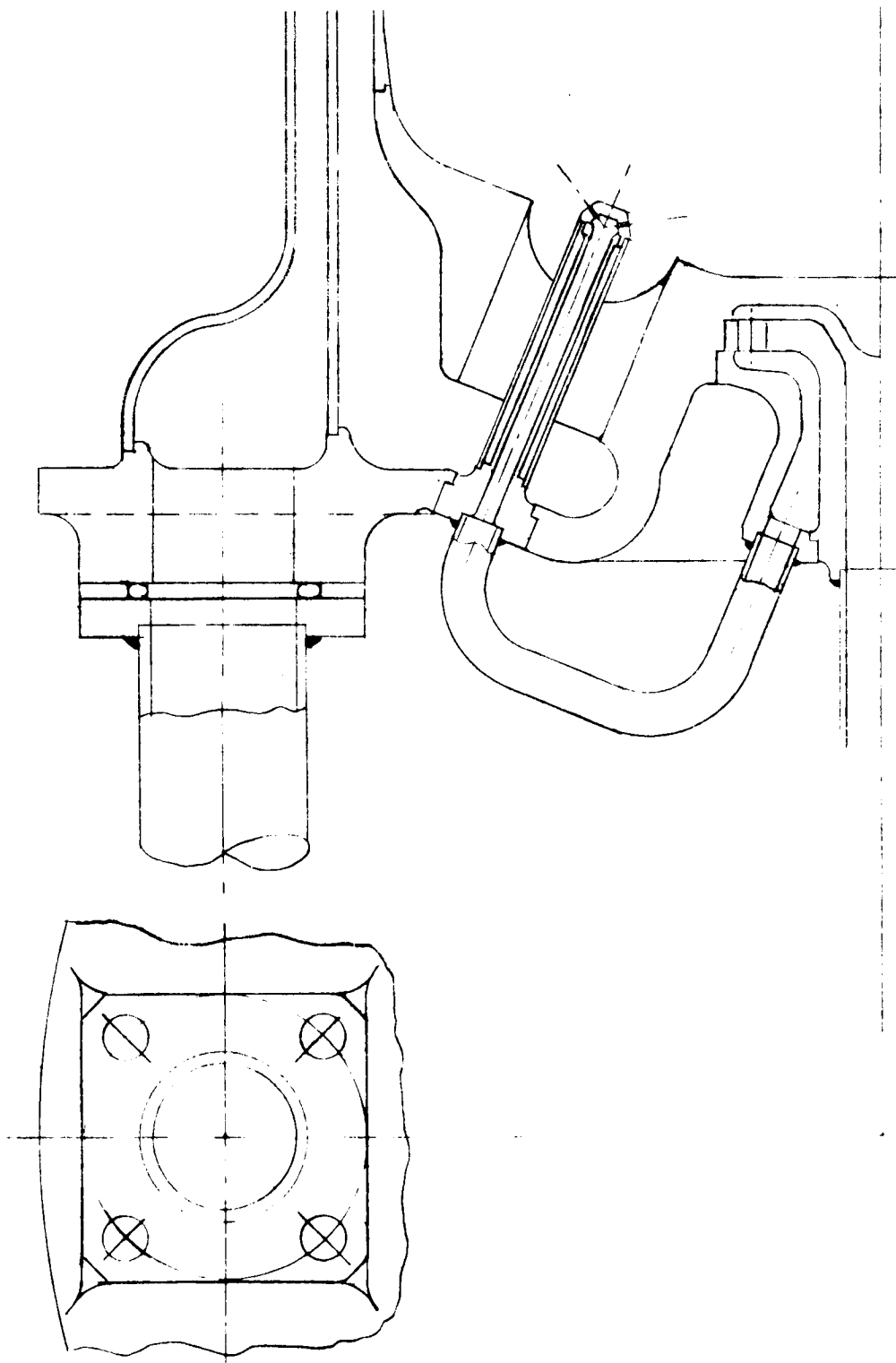


Figure 47 SI. Coaxial Injector

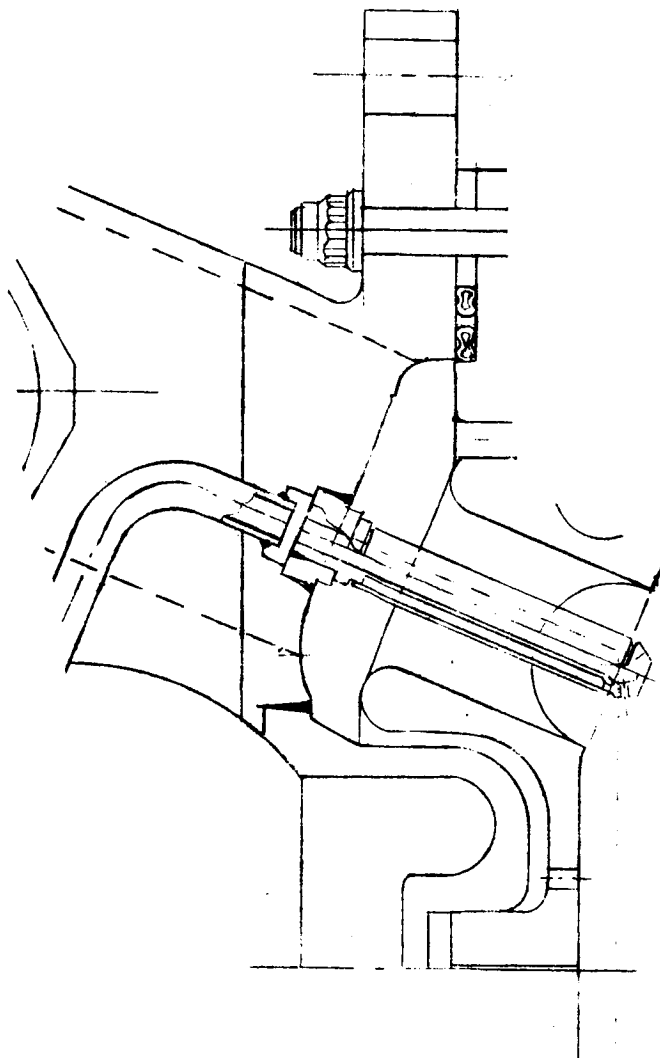


Figure 48 SI. Columbiuim/L-605 Injector with Center Fuel Cooling

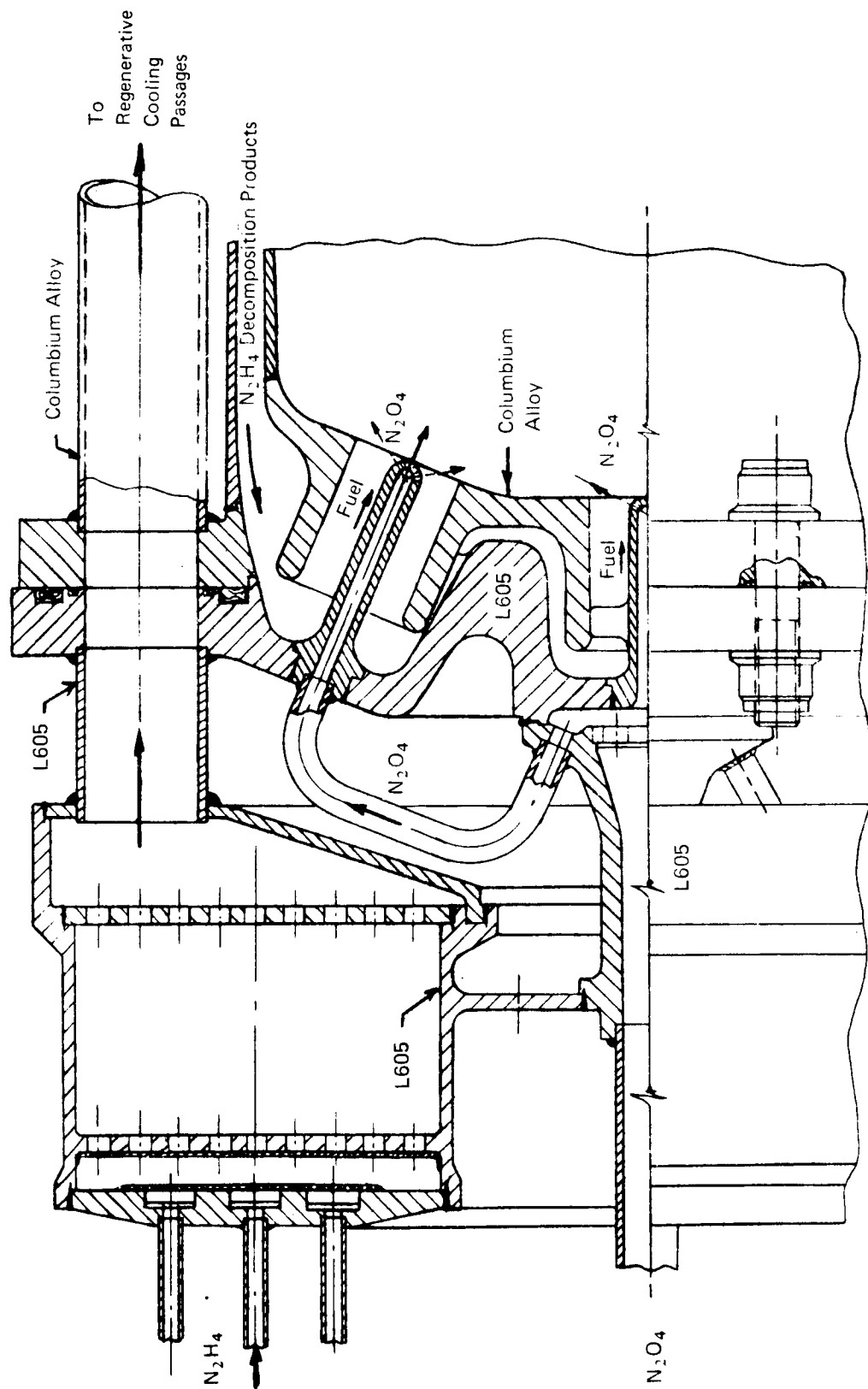
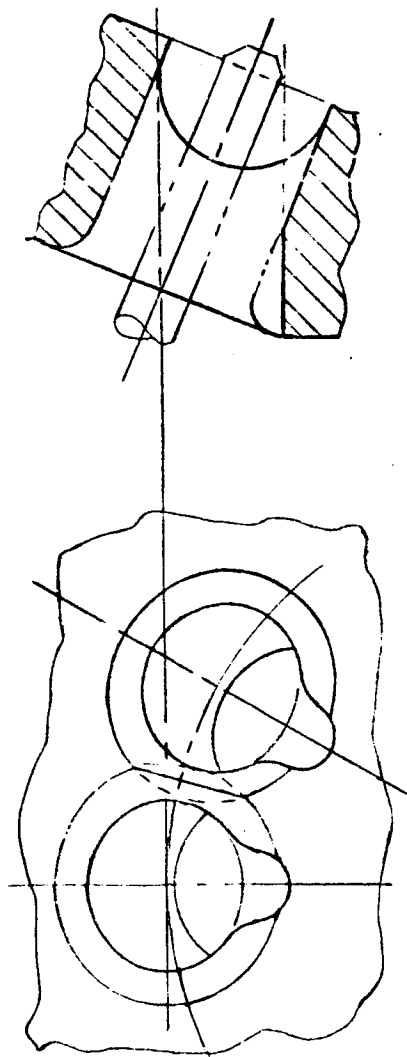


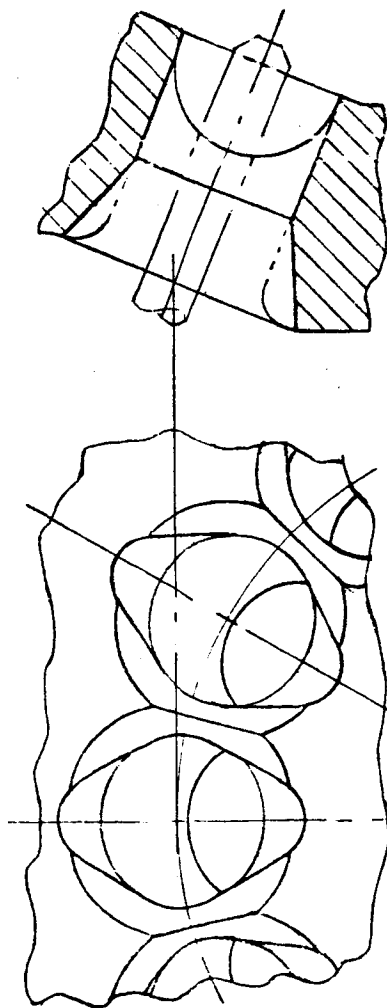
Figure 49 SI. Bimodal Engine, Regeneratively Cooled L-605 Reactor and Secondary Injector Back Plate, Columbium Alloy Thrust Chamber. Six Cylindrical Integral Reactors



CONFIG A

ENTRANCE OF FUEL ORIFICES
SLOTTED LOCALLY

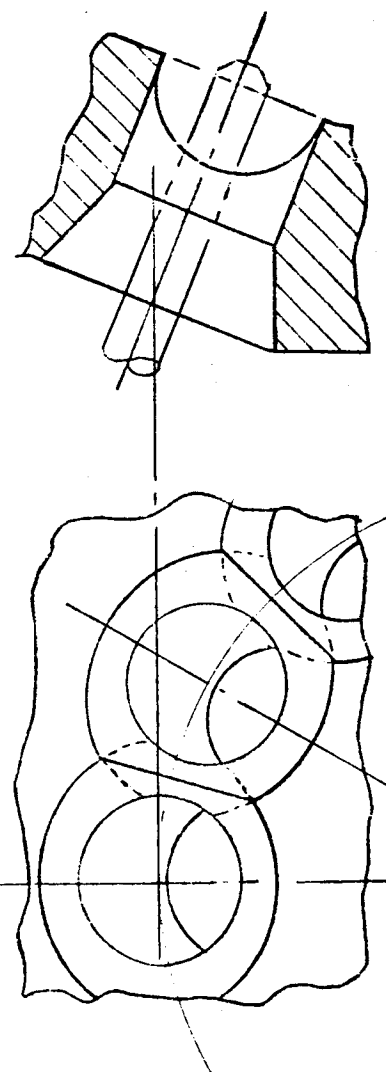
- PROBABLE FUEL FLOW
MALDISTRIBUTION



CONFIG B

ENTRANCE OF FUEL ORIFICES
TAPERED IN AN ELLIPTICAL
CONE SHAPE

- ALLOWS MAXIMUM WEB
THICKNESS BETWEEN FUEL
ORIFICES
- POSSIBLE FUEL FLOW
MALDISTRIBUTION - BUT
MINIMUM



CONFIG C

ENTRANCE OF FUEL ORIFICES
TAPERED IN A CIRCULAR SHAPE

- REDUCES WEB THICKNESS
CONSIDERABLY - UNSATISFACTORY
- PROVIDES UNIFORM FLOW
CONDITIONS

Figure 50 SI. Fuel Orifice Variations (To Allow Axial Removal of Oxidizer Orifices)

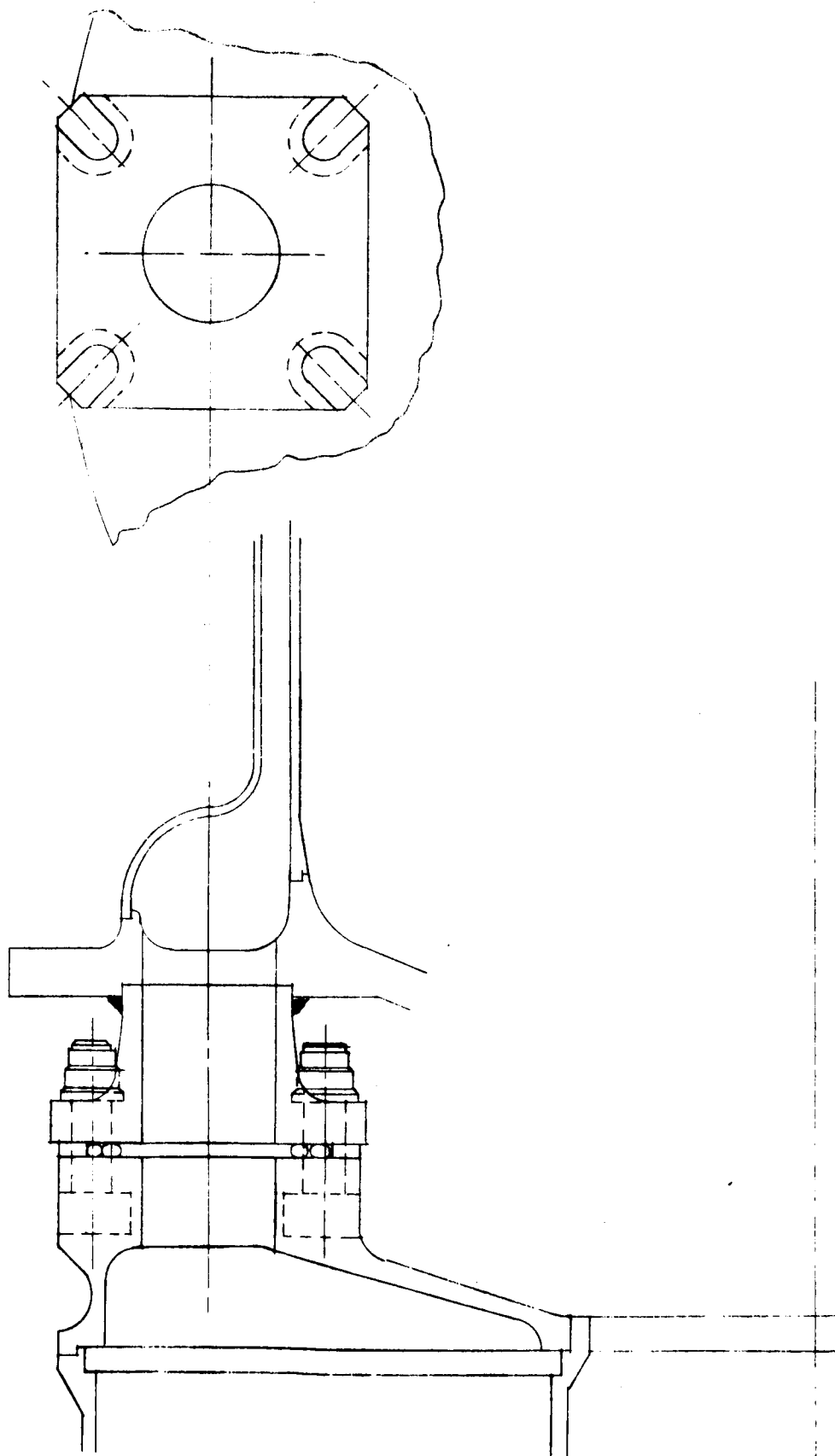


Figure 51 SI. Nut and Bolt Installation

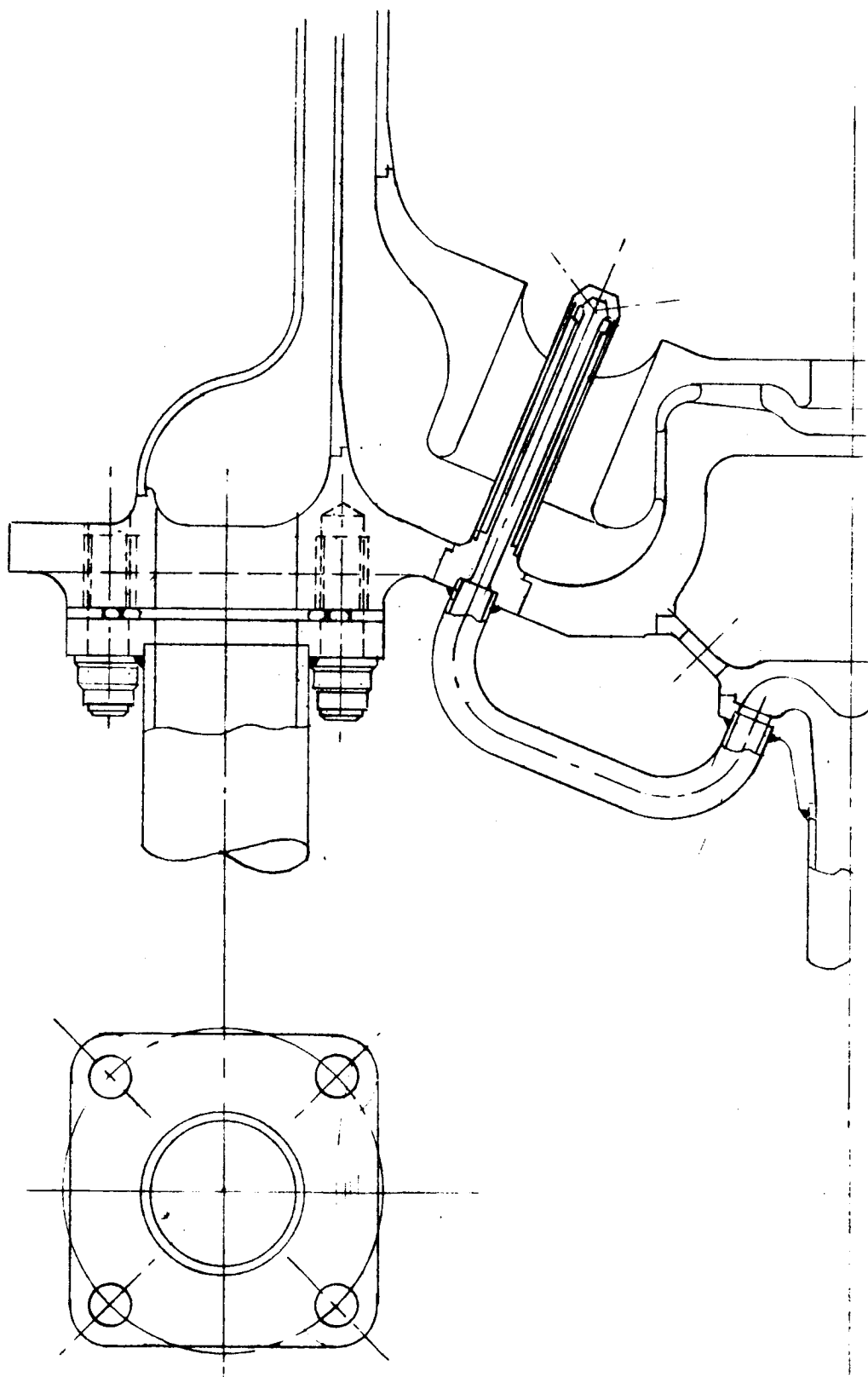


Figure 52 SI. Stud and Nut Installation

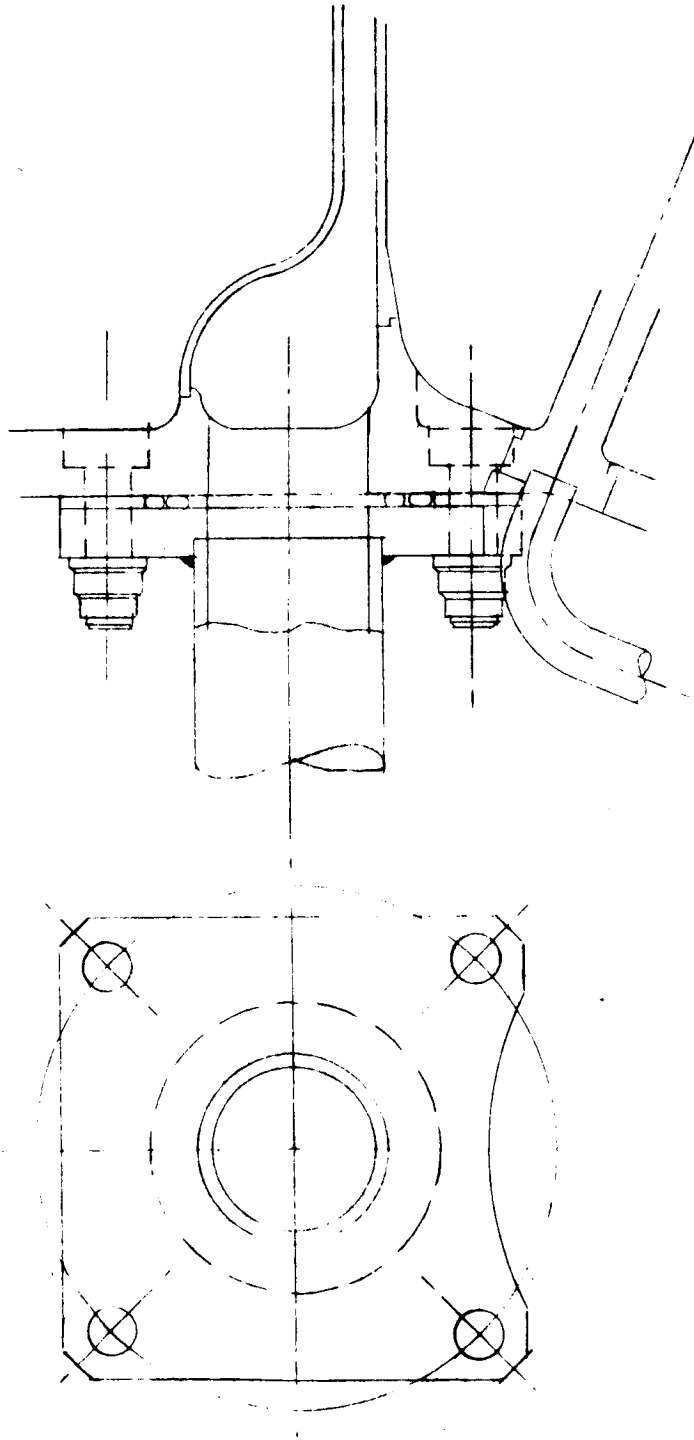


Figure 53 SI. Stud and Nut (Welded Stud)

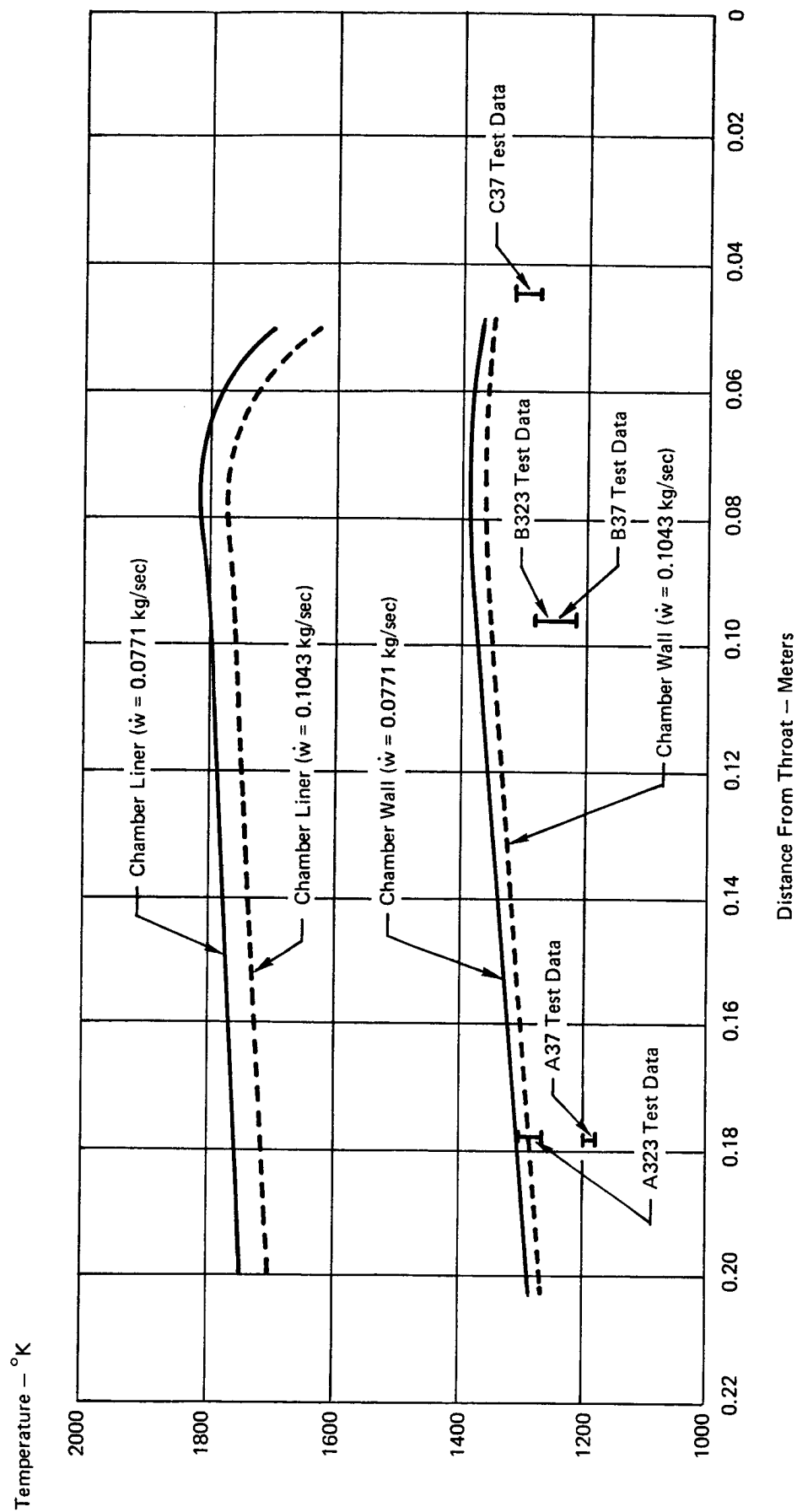


Figure 54 SI. Chamber and Liner Temperatures Test DJ-339

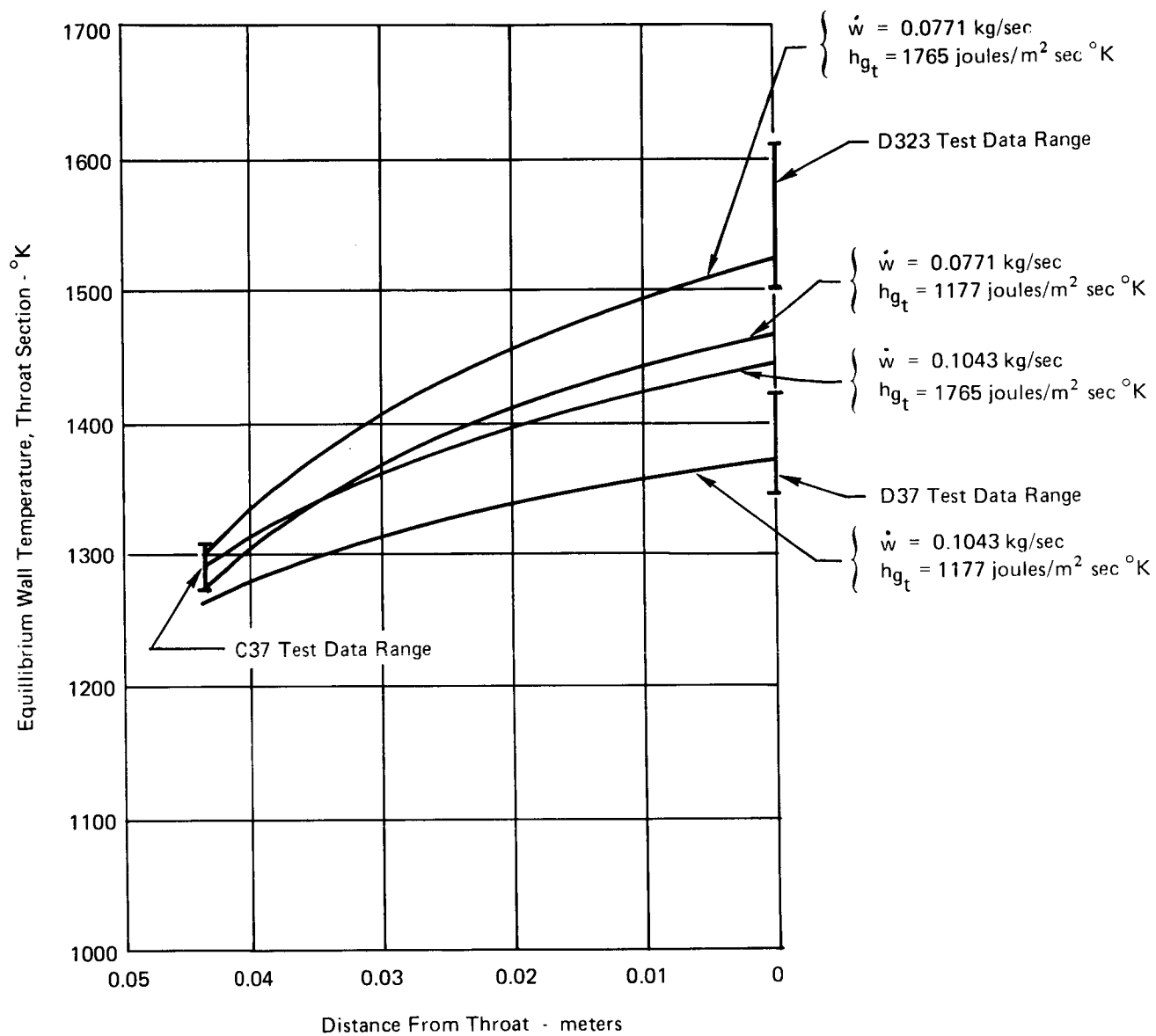


Figure 55 SI. Test DJ 339 - Throat Location

95% c*
Gap (Measured Cold) = 0.203 cm
Film Coolant Flow Rate = 0.0907 kg/sec
Throat Station $h_g = 1765 \text{ joules/m}^2 \text{ sec } ^\circ\text{K}$

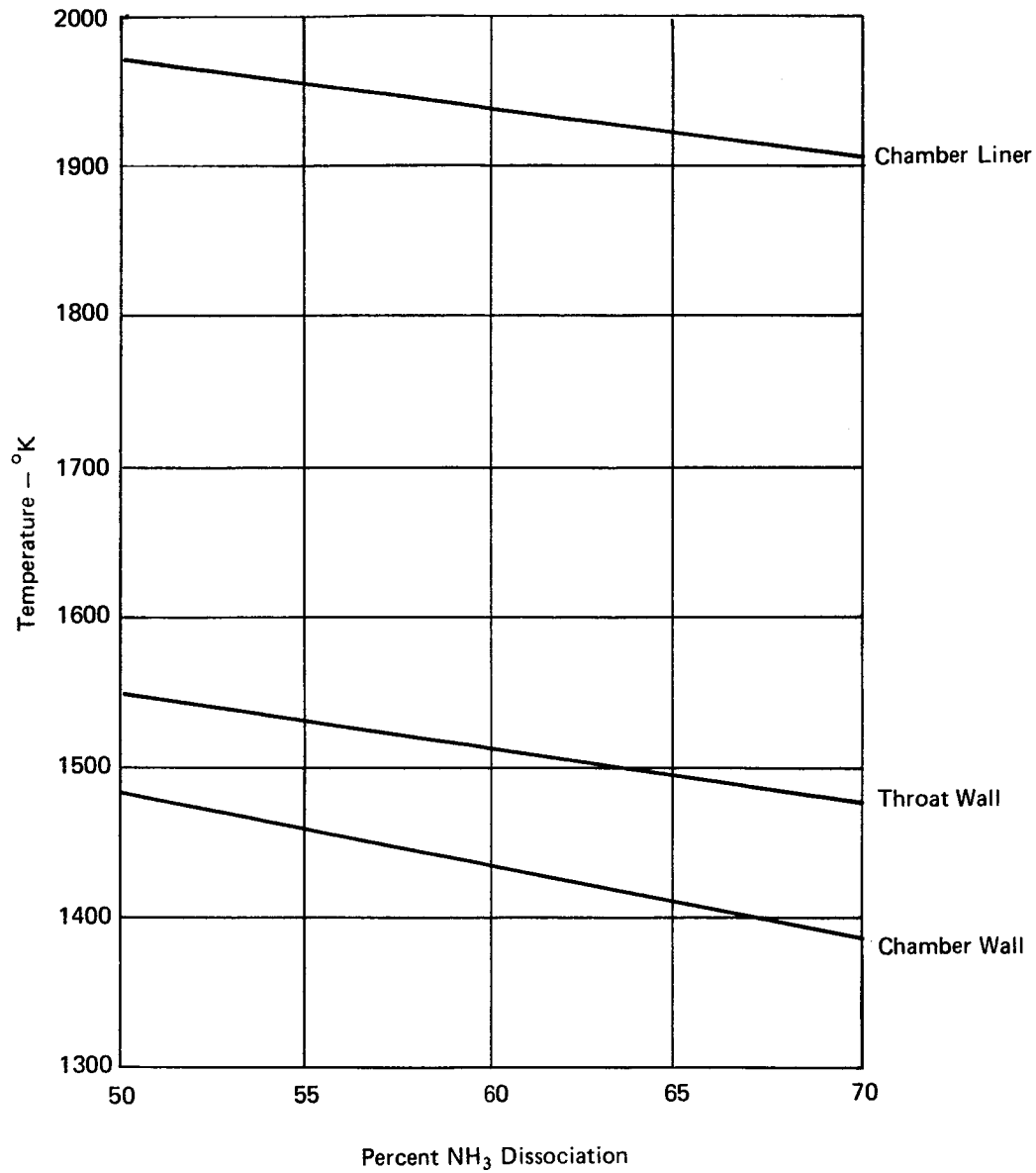


Figure 56 SI. Influence of Ammonia Dissociation on Liner and Wall Temperatures

95% c^*
60% NH_3 Dissociation
Gap (Measured Cold) = 0.203 cm
Throat Station $h_g = 1765 \text{ joules/m}^2 \text{ sec } ^\circ\text{K}$

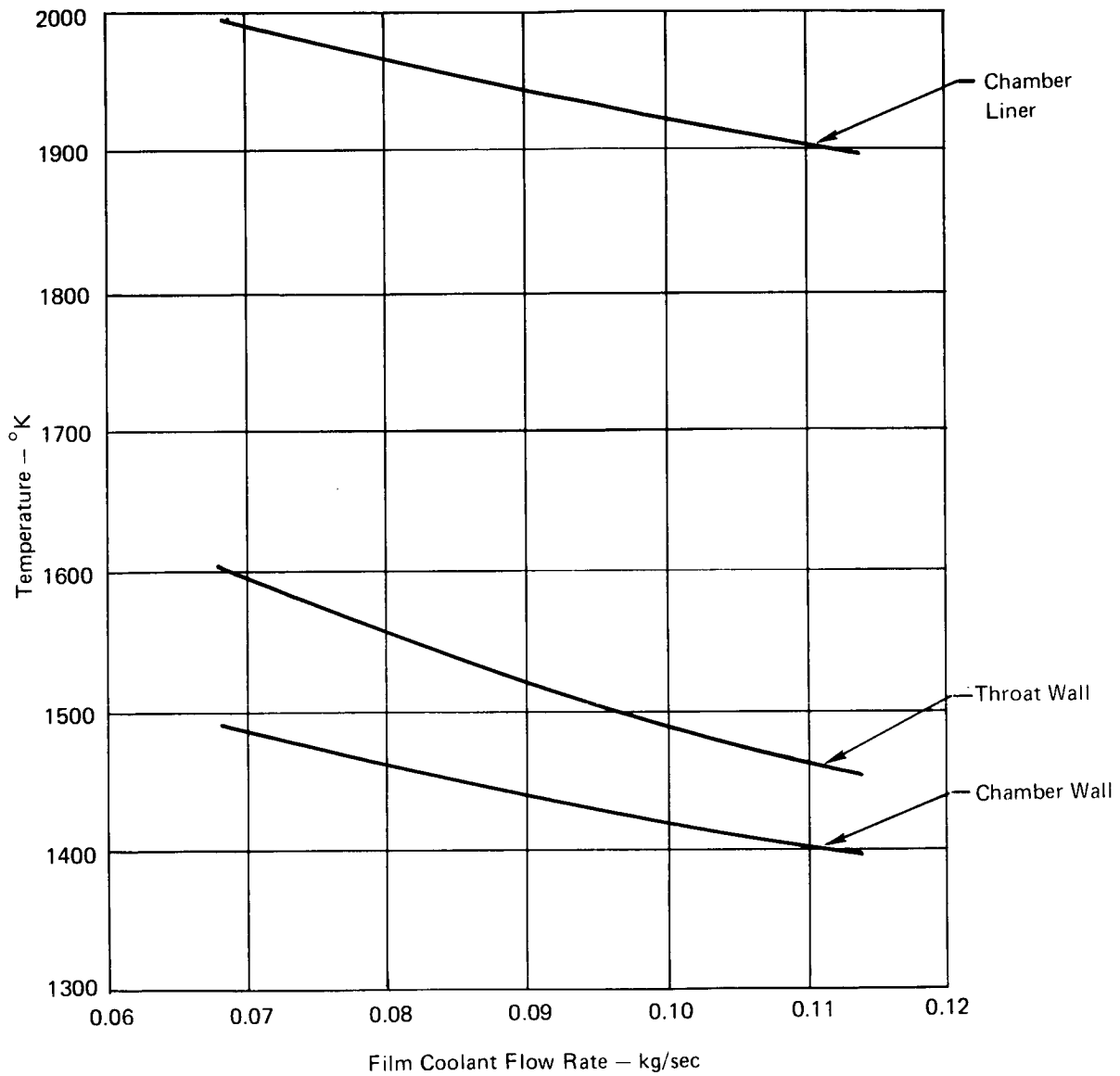


Figure 57 SI. Influence of Film Coolant Flow Rate on Liner and Wall Temperatures

95% c^*
60% Dissociation
Film Coolant Flow Rate = 0.0907 kg/sec
Throat Station $h_g = 1765 \text{ joules/m}^2 \text{ sec } ^\circ\text{K}$

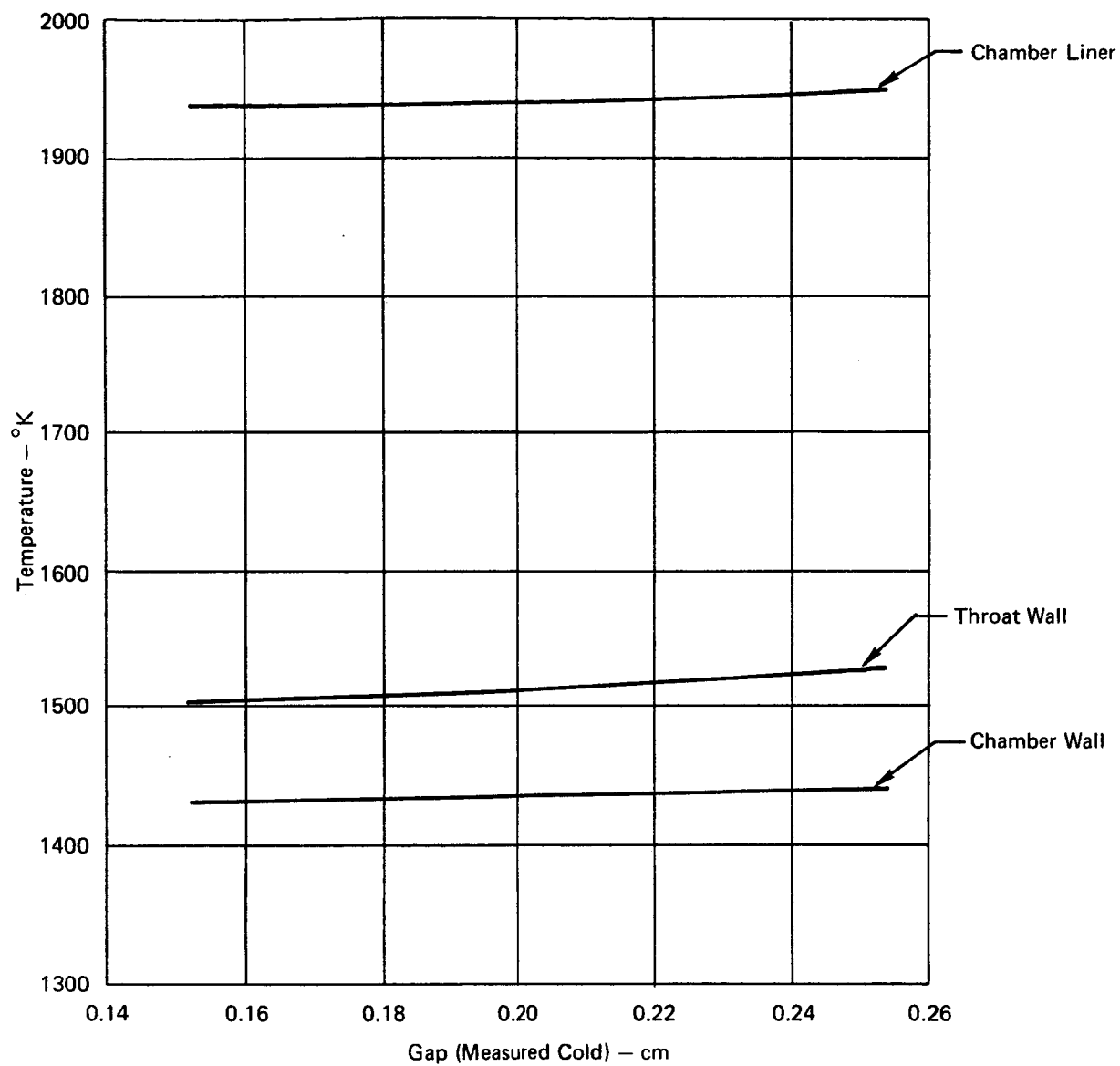


Figure 58 SI. Influence of Annular Gap on Liner and Wall Temperatures

60% NH_3 Dissociation
Gap (Measured Cold) = 0.203 cm
Film Coolant Flow Rate = 0.0907 kg/sec

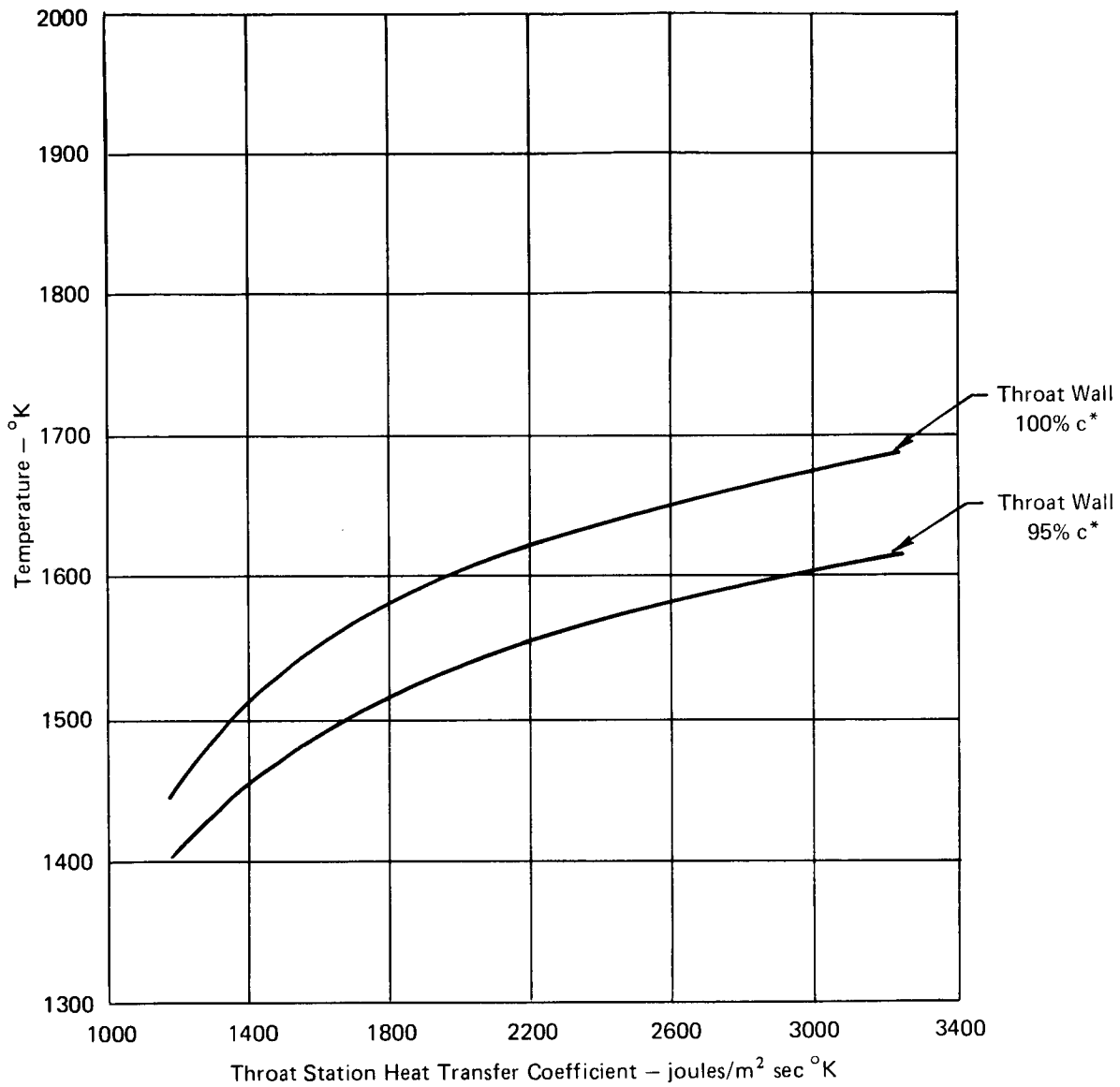


Figure 59 SI. Influence of Heat Transfer Coefficient on Throat Station Wall Temperature

60% NH_3 Dissociation
Gap (Measured Cold) = 0.203 cm
Film Coolant Flow Rate = 0.0907 kg/sec

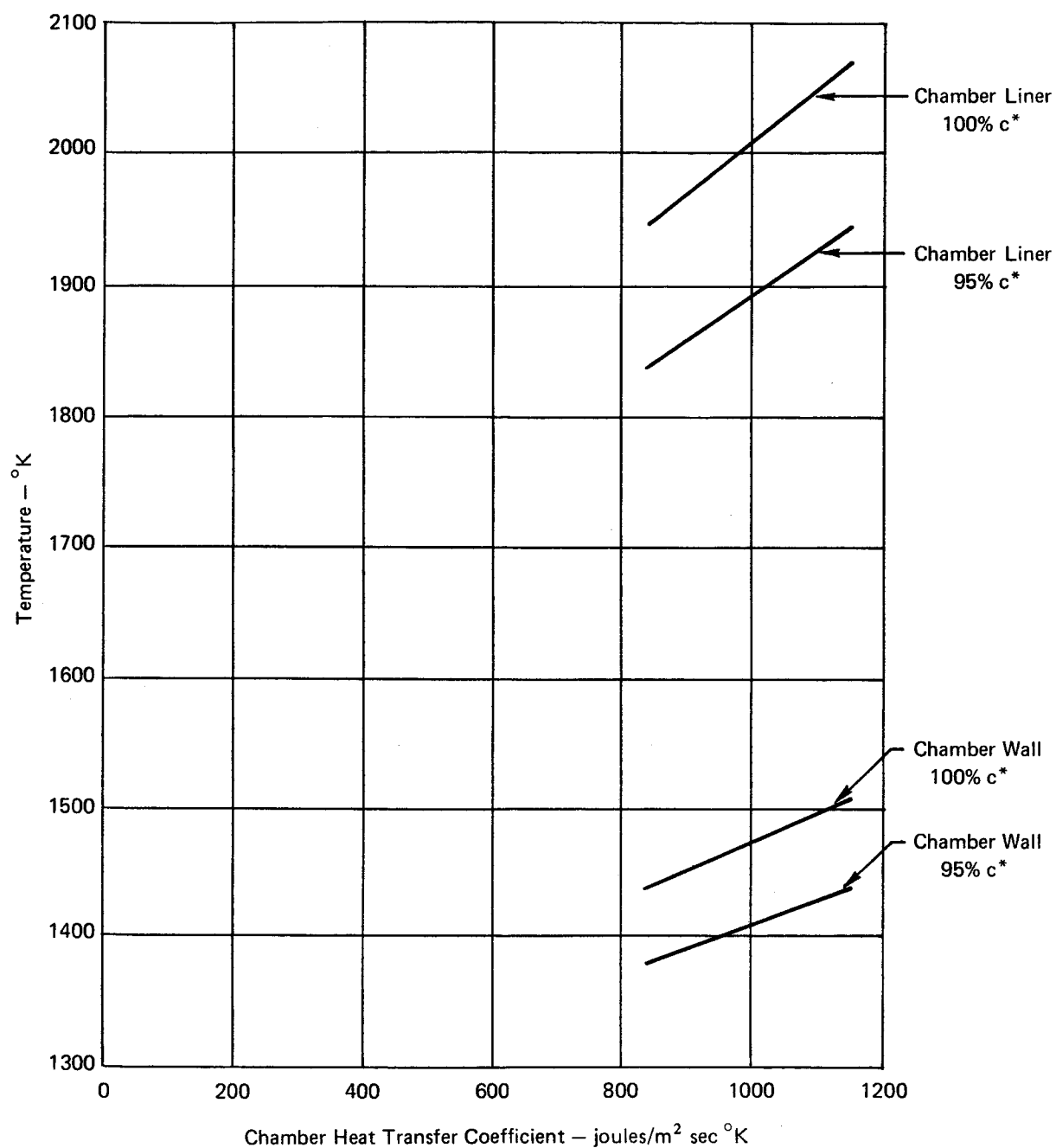


Figure 60 SI. Influence of Chamber Heat Transfer Coefficient
on Chamber Liner and Wall Temperatures

95% c*
 60% NH₃ Dissociation
 Gap (Measured Cold) = 0.203 cm
 Film Coolant Flow Rate = 0.0907 kg/sec
 Throat Station $h_g = 1770 \text{ joules/m}^2 \text{ sec}^\circ \text{K}$

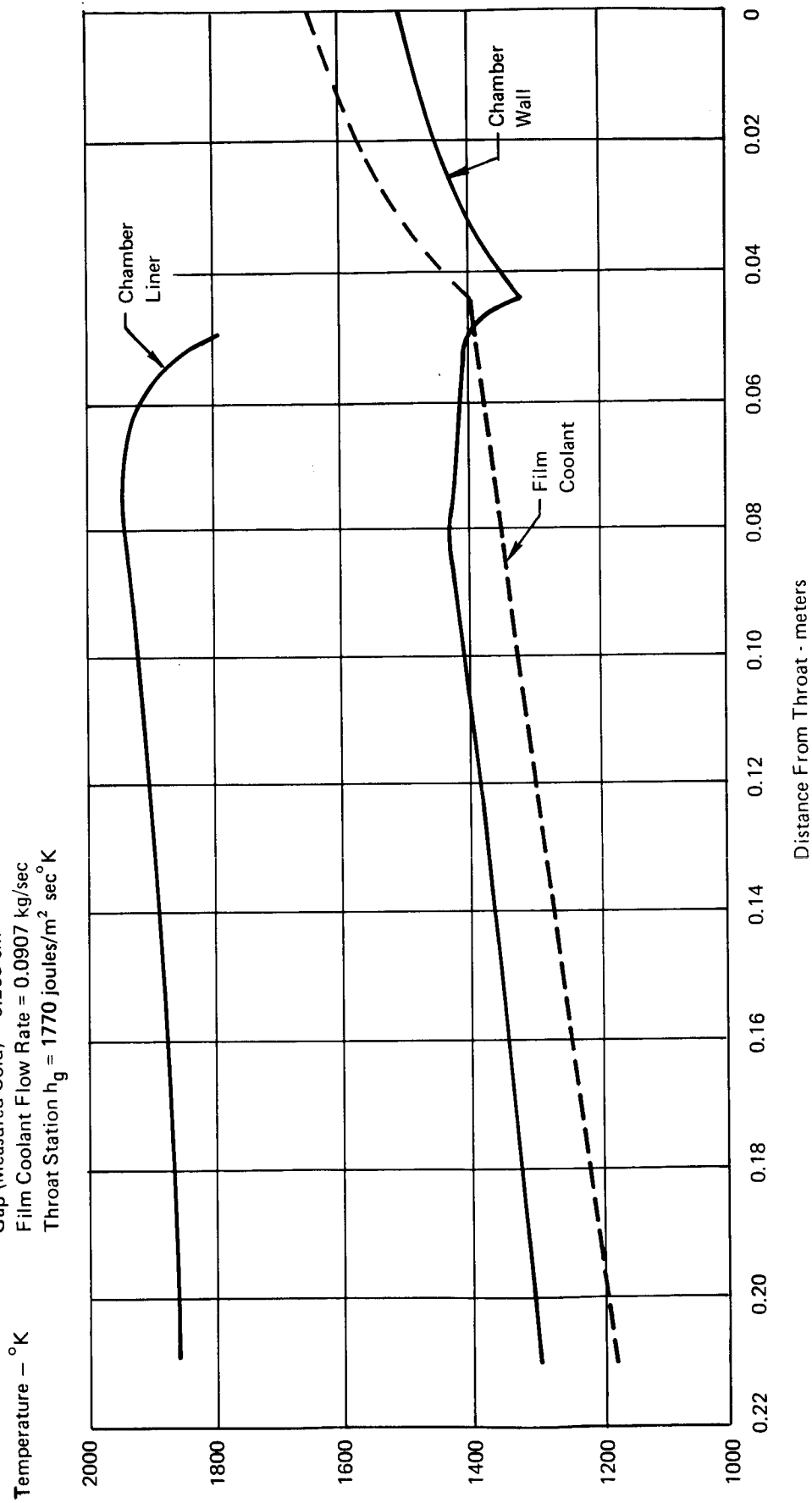


Figure 61 SI. Axial Temperature Distribution of Film Coolant, Liner and Chamber Wall

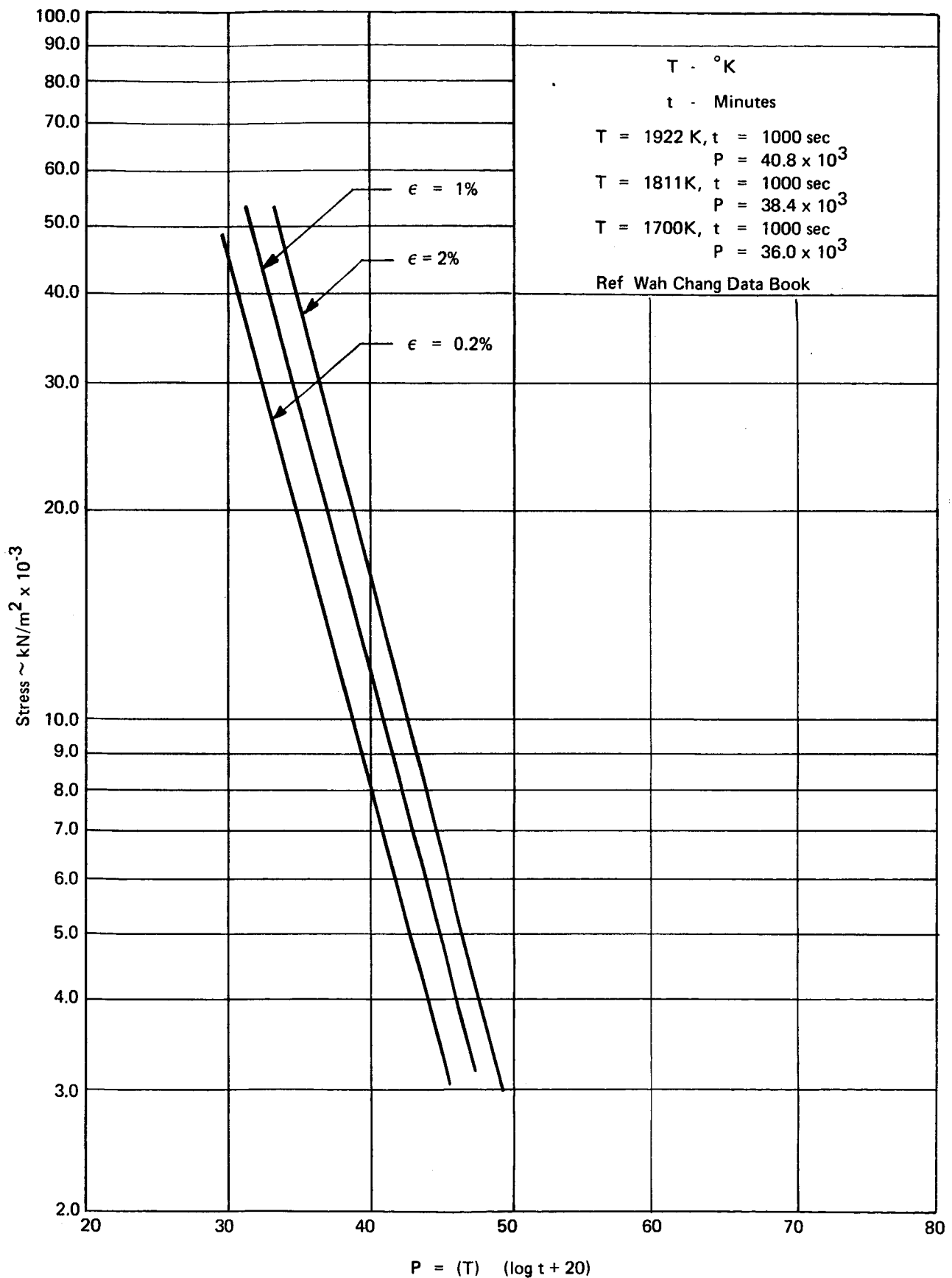


Figure 62 SI. Larsen-Miller Master Plot for Recrystallized C103

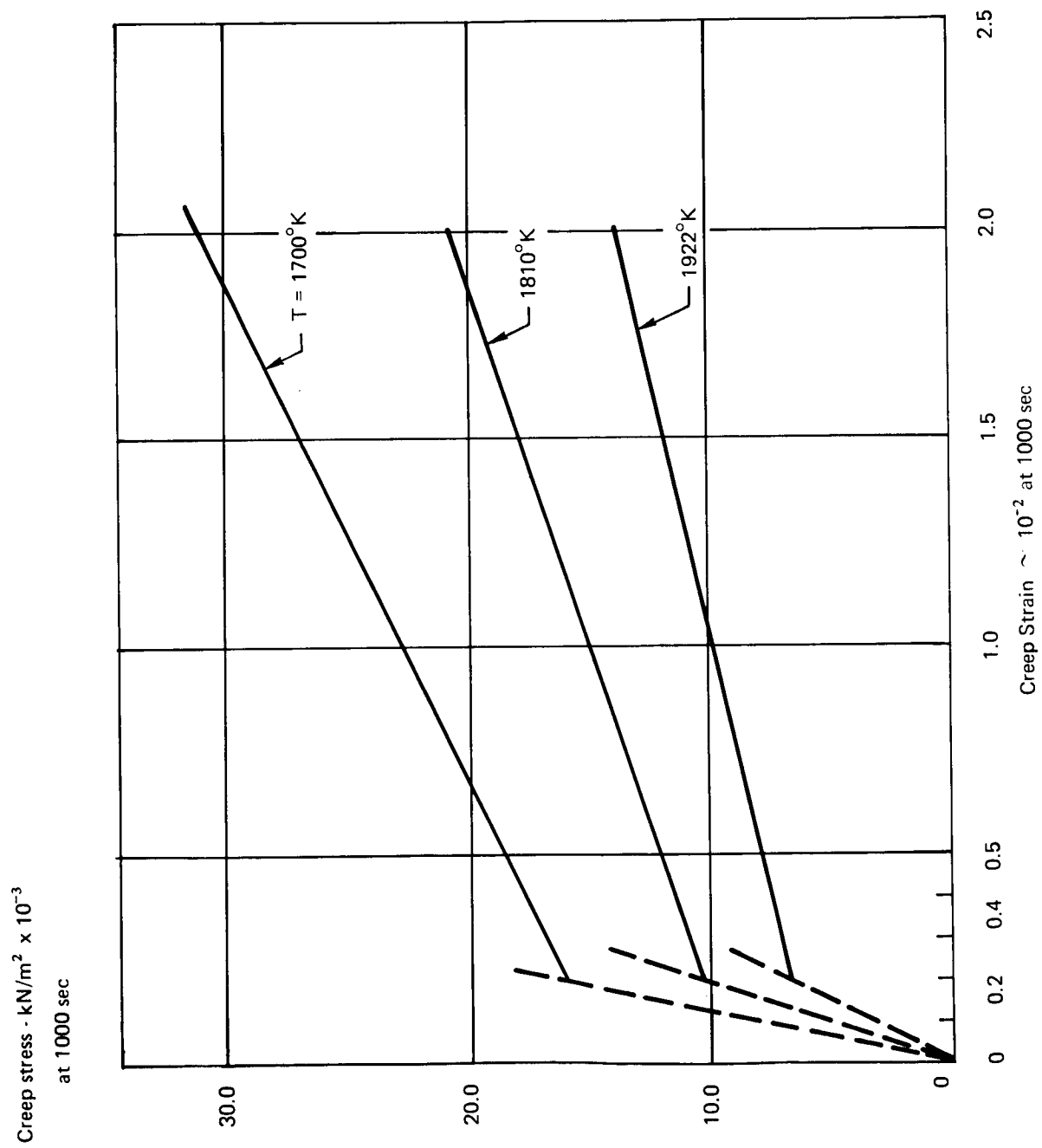


Figure 63 SI. Material - C-103 Creep Characteristic Stress - Strain Diagrams at $t = 1000$ sec

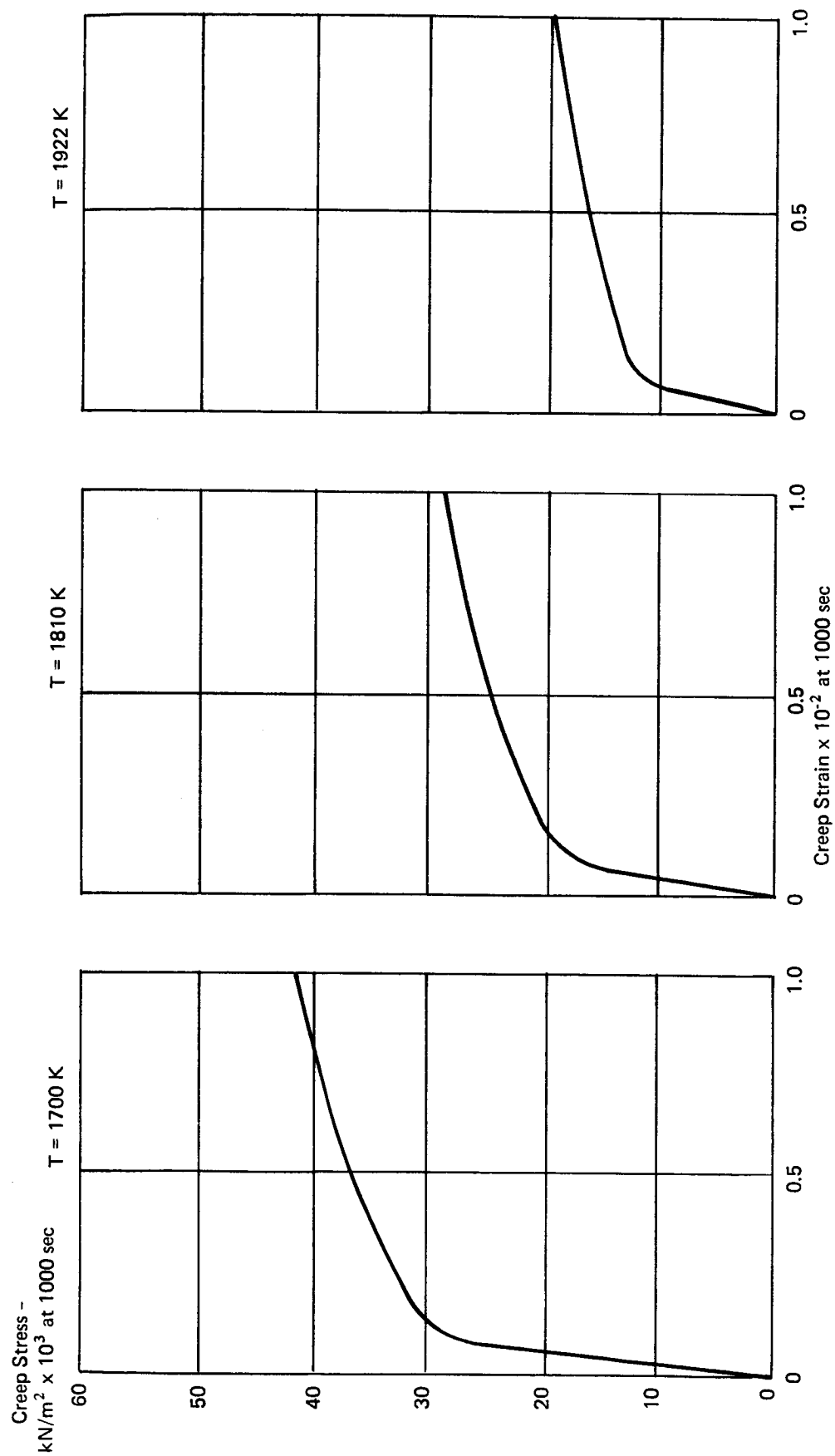


Figure 64 SL. Material - SCb-291 Creep Characteristic Stress - Strain Diagram at $t = 1000$ sec

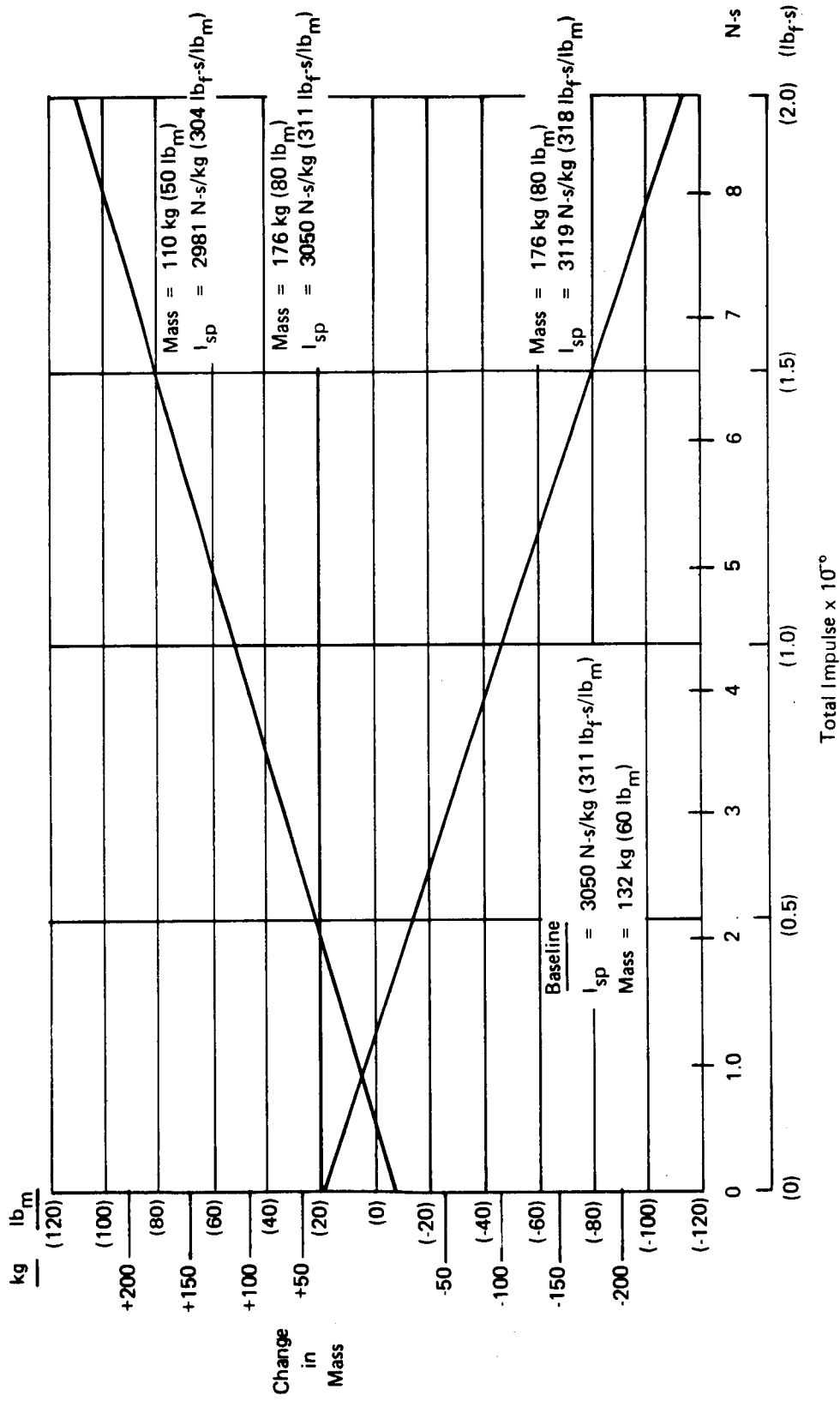
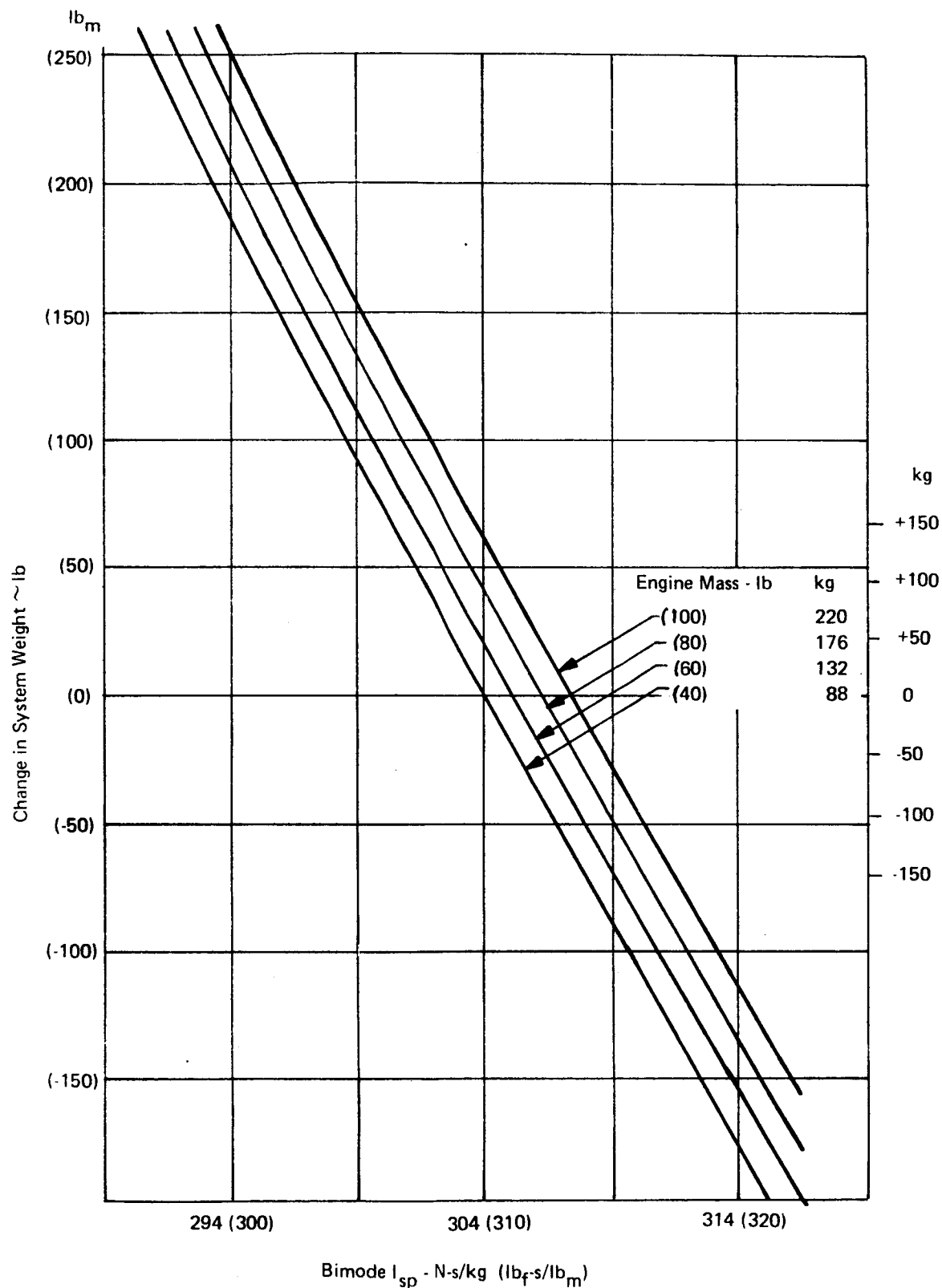


Figure 65 SI and 65. System Weight Comparison versus Total Impulses, Bimode Engine Weight and I_{sp}



Total Impulse - N-s	lb _f -s
Bimode 6.75×10^6	1.52×10^6
Mono 1.6×10^6	0.36×10^6

Figure 66 SI and 66. Bimode Engine System Weight versus I_{sp} and Engine Weight

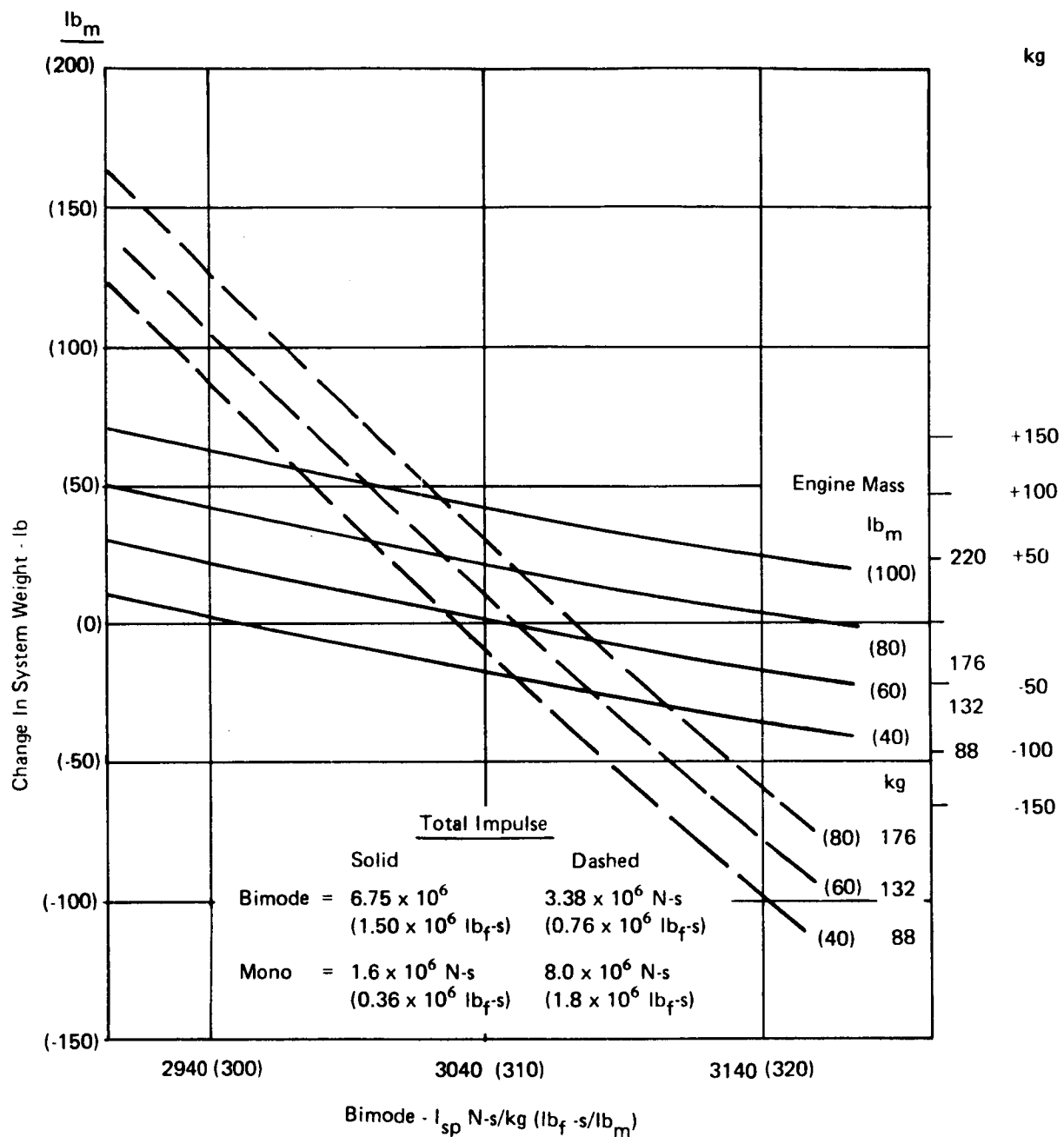


Figure 67 SI and 67. Bimode Engine System Weight versus I_{sp} and Engine Weight

SYSTEM WEIGHT MODEL BINODE SYSTEM

01/12/73

PRESSURE SCHEDULE - NOMINAL CONDITIONS - 1 ENGINE FIRING

	FUEL	OX
ENGINE CHAMBER	130.	
INJECTOR DROP	50.	50.
ORIFICE DROP	90.	90.
VALVE DROP	30.	30.
ENGINE INLET	300.	300.
FEED LINE DROP	1.	1.
PROPELLANT TANK	301.	301.
GAS MANIFOLD DROP	1.	1.
PRIMARY REG OUT	302.	
SECONDARY REG OUT	310.	
REG LOCKUP PRESSURE	307.	
RELIEF VALVE RESEAT	325.	
MAX RELIEF PRESSURE	365.	
TANK WORKING PRESSURE	365.	
MIN REG INLET	510.	
HIGH PRESS LINE DROP	50.	
MINIMUM SOURCE	560.	
HELIUM STORAGE PRESSURES		
MINIMUM AT 41. DEG F	3795.	
NOMINAL AT 72. DEG F	4000.	
MAXIMUM AT 103. DEG F	4265.	
PREPRESSURE AT 103. DEG F	287.	

10% PRESSURANT RESERVE INCLUDED

PROPELLANT TANK -SURFACE TENSION

MIXTURE RATIO MISMATCH =	0.03		
EXPULSION EFFICIENCY	0.99		
PROPELLANT MARGIN =	0.03		
MIXTURE RATIO LIMITS	1.15	1.12	1.18

SYSTEM WEIGHT SUMMARY

ISP A = 311.0

ISP M = 234.0

COMPONENT	UNIT WEIGHT	FORWARD MODULE NO	MODULE WEIGHT	AFT MODULE NO	MODULE WEIGHT	TOTAL NO	WEIGHT
ENGINES	60.0	1	60.0	0	0.0	1	60.0
FLUID LINES	10.0	1	10.0	0	0.0	1	10.0
FUEL TANK	183.6	2	367.1	0	0.0	2	367.1
OXIDIZER TANK	183.6	1	183.6	0	0.0	1	183.6
HELIUM TANK	163.8	2	327.6	0	0.0	2	327.6
REGULATOR	3.0	2	6.0	0	0.0	2	6.0
ISOLATION VALVES	4.5	4	18.0	0	0.0	4	18.0
MISC HARDWARE	15.0	1	15.0	0	0.0	1	15.0
TOTAL DRY WEIGHT			987.2		0.0		987.2
USEABLE PROPELLANT			6602.1		0.0		6602.1
RESIDUAL PROPELLANT			142.4		0.0		142.4
HELIUM			27.9		0.0		27.9
TOTAL WET WEIGHT			7759.7		0.0		7759.7

WEIGHT SUMMARY CHECK

PRESSURANT TANK VOLUME NEEDED	3330.	0.
PROPELLANT TANK VOLUME LIQUID	55562.	0.
SHELL	56117.	56117.

Figure 68 SI and 68. Specific Impulse Values

SYSTEM WEIGHT MODEL BIMODE SYSTEM

01/12/73

PRESSURE SCHEDULE - NOMINAL CONDITIONS - 1 ENGINE FIRING

	FUEL	OK
ENGINE CHAMBER	130.	
INJECTOR DROP	50.	50.
ORIFICE DROP	90.	90.
VALVE DROP	30.	30.
ENGINE INLET	300.	300.
FEED LINE DROP	1.	1.
PROPELLANT TANK	301.	301.
GAS MANIFOLD DROP	1.	1.
PRIMARY REG OUT	302.	
SECONDARY REG OUT	310.	
REG LOCKUP PRESSURE	307.	
RELIEF VALVE RESET	325.	
MAX RELIEF PRESSURE	365.	
TANK WORKING PRESSURE	365.	
MIN REG INLET	510.	
HIGH PRESS LINE DROP	50.	
MINIMUM SOURCE	560.	
HELIUM STORAGE PRESSURES		
MINIMUM AT 41. DEG F	3795.	
NOMINAL AT 72. DEG F	4000.	
MAXIMUM AT 103. DEG F	4265.	
PREPRESSURE AT 103. DEG F	287.	
10% PRESSURANT RESERVE INCLUDED		

PROPELLANT TANK -SURFACE TENSION

MIXTURE RATIO MISMATCH =	0.03		
EXPULSION EFFICIENCY	0.99		
PROPELLANT MARGIN =	0.03		
MIXTURE RATIO LIMITS	1.15	1.12	1.18

SYSTEM WEIGHT SUMMARY

ISP A = 300.0

ISP M = 234.0

COMPONENT	UNIT WEIGHT	FORWARD MODULE NO	MODULE WEIGHT	AFT MODULE NO	MODULE WEIGHT	TOTAL NO	WEIGHT
ENGINES	60.0	1	60.0	0	0.0	1	60.0
FLUID LINES	10.0	1	10.0	0	0.0	1	10.0
FUEL TANK	186.9	2	373.9	0	0.0	2	373.9
OXIDIZER TANK	186.9	1	186.9	0	0.0	1	186.9
HELIUM TANK	168.0	2	335.9	0	0.0	2	335.9
REGULATOR	3.0	2	6.0	0	0.0	2	6.0
ISOLATION VALVES	4.5	4	18.0	0	0.0	4	18.0
MISC HARDWARE	15.0	1	15.0	0	0.0	1	15.0
TOTAL DRY WEIGHT			1005.7		0.0		1005.7
USEABLE PROPELLANT			6786.1		0.0		6786.1
RESIDUAL PROPELLANT			147.0		0.0		147.0
HELIUM			28.5		0.0		28.5
TOTAL NET WEIGHT			7967.3		0.0		7967.3
WEIGHT SUMMARY CHECK							
PRESSURANT TANK VOLUME NEEDED			8594.		0.		
PROPELLANT TANK VOLUME LIQUID			56783.		0.		
SHELL			57351.		57351.		

Figure 69 SI and 69. Specific Impulse Values

SYSTEM WEIGHT MODEL BIMODE SYSTEM

01/12/73

PRESSURE SCHEDULE - NOMINAL CONDITIONS - 1 ENGINE FIRING

	FUEL	OX
ENGINE CHAMBER	130.	
INJECTOR DROP	50.	50.
ORIFICE DROP	90.	90.
VALVE DROP	30.	30.
ENGINE INLET	300.	300.
FEED LINE DROP	1.	1.
PROPELLANT TANK	301.	301.
GAS MANIFOLD DROP	1.	1.
PRIMARY REG OUT		302.
SECONDARY REG OUT		310.
REG LOCKUP PRESSURE		307.
RELIEF VALVE RESEAT		325.
MAX RELIEF PRESSURE		365.
TANK WORKING PRESSURE		365.
MIN REG INLET		510.
HIGH PRESS LINE DROP		50.
MINIMUM SOURCE		560.
HELIUM STORAGE PRESSURES		
MINIMUM AT 41. DEG F	3795.	
NOMINAL AT 72. DEG F	4000.	
MAXIMUM AT 103. DEG F	4265.	
PREPRESSURE AT 103. DEG F	287.	
10% PRESSURANT RESERVE INCLUDED		

PROPELLANT TANK -SURFACE TENSION

MIXTURE RATIO MISMATCH =	0.03		
EXPULSION EFFICIENCY	0.99		
PROPELLANT MARGIN =	0.03		
MIXTURE RATIO LIMITS	1.15	1.12	1.18

SYSTEM WEIGHT SUMMARY

ISP A = 320.0

ISP1= 234.0

COMPONENT	UNIT WEIGHT	FORWARD NO	MODULE WEIGHT	AFT NO	MODULE WEIGHT	TOTAL NO	WEIGHT
ENGINES	60.0	1	60.0	0	0.0	1	60.0
FLUID LINES	10.0	1	10.0	0	0.0	1	10.0
FUEL TANK	181.0	2	361.9	0	0.0	2	361.9
OXIDIZER TANK	181.0	1	181.0	0	0.0	1	181.0
HELIUM TANK	160.6	2	321.1	0	0.0	2	321.1
REGULATOR	3.0	2	6.0	0	0.0	2	6.0
ISOLATION VALVES	4.5	4	18.0	0	0.0	4	18.0
MISC HARDWARE	15.0	1	15.0	0	0.0	1	15.0
TOTAL DRY WEIGHT			973.0		0.0		973.0
USEABLE PROPELLANT			6461.0		0.0		6461.0
RESIDUAL PROPELLANT			138.3		0.0		138.3
HELIUM			27.5		0.0		27.5
TOTAL NET WEIGHT			7600.4		0.0		7600.4

HEIGHT SUMMARY CHECK

PRESSURANT TANK VOLUME NEEDED	3215.	0.
PROPELLANT TANK VOLUME LIQUID	54625.	0.
SHELL	55171.	55171.

Figure 70 SI and 70. Specific Impulse Values

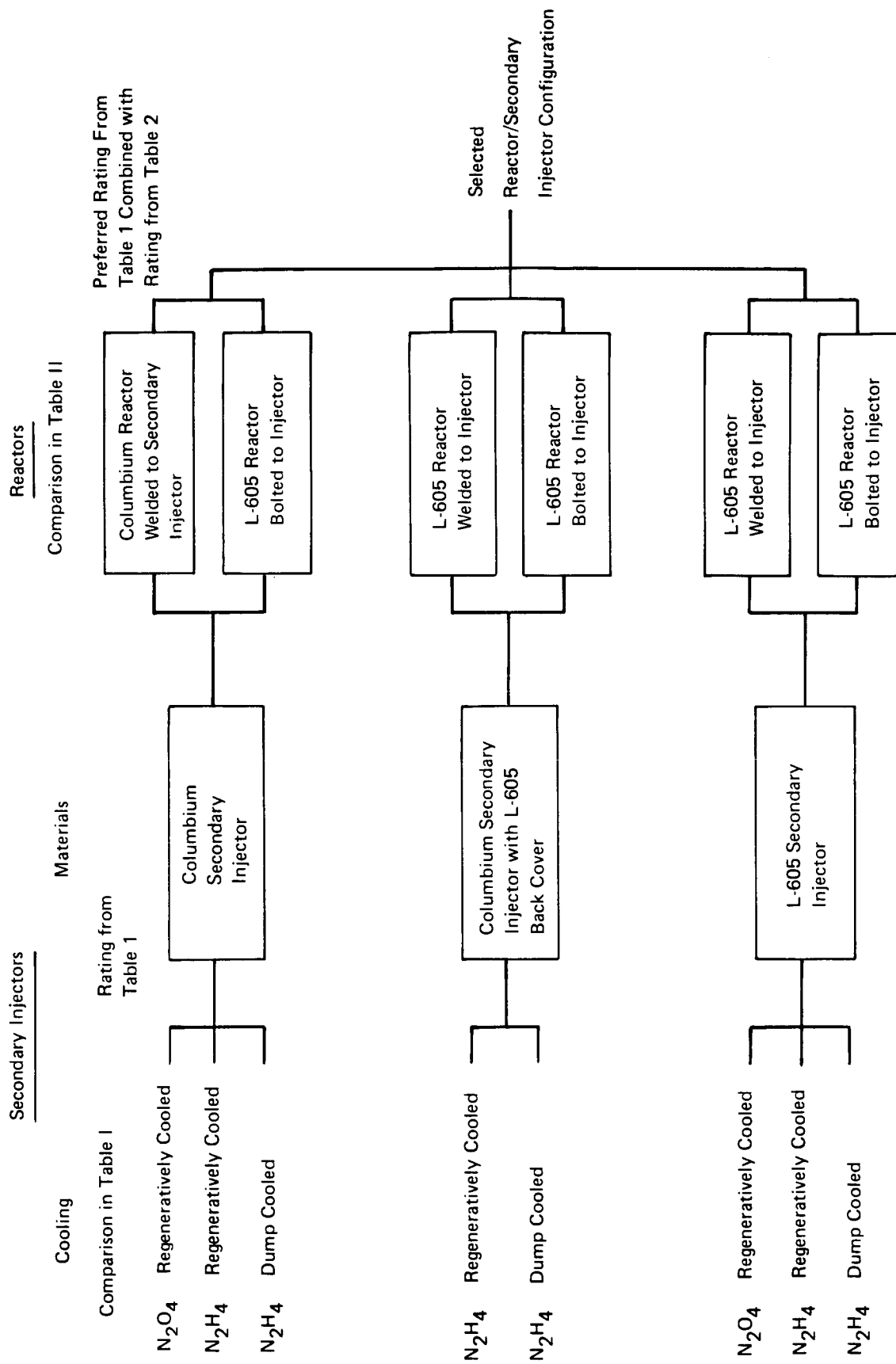


Figure 71 SI. Reactor Located at Secondary Injector Station

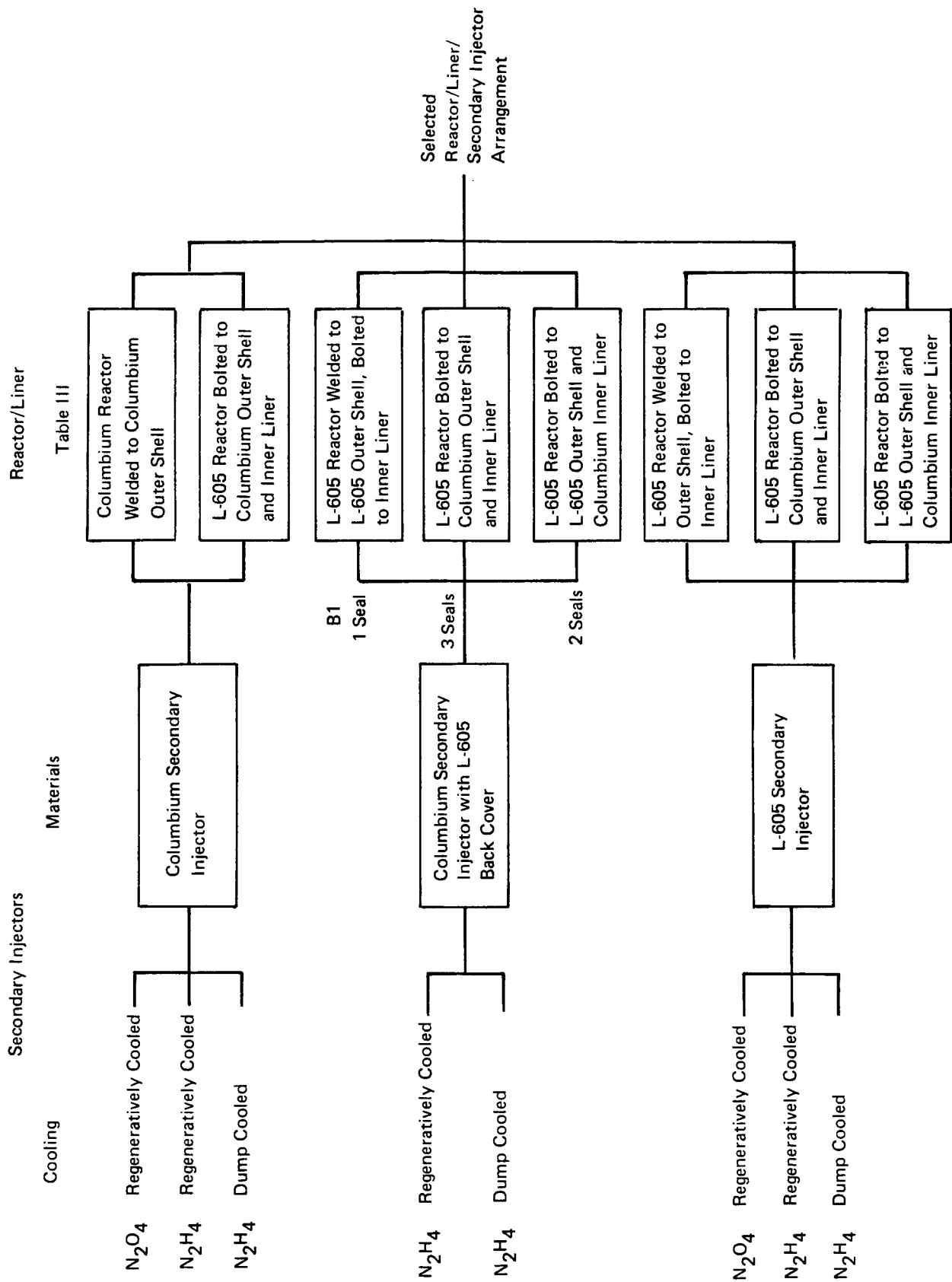


Figure 72 SI. Regeneratively Cooled Thruster, Reactor Located at Nozzle Extension Interface

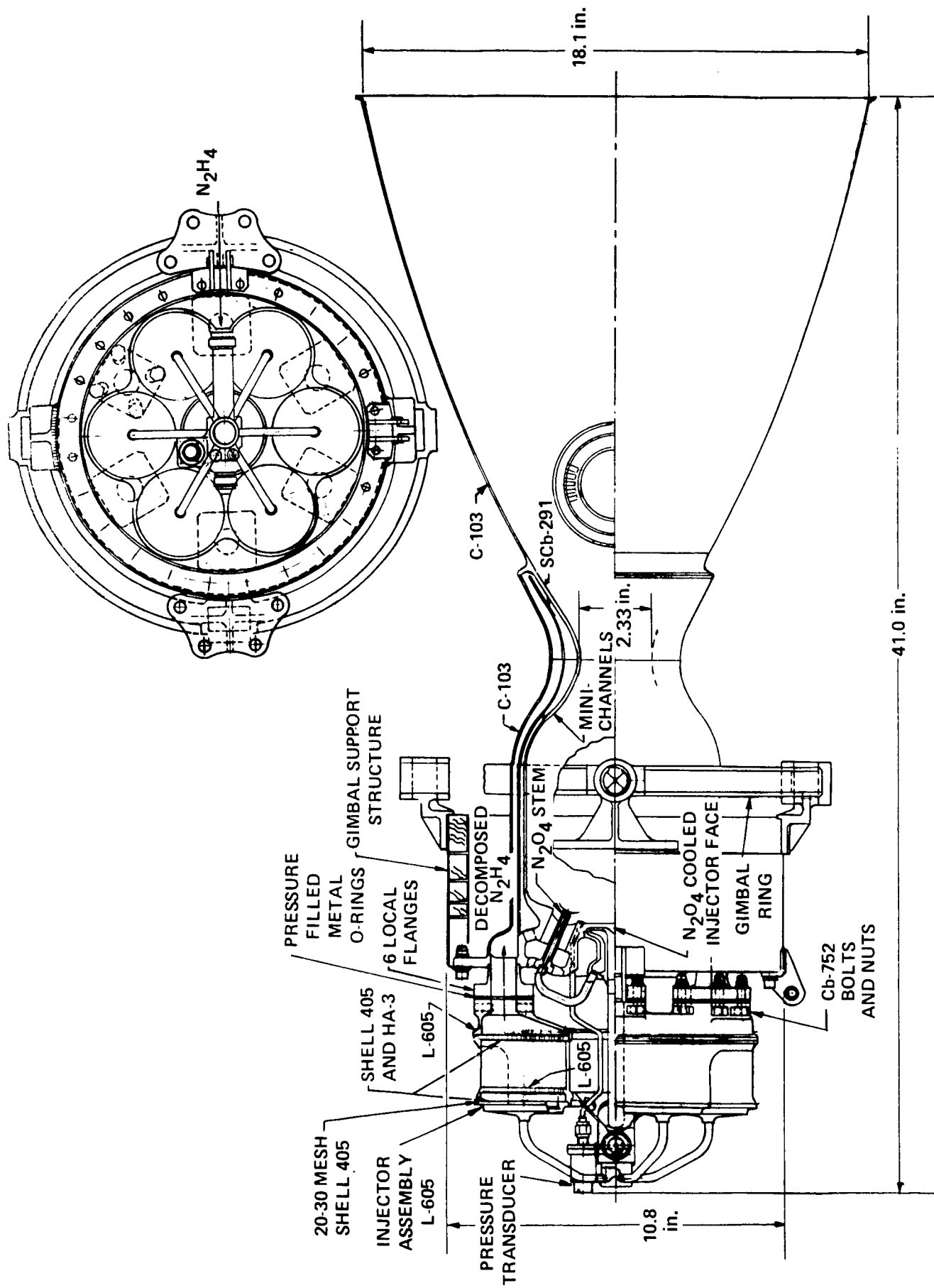


Figure 73 SL. Prototype Regenerative Cooled Bimodal Thrust Chamber with Integral Six Cylindrical Reactor at Injector

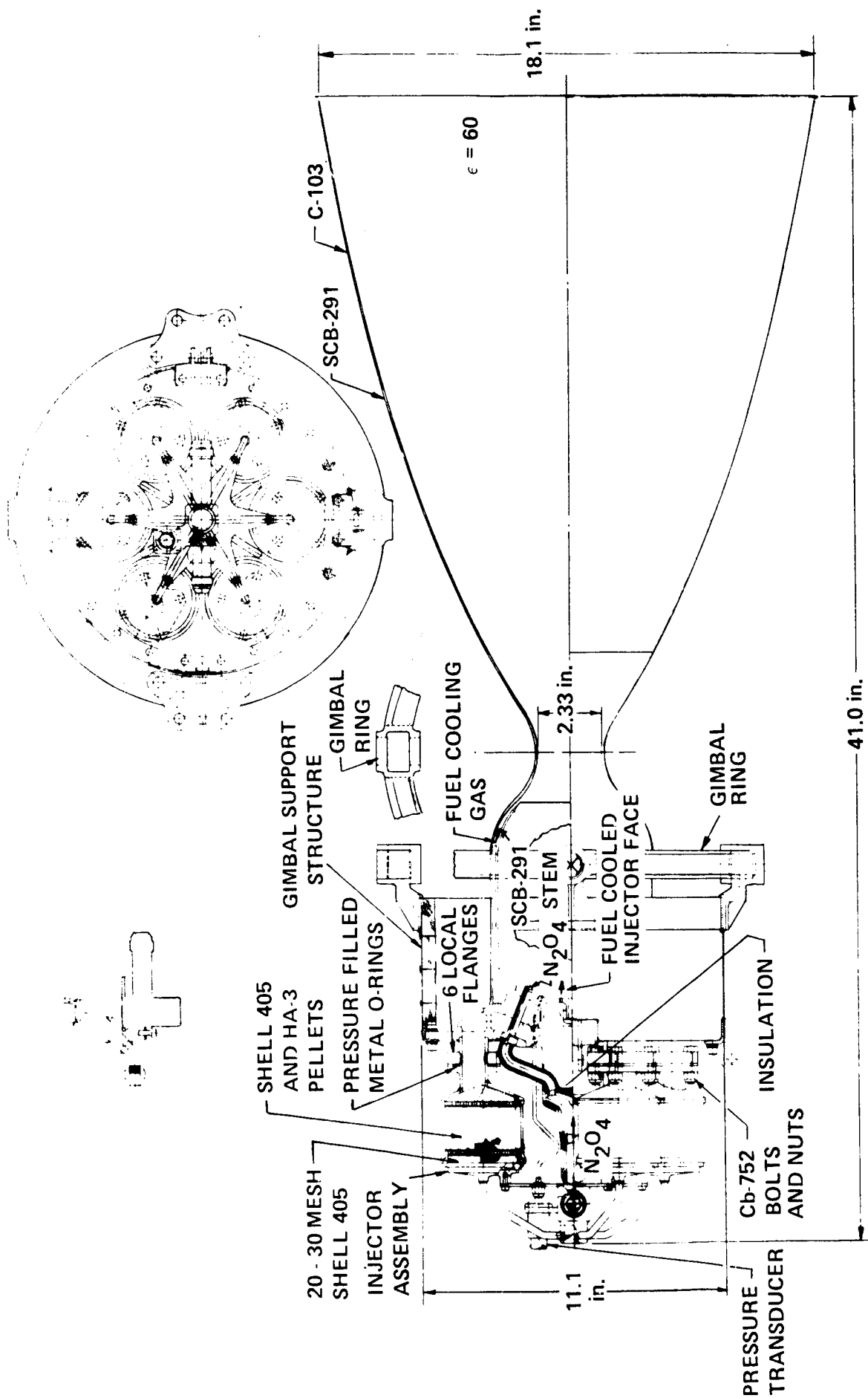


Figure 75 SI. Prototype Film Cooled Bimodal Thrust Chamber with Six Individual Cylindrical Reactors at Injector

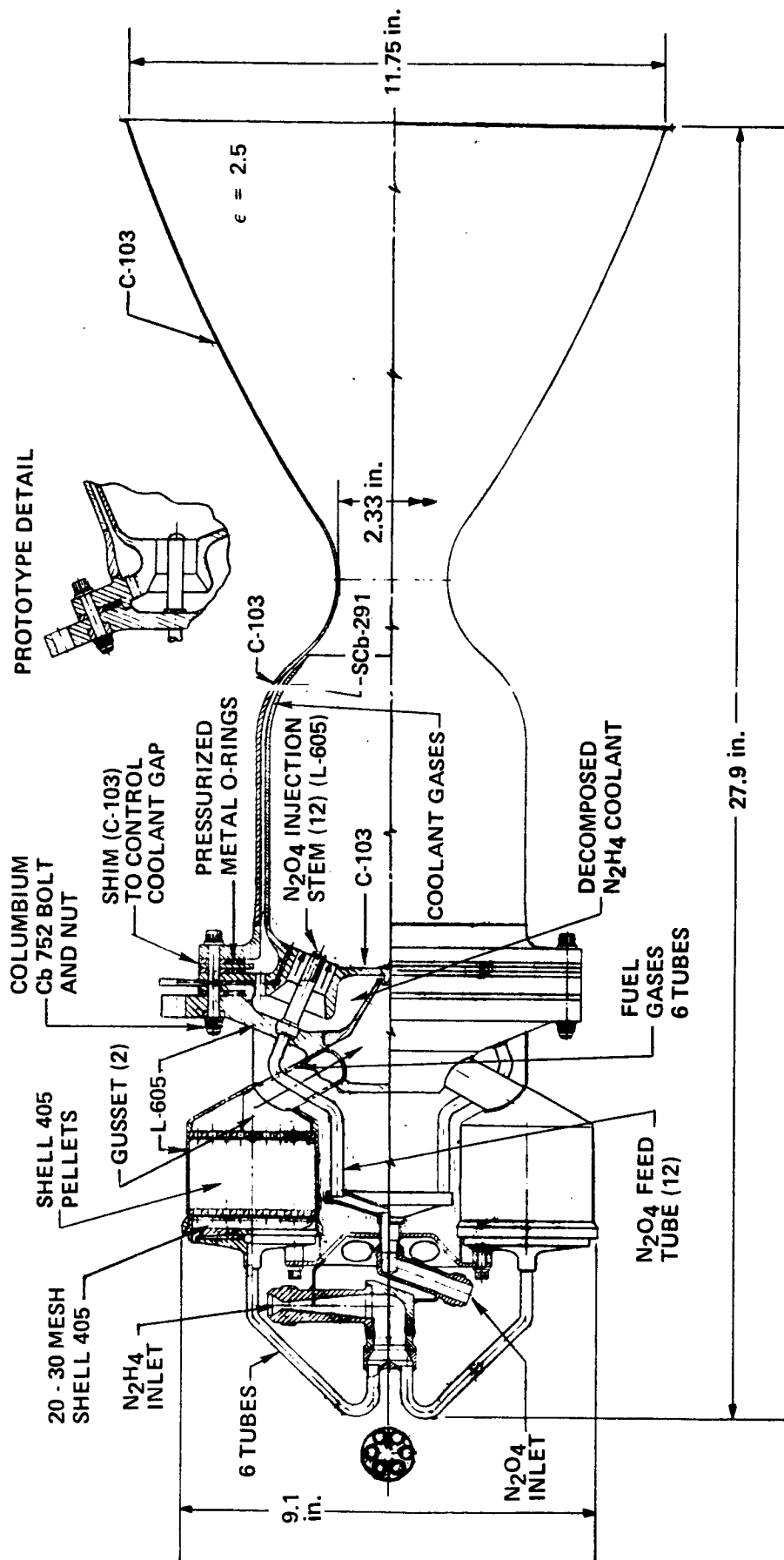


Figure 76 Sl. Preprototype Film Cooled Thrust Chamber with 100% Fuel Cooled Injector Face

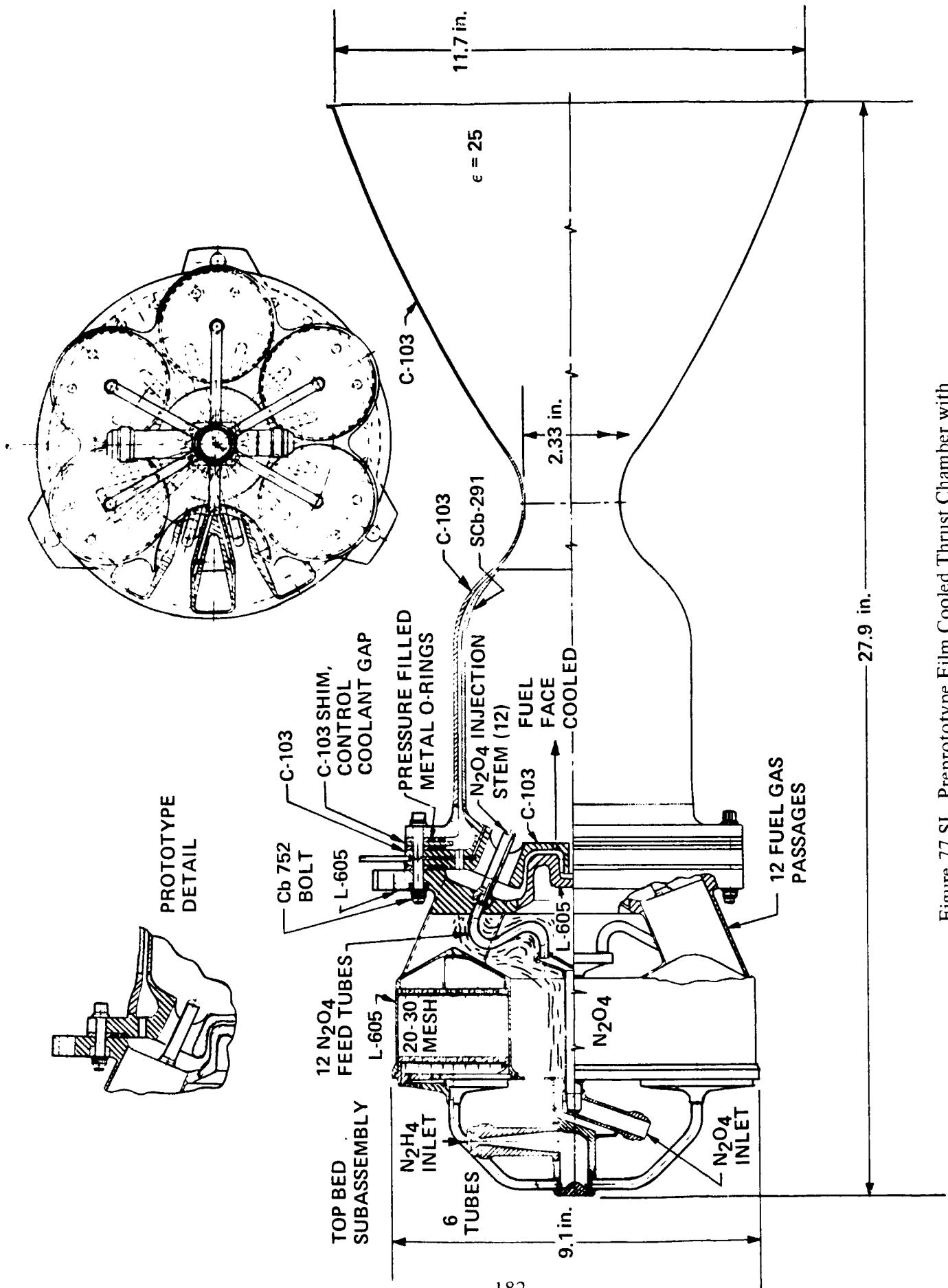


Figure 77 SI. Preprototype Film Cooled Thrust Chamber with 6% Fuel Cooled Injector Face

FIGURES ENGLISH

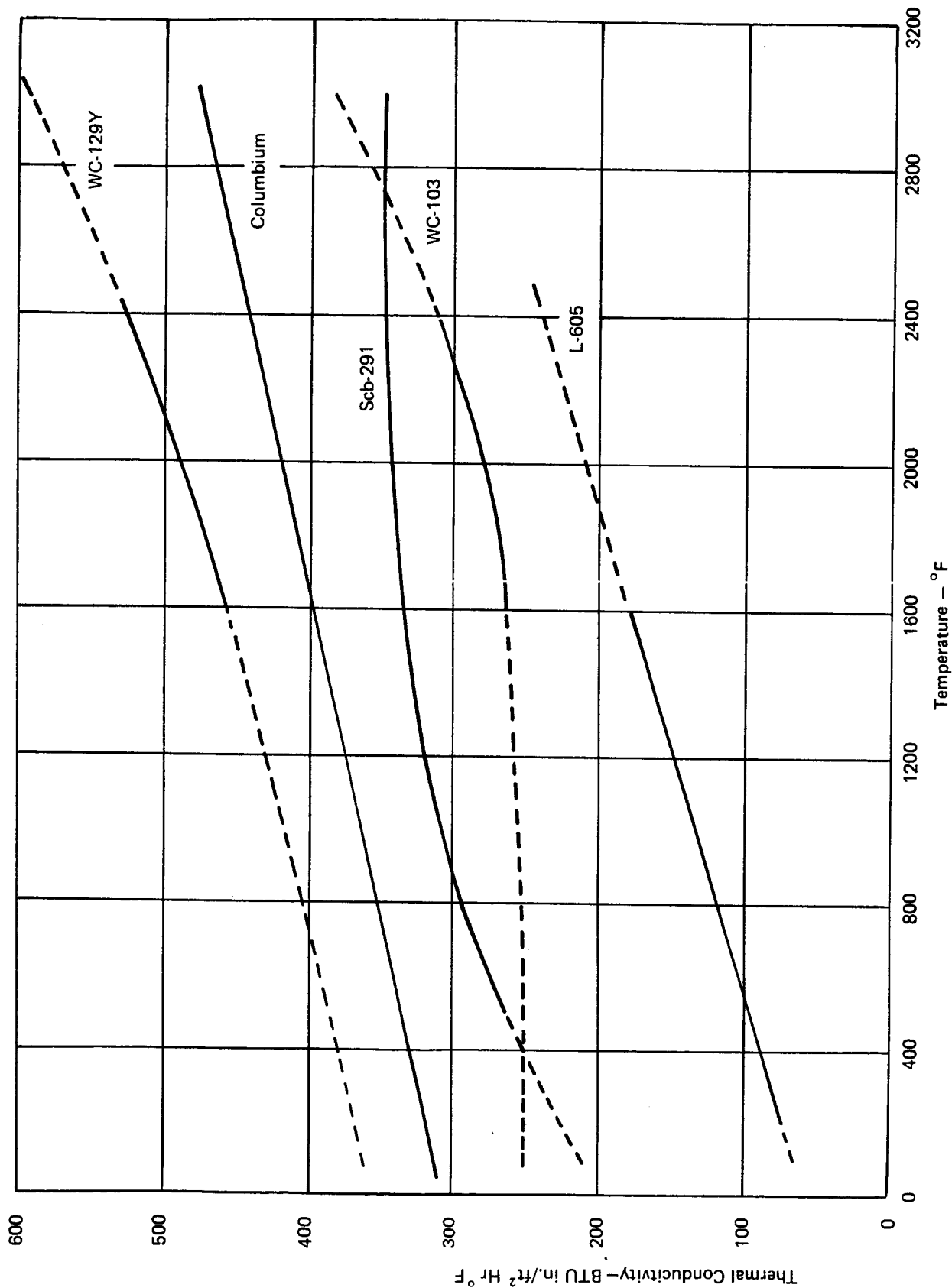


Figure 20. Thermal Conductivity

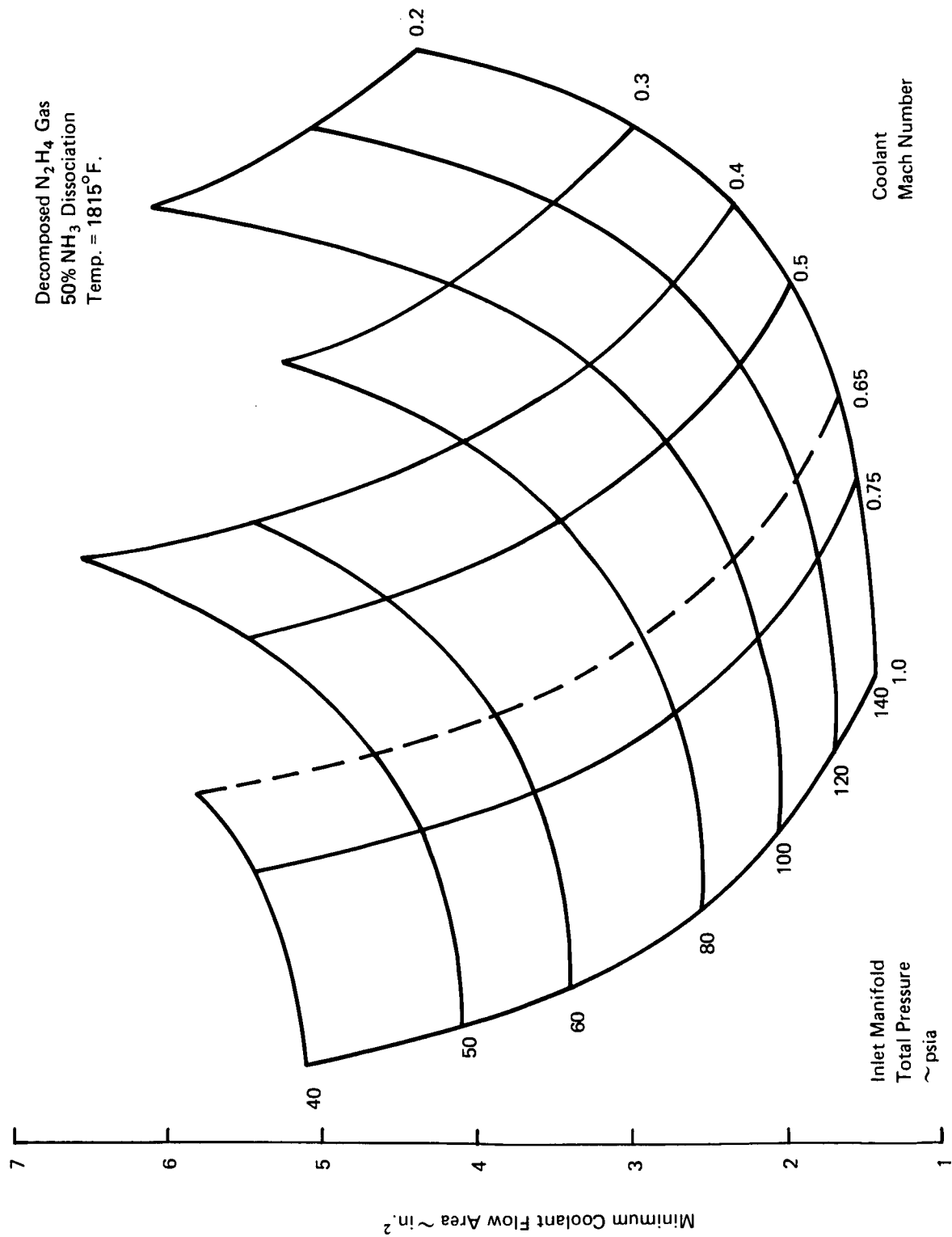


Figure 21. Influence of Inlet Manifold Pressure on Cooling Passage Design Variables

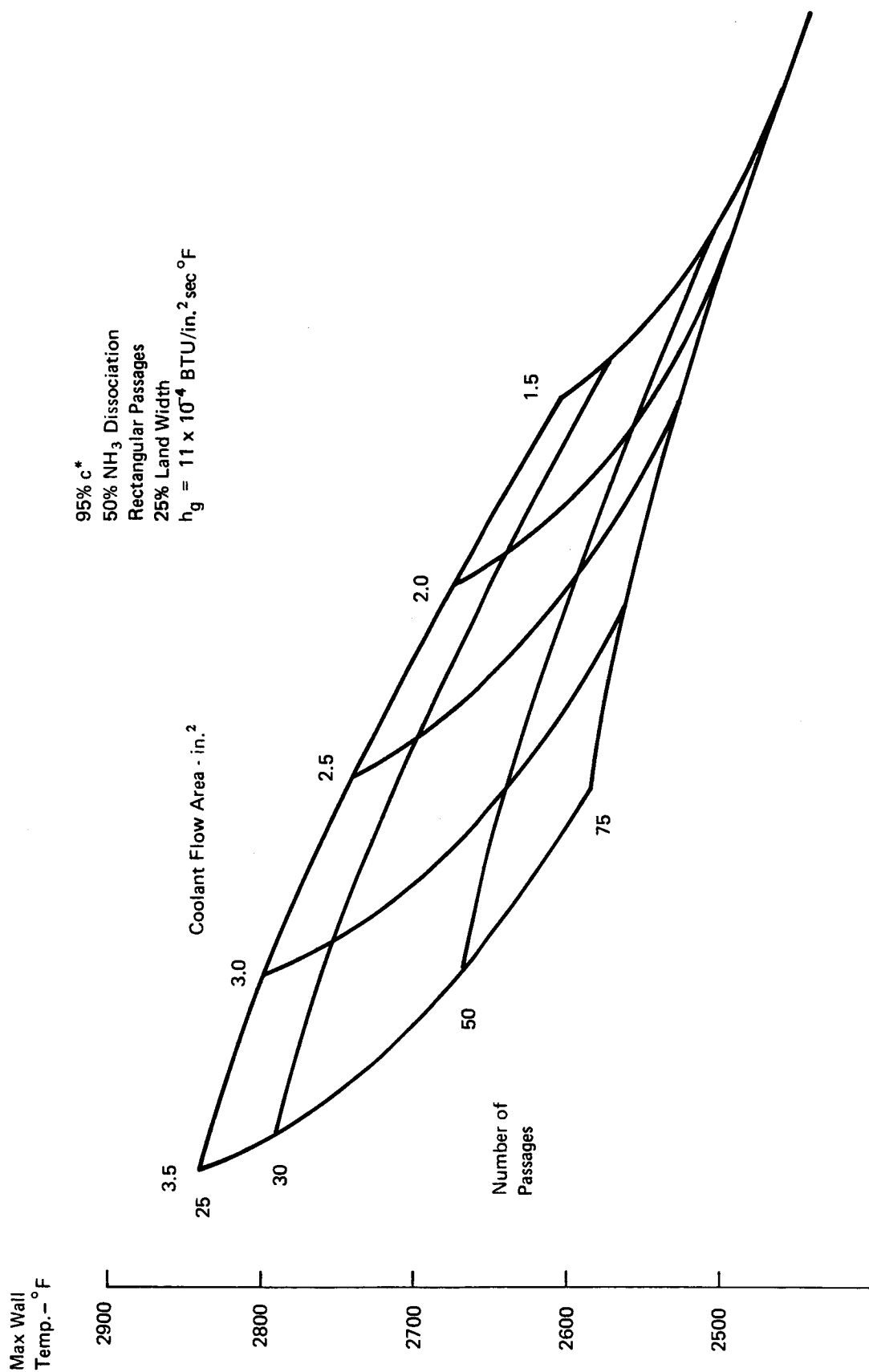


Figure 22. Influence of Coolant Passage Design Parameters on Maximum Throat Temperature

95% c*
 50% NH₃ Dissociation
 Rectangular Passages
 Total Pressure = 80 psia (Monomode)
 25% Land Width
 $h_g = 11 \times 10^{-4} \text{ BTU/in.}^2 \text{ sec } ^\circ\text{F}$

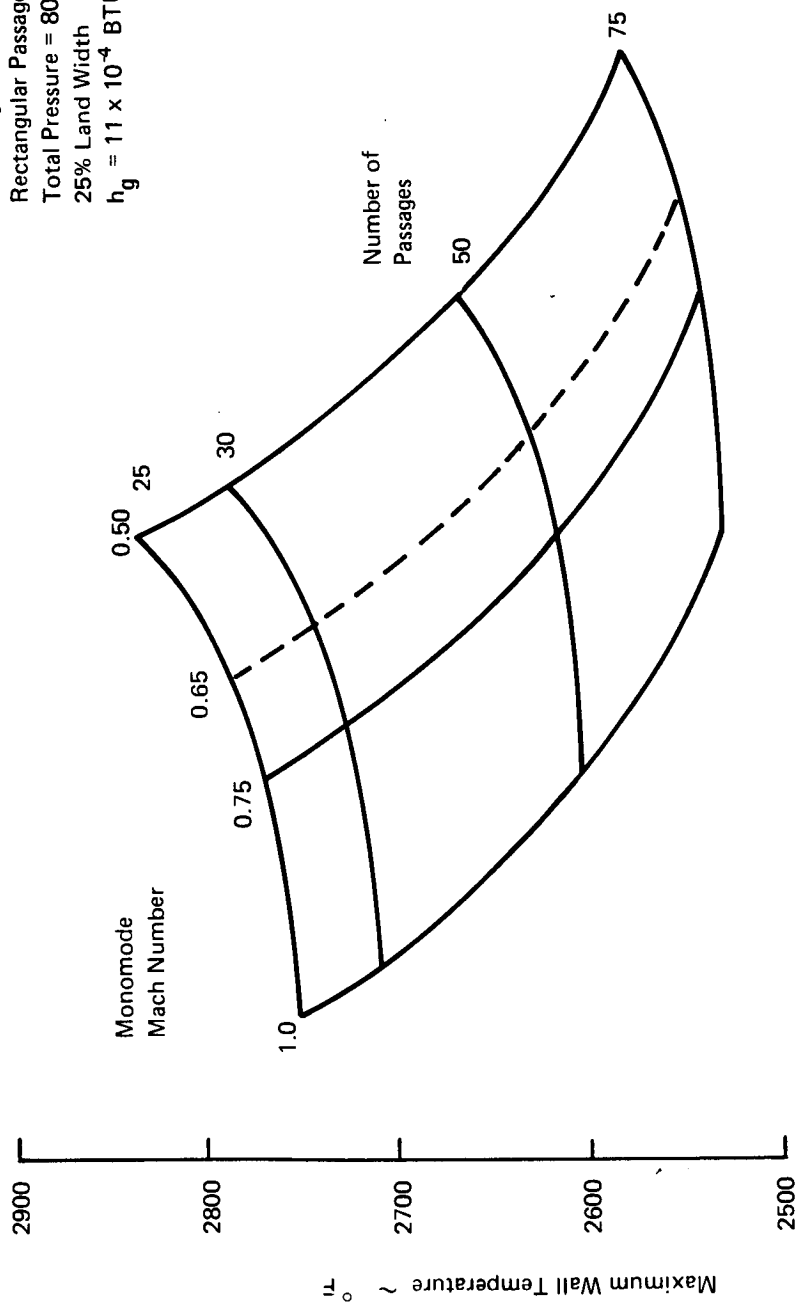


Figure 23. Influence of Coolant Passage Design Parameters on Maximum Throat Temperature

95% c*
 50% NH₃ Dissociation
 50 Rectangular Passages
 25% Land Width
 $h_g = 11 \times 10^{-4} \text{ BTU/in.}^2 \text{ sec } ^\circ\text{F}$

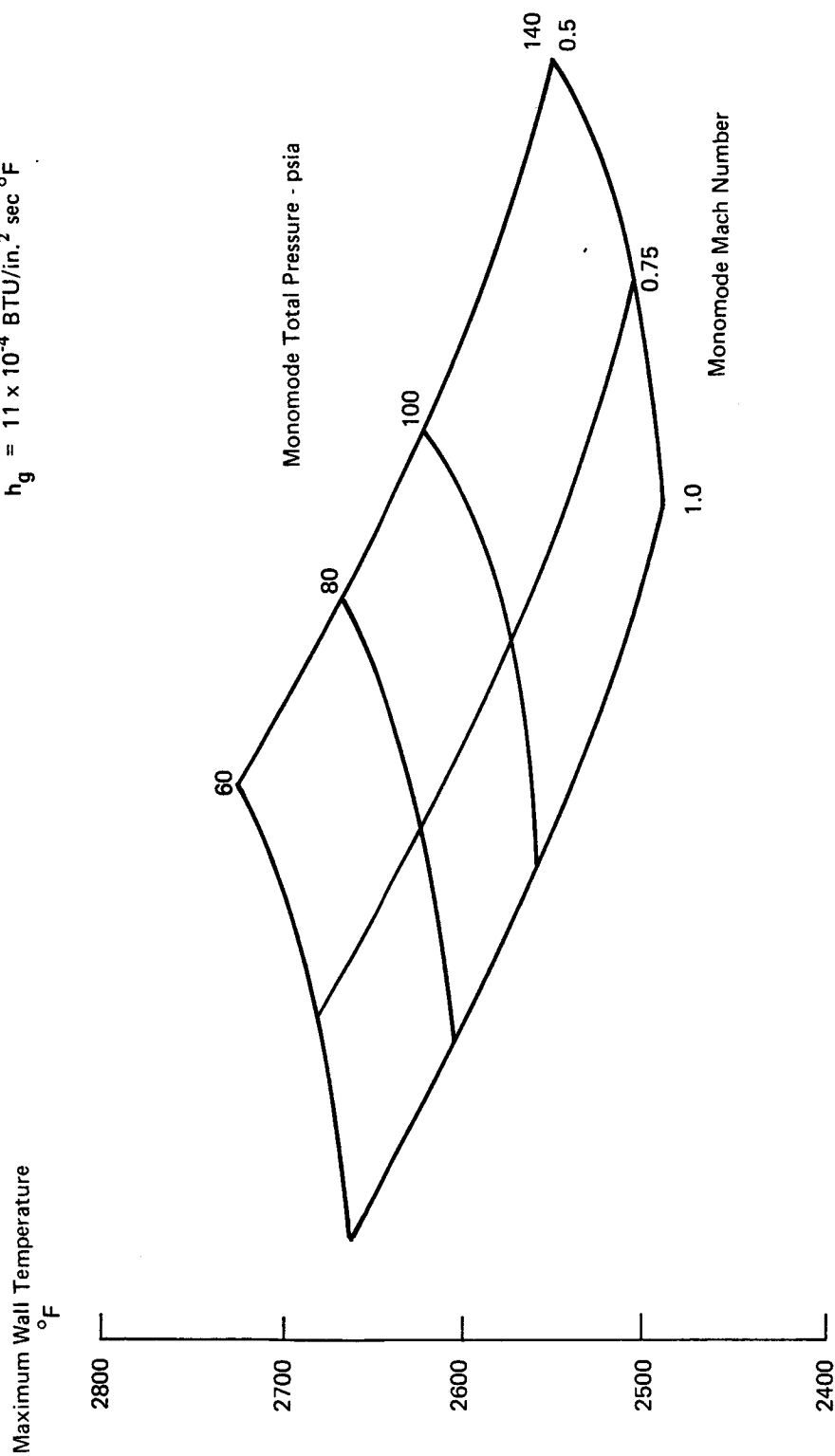


Figure 24. Influence of Coolant Passage Design Parameters on Maximum Throat Temperature

95% c*
 50% NH₃ Dissociation
 50 Rectangular Passages
 Mach Number = 0.75
 Total Pressure = 80 psia
 $h_g = 11 \times 10^{-4} \text{ BTU/in.}^2 \text{sec } ^\circ\text{F}$

} Monomode

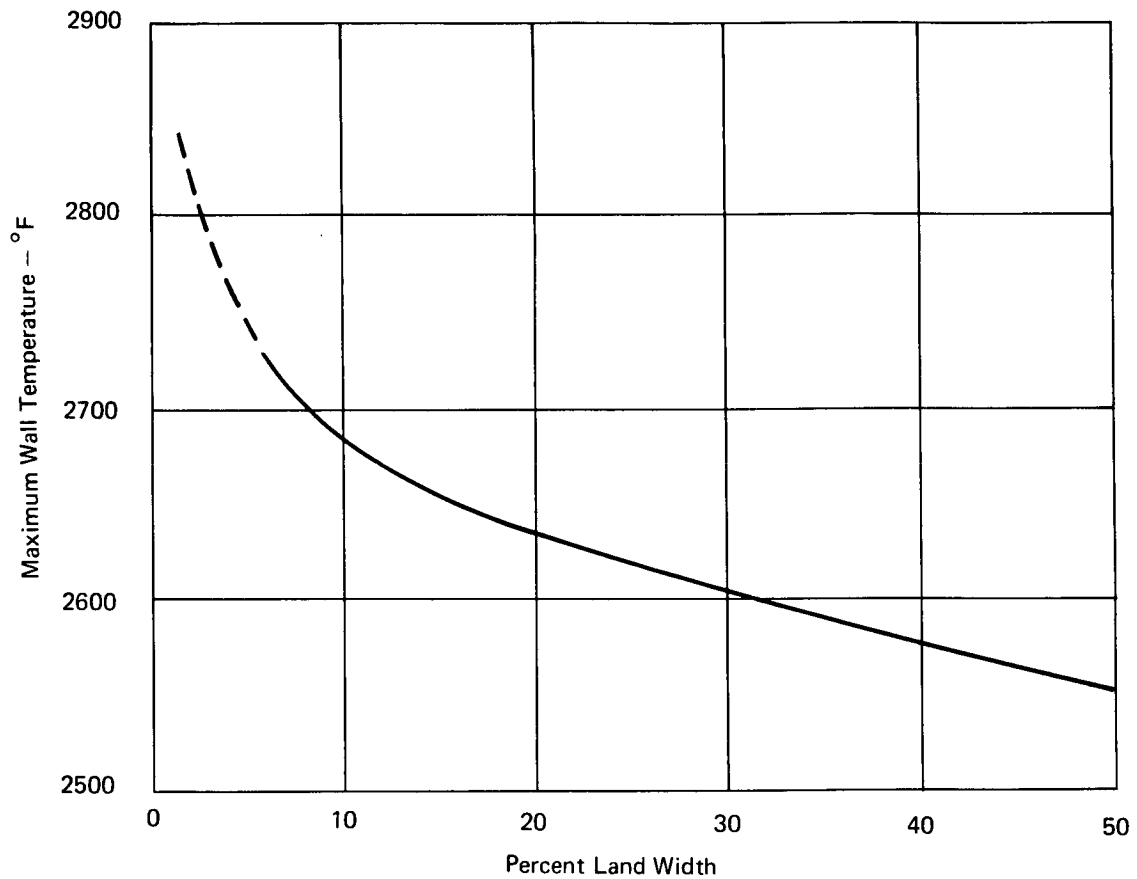


Figure 25. Influence of Percent Land Width on Maximum Throat Temperature

95% c*
 50% NH₃ Dissociation
 50 Rectangular Passages
 $h_g = 11 \times 10^{-4}$ BTU/in. sec °F

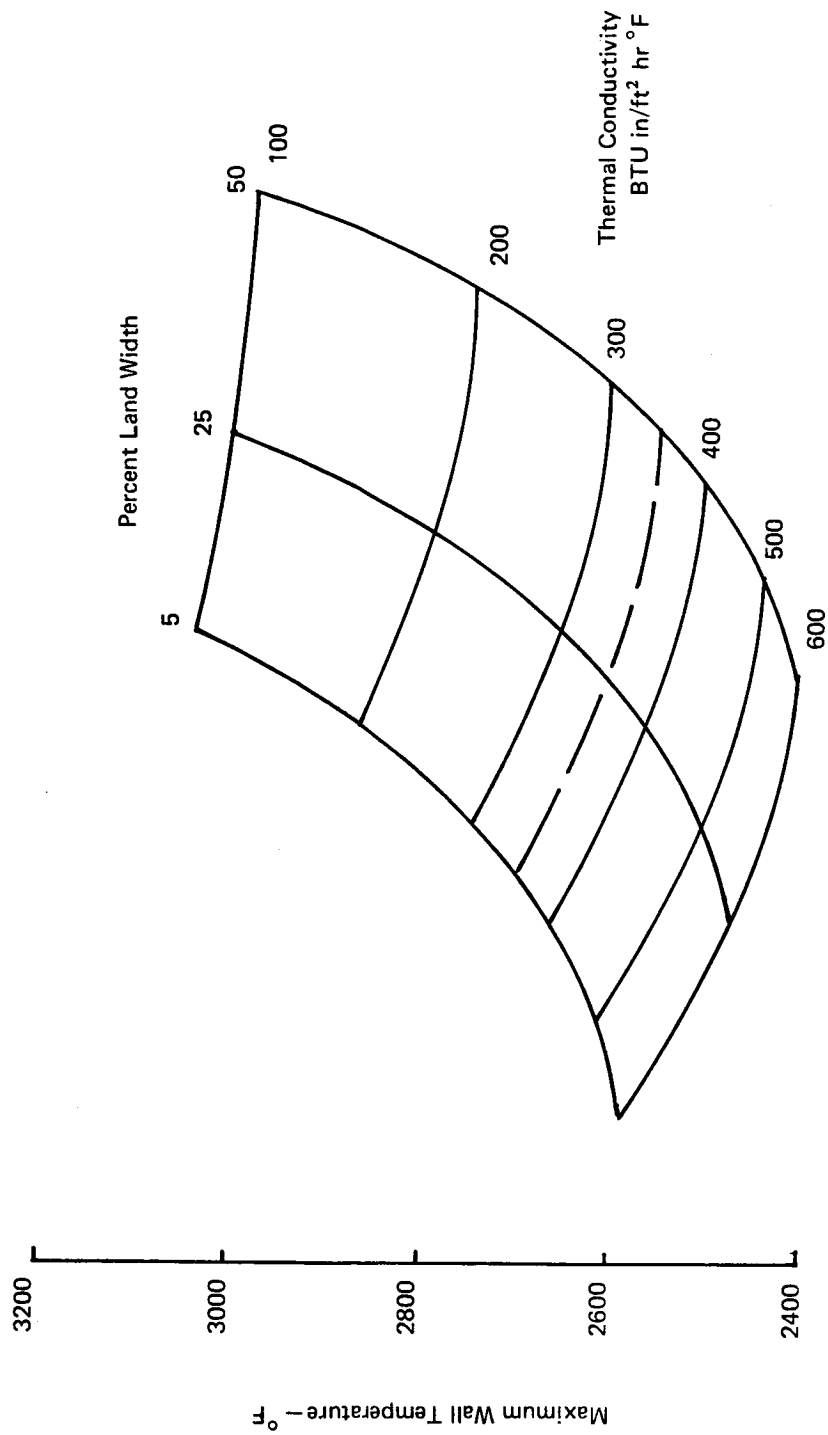


Figure 26. Influence of Wall Thermal Conductivity and Land Width on Maximum Throat Temperature

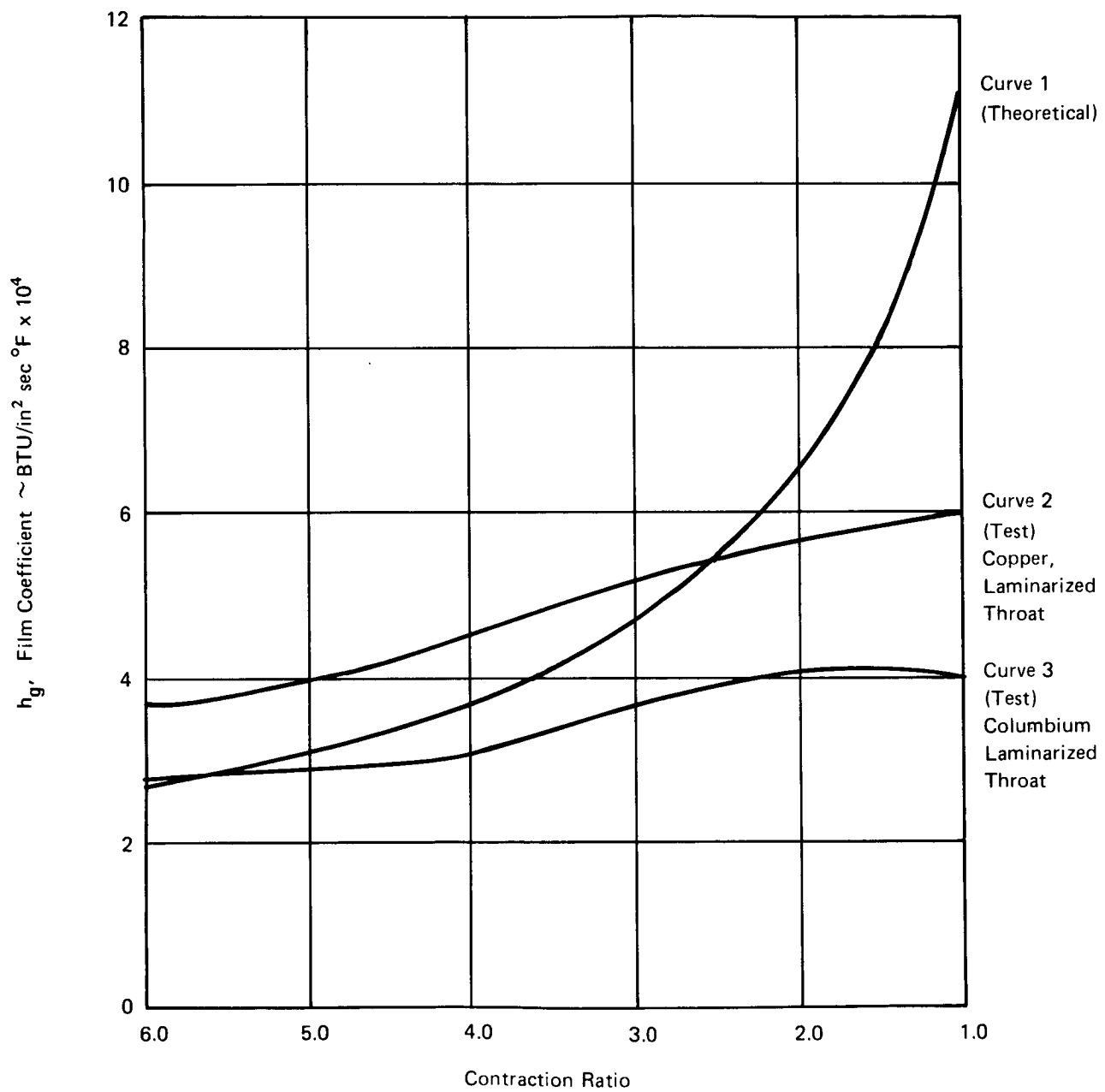


Figure 27. Hot Gas Film Coefficient versus Contraction Ratio

95% c*
 50% NH₃ Dissociation
 Rectangular Passages
 25% Land Width
 $h_g = 6 \times 10^{-4} \text{ BTU/in.}^2 \text{ sec } ^\circ\text{F}$

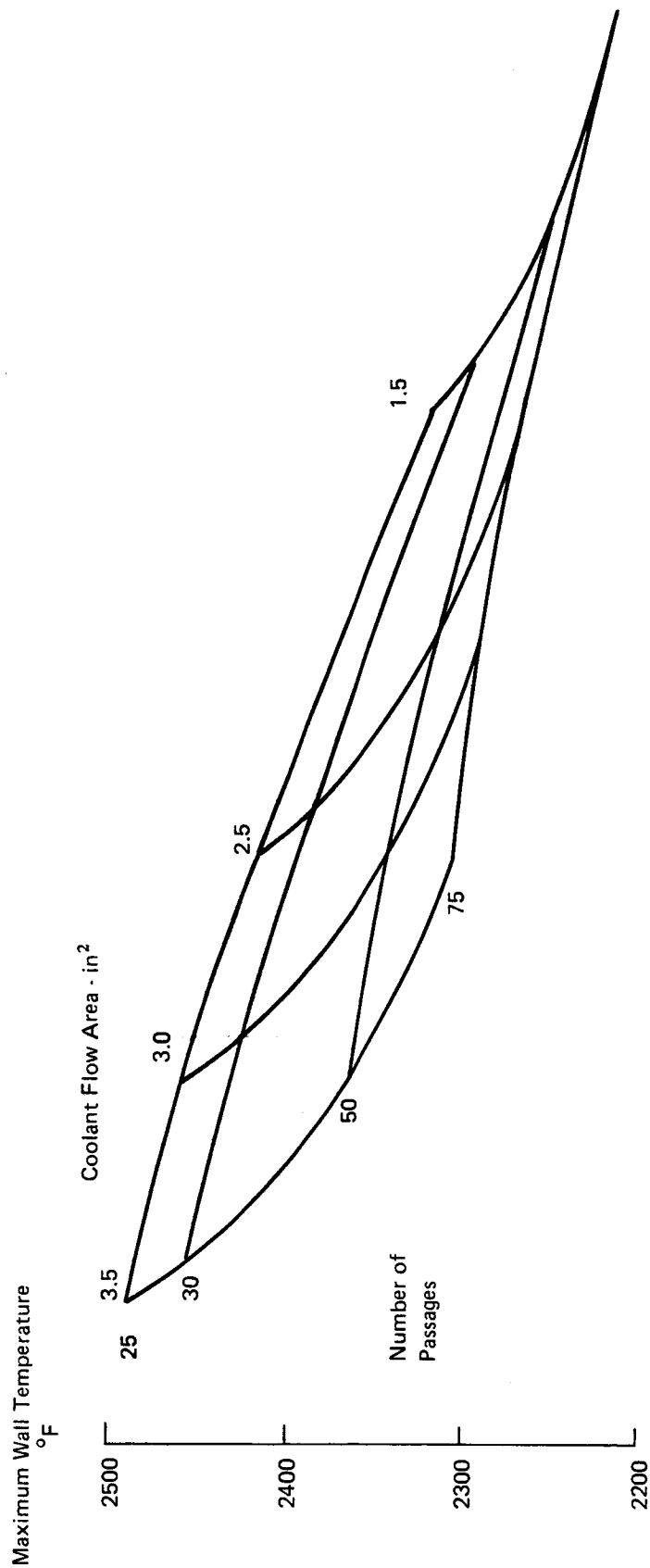


Figure 28. Influence of Coolant Passage Design Parameters on Maximum Throat Temperature

95% c^*
 50% NH_3 Dissociation
 Rectangular Passages
 Total Pressure = 80 psia (Monomode)
 25% Land Width
 $h_g = 6 \times 10^{-4} \text{ BTU/in.}^2 \text{ sec } ^\circ\text{F}$

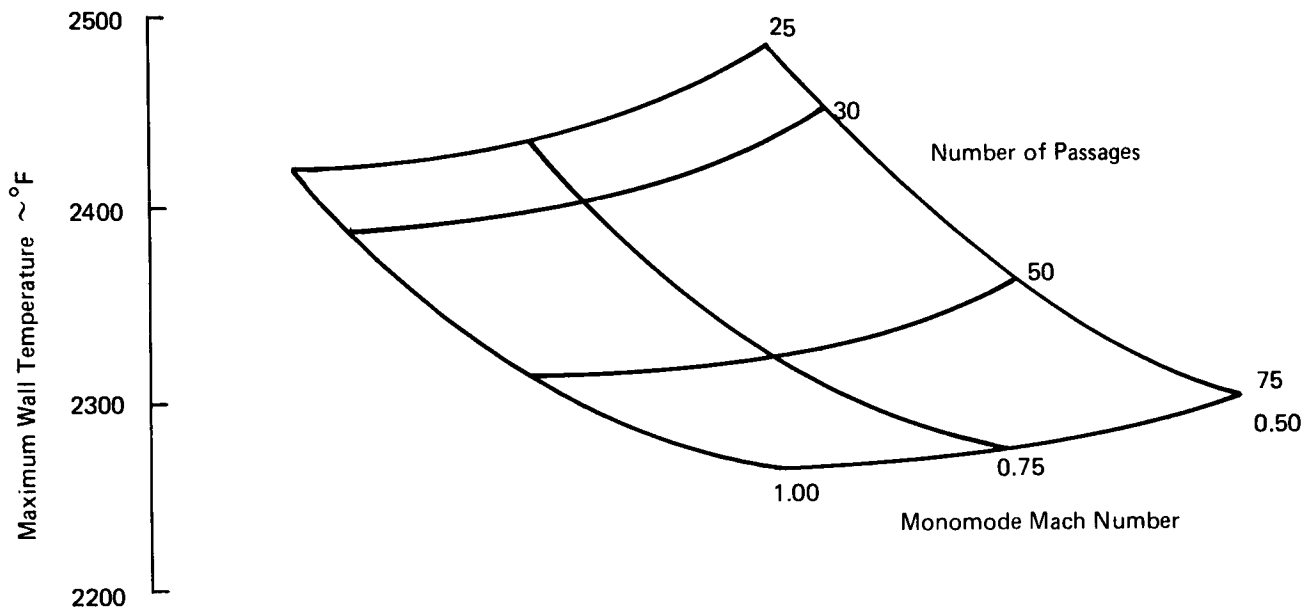


Figure 29. Influence of Coolant Passage Design Parameters on Maximum Throat Temperature

95% c*
 50% NH₃ Dissociation
 50 Rectangular Passages
 25% Land Width
 $h_g = 6 \times 10^{-4} \text{ BTU/in.}^2 \text{ sec } ^\circ\text{F}$

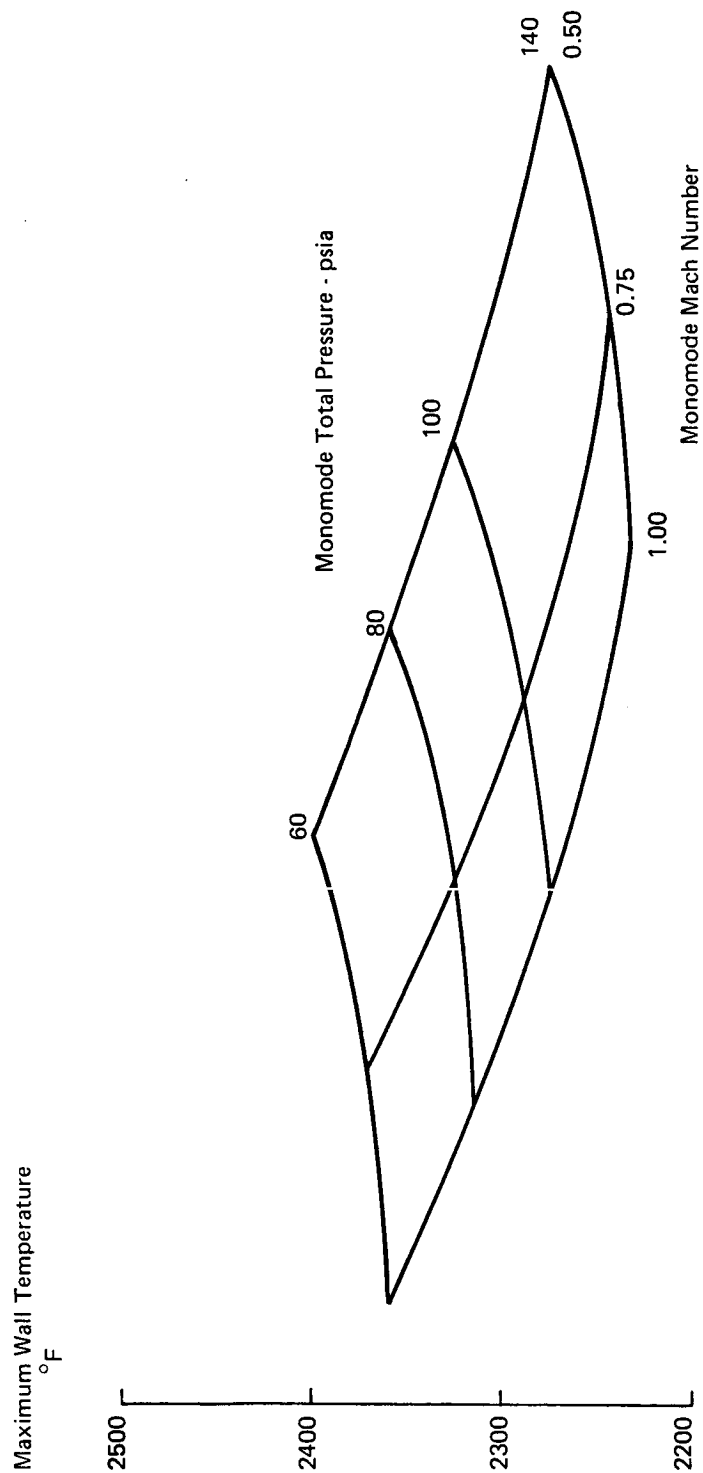


Figure 30. Influence of Coolant Passage Design Parameters on Maximum Throat Temperature

95% c^*
 50% NH_3 Dissociation
 50 Rectangular Passages
 Mach Number = 0.75
 Total Pressure = 80 psia
 $h_g = 6 \times 10^{-4} \text{ BTU/in.}^2 \text{ sec } ^\circ\text{F}$

} Monomode

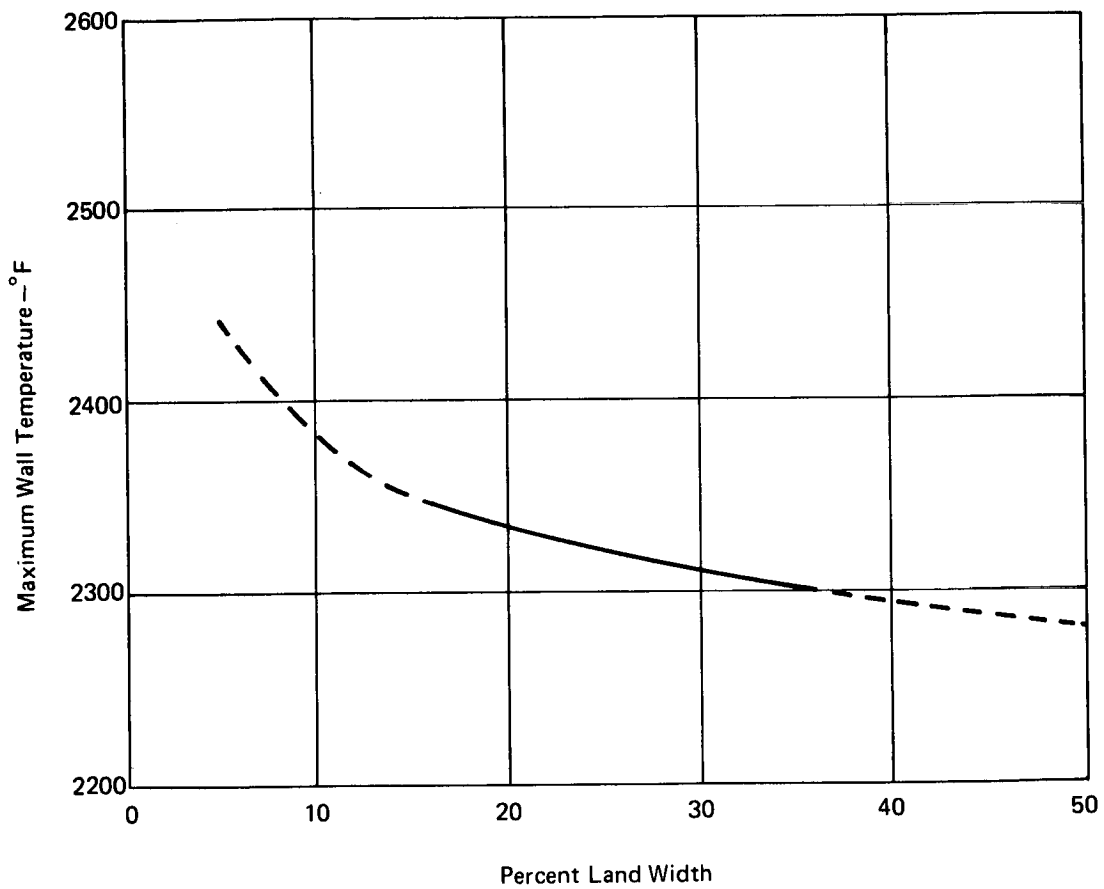


Figure 31. Influence of Percent Land Width on Maximum Throat Temperature

Wall Thickness = 0.07 in.

$h_g = 11 \times 10^{-4} \text{ BTU/in.}^2 \text{ sec } ^\circ\text{F}$
(Theoretical, Curve 1)

$T_g = 4411^\circ\text{F}$, 95% c*

$h_g = 6.0 \times 10^{-4} \text{ BTU/in.}^2 \text{ sec } ^\circ\text{F}$
(Test, Curve 2)

$T_g = 5002^\circ\text{F}$, 100% c*

$h_g = 6.00 \times 10^{-4} \text{ BTU/in.}^2 \text{ sec } ^\circ\text{F}$
(Test, Curve 2)

$T_g = 4411^\circ\text{F}$, 95% c*

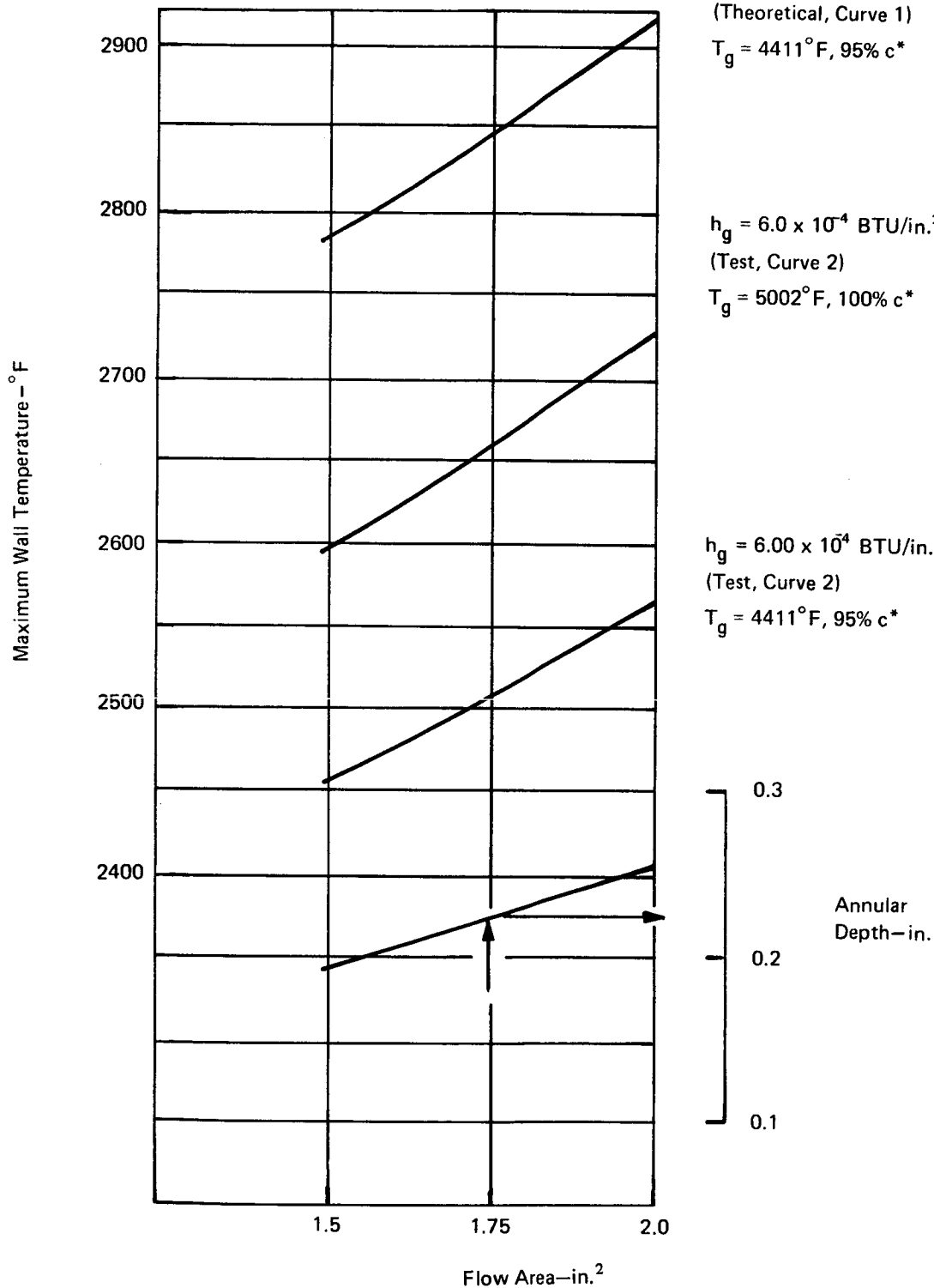


Figure 32. Annular Passage Wall Temperature at the Throat

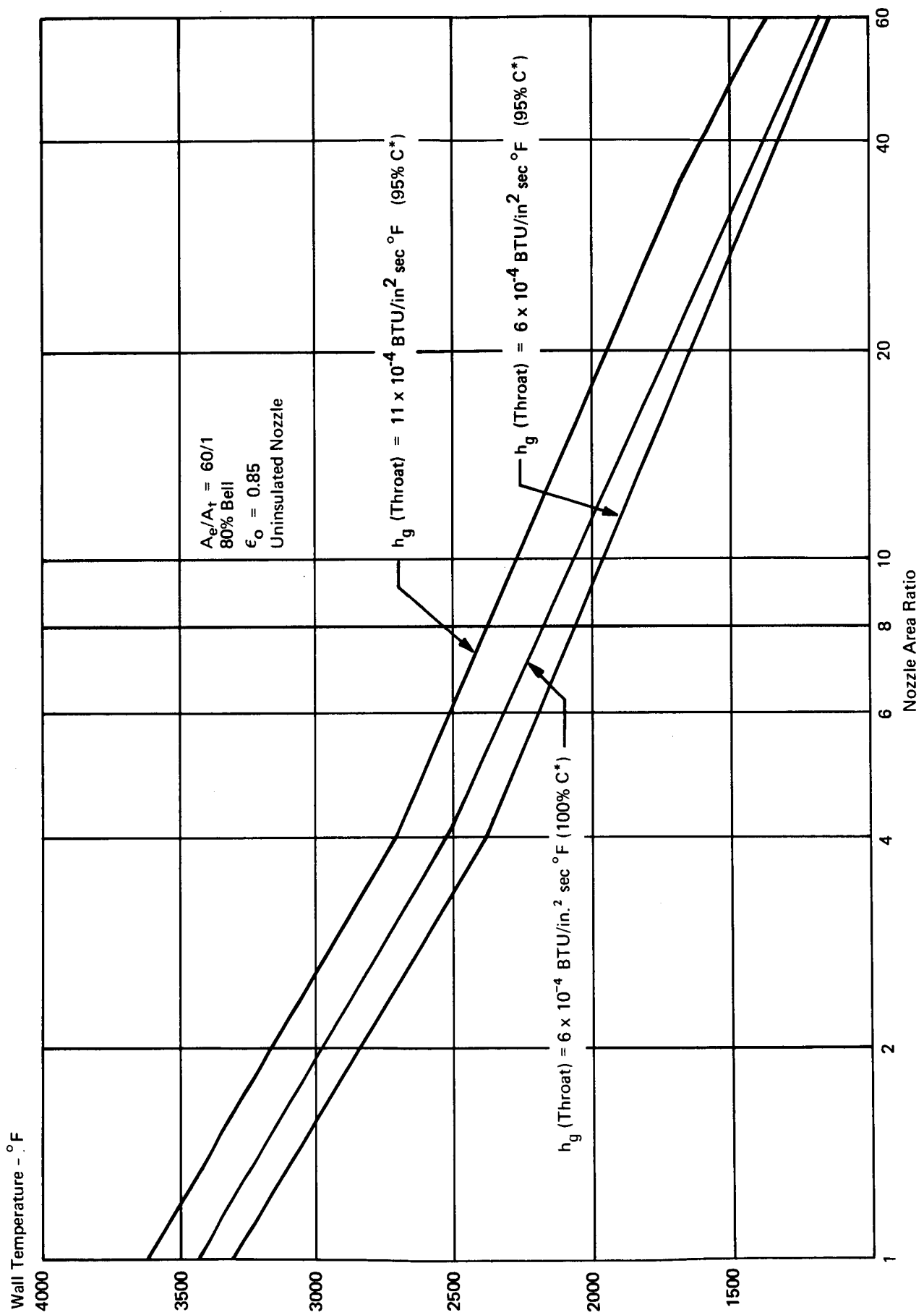


Figure 33. Nozzle Extension Temperature versus Area Ratio

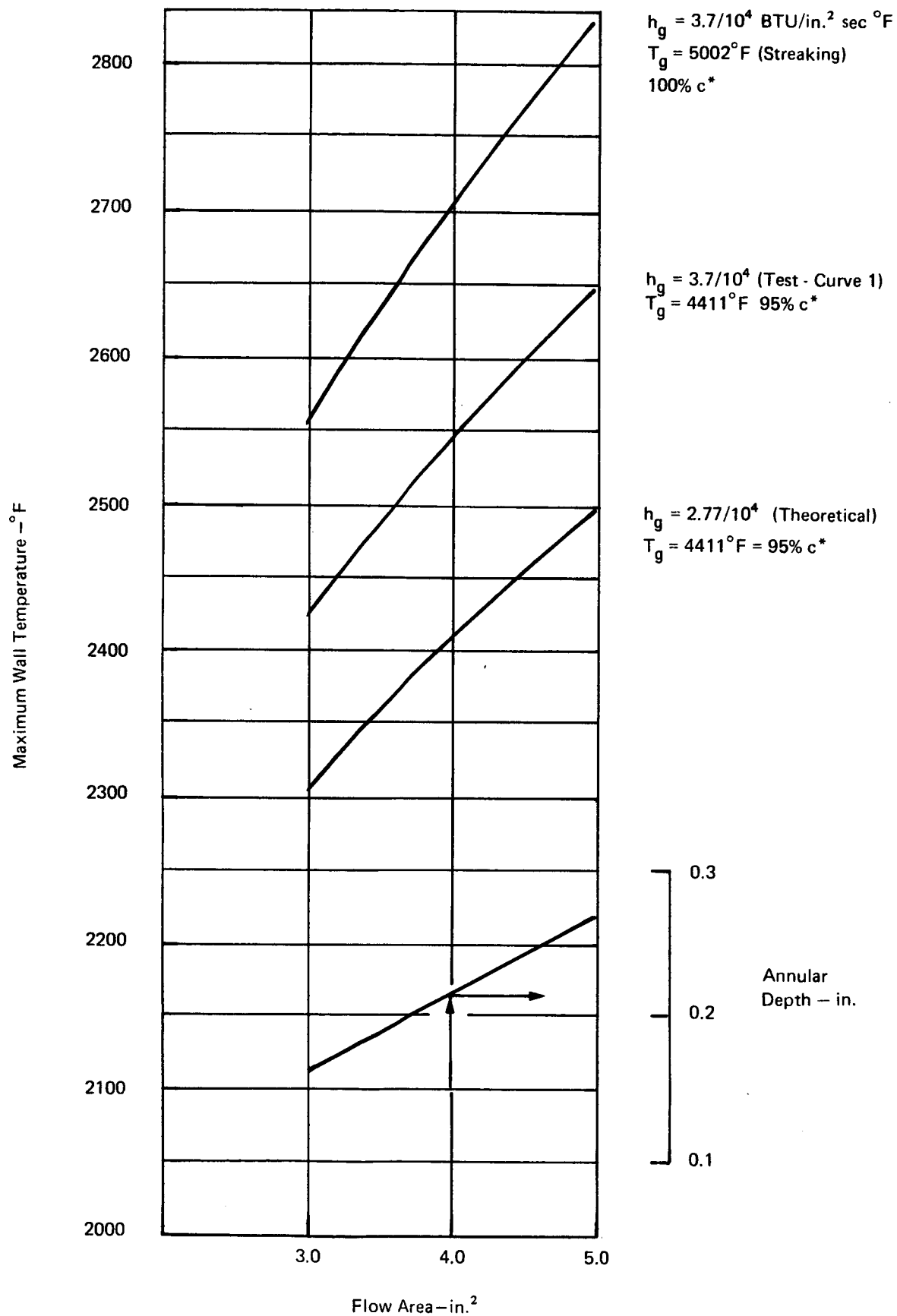


Figure 34. Annular Passage Wall Temperature — Chamber

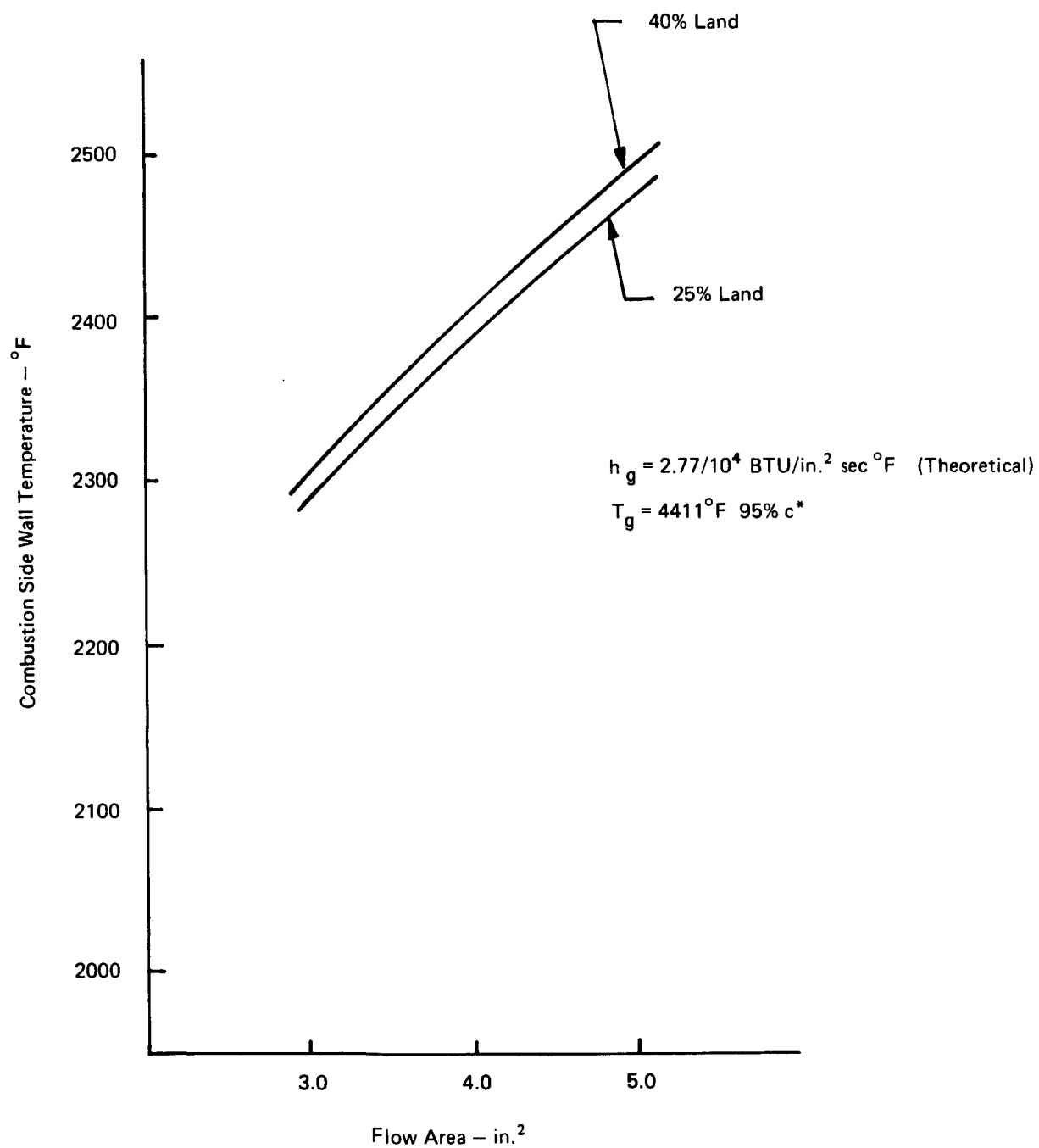


Figure 35. Drilled Passages Wall Temperature – Chamber

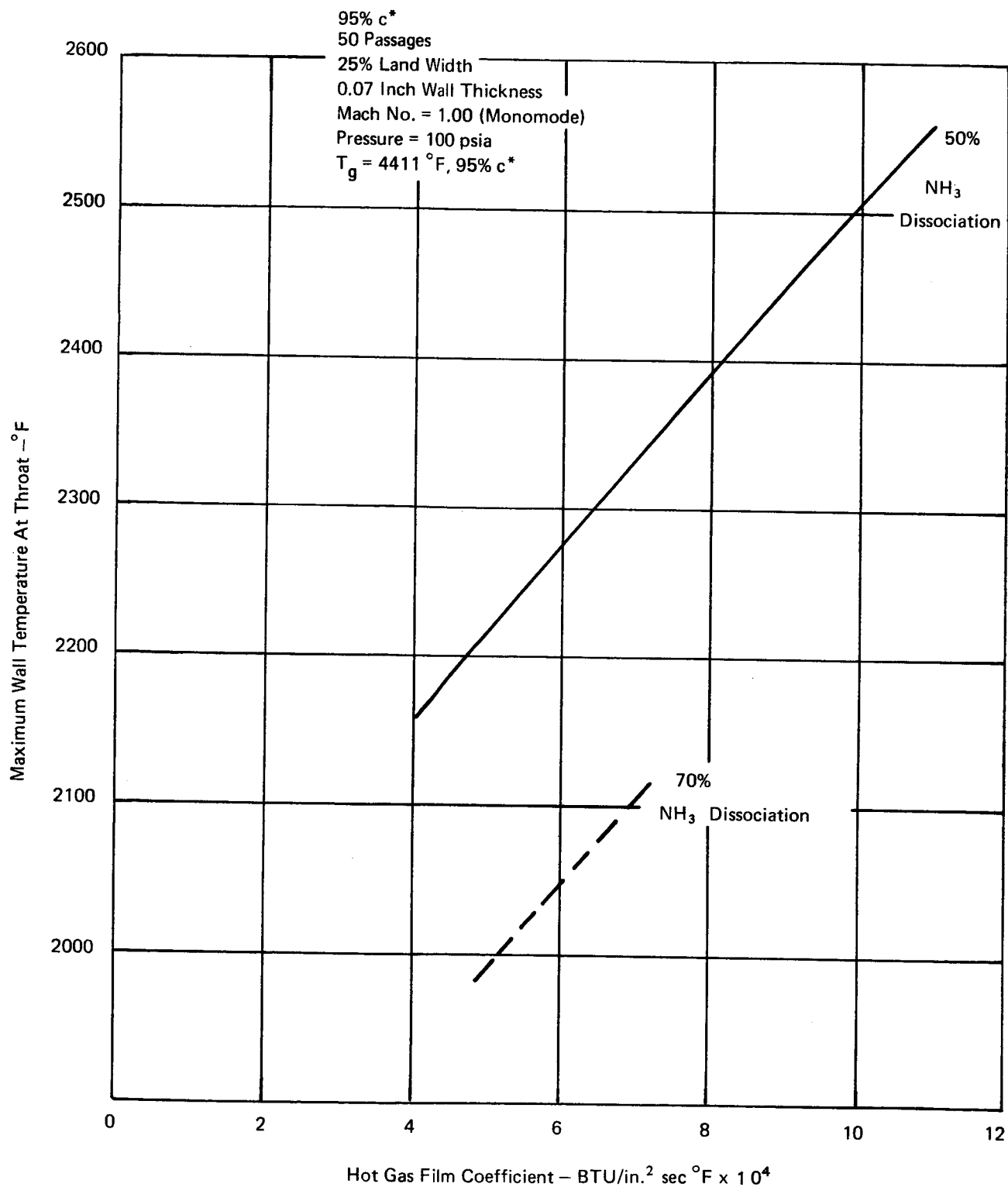


Figure 36. Wall Temperature at Throat Station versus Hot Gas Film Coefficient

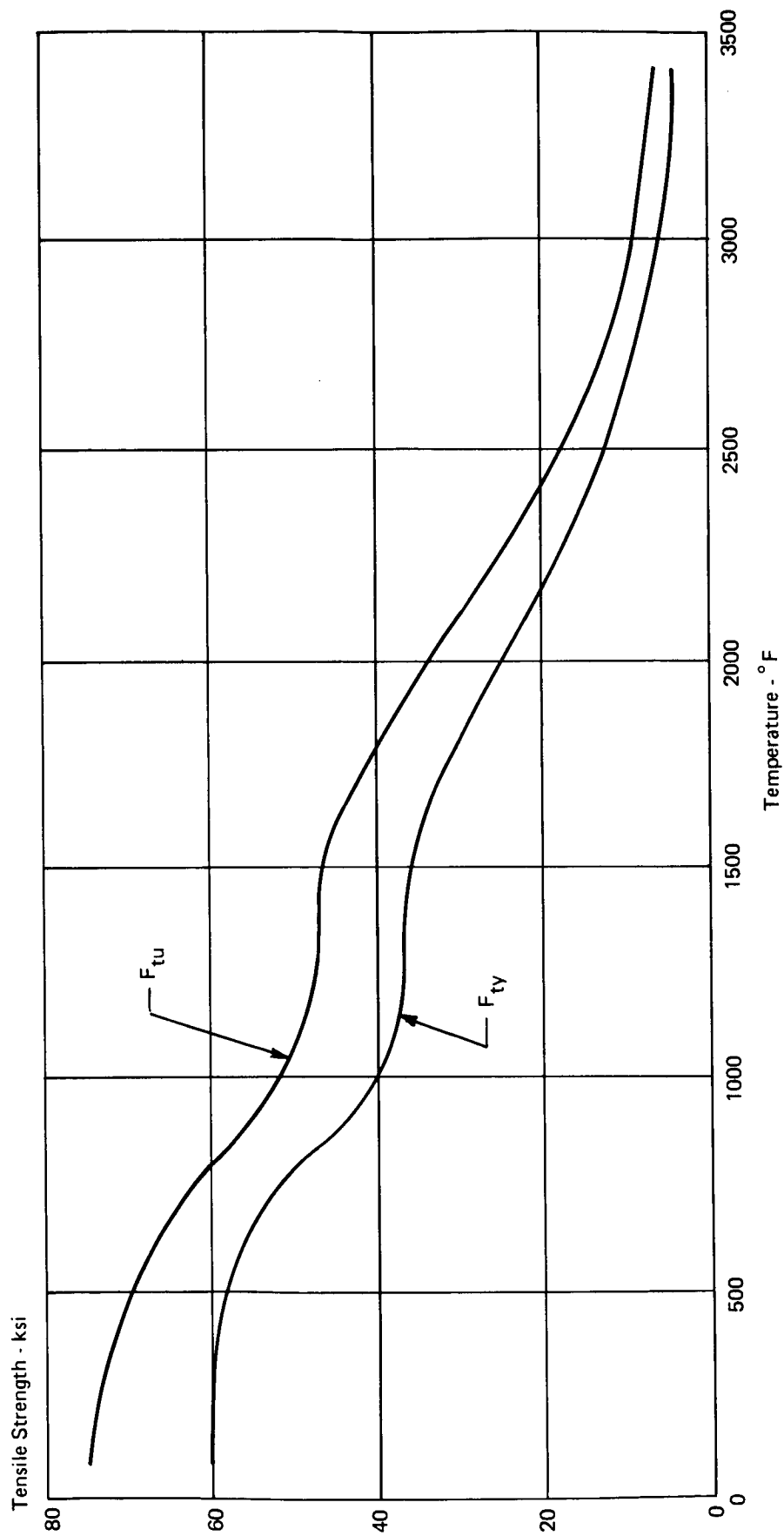


Figure 37. Tensile Strength versus Temperature SCb-291 Columbium

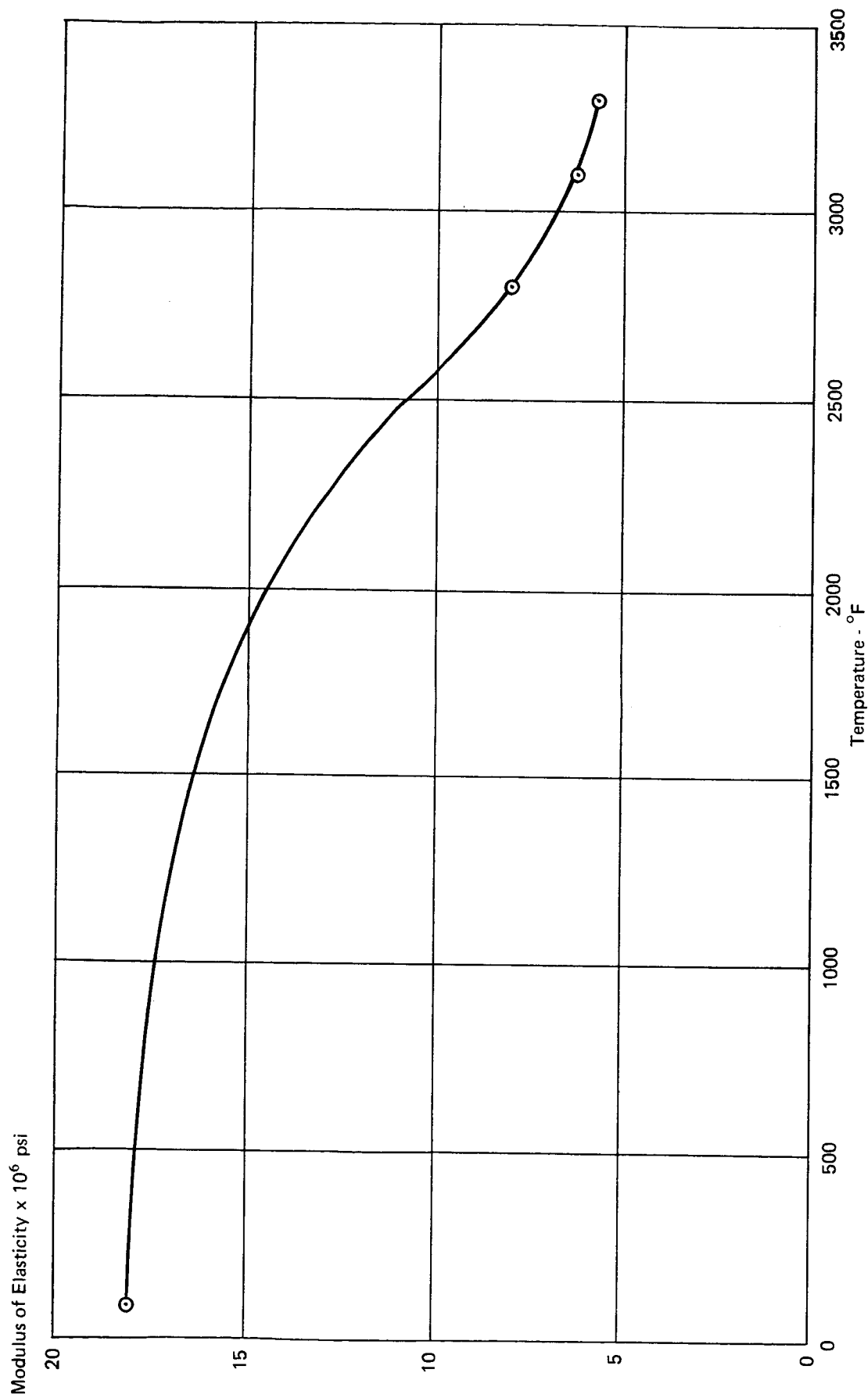


Figure 38. Effect of Temperature on Modulus of Elasticity for SCb-291 Columbian

Creep Stress ~ ksi

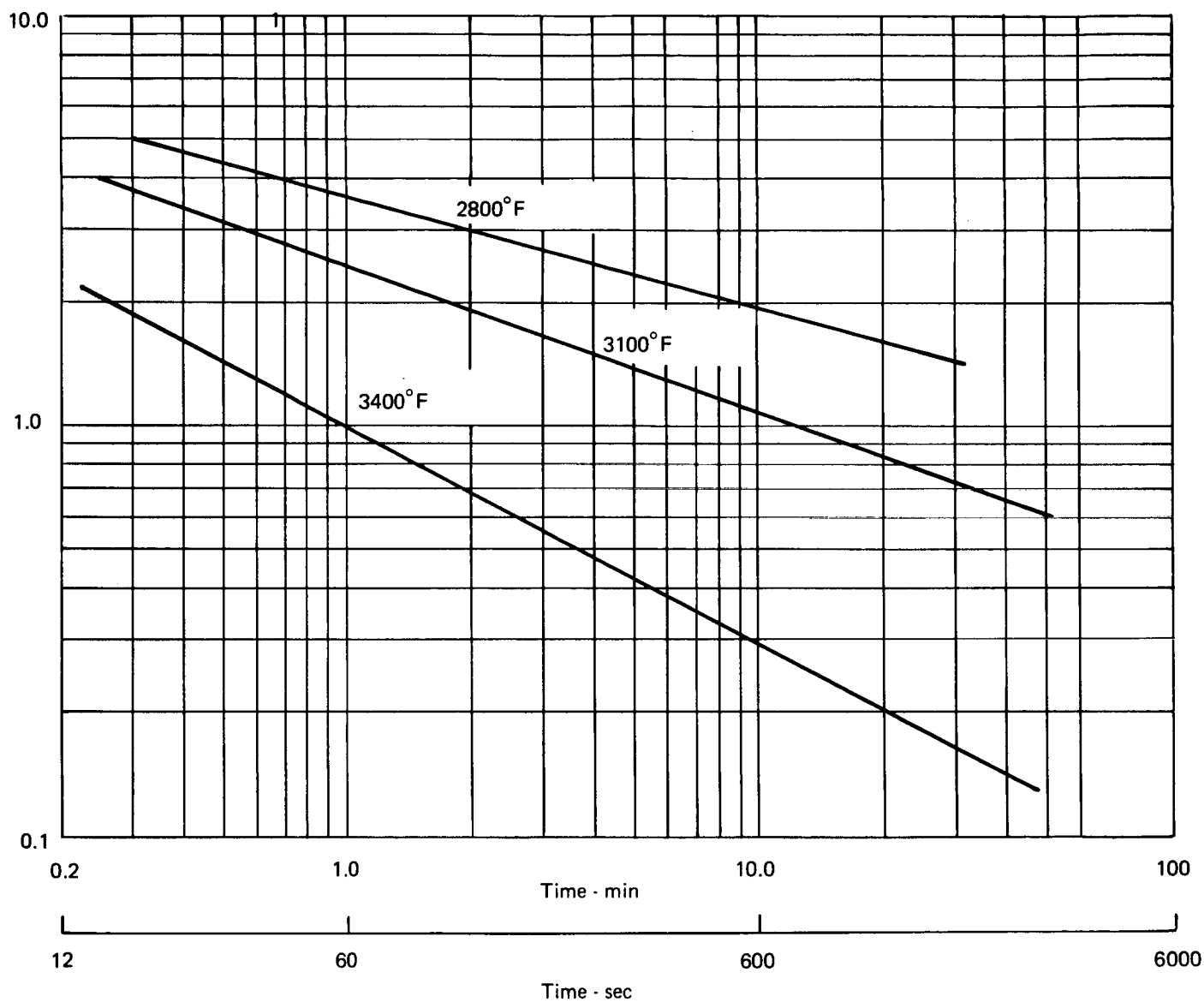


Figure 39. Material SCb-291 Stress Necessary to Produce a Creep Strain of 0.05% at Temperature

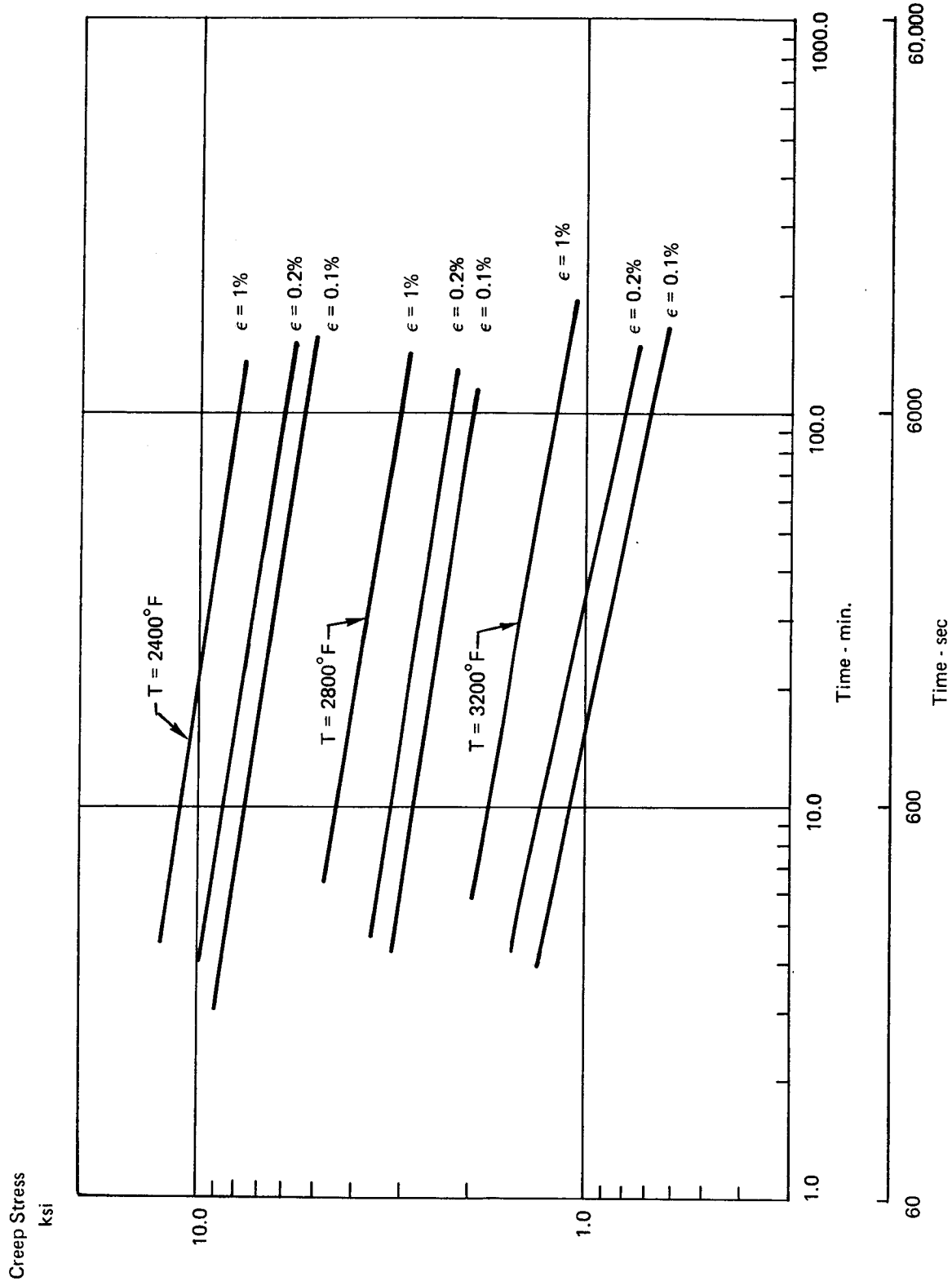


Figure 40. Material - SCb-291 Stress Necessary to Produce Indicated Creep Strain at Temperature

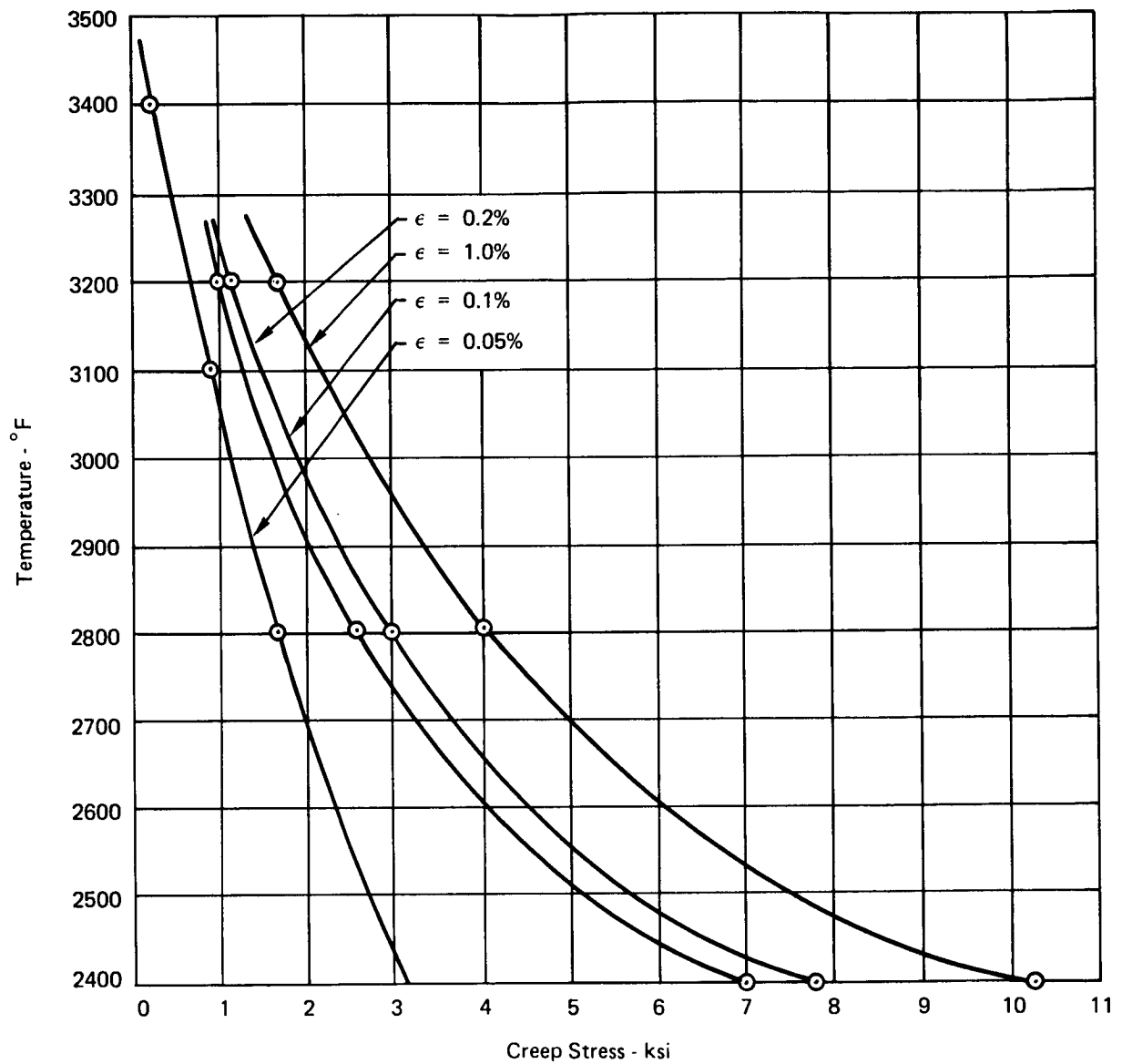


Figure 41. Material - SCb-291 Stress versus Temperature for Indicated Creep Strain at $t = 1000$ sec

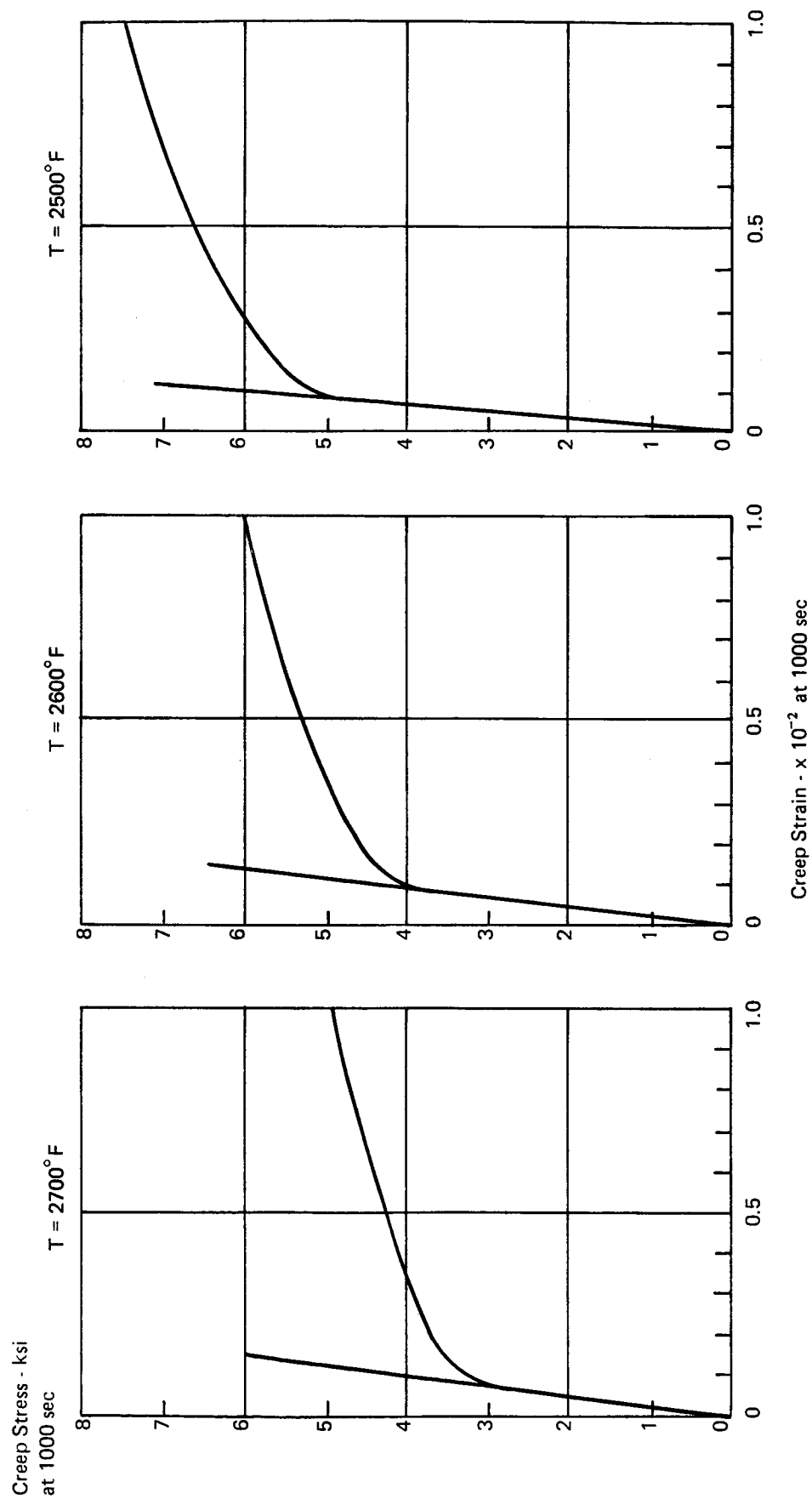


Figure 42. Material - SCb-291 Creep Characteristic Stress-Strain Diagrams at $t = 1000$ sec

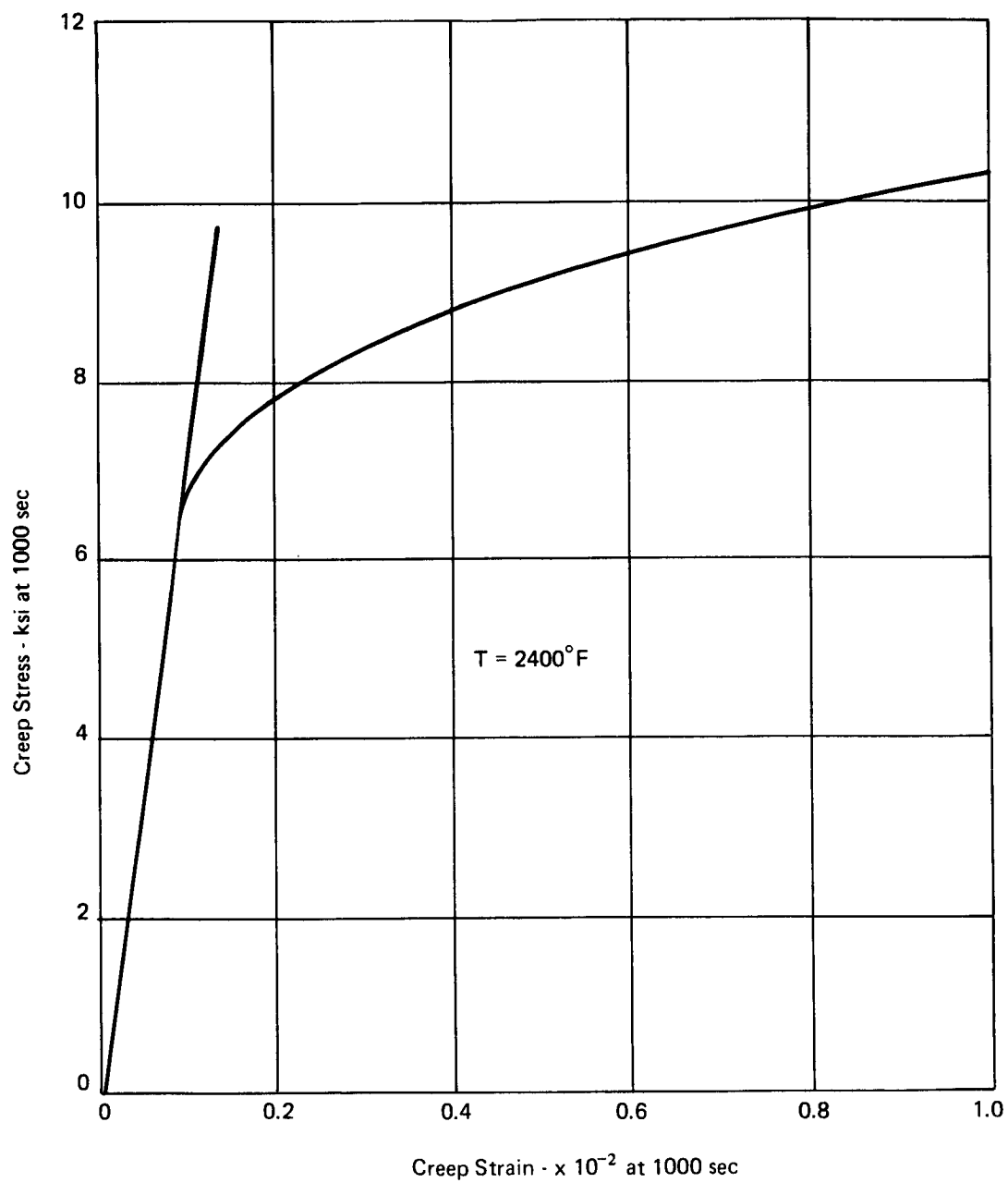


Figure 43. Material - SCb-291 Creep Characteristic Stress-Strain Diagram at $t = 1000$ sec

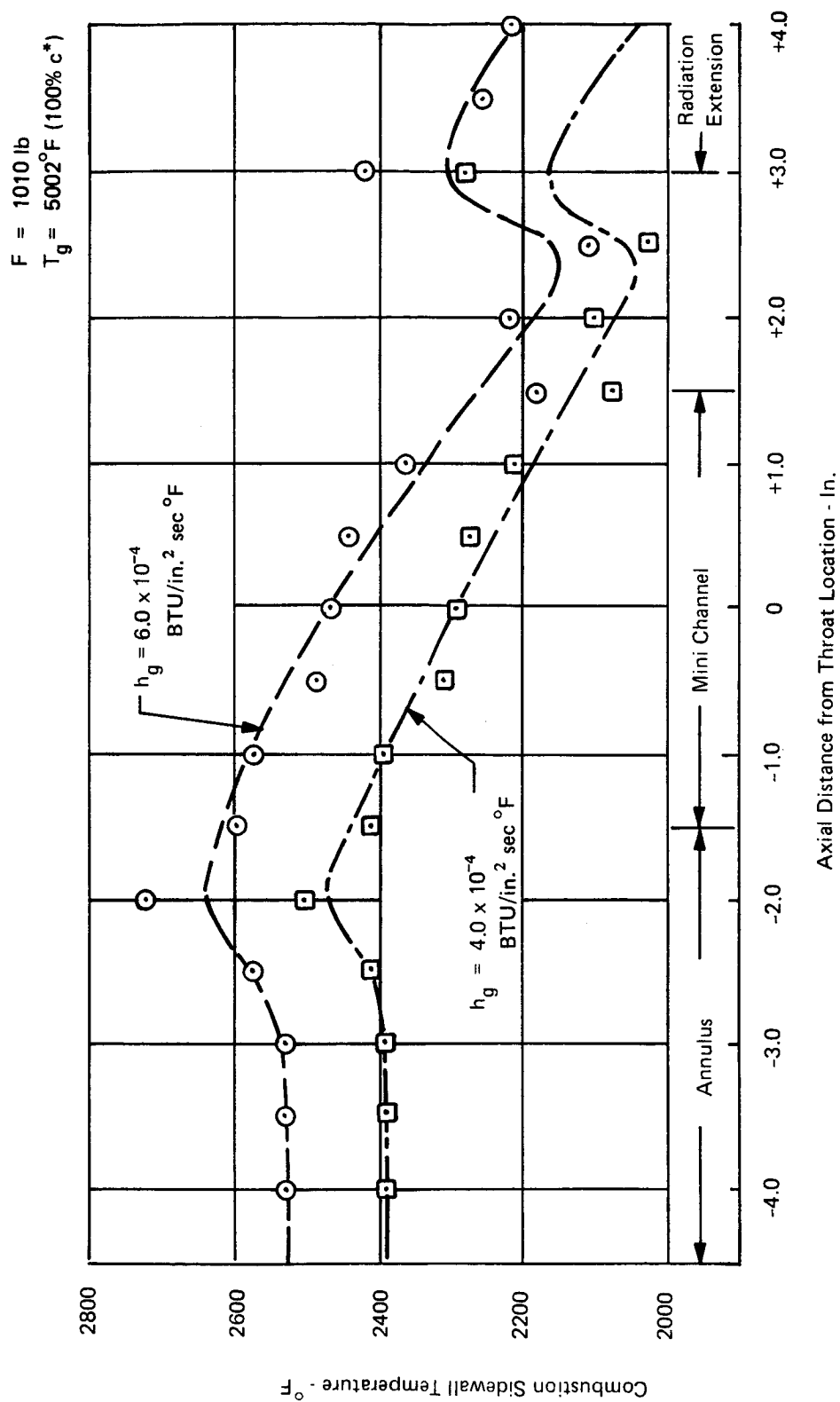


Figure 44. Bimode Engine Axial Temperature versus Distance

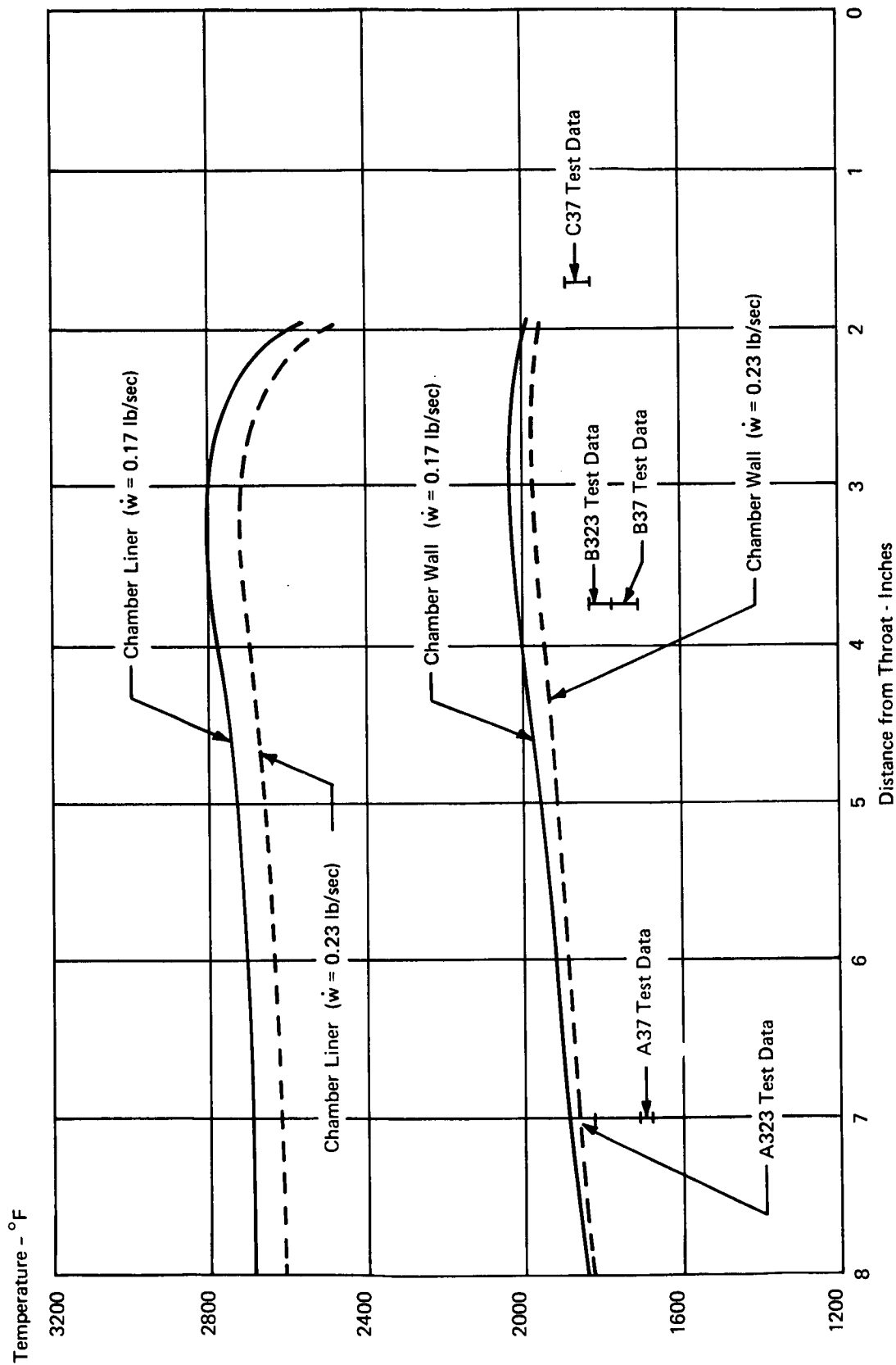


Figure 54. Chamber and Liner Temperatures, Test DJ 339

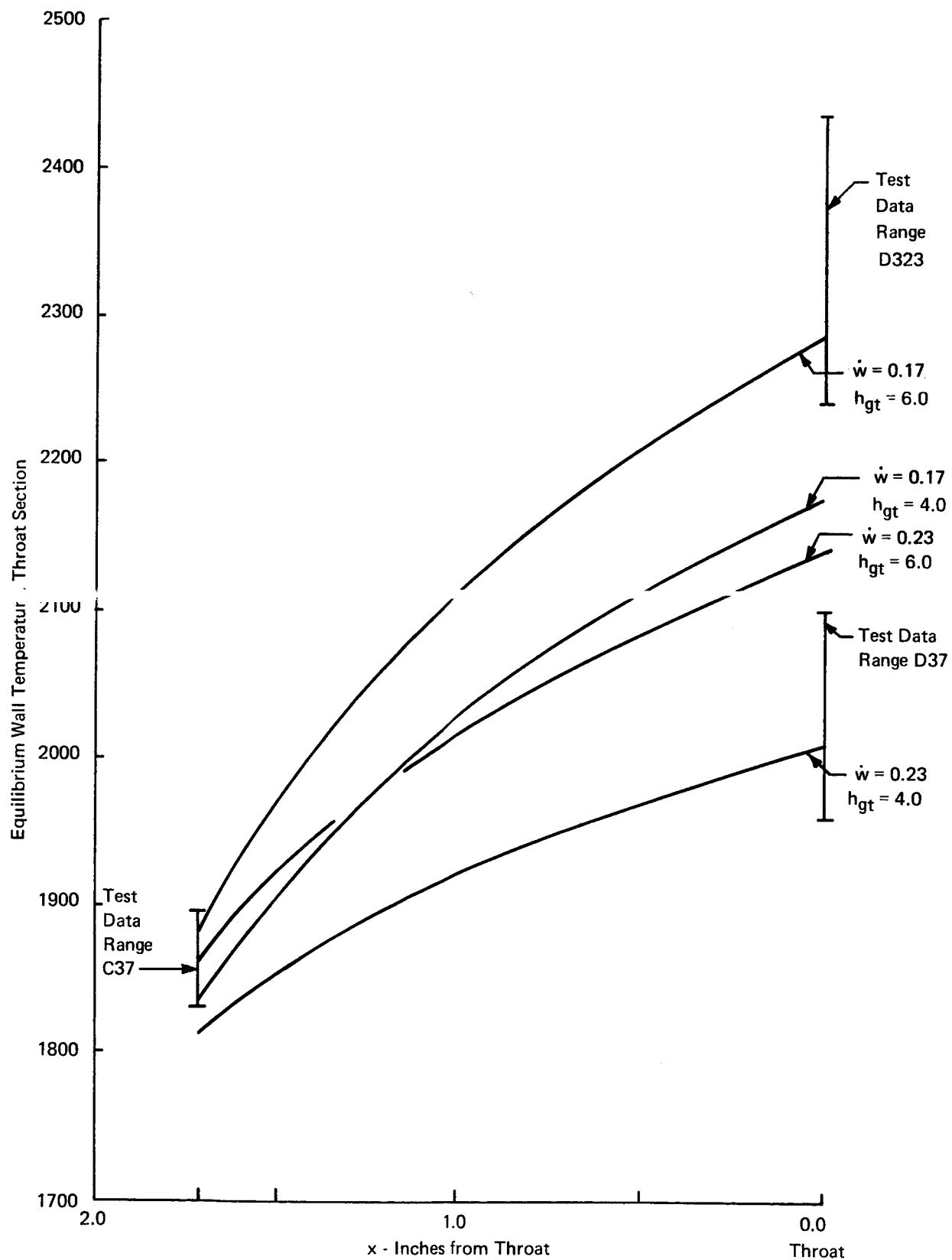


Figure 55. Throat Location, Test DJ 339

95% c*
Gap (Measured Cold) = 0.080 in.
Film Coolant Flow Rate = 0.20 lb/sec
Throat Station $h_g = 6 \times 10^{-4}$ BTU/in.² sec[°]F

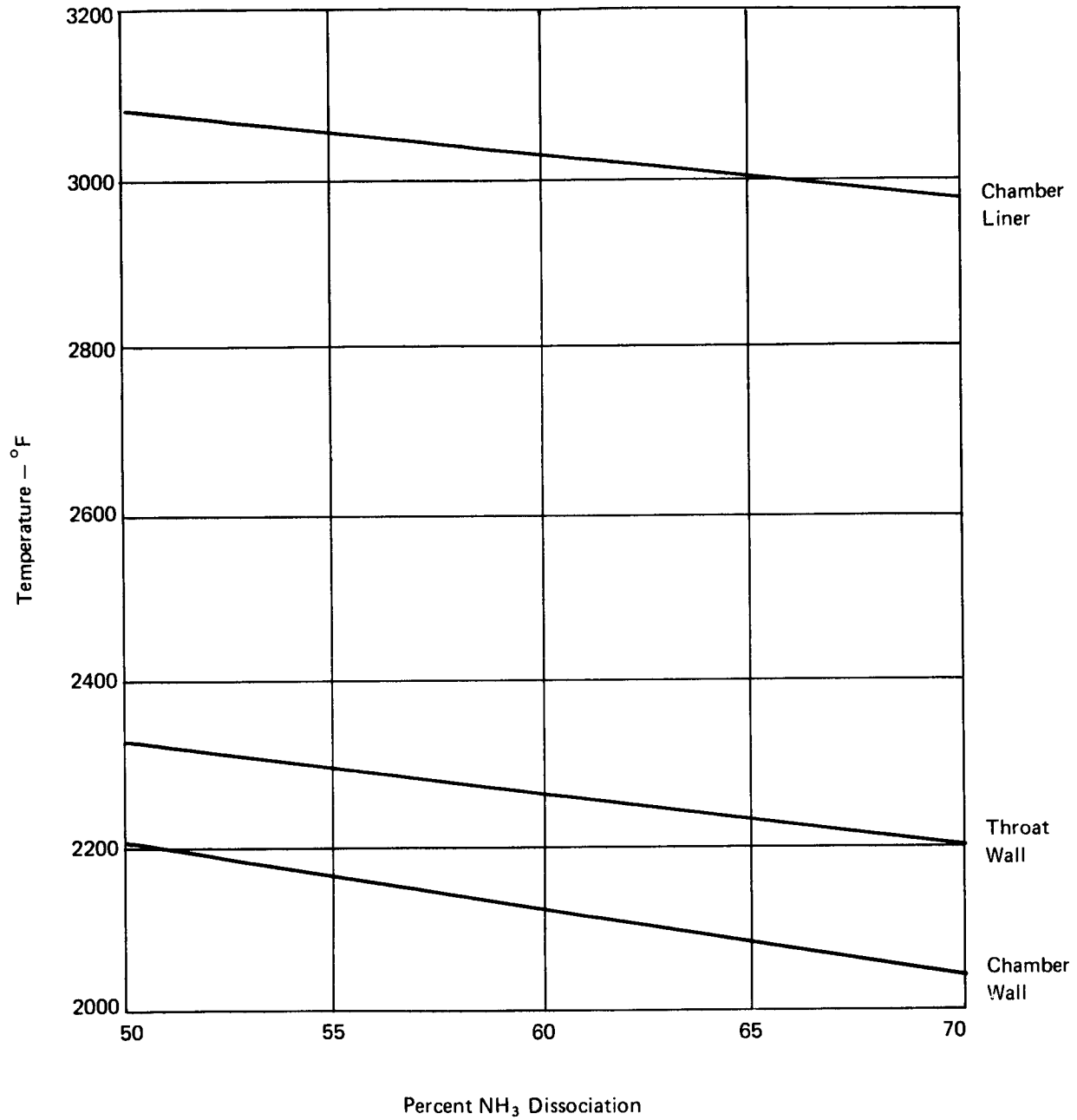


Figure 56. Influence of Ammonia Dissociation on Liner and Wall Temperatures

95% c^*
60% NH_3 Dissociation
Gap (Measured Cold) = 0.080 in.
Throat Station $h_g = 6 \times 10^{-4} \text{ BTU/in.}^2 \text{ sec}^\circ\text{F}$

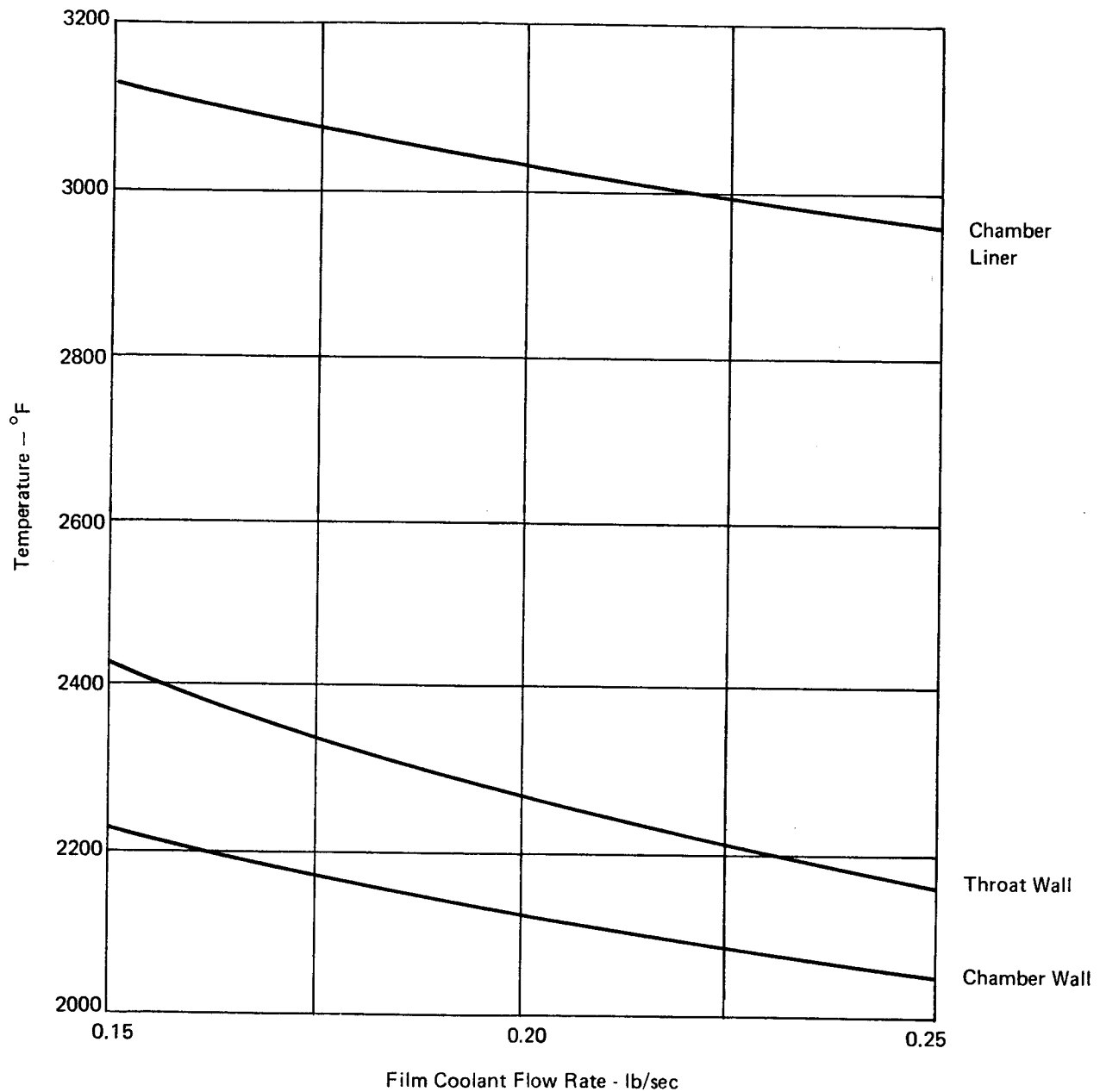


Figure 57. Influence of Film Coolant Flow Rate on Liner and Wall Temperatures

95% c^*
60% NH_3 Dissociation
Film Coolant Flow Rate = 0.20 lb/sec
Throat Station $h_g = 6 \times 10^{-4} \text{ BTU/in.}^2 \text{ sec}^\circ\text{F}$

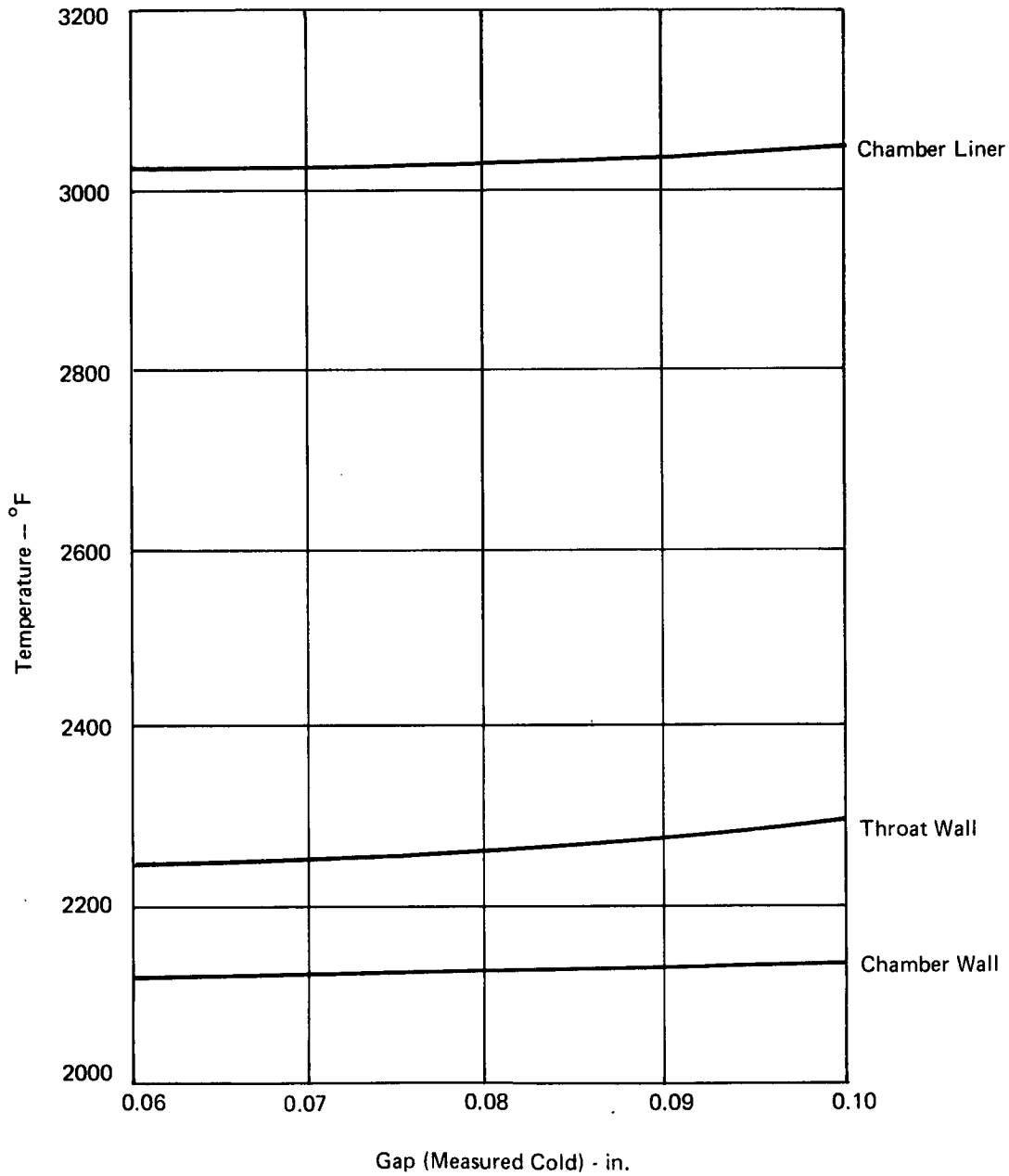


Figure 58. Influence of Annular Gap on Liner and Wall Temperatures

60% NH_3 Dissociation
Gap (Measured Cold) = 0.080 in.
Film Coolant Flow Rate = 0.20 lb/sec

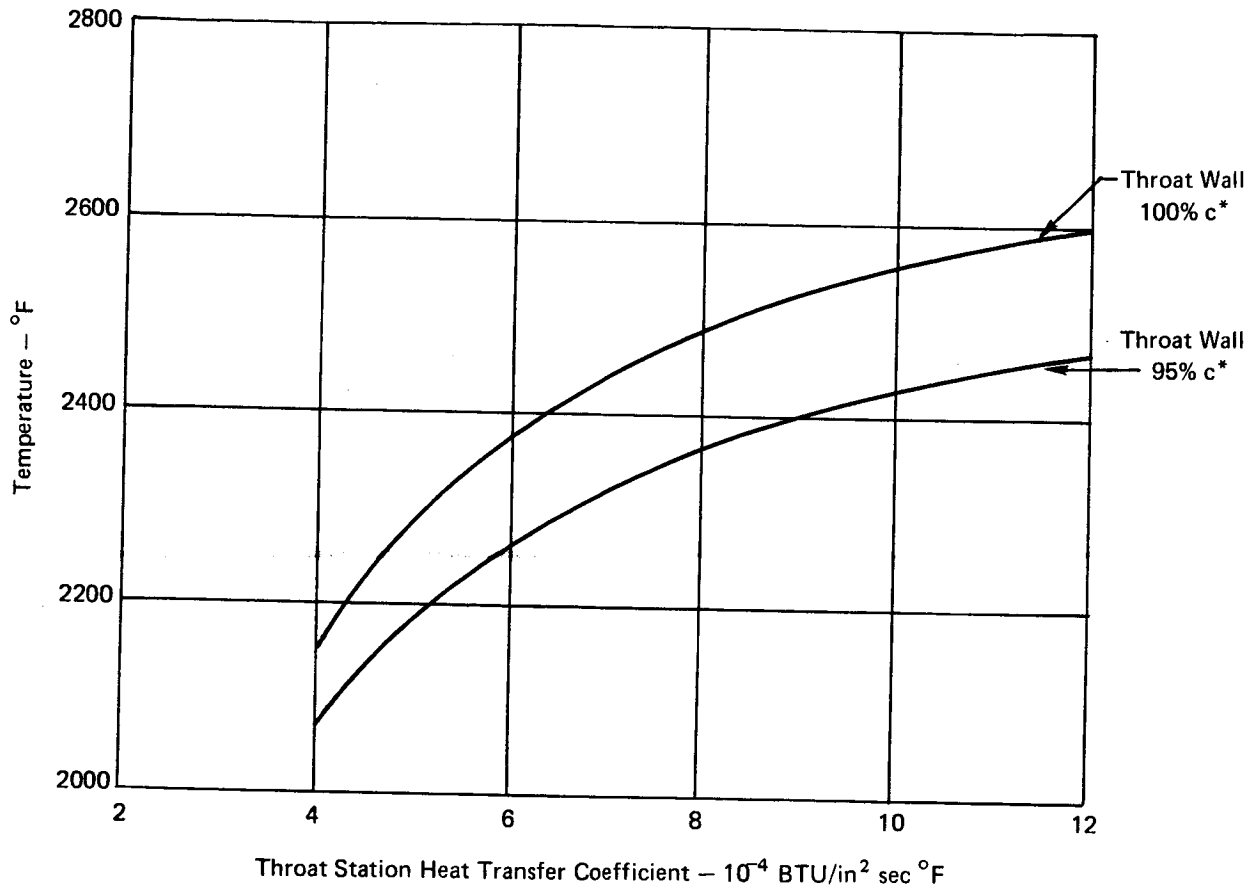


Figure 59. Influence of Heat Transfer Coefficient on Throat Station Wall Temperature

60% NH₃ Dissociation
Gap (Measured Cold) = 0.080 in.
Film Coolant Flow Rate = 0.20 lb/sec

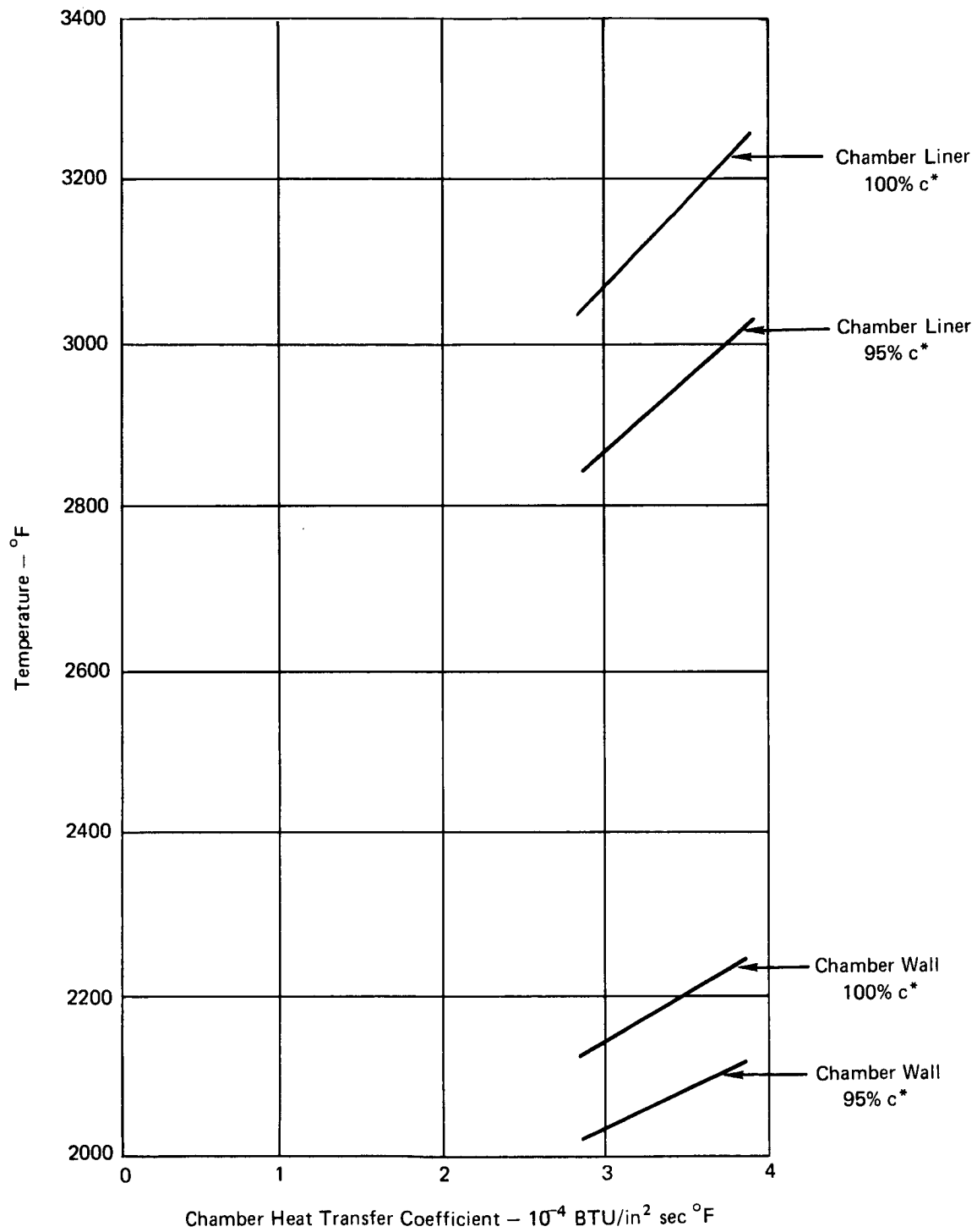


Figure 60. Influence of Chamber Heat Transfer Coefficient on Chamber Liner and Wall Temperatures

95% c*
 60% NH₃ Dissociation
 Gap (Measured Cold) = 0.080 in.
 Film Coolant Flow Rate = 0.20 lb/sec
 Throat Station $h_g = 6 \times 10^{-4}$ BTU/in² sec °F

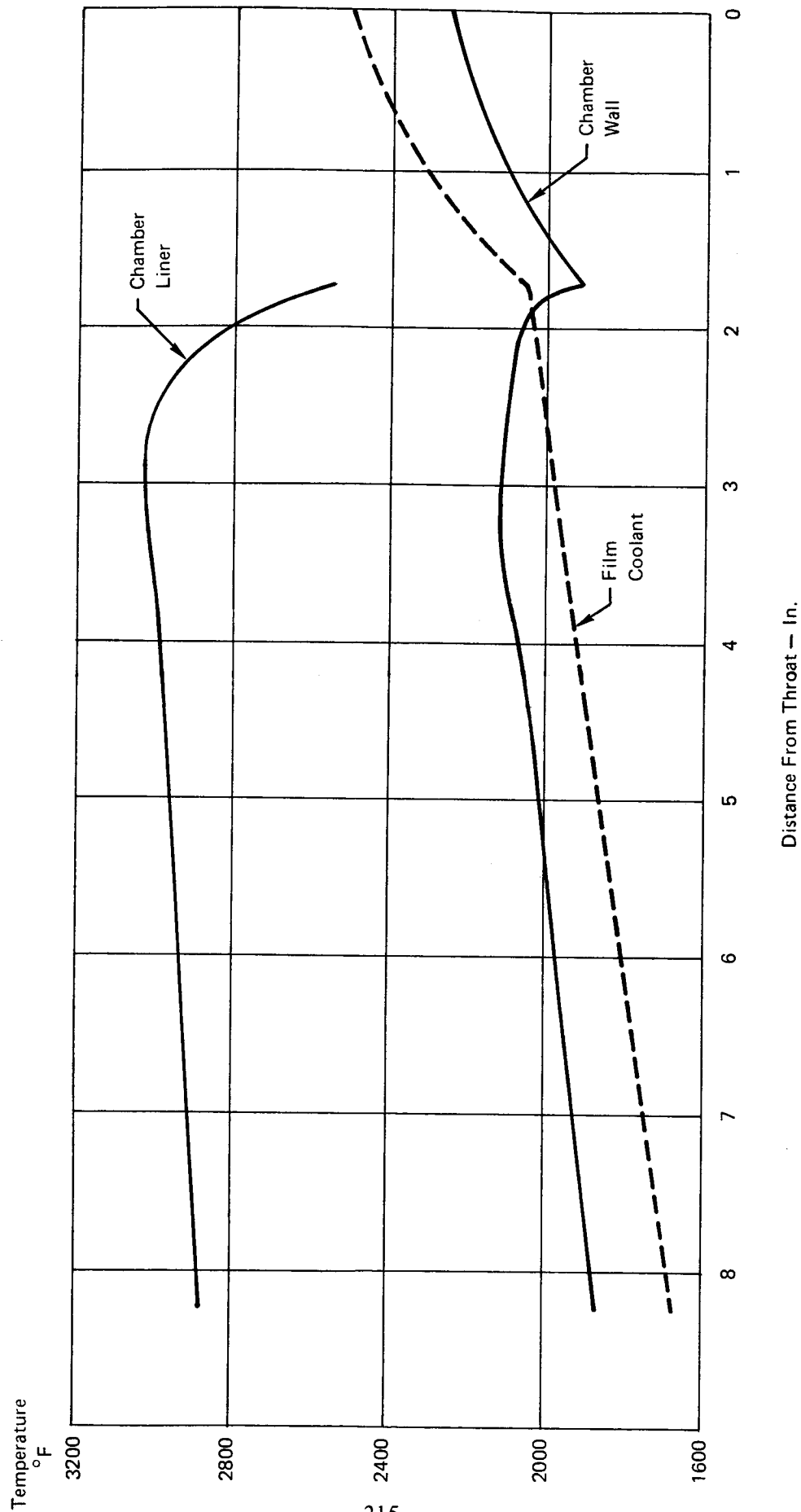


Figure 61. Axial Temperature Distribution of Film Coolant, Liner and Chamber Wall

Stress - ksi

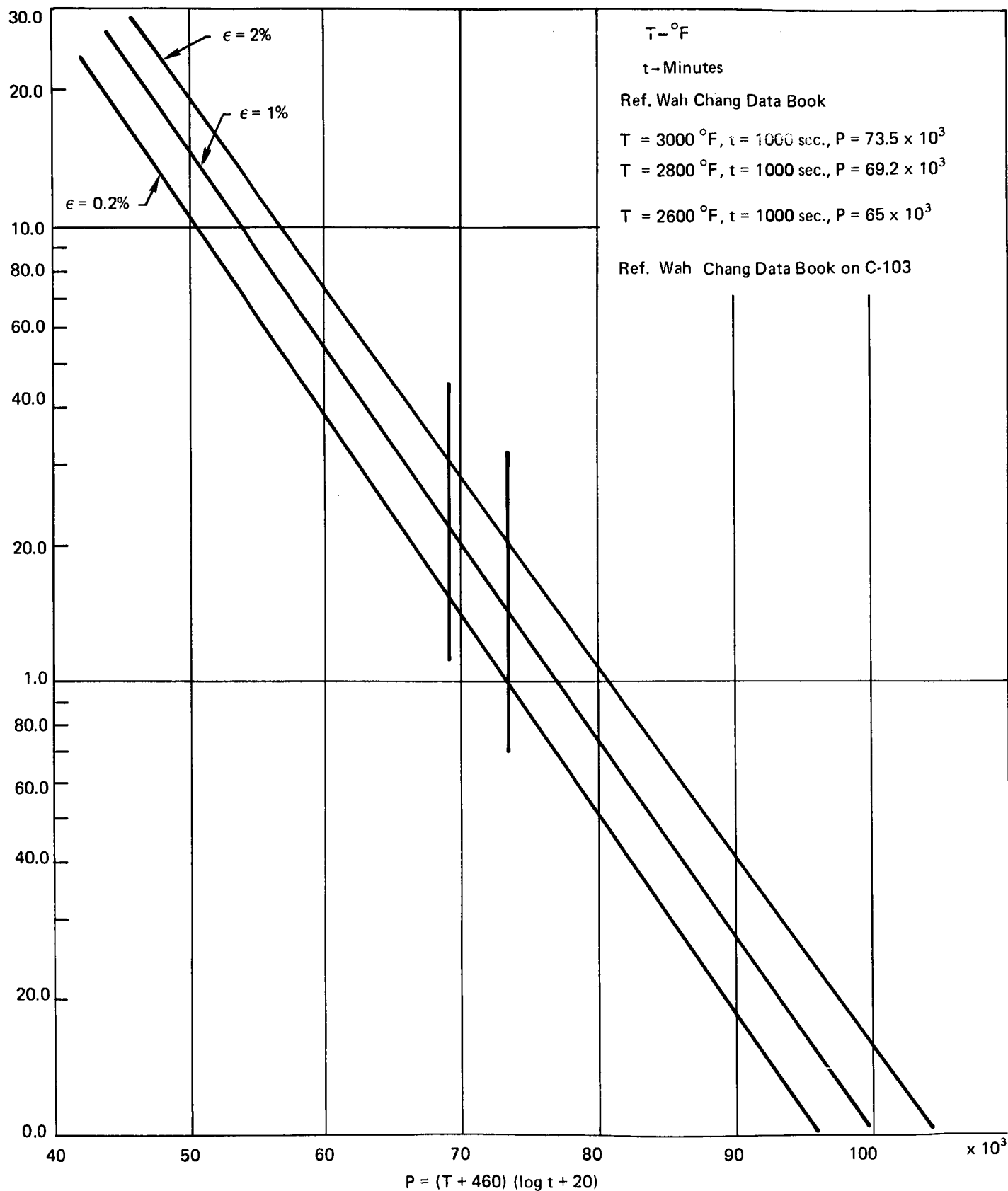


Figure 62. Larson - Miller Master Plot for Recry C-103

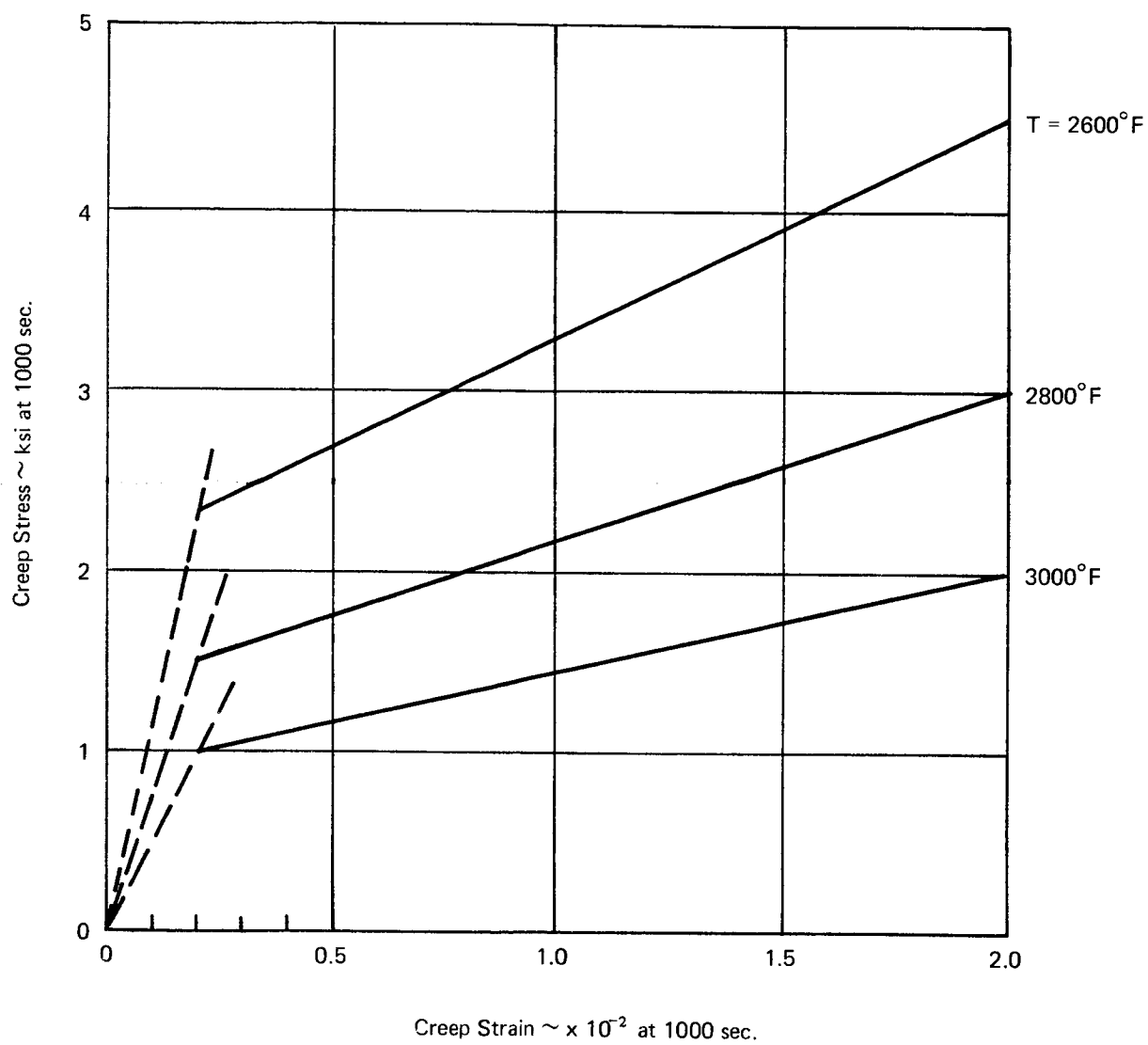


Figure 63. Material - C-103 Creep Characteristic Stress-Strain Diagrams at $t = 1000$ sec

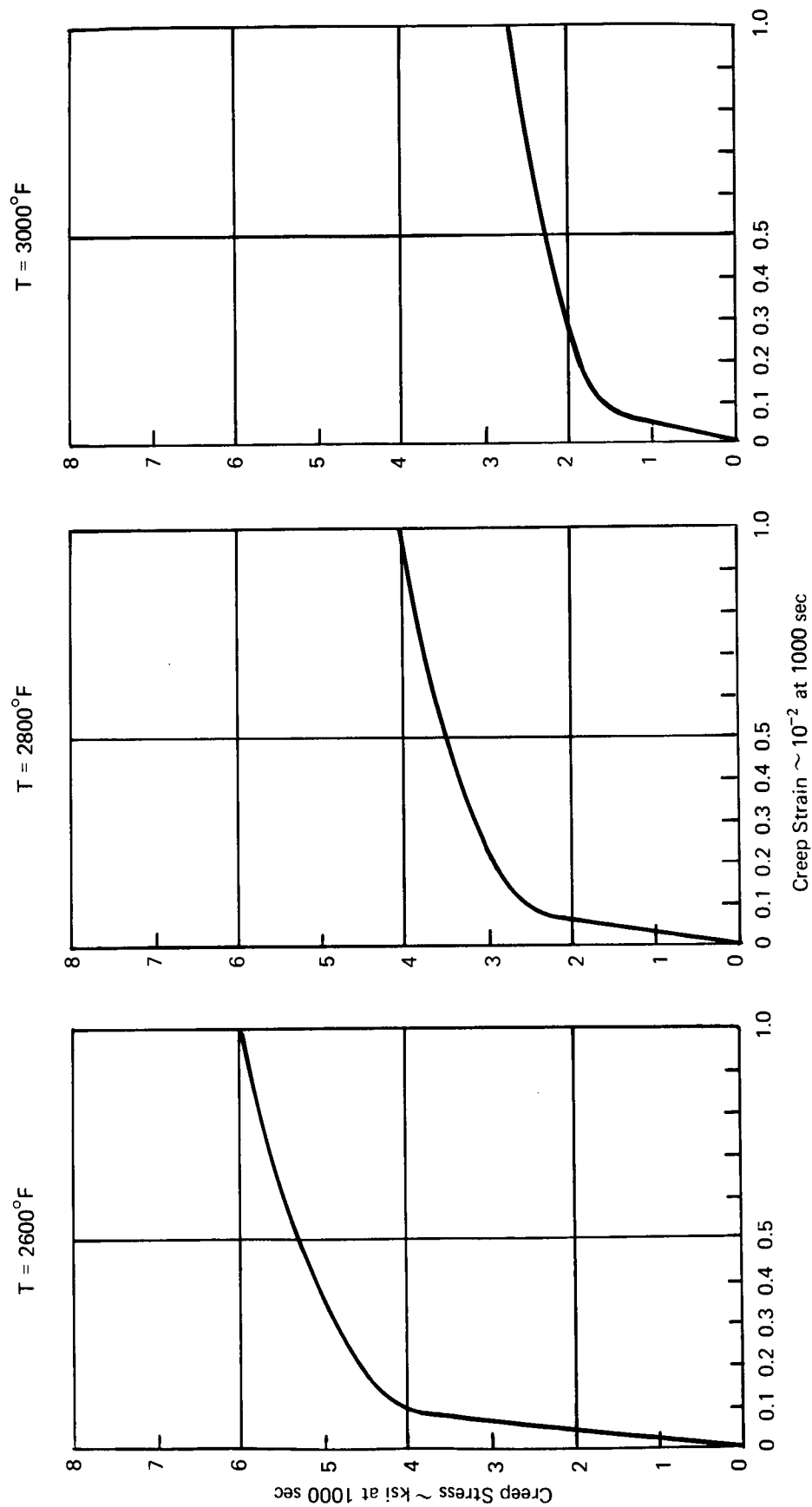


Figure 64. Material - SCb-291 Creep Characteristic Stress Strain Diagrams at $t = 1000$ sec